

Louisiana State University

LSU Scholarly Repository

LSU Doctoral Dissertations

Graduate School

4-9-2020

The Long-Term Outlook of the Mississippi-Atchafalaya Bifurcation: A Convergence of Engineering, Economics, and Deltaic Evolution

Thomas Mitchell Andrus

Louisiana State University and Agricultural and Mechanical College

Follow this and additional works at: https://repository.lsu.edu/gradschool_dissertations



Part of the [Civil Engineering Commons](#), [Geological Engineering Commons](#), [Geology Commons](#), [Geomorphology Commons](#), [Hydraulic Engineering Commons](#), and the [Hydrology Commons](#)

Recommended Citation

Andrus, Thomas Mitchell, "The Long-Term Outlook of the Mississippi-Atchafalaya Bifurcation: A Convergence of Engineering, Economics, and Deltaic Evolution" (2020). *LSU Doctoral Dissertations*. 5218. https://repository.lsu.edu/gradschool_dissertations/5218

This Dissertation is brought to you for free and open access by the Graduate School at LSU Scholarly Repository. It has been accepted for inclusion in LSU Doctoral Dissertations by an authorized graduate school editor of LSU Scholarly Repository. For more information, please contact gradetd@lsu.edu.

**THE LONG-TERM OUTLOOK OF THE MISSISSIPPI –
ATCHAFALAYA BIFURCATION: A CONVERGENCE OF
ENGINEERING, ECONOMICS, AND DELTAIC EVOLUTION**

A Dissertation

Submitted to the Graduate Faculty of the
Louisiana State University and
Agricultural and Mechanical College
in partial fulfillment of the
requirements for the degree of
Doctor of Philosophy

in

The Department of Geology and Geophysics

by

Thomas Mitchell Andrus
B.S., Louisiana State University, 1997
M.S., Louisiana State University, 2007
May 2020

To Evelyn, Kate, and Thomas

May your dreams be big and your desire to pursue them even bigger.

ACKNOWLEDGMENTS

As a lifelong resident of Louisiana, I continue to be amazed at the diversity of its culture, history, and physical settings that make it unique and vital to the nation. As our environment changes and our people adapt, it is essential that our plans to restore and protect both work in unison. As I examined this possibility for the Mississippi-Atchafalya bifurcation, I realized the depth of scientific, engineering, and political will it took to control it. The magnitude and longevity of this accomplishment leaves little doubt that it could be summoned again.

I would like to thank my business partners and coworkers at Royal Engineers and Consultants for walking with me on this seven-year journey. As I pursued this on a part-time and remote basis, the support I received in the form of tuition, expenses, and most of all, trust in me to manage the balance between academic and company responsibilities, will hopefully pay dividends many times over.

For a major advisor, I was fortunate enough to have Dr. Sam Bentley who piqued my interest in coastal geology and deltaic processes over fifteen years ago and has served as a valuable mentor and friend along the way. He never failed to navigate me through academic hurdles and provide superior scientific tutelage that enabled me to bring my ideas to life. I will always be grateful for his guidance. Thanks also to Dr. Clint Willson guiding me towards the river engineering and modeling resources that were the right fit for my needs. To Dr. Doug Edmonds of Indiana University for sharing the Delft 3D model he originally developed for the Mississippi and Atchafalya River channels and bifurcation. To Dr. Rex Caffey for sharing his economic insights with respect to river diversions and other coastal restoration methodologies. To Dr. Peter Clift, Dr. Carol Wilson, and Dr. Richard Shaw for challenging me through my general exams and defense requirements.

To my wife, Hallie, thank you for the sacrifices you endured and believing in me as I saw this through to completion. Your patience, love, and understanding has been truly remarkable. Thank you for picking up the slack when the work had to be done and reminding me when higher priorities took precedence. None were bigger than raising our children, Evelyn, Kate, and Thomas. This work is for you, may you find joy and purpose in your pursuits.

TABLE OF CONTENTS

ACKNOWLEDGMENTS	iii
ABSTRACT.....	vi
CHAPTER 1: INTRODUCTION	1
1.1 Introduction.....	1
1.2 Sustainability Decline in the LMR	3
1.3 Transition of the Holocene Delta Cycle into the Anthropocene: Correlation of Regressive and Transgressive Phases in MRDP	7
1.4 Sediment Diversion Review and Considerations.....	16
1.5 Dissertation Structure.....	21
CHAPTER 2: THE CAPTURE TIMESCALE OF AN UNCONTROLLED MISSISSIPPI – ATCHAFALAYA BIFURCATION WITH FUTURE LOWER RIVER STRATEGY IMPLICATIONS	24
2.1 Introduction and Purpose	24
2.2 Overview of Holocene River Avulsions of the Mississippi River.....	27
2.3 Atchafalaya River Diversion and Anthropogenic Influences	30
2.4 Previous Research.....	32
2.5 Methods.....	41
2.6 Results and Discussion	44
2.7 Conclusions.....	57
CHAPTER 3: PROJECTED LONG-TERM DELTA-BUILDING RESPONSES TO FLOW MODIFICATIONS AT THE MISSISSIPPI – ATCHAFALAYA BIFURCATION..	60
3.1 Introduction and Purpose	60
3.2 Methods.....	65
3.3 Results.....	83
3.4 Discussion.....	90
3.5 Conclusions.....	94
CHAPTER 4: A FIRST ORDER COST-BENEFIT ANALYSIS OF MODELED COASTAL LAND-BUILDING POTENTIAL OF THE MISSISSIPPI AND ATCHAFALAYA RIVER-DELTA SYSTEMS	96
4.1 Introduction and Purpose	96
4.2 Methods.....	101
4.3 Results.....	121
4.4. Discussion.....	126
4.5. Conclusions.....	131
CHAPTER 5: SUMMARY AND CONCLUSIONS.....	133
APPENDIX A: MODELED STAGE AND LEVEE PLOTS.....	138
APPENDIX B: RIVER LEVEE CONSTRUCTION COSTS EXAMPLE USACE BID TABULATIONS.....	151
REFERENCES	153
VITA	174

ABSTRACT

The most recent and currently active delta lobe of the Mississippi River (MR) is the Atchafalaya-Wax Lake lobe, which was initiated approximately 400 years ago as a result of MR stream capture by the Atchafalaya River (AR). This capture process accelerated in the early to mid-1900s but further progress was prevented by construction and operation of the Old River Control Structure (ORCS) Complex. Many recent studies indicate that MR system below the ORCS is on a retreating geologic trajectory due to contributing factors such as sea level rise, subsidence, faulting, and declining hydraulic stream power. Diversions along the Lower MR currently being planned would partially alleviate these risks by altering the Lower MR hydraulics and capturing land-building sediment.

This study uses both 1D and 2D numerical modeling techniques to evaluate the long-term effects of current water and sediment regulation mandates and alternatively explore the long-term land-building potential of progressively continuing the avulsion at the MR-AR bifurcation in a controlled manner. Riverine hydraulic and sediment transport modelling was performed using Delft 3D coupled with a spreadsheet which used a 1D spatially averaged equation to calculate delta growth. A 150-year model duration was used to account for flow and system adjustments, implementation of current restoration plans, and to sufficiently analyze delta response trends into the future. The study tests 12 scenarios (1 No Change scenario, 8 increased AR flow scenarios, and 3 increased MR flow scenarios) where flow adjustments are made gradually over time in 5% increments.

The 150-year resulting land areas built for the MR vs. the AR at discrete flow percentages demonstrate a clear land-building capacity advantage in the AR. For common flow percentages, the AR builds 1.7 times more land at 30% of the total river flow and 3.0 times more land at 70%

of the total river flow. Reconnaissance-level cost impact analysis on river levees and navigational dredging to accommodate flow, stage, and sediment load alterations indicate that flow diversion of up to 60% of total river flow into the AR could result in a cost-effective flood alleviation and deltaic land-building strategy over the next 150 years.

CHAPTER 1: INTRODUCTION

1.1 Introduction

Humans have populated the world's river deltas since the beginning of civilization because of their rich resources and dynamic ecosystems. Today, river deltas of the earth are home to over 500 million people and coastal regions altogether are populated by approximately 1.2 billion people (Nichols and Small, 2002; Giosan, 2014). They provide a diverse range of ecosystem services such as fertile soil and water supply for agriculture, habitat and nursery for coastal fisheries, storm protection, recreation and tourism, air and water quality regulation, etc. (Syvitski et al., 2009; Chapman et al., 2016; REC and EE, 2016). At present, many of the world's deltaic plains are in peril due to natural and anthropogenic phenomena. Prior to the industrial age, human activities benefited delta growth processes and their ability to counteract natural degradation factors such as subsidence, sea-level rise, and wave erosion. Agricultural, mining, and logging practices introduced additional sediment influx into river systems and ultimately to deltaic destinations (Syvitski and Higgins, 2012). Human engineering to create reservoirs for drinking water and combat river flooding throughout major drainage basins is now a major influence on the growth and evolution of heavily populated delta regions (Syvitski and Saito, 2007; Giosan et al., 2014). Today, sediment supply is increasingly limited by levees, pumps, dams, and water control structures which have greatly modified sediment transport and storage patterns and pre-Anthropocene deltaic morphology.

Mississippi River Drainage Basin

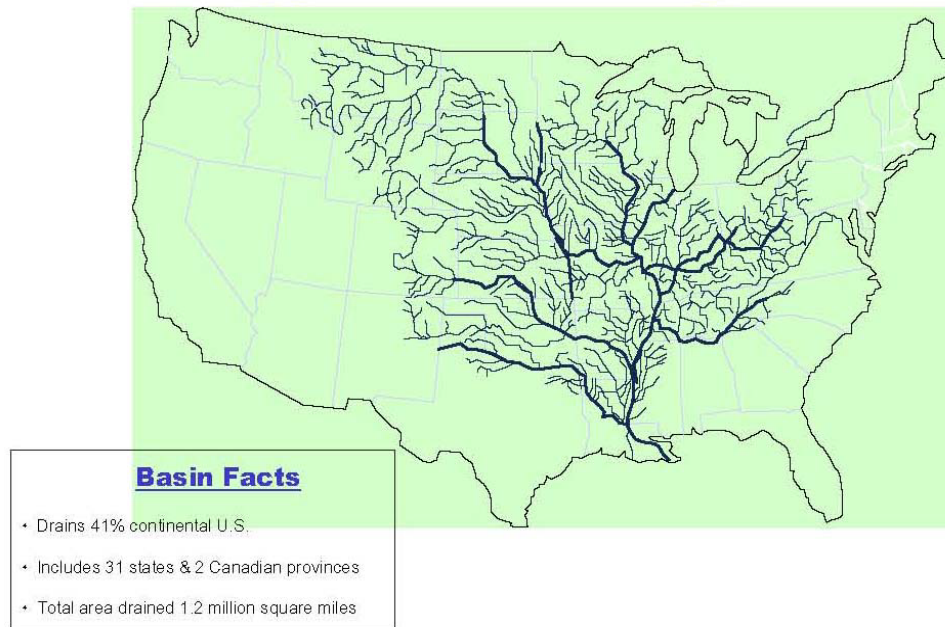


Figure 1.1. Mississippi River Drainage Basin (USACE, 2004).

One of the most acute examples of these human impacts is in the source to sink system of the Mississippi River (MR). Currently, the MR drainage basin shown in Figure 1.1 covers more than 3,225,000 km² and encompasses 41% of the contiguous United States and a portion of two Canadian provinces (USACE, 2004). This enormous drainage basin once delivered approximately 400 million tons of sediment to the Mississippi River deltaic plain (MRDP) annually, before it was modified by approximately 3500 km of levees, 86 dams, and spillways that divert and capture sediment (Meade and Moody, 2010; Kemp et. al. 2014). Prior to these modifications, the MR maintained approximately 40% of its total deltaic plain through active delta lobes at any one time, leaving the remaining coastline in retreat (Kolb and van Lopik, 1958; Roberts, 1997; Bentley et al., 2014). Currently the sediment supply has been cut in half to approximately 200 million tons per year carried to the delta plain, not all of which reaches major coastal outlets which generate land-building processes (Allison et al., 2012; Kemp et. al. 2014). Consequently, it is estimated that the river is maintaining less than 10-15% of the coast due to

drastically decreased sediment loads resulting from upriver dam construction, increased sediment storage within the river levee system, and sediment and nutrient bypassing into the Gulf of Mexico (GOM) (Barras et al., 2003; Day et al., 2007).

1.2 Sustainability Decline in the LMR

During transgressive phases of the Holocene MR delta cycle, progressive hydraulic inefficiency plus a reduction in gradient as a result of continued progradation, results in eventual stream capture upriver. As this occurs, subsidence-driven processes coupled with marine reworking overtake accretionary delta growth. This phase generally occurs faster for delta lobes located within the entrenched alluvial valley vs. those that have developed over a shallow Pleistocene base (e.g. St. Bernard delta) (Roberts, 1997). The PBD composition of very thick (~100 m) and compressible prodelta clays makes it prone to subsidence while its shelf edge proximity increases its susceptibility to marine degradation. While this process was artificially prolonged by the prevention of stream capture into the AR, decreases in hydraulic efficiency have continued.

Recent research and observations indicate that hydraulics in the LMR have changed significantly and that the combined effects of sea-level rise, subsidence, and channel infilling have reduced the ability of the MR to transport sand through the PBD (Kemp et. al., 2014; Bentley et al., 2016). This has resulted in an increased backwater effect during high river stages and a migration of flow through outlets upstream of head of passes. Dredging records over the last 30 years also show increasing depositional rates in upstream reaches combined with diminishing volumes and sand content in Southwest Pass. Additionally, four zones of adverse (negative downstream) bed slopes occur in the 500 km of the LMR below the MR-AR bifurcation. Two of these zones which occur in the PBD are caused by the onset of deltaic

shoaling and upstream migration of sand deposition. The steepest occurs along a 100 km stretch between New Orleans and Bohemia and could be due to drastic increases in subsidence rates over that stretch (Dokka et al., 2006) in addition to faults crossing the river in this vicinity (Gagliano et al., 2003). The fourth negative downstream slope occurs much farther upstream near the ORCS as a result of the water diverted to the AR (Harmar and Clifford, 2007; Kemp et al., 2014).

Monitoring surveys of river reaches just below the MR-AR diversion have shown gradual sedimentation, bar adjustment to flow diversion, and loss of cross-sectional area since the late 1800's which indicate natural underlying conditions conducive to avulsion (Latimer and Schweizer, 1951; Fisk, 1952; Kesel et al., 1992; Hudson and Kesel, 2006). Depositional trends just downstream of the ORCS have increased in recent years due to river engineering including diversion, revetment, and dike construction (Wang and Xu, 2016). More specifically, a massive mid-channel bar has developed next to the ORCS contributing to the negative slope in this stretch of the river because of the loss of flow and associated energy to transport sand. This bar also situated in a meander where the thalweg stops abruptly and abnormally near the hydropower intake which delivers 80% of the diversion discharge. This gives some indication that the helical flow that normally occurs in a meander and contributes to sand transport is disrupted (Heath et al., 2015; Knox and Latrubesse, 2016). Lastly, multibeam surveys after the 2011 flood indicate extreme scour just downstream from the ORCS further contributing to the precarious situation surrounding the long-term stability of the ORCS and the downstream LMR (Knox and Latrubesse, 2016).

In recent studies, researchers also have raised concerns over rising stage levels induced by increased sedimentation within the MR system. Between OR and the PBD, the sediment storage

rate within the channel and floodplain was measured at 103 Mt/yr between 2008 and 2010 by Allison et al., 2012. While some portion of this volume is deposited in the unleveed floodplain above Baton Rouge, the majority contributes to bed aggradation in the river channel (Smith and Bentley, 2014; Bentley et al., 2016). Stage measurements by the USACE (2014) at St. Francisville (~66km downstream of the ORCS) between 1951 and 2010 showed rises of 1.5 m and 4 m for flows of 8,400 m³/s and 28,000 m³/s, respectively. Comparison of 1973 vs. 2011 flood records (the only two years in which the Morganza Spillway was opened) from the USGS Vicksburg (RK 700) dataset show that between January and April during those floods prior to Morganza Spillway opening, the 1973 flood had a 46% higher average discharge and a 36% higher maximum discharge. Even so, the flood of 2011 produced approximately a 2 m higher peak stage (Kolker et al., 2014). Stage-discharge curves produced by Kemp et al. in 2014 at Tarbert Landing (RK 510) and Baton Rouge (RK 367) showed that stage was consistently 0.6 m and 0.4 m higher in 2011 than in 1973 at Tarbert Landing and Baton Rouge, respectively, with peak stage differences greater than 1m. In a similar analysis at Tarbert Landing, in 2016 Wang and Xu compared stage-discharge rating curves from 1988, 1999, and 2015. Stage increases over the 27-year period ranged from 1.3 m at lower flows to 1.5 m at higher flows. When these trends are projected forward using geomorphological and riverine modeling tools such as the Delft 3D model used in this study, results reveal that sedimentation will continue to be problematic within the MR branch where stages could increase by up to 3 m in the lower reaches at average annual peak flows, potentially placing the river levee system at New Orleans and below in jeopardy in the next 75 years. Additionally, rising stages from OR to the GOM diminish the sustainability of the LMR and ORCS as currently operated and maintained (Andrus, 2020).

To combat rising river stages during flood conditions in the LMR, the USACE incorporated two major floodways into the MR&T system downstream of the ORCS. The present project design flood was developed in 1956 when the Mississippi River Commission (MRC) assisted by the National Weather Service made a complete review of the adequacy of the MR&T project (USACE, 2015). As the river approaches the design flood flow conditions, decisions are made by the MRC with recommendations from the USACE New Orleans District (NOD) to open and operate the Morganza and Bonnet Carré structures in order to protect levees and riverside communities. The Morganza has only been opened and operated twice during the historic 1973 and 2011 floods, while the Bonnet Carré Spillway has been opened fourteen times since its construction in the 1930's (USACE, 2014, 2019). Six of these openings have occurred since 2008, with it being opened twice in one year for the first time in 2019. 2019's second opening

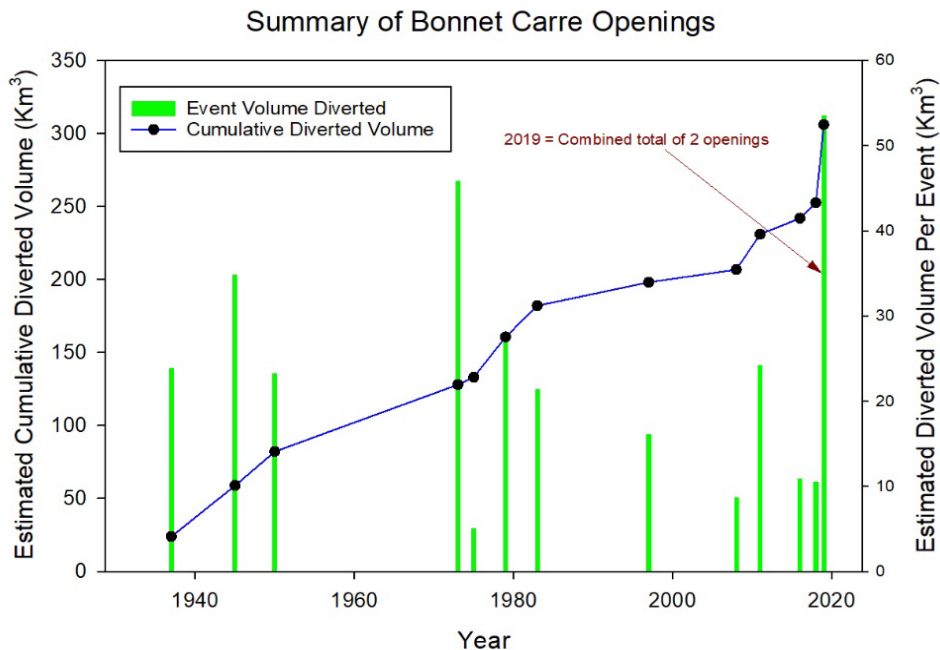


Figure 1.2. Historic of Bonnet Carré Spillway Openings (Estimated using data from USACE, 2014, 2019).

was also for a record 79 days bringing the total days opened in 2019 to 122. Figure 1.2 shows the estimated volume of water diverted for each opening as well as the cumulative volume

diverted over the life of the spillway (~35% of the total volume has been diverted in the last 11 years). While these recent increases in frequency and duration are largely driven by weather patterns within the MR drainage basin, they are also indicative of the increased sedimentation rates and rising stage-discharge relationships.

1.3 Transition of the Holocene Delta Cycle into the Anthropocene: Correlation of Regressive and Transgressive Phases in MRDP

Over the past 7,500 years during the Holocene glacial high stand, the MR avulsed five times (Fisk, 1952; Coleman et al., 1998; Aslan et al., 2005) producing six delta complexes (Frazier, 1967; LCWCRTF and WCRA, 1998; Kulp et al., 2005; Blum and Roberts, 2009, 2012). While the age, duration, and spatial extent of these delta lobes are debated (Condrey et al., 2014), on average, the MR has historically switched courses within the MRDP every 1000 – 1500 years (Coleman 1988; Aslan et al., 2005). Roberts (1997) schematically summarized the “delta cycle” as an orderly progression of delta-building events that results from cyclic deposition on different temporal and spatial scales. Components of the dynamic and progressive stages of the delta cycle include stream capture and establishment of a well-defined channel network as part of the rapid regressive phase, while the slower transgressive phase includes stream abandonment, subsidence, and marine reworking to form beaches, spits, barrier islands, and finally submarine shoals.

While the MR delta cycle has continued up to the present day, it has been largely influenced by human activities and intense river engineering in the last two centuries which mark the advent of the Anthropocene (Zalasiewicz et al. 2011). Recent research on global deltas has shown anthropogenic activities such as agriculture, mining, reservoir construction, transportation infrastructure, oil and gas extraction, water diversions, flood control, and navigational channels now heavily impact and many times dominate sediment dispersal and depositional patterns at

today's river mouth locations (Syvitski et al., 2005; Fan et al., 2006; Syvitski and Saito, 2007; Bergillos et al., 2016; Yang et al., 2017). Many of these factors are at play in the MRDP's currently active and interconnected regressive (AWL) and transgressive (PBD) lobes.

Deposition on the currently active PBD complex began ~1.2 to 1.3ka when the MR avulsed near New Orleans (Fisk, 1952; Tornqvist et al., 1996; Coleman et al., 1998; Aslan et al., 2005) and has created a shelf-edge fluvially-dominated delta overlaying prodelta deposits of >100 m thick (Coleman and Roberts, 1988; Kulp et al., 2002). Progradation began to decline in the 1930's and 40's but continued up until the late 1970's and now the PBD is considered to be in a state of retrogradation (Maloney et al., 2018). Contributing factors include declining sediment loads due to upstream dam construction (Keown et al., 1986; Kesel, 1988; Meade and Moody 2010; Blum and Roberts, 2012), increasing diversion of sediment and water into the AR distributary (Latimer and Schweizer, 1951; Fisk 1952), reduction in overbank flows due to levee construction (Kessel, 1988), hydrocarbon extraction (Morten et al., 2005), significant upstream floodplain and channel storage of sediment (Allison et al., 2012; Smith and Bentley, 2014), loss of stream power and upstream migration of flows and sediment depocenters (Kemp et al., 2014; Bentley et al., 2016), and natural transgressive processes such as subsidence, sea-level rise, and marine reworking (Muto and Steel, 1992; Roberts, 1997; Dokka et al., 2006; Tornqvist et al., 2008; Blum and Roberts, 2012; Jankowski et al., 2017).

Land loss coastwide in the MRDP between 1932-2010 was estimated to be 4877km² with approximately 25% of the deltaic area in the PBD gone (Couvillion et al., 2011). Estimated coastwide land loss rates to subaerial wetlands have ranged from 50 – 100 km²/yr (Gagliano et al., 1981; Van Beek and Meyer-Arendt, 1982; Morton et al., 2005; Couvillion et al., 2011), with the majority of the losses both coastwide and in the PBD occurring between the 1930's and

1970's. Delta front progradation in the subaqueous portions of the PBD began to decline over this time period as well and has now been retreating since 1979 at South Pass and Pass a Loutre > 20m/yr, while Southwest Pass likely is only slightly prograding due to the location of the navigational dredging disposal site located near the mouth of the pass. Lastly, estimated sediment mass accumulation rates along the delta front have decreased since the late 1800's by ~73% (Maloney et al., 2018).

Delta complexes are built through depositional responses associated with overbank splaying and bay-filling within the footprint of a major lobe (Welder, 1959). Coleman and Gagliano (1965) investigated the concept of cyclic MR deposition on a variety of scales and emphasized that major delta lobes are active for approximately 1000-1500 years, whereas subdeltas complete their cycles of growth and deterioration in about 100-150 years. Even smaller "crevasse splays" and "bay-filling" episodes build and become abandoned within the time-scale of a few decades (Roberts and Coleman, 1996). Each subdelta within a major delta complex roughly follows a "bell-shaped" (this is roughly demonstrated by the data presented in Figure 4) curve over its active lifecycle where coarsening-upward sedimentary facies develop and are capped by highly organic, fine-grained sediments as depositional activity wanes. Currently, the last remaining active subdeltas in the PBD are in a state of decline associated with their destructional phases (Coleman and Gagliano, 1964; Wells and Coleman, 1987). Extents of these historic subdeltas are depicted in Figure 1.3 and overlay the remnant wetlands that remain along with the skeletal distributaries outlined by natural levees and passes maintained for navigation (Bentley et al., 2016).

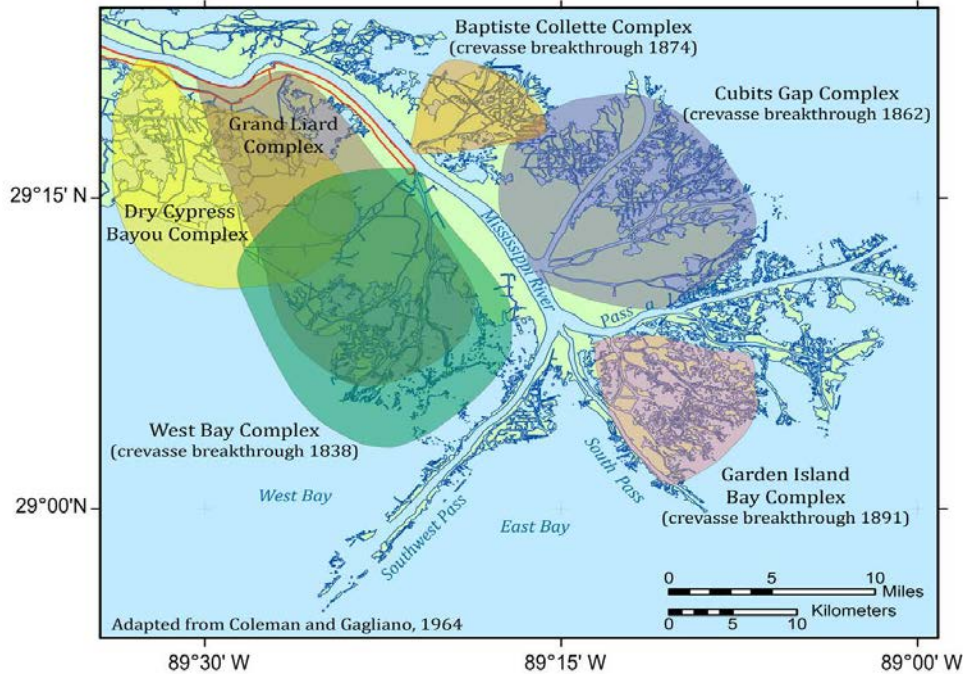


Figure 1.3. Historic (Dry Cypress Bayou and Grand Liard – Active prior to the 1800s) and Last Remaining Active (Baptiste Collette, Cubits Gap, West Bay, Garden Island Bay) Subdelta Complexes of the Plaquemines-Balize Delta (After Coleman and Gagliano, 1964 and From Bentley et al., 2016).

Extensive mapping analysis was performed by Wells and Coleman (1987) who used historic nautical maps, charts and aerial photographs to digitize subaerial wetland areas in the four latest PBD subdeltas from 1840-1980. This data set was then extended to 2002 using satellite imagery (Coleman, 2006). This combined growth curve data set is presented in Figure 4 alongside a similar analysis from the AWL by Majersky et al. (1997) which plots the rapid embryonic growth of its two bayhead deltas, namely Wax Lake Delta (WLD) and the Lower Atchafalaya Delta (LAD) between 1973-1994 coinciding with a sharp decline in the PBD delta area. This transition follows closely after rapid acceleration of stream capture of flow and sediment through the MR-AR bifurcation which occurred in the previous two decades leading up to the construction of the ORCS which suspended flow into the AR at 30% in 1962 (Latimer and Schweizer, 1951, Fisk, 1952). Another significant contributing factor to the decline in sediment delivery to the PBD was large dam construction in the upper MR Basin, primarily on the

Missouri River (Kesel, 1988; Meade and Moody, 2010; Blum and Roberts, 2014; Bentley et al., 2016). Figure 1.4 demarks these sediment load altering events along with the great flood of 1973 which stimulated wetland growth in both the PBD and AWL deltas, although the PBD returned to previous rates of decline shortly thereafter.

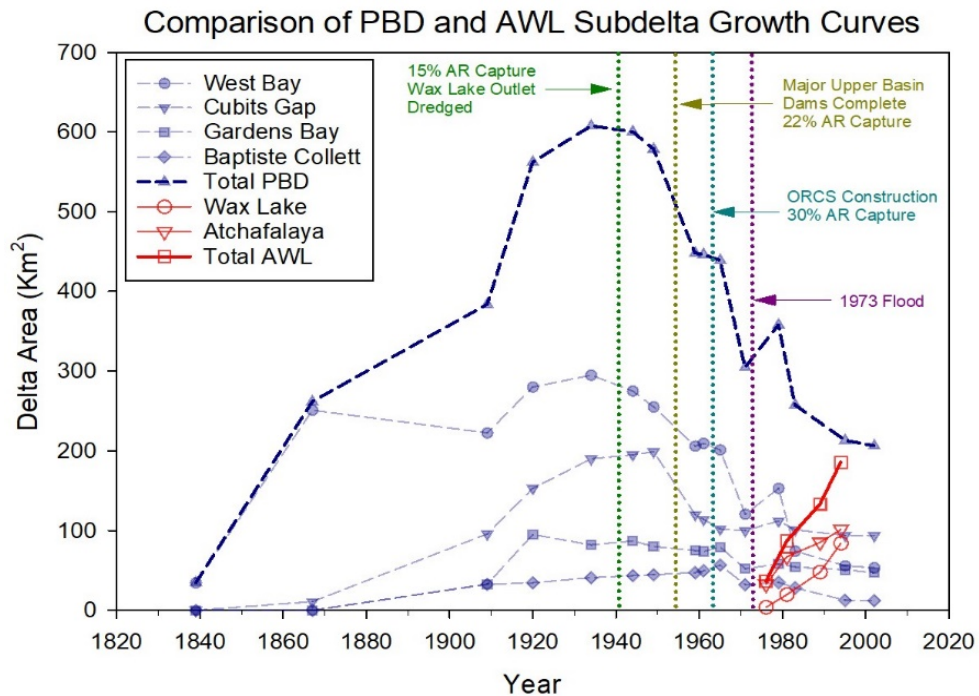


Figure 1.4. Documented Subdelta Growth Rates from the PBD and AWL Delta Complexes with Major Anthropogenic System Alterations (PBD data from Wells and Coleman, 1987 and Coleman, 2006; AWL data from Majerski et al., 1997; AR Capture Percentages from Latimer and Schweizer, 1951).

Wells and Coleman (1987) reported a long-term average growth rate of the composite PBD subdelta curve during the regressive period of approximately 1840-1940 to be 5.2 km²/y with a maximum rate of 7.0 km²/y occurring in the West Bay subdelta between 1845-1875. Average rates of deterioration between 1920-1971 ranged from 1.0 to 4.1 km²/y with a maximum of 12.9 km²/y in the Baptiste Collette subdelta in the late 1940's. In the AWL plots, Majersky et al. (1997) used a digital terrain model to estimate delta area above -0.6 m NGVD which includes both subaerial lands and subaqueous flats, for an average growth rate of 8.8 km²/y (4.0 km²/y for

WLD and 4.5 km²/y for LAD, respectively) over the 21-year study period. An early study by Rouse et al. (1978) reported a growth rate of 6.5 km²/y between 1973-1976 post high flood years. Roberts et al. (1997) estimated a combined growth rate of 7.3 km²/y (2.5 km²/y for WLD and 4.5 km²/y for LAD, respectively). Using a similar terrain model as Majersky et al. (1997), Fitzgerald (1998) estimated a WLD growth rate of 3.0 km²/y and Kim et al., 2009 estimated a land area in the WLD subdelta of 100 km² in 2005 equating to a growth rate of 3.1 km²/yr. Allen et al. (2012) used remote sensing imagery and inundation measures to estimate a much lower growth rate of 1.0 km²/y for the WLD between 1983 and 2011. Similarly, Couvillion et al. (2011) estimated a combined growth rate of ~2 km²/y for the AWL between 1973 and 2011. Rosen and Xu (2013) estimated an annual land growth rate for the AWL of 2.8 km²/y between 1989 and 2010. Lastly, Carle et al. (2015) estimated 6.5 km² of land gain at mean water level in the WLD in just one year as a result of the major flood of 2011.

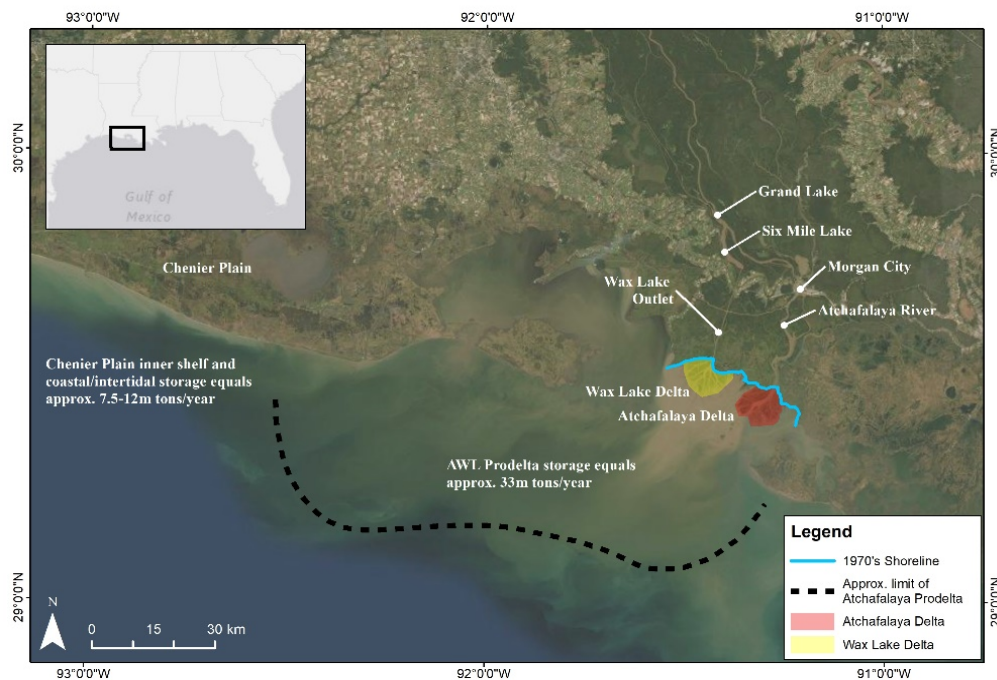


Figure 1.5. Atchafalaya/Wax Lake Deltaic System Vicinity Map (Sediment storage rates from Bentley et al., 2016).

The AWL system subaerial deltas, approximate prodelta boundary, and sediment storage rates are shown in Figure 1.5. Up until the 1950's most of the sediment deposition along the AR branch occurred in the Atchafalaya Basin filling interior lakes and forming lacustrine deltas in Grand Lake and Six Mile Lake. The dredging of Wax Lake Outlet (WLO) in 1941 as an additional flood relief measure to Morgan City, providing additional sediment transport capacity to Atchafalaya Bay as Six Mile Lake filled to capacity. At this time many oyster reefs existed in Atchafalaya Bay with some fine-grained riverine deposits (Thompson, 1951, 1955). Researchers then began to document distinct phases of subaqueous deltaic development: (1) deposition of prodelta clays and silty clays from the middle of the 19th century to about 1952, (2) the initiation of coarser-grained deposition about 1952 (mostly silts), and (3) introduction of bedload sands in the early 1970s (Cratsley, 1975; Shlemon, 1975).

Development of this subaqueous delta served as a subaerial land-building primer to the next extreme high-water event. This event occurred in 1973 with two subsequent high-water years which produced a three-year period of greatly increased sediment flux. The average annual discharge down the AR measured at Simmesport was 5,781 m³/s between 1935 and 2001. During the high flood years of 1973-1975 annual mean discharges reached 9,945 m³/s with peak discharge in 1973 of about 20,000 m³/s. Accordingly, average sediment discharge was approximately 75.2 Mt/y with a peak of 143.2 Mt/y (USACE, 2002). This resulted in sudden appearance and rapid growth of sand-rich lobes directly linked to the transfer of stored channel sands to the bay (Roberts et. al., 2003).

Further research has shown that a silt-rich prodelta has been forming on the Atchafalaya shelf opposite of Atchafalaya Bay for the last century. In some areas this prodelta has been accumulating at rates greater than 10 cm/yr and prograding seaward as a result of sediment

bypassing the subaerial deltas and contributing to foundational sediment facies (Allison and Neill, 2002). A significant portion of the prodelta composition is sand, possibly as result of bedload transport through the dredged navigation channel. Additionally, significant redistribution and advection of fine-grained sediments is occurring to the west, further distributing prodelta deposits which can eventually be trapped in down-drift settings such as the Chenier Plain shelf or intertidal zone (Bentley et al., 2003; Ramatchandirane, 2013; Bentley et al., 2016). And while these two deltas do experience sediment bypassing, there is more potential the bypassed fluxes to contribute to prodelta building blocks on the shallow Atchafalaya Shelf (Allison and Neil, 2002) or to be trapped in coastal ponds in down-drift settings such as the chenier plain (Ramatchandirane, 2013). Additionally, the sediment-laden river plumes dispersing into the shelf from the AWL are fine-grained in nature and form a fluid mud layer due to water level set-down during cold front passages, which effectively dampens the wave energy and reduces erosion of deltaic deposits and associated wetland growth (Wells, 1983; Sheremet and Stone, 2003; Siadatmousavi et al., 2012; Safak et al., 2017). These combined riverine, coastal, and anthropogenic processes have also resulted in an interbedded wedge deposit of very shallow slope ($0.03 - 0.05^\circ$), making it less susceptible to mass movements or slides than its shelf-edge PBD counterpart (Coleman and Garrison, 1977; Allison and Neill, 2002, Guidroz, 2009; Maloney et al., 2018).

Groundwork for Land-building in the AWL lobe was laid by basin infilling processes and jump-started by the 1973 flood. The prodelta front has since steadily progressed in development and recently experienced another major flooding event in 2011 comparable in magnitude to the 1927 and 1973 floods. The peak flow rate reached in the AR was approximately $23,000 \text{ m}^3/\text{s}$, slightly higher than that of the 1973 flood event (Kolker et. al. 2014). Kolker et. al. (2014) led a

field study in which sediment cores were collected and analyzed for the naturally occurring radionuclide ^7Be . ^7Be has a short half-life (53 days) and is an excellent indicator of event scale sediment dynamics (Sommerfield et al., 1999; Allison et al., 2000; Bentley et al. 2003; Andrus, 2007; Kolker et al. 2012;). The total depth of ^7Be penetration in sediment cores taken from the Atchafalaya shelf ranged from 2 to 11 cm. When converted and annualized, depositional rates ranged from 6 to 17 cm/yr. Similar cores were collected in the WLD and indicate that depth of deposition ranged from 0 to 5 cm during the flood, with the lowest values found near the head of the delta and the highest values near the delta front. Similar measurements from a 1999 study on the Atchafalaya shelf during a $\sim 10,200 \text{ m}^3/\text{s}$ flood showed deposition of 1 to 3 cm (Allison et al. 2000). These results suggest that while the Mississippi-Atchafalaya River system is supply limited, the 2011 flood shifted the AWL depocenter to the shelf and produced an order of magnitude greater deposit layer (Kolker et al. 2014). This is an important result as much of this event layer will be preserved and will likely contribute the progradation of the delta front in the absence of a hurricane. While some resuspension is expected as cold fronts pass over the region, the layer is much thicker than the depth at which sediments will be resuspended on the Atchafalaya Shelf (about 1 cm; Allison et al., 2000).

The aforementioned study also drew important contrasts between the AWL and PBD systems and their sustainability. Results of salinity and turbidity measurements during 2011 revealed that the Atchafalaya Shelf was more river-dominated than the Mississippi Shelf as low salinity waters were observed over a much greater area. Along the Mississippi Shelf, low salinity waters were confined to jet-like features consistent with previous studies (Wright and Coleman, 1974; Wright, 1977; Falcini et al., 2012). Maximum turbidity on the Atchafalaya Shelf was also significantly higher and stratified differently with fluid mud-like conditions at the bottom of the

water column. Hence, the AR likely had greater influence on the distribution of water, salt, and sediment on its continental shelf than the Mississippi River (Kolker et al., 2014). This can be attributed to a number of factors such as the shallow and open nature of the Atchafalaya Shelf, as well as its axis of discharge which is normal to the shelf, which encourages onshore winds to constrain currents close to the coast (Walker and Hammack, 2000; Kolker et al., 2014); the design of the MR&T system which diverts flood waters to the Atchafalaya and away from the Mississippi to protect infrastructure and population centers; the constricted configuration of the LMR which forces river water into the GOM through a confined levee system and then through a series of small passages, diversion, and distributaries; and the close proximity of the PBD to the open ocean which promotes both the advection and diffusion of river waters across the continental shelf and associated pelagic regions (McKee et al., 2004; Walker et al., 2005).

1.4 Sediment Diversion Review and Considerations

Since the early 1800s, the engineers, private landowners and Federal agencies have debated the efficacy of levees vs. controlled diversions as the best management strategy for engineering the MR to maintain navigation and flood control (Barry, 1997; Reuss, 2004). These debates culminated in the MR&T program which has been successful at protecting against devastating floods and bolstering commerce, but at the same time the levees built under the plan have cut off vital sediment and freshwater supplies vital to coastal wetlands in the MRDP. Engineered diversions such as the ORCS, Morganza Spillway, Bonnet Carré Spillway and the WLO have been incorporated into this flood control plan to provide outlets which relieve pressure from the levee system mostly during flood stages. While not their primary purpose, these diversions have delivered sediments which have contributed to significant land building and wetland creation. Today, current ecosystem restoration plans aim to maximize wetland building through diversions

to mimic natural deltaic land-building processes by restoring the delivery of freshwater, sediment and nutrients (Roberts et al., 2003; Snedden et al., 2007; Kim et al., 2009; CPRA, 2012, 2017). These proposed diversions are anthropogenic countermeasures to coastal land loss and ecosystem deterioration largely caused by other anthropogenic activities. Construction of subdeltas like those discussed in Section 1.2 are similar in scale to proposed river-sediment diversions, thereby serving as a geologic analog (Peyronnin et al., 2017; CPRA, 2017). While some diversions like West Bay are uncontrolled, most use engineered structures that can be operated to optimize a variety of physical and ecological factors such as discharge, sediment intake, velocity, stage as well as impacts to fisheries in the receiving basin and navigation in the river (Allison and Meselhe, 2010; De Mutsert et al., 2012; Peyronnin et al., 2017). Table 1.1 lists MR diversions which have been constructed in addition to those which are currently being planned for. The locations of these diversions are also shown in Figure 1.6.

Even though it has been established that the LMR has entered a transgressive phase of retreat and yielding to energetic oceanic processes in open bay areas at its outermost GOM boundary, these diversions have had some success. Sand deposition in the Bonnet Carré Spillway near Lake Pontchartrain has accreted between 2 and 3 cm/yr as a result of periodic openings to reduce flood stages in the river (Day et al., 2012; Nittrouer et al., 2012; Allison et al., 2013). The purpose of the Caernarvon freshwater diversion is to control salinity in Breton Sound but has incidentally created a sizeable subdelta in Big Mar (Lopez et al., 2014). Similarly, the Davis Pond diversion has created a significant subdelta deposit and vegetated wetlands (Day et al., 2016; Keogh et al., 2019). Since 1995 the Bohemia Spillway has experienced no net land loss with slight gains from navigation and oil gas canal filling as a result of pulsed MR flows (LPBF, 2019). The West Bay Diversion is the only diversion designed and constructed to date with the sole purpose of

building and sustaining wetlands by naturally mimicking crevasse splay processes in an uncontrolled manner. Since its opening in 2003, diversion flows have formed a distributary channel for efficient sediment delivery and sediment accumulation has outpaced relative sea level rise (RSLR) with depositional rates between 1 and 3 cm/yr between 2003 and 2009 (Andrus and Bentley, 2007; Kolker, 2012). Just after the flood of 2011, estimates of subaerial deltaic deposits were over 4 km² and total aggrading deltaic regions including subaqueous deposits were approximately 23 km² covering nearly 60% of the West Bay receiving area (Andrus et. al., 2012). It has also been shown through numerical modeling that Sediment Retention Enhancement Devices (SREDS) constructed as part of the project have contributed retention of these deposits by reducing wave resuspension (Andrus et al., 2012; Allison et al., 2017).

With a greater academic focus on understanding deltaic systems in recent years, the scientific community has developed various broad predictive relationships and forecasting models which project delta plain growth associated with sediment diversions (Parker et al., 1998, 2006, 2008; Kostic and Parker, 2003; Syvitski and Saito, 2007; Paola et al., 2011; Dean et al., 2012). Many numerical modeling efforts (Storms, Stive et al., 2007; Geleynse, Storms et al., 2010; Edmonds and Slingerland, 2007; Edmonds and Slingerland, 2010; Geldynse, Storms et al., 2011; Hillen, 2009; Caldwell and Edmonds, 2014) evaluate idealized delta-building scenarios at relevant scales of interest to examine the relationships between delta processes and dominant forcing functions with the resulting morphology, stratigraphy, and distributary network formation. Others have developed numerical models for specific riverine and estuarine systems, particularly in the MRDP, to evaluate many hydrodynamic and biophysical variables associated with riverine sediment diversions and their deltaic responses (Kim et al., 2009; Hanegan, 2011; Edmonds,

2012; Meselhe et. al., 2012; Gaweesh and Meselhe, 2016; Meselhe et. al., 2016; CPRA, 2017). These models are informed by relevant research on factors which influence diversion performance such as riverine sediment supply and bed geomorphology (Galler and Allison, 2008; Nittrouer et al., 2011; Allison et al., 2012; Nittrouer and Viparelli, 2014; Smith and Bentley, 2014; Bentley et al., 2016; Kemp et al., 2016; Magliolo, 2017; Bentley and Magliolo, 2018; Wang and Xu, 2018a, 2018b), river stage, discharge, and backwater effects (Nittrouer et al., 2011; Edmonds, 2012; Lamb et al., 2012; Kemp et al., 2014) and physical characteristics of potential bay receiving areas such as subsidence, sediment erodibility and retention, land loss rates, and morphodynamics, among others (~90 papers identified by Xu et al., 2019).

Table 1.1 Summary of Constructed and Proposed Mississippi River Diversions

<i>Diversion</i>	<i>River Mile (Above Head of Passes)</i>	<i>River KM (Above Head of Passes)</i>	<i>Description of Control Structure</i>	<i>Direction of Diversion</i>	<i>Purpose</i>	<i>Maximum Design Discharge (cfs)*</i>	<i>Maximum Design Discharge (cms)*</i>	<i>Date Completed</i>
1. Old River Control Structure Complex								
Low-Sill	315	506	Controlled Spillway	West	Maintain Distribution of Flow and Sediment	500,000	14,159	1962
Overbank	315	506	Controlled Spillway	West	Flood Control	150,000	4,248	1962
Auxiliary	312	502	Controlled Spillway	West	Maintain Distribution of Flow and Sediment	350,000	9,911	1986
Hydropower	317	509	Controlled Spillway	West	Power Generation	170,000	4,814	1990
2. Morganza	285	459	Controlled Spillway	West	Flood Control	600,000	16,990	1963
3. Bonnet Carré	133	214	Controlled Spillway	East	Flood Control	250,000	7,079	1932
4. Davis Pond	122	196	Controlled Box Culverts	West	Freshwater Diversion	10,050	285	2003
5. Caernarvon	85	137	Controlled Box Culverts	East	Freshwater Diversion	8,000	227	1991
6. Mid Barataria	61	98	Controlled Spillway	West	Sediment Diversion	75,000	2,124	In Planning
7. Mid Breton	69	110	Controlled Spillway	East	Freshwater Diversion	35,000	991	In Planning
8. Bohemia Spillway	45	72	Uncontrolled Spillway	East	Flood Control	350,000	9,911	1926
9. West Bay	5	7	Uncontrolled Channel	West	Sediment Diversion	50,000	1,416	2003

*While flow rates listed are maximum design capacity, actual flow rates are generally lower and are dictated by operational plans of each structure. Factors such as seasonal variations in river flow, high river flood alleviation, receiving basin interests such as property, agriculture, and fisheries all factor in to operational decision-making. The originally designed dredge section for West Bay was for 20,000 cfs/566 cms at a 50% river stage with plans to increase the section to 50,000 cfs/1,416 cms after monitoring. The uncontrolled nature of this opening has evolved to this point and beyond naturally (Andrus, 2007).

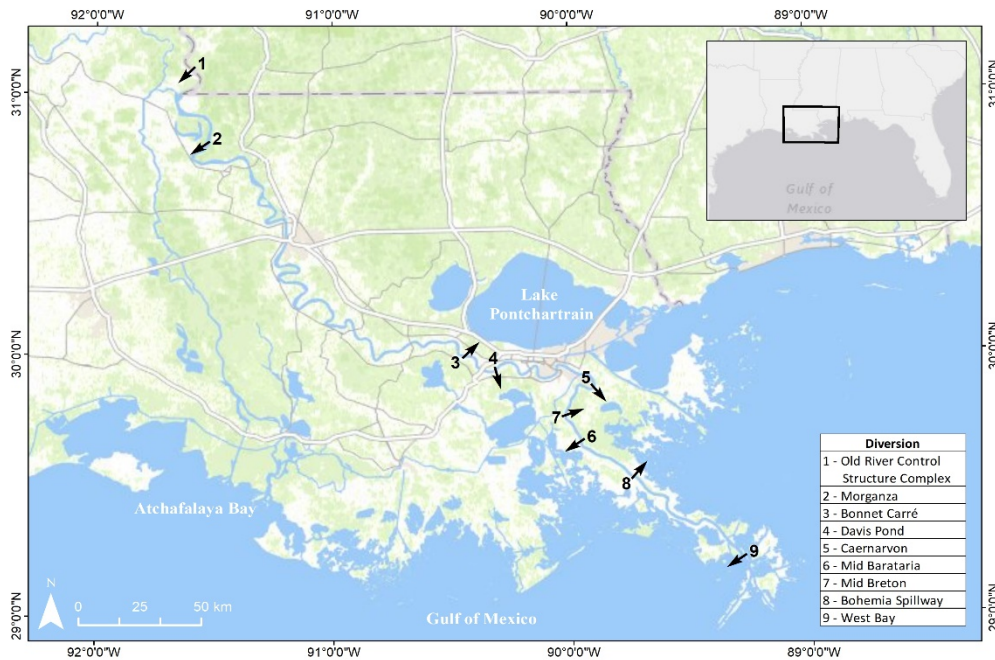


Figure 1.6. Locations of Existing and Planned Mississippi River

1.5 Dissertation Structure

Authorized by the MRC in the early 1950's, two landmark studies of the Atchafalaya Basin and the problem of the MR diversion were undertaken to investigate engineering and geological aspects of whether the enlargement of OR and AR would ultimately capture the MR's discharge. These efforts predicted that the future of the diversion at the Mississippi-Atchafalaya junction would reach a critical stage of capture of 40% by the 1970's and beyond this point would be rapid and uncontrollable. Because the core work to warrant the construction of the ORCS was undertaken nearly 70 years ago, Chapter 2 revisits the basis of the resulting predictions, discusses significant developments that have occurred in the MR and AR to date, and evaluates how both branches could evolve moving forward. Since the 1950s many useful datasets and tools have been compiled and developed which were used to conduct hydraulic and sediment transport modelling simulations. Chapter 2 uses the Delft3D software suite to retest the capture hypothesis by accounting for complex hydrodynamic interactions from the MR-AR bifurcation

to the Gulf of Mexico with the intent of investigating long-term avulsion dynamics and their responses to an oscillating flow regime which mimics annual hydrograph variations.

Recognizing that coastal planners, scientists and engineers consider engineered river diversion as a viable restoration tool in the next century, operations of current and future diversions and land-building potential in the MR and AR branches could depend heavily on flow and sediment management strategies at the MR-AR bifurcation. Chapter 3 uses both 1D and 2D numerical modeling techniques to evaluate the long-term effects of current water and sediment regulation mandates and test alternative regulation strategies with respect to delta-building goals. Riverine hydraulic and sediment transport modelling was performed using the Delft 3D tested in Chapter 2 coupled with a spreadsheet which used a 1D spatially averaged equation developed by Dean et. al. (2012) to calculate delta growth. A 150-year model duration was used to account for flow and system adjustments, implementation of current restoration plans, and to sufficiently analyze delta response trends into the future. The study tests twelve MR/AR flow scenarios (1 No Change scenario, 8 increased AR flow scenarios, and 3 increased MR flow scenarios) where flow adjustments are made gradually over time in 5% increments.

Environmental benefits predicted by models in Chapter 2 are reported in terms of deltaic land area. The cost effectiveness of producing these benefits is evaluated in Chapter 3. Cost analyses focus on river management costs as economic indicators that are directly related to river discharge, stage, and sedimentation rates. Alterations in flow and sediment at the MR-AR bifurcation cause long-term changes in stage heights which require levee enlargements to maintain flood protection and changes in depositional rates which alter dredging requirement needed to maintain navigational channels. Modeled changes in these parameters are used to calculate levee enlargement and dredging quantities and historic prices were gathered to project

river management cost into the future for each of the twelve MR/AR flow scenarios. These costs are then compared against land-building projections to determine the most cost-effective MR/AR operational scenario. Conclusions discuss additional river maintenance categories that could impact river management schemes, effect land-building efficiencies, and provide more comprehensive costs implications.

CHAPTER 2: THE CAPTURE TIMESCALE OF AN UNCONTROLLED MISSISSIPPI – ATCHAFALAYA BIFURCATION WITH FUTURE LOWER RIVER STRATEGY IMPLICATIONS

2.1 Introduction and Purpose

Since the 1930s in coastal Louisiana many factors, both natural and manmade, have contributed to the loss of approximately 4,870 km² of land. Analyses predict that this number could double in the next 50 years with no action. With such an expansive continental footprint and influence over the history and future of the Louisiana coastline, the Mississippi River (MR) system is the greatest potential source of solutions to the land loss problem because of the sediment it carries (CPRA, 2012, 2017). Formation and maintenance of the MR deltaic plain is the direct result of water, sediment, and nutrient delivery from its drainage basin which is many orders of magnitude larger (Giosan and Freeman, 2014). The present sea-level high stand has given rise to delta-building processes of the MR that are cyclic in nature and involve a wide array of depositional environments. Through alternating regressive (fluvial/depositional) and transgressive (marine/erosional) phases, the MR has occupied at least six major courses in the deltaic plain during the Holocene geologic period as depicted in Figure 1 (Roberts, 1997; Blum and Roberts, 2012). Throughout this period the river has delivered sediment to the coast to build land at its mouth, annually extending the length of the river channel until a major flood or other disturbance causes the river to avulse, or change course, seeking a shorter, more efficient path to the Gulf of Mexico (GOM). Historically these processes have maintained approximately 40% of the total MR deltaic plain through active delta lobes at any one time, leaving the remaining coastline in retreat (Kolb and van Lopik, 1958; Roberts, 1997; Bentley et al., 2014). Currently, it is estimated that the river is maintaining less than 10-15% of the coast due to drastically decreased sediment loads resulting from upriver dam construction, increased sediment storage within the river levee system, and sediment and nutrient bypassing into the GOM (Barras et al.,

2003; Day et al., 2007). Hence, restoration planning should make every effort to maximize delta areas maintained by the river which begins with understanding its most recent avulsion.

The most recent and currently active delta lobe is the Atchafalaya-Wax Lake lobe, which was initiated approximately 400 years ago and is the result of ongoing MR stream capture by the Atchafalaya River (AR) (Fisk, 1944, 1952; Gagliano and Van Beek, 1975; Tye and Coleman 1989a, b; Roberts, 1997, 1998; Coleman et al., 1998; Aslan et al., 2005). This capture process accelerated in the early to mid-1900s but further progress was prevented by construction and operation of the Old River Control Structure (ORCS) Complex. The complex originally became operational in 1963 with the low sill and overbank structures, was modified in 1986 with the auxiliary structure, and was completed in 1990 with the hydroelectric station as shown in Figure 2.1. Although this structure complex has limited flow from the Mississippi to the Atchafalaya to 30% of the total combined flow of the Mississippi and Red Rivers (RR) at the latitude of Old River (OR), the deltaic process has continued to advance in the Atchafalaya Basin, Wax Lake and Lower AR Outlets, and in the Wax Lake and Atchafalaya Deltas.

Authorized by the Mississippi River Commission (MRC) in the early 1950's, two landmark studies of the Atchafalaya Basin and the problem of the MR diversion were undertaken to investigate engineering (Latimer and Schweizer, 1951) and geological (Fisk, 1952) aspects of whether the enlargement of Old and Atchafalaya Rivers would enlarge their cross-sectional areas and capture the Mississippi River's discharge. As part of these efforts it was predicted that the future of the diversion at the Mississippi-Atchafalaya junction would reach a critical stage of capture of 40% in 20 years. In fact, it was predicted that by the 1970's further capture beyond this point would be rapid and uncontrollable. Impelled by this recommendation, Congress

authorized the U.S. Army Corps of Engineers (USACE) to construct the ORCS which suspended this capture process.

Because the core work to warrant the construction of the ORCS was undertaken nearly 70 years ago, the purpose of this study is to revisit the basis of the resulting predictions, discuss significant developments that have occurred in the MR and AR to date, and evaluate how both branches could evolve moving forward. For instance, since the 1950s many useful datasets and tools have been compiled and developed which can be used to conduct hydraulic and sediment transport modelling simulations. This study uses the Delft3D software suite to retest the capture hypothesis by accounting for complex hydrodynamic interactions from the MR/AR bifurcation to the Gulf of Mexico. We also evaluate the effectiveness of the model to predict future flow, stage, and sediment transport trends in the MR and AR branches under currently implemented management controls. Results could have larger implications in long-term water and sediment

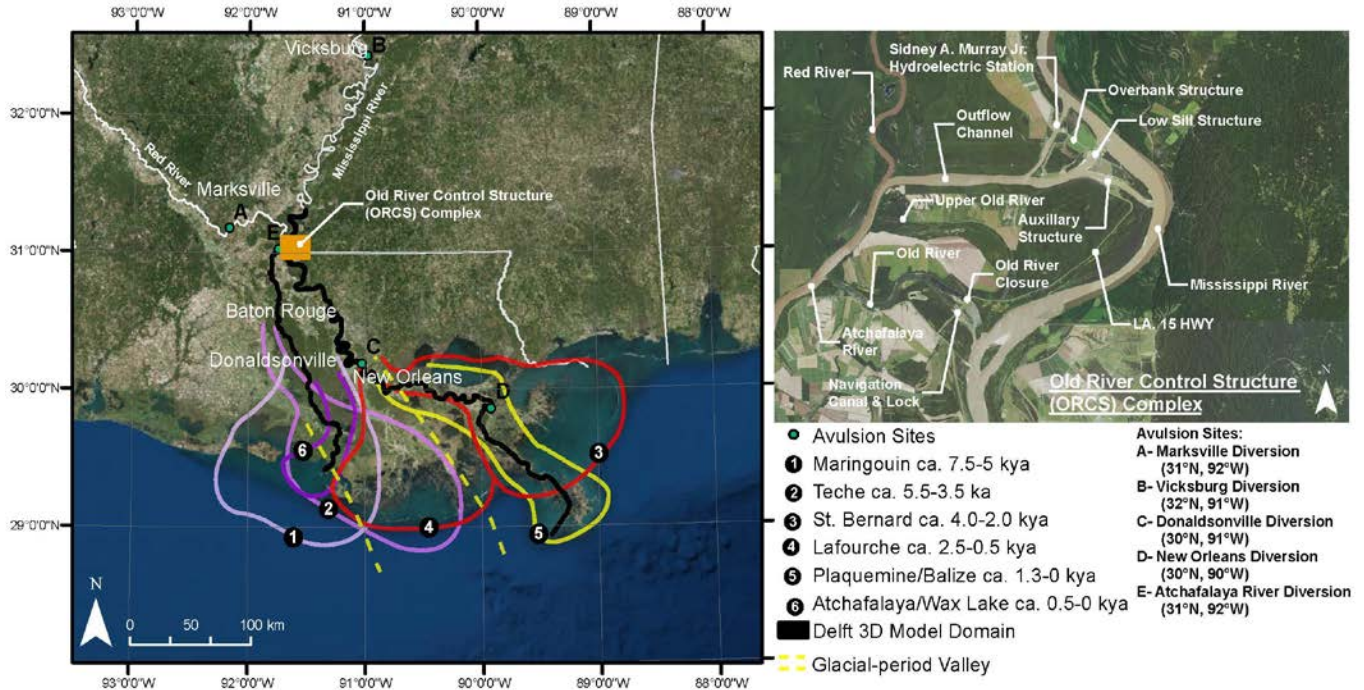


Figure 2.1. Study area depicting Holocene deltas of the Mississippi River (Blum and Roberts, 2012; from Roberts, 1997), Historic avulsion Mississippi River avulsion sites (from Fisk, 1952 and Aslan et al., 2005), Components of the Old River Control Structure Complex managed by the U.S. Army Corps of Engineers, and the Delft3D Model Domain used in this study (from Edmonds, 2012)

management strategies to protect infrastructure, maintain navigation, and combat land loss in the Lower Mississippi River (LMR) deltaic plain.

2.2 Overview of Holocene River Avulsions of the Mississippi River

An avulsion is the abandonment of a part or whole of a channel belt by a stream in favor of a new course (Allen, 1965). There are many naturally occurring factors which contribute to avulsion events in river systems resulting in abandonment of long-occupied courses and establishment of new main channels. When an avulsion occurs near the coastline it can change delta position. Distribution of Holocene avulsion sites can be driven by gradient advantage, relative sea level rise, neotectonics, discharge and channel sedimentation rates, human influence, backwater controls, and substrate composition (Stouthamer and Berendsen, 2000; Aslan et al., 2005; Zheng et al., 2019). These phenomena are generally associated with large alluvial rivers with avulsion frequency linked to degree of channel-bed aggradation relative to the floodplain (Bridge and Leeder, 1979; Schumm et al., 1986; Bryant et al., 1995; Mackey and Bridge, 1995; Slingerland and Smith, 1998; Jerolmack and Mohrig, 2007; Stouthamer and Berendsen, 2007; Jerolmack, 2009; Hajek and Wolinsky, 2012; Hajek and Edmonds, 2014). Avulsion frequencies for coastal rivers can range from 10-2000 years. For example, the Mississippi River has historically switched courses in its lower reaches every 1000 – 1500 years (Coleman 1988; Aslan et al., 2005), the primary channel belt in the Rhine-Meuse delta every 500 – 1000 years (Törnqvist, 1993; Stouthamer and Berendsen, 2000; Stouthamer and Berendsen, 2007), the Upper Rhone delta every 1500 years (Jerolmack, 2009), the channel at the Po River delta every 500 years, the Brahmaputra River valley every 1800 years (Pickering et. al. 2014), and about 10 years at the Yellow River delta which is much shorter than other world deltas due to its high

sediment load and fast accretion (Wang and Liang, 2000; Saito et. al., 2001; Shi and Zhang, 2003; Xu, 2008; Zheng et. al., 2017).

Over the past 7,500 years during the latest glacial high stand, the Mississippi River avulsed five times (Fisk, 1952; Coleman et al., 1998; Aslan et al., 2005) producing six delta complexes (Frazier, 1967; LCWCRTF and WCRA, 1998; Kulp et al., 2005; Blum and Roberts, 2009, 2012). While these studies agree on the ordered delta complex sequence of Maringouin, Teche, St. Bernard, Lafourche, Plaquemines/Balize, Atchafalaya/Wax Lake from oldest to youngest, the age, duration, and spatial extent of these delta lobes are debated (Condrey et al., 2014). Further disparity exists in the sequence between these studies and those of Fisk (1952) which places the inception of the St. Bernard delta lobe after that of the Lafourche lobe. Coleman et al. (1998) recounted subsequent studies by McIntire (1954) and Frazier (1967) which used comprehensive ¹⁴C dating to reverse this chronological order by identifying major deltaic plain depositional pulses. As a result of this undertaking, sixteen separate lobes were identified as part of the Teche, St. Bernard, Lafourche, and Plaquemines/Balize delta complexes. Frazier's work began to highlight the complex nature of the nested series of deltas and subdeltas that operate on overlapping spatial and temporal scales. Acknowledgement of these complexities by today's researchers, planners, and engineers is key to understanding anthropogenic influences associated with the currently active avulsion at the MR-AR bifurcation.

Figure 2.1 shows the Blum and Roberts (2012) depiction of the historic MR delta complexes and relates them to five historic avulsion sites. Avulsion site A (Marksville Diversion: ~31°N, ~92°W) occurred near the Marksville Hills and the present-day OR location where the river left the Teche course to the east to initiate a river segment which has been used first to develop the St. Bernard lobe then eventually transitioning to the Lafourche and Modern Mississippi courses.

This course was further developed when avulsion site B (Vicksburg Diversion: $\sim 32^{\circ}\text{N}$, $\sim 91^{\circ}\text{W}$) occurred near Vicksburg, MS, taking a more direct path to the deltaic plain along the eastern valley wall and leading to further development of the Lafourche delta complex through Donaldsonville, LA. It is likely that avulsion site C (Donaldsonville Diversion: $\sim 30^{\circ}\text{N}$, $\sim 91^{\circ}\text{W}$) served as an active two-way bifurcation feeding both the St. Bernard and Lafourche Delta complexes for hundreds of years until it was eventually rapidly abandoned as the river shifted to the more favorable easterly course towards New Orleans, LA. Thereafter, the downstream end of the modern course was transferred south at avulsion site D (New Orleans Diversion: $\sim 30^{\circ}\text{N}$, $\sim 90^{\circ}\text{W}$) to form the modern Plaquemines/Balize delta. Lastly, the main focus of this paper is the historic and future development of the AR and its connection through OR over the last few centuries now represents avulsion site E (Atchafalaya River Diversion: $\sim 31^{\circ}\text{N}$, $\sim 92^{\circ}\text{W}$) which is driving the embryotic growth phases of Atchafalaya/Wax Lake Delta Complex (Fisk, 1952; Coleman et al., 1998; Aslan et al., 2005).

In the cases of each of these five avulsions, a significant gradient advantage existed between the new diversion channel and the older, more mature river course. For avulsion sites A-D, Fisk (1952) forensically measured these gradient advantages, which ranged from 3:2 to 2:1 for diverted to parent course gradients, by estimating elevation changes from the point of diversion to both the younger and older mapped delta positions. Comparatively, the gradient advantage of the AR over the MR at its present point of diversion at OR (avulsion site E) is approximately 3:1, making it the most advantageous for stream capture of the five historic sites, from a gradient perspective.

While gradient advantages are required for avulsion, they are not the most prominent controlling factor in determining avulsion location. Virtually every outer bend of the meander

belts in the LMR Flood Plain between Vicksburg and New Orleans has sufficient gradient advantage for avulsion, which is defined by Slingerland and Smith (1998) to be cross-valley to down-valley slopes of > 8 . Of the fifteen locations analyzed by Aslan et al. (2005), every location exceeded this threshold and all but one was > 30 . Rather than gradient advantage alone, further analysis demonstrated that erodible sandy/silty substrates deposited by crevasse-splay events and reoccupation of flood plain channels were of primary importance in the Atchafalaya Diversion. More specifically, prior to approximately a thousand years ago, Yellow Bayou, Moreau Bayou, and Pelousas Bayou were crevasse channels of the previous course of the Mississippi in the vicinity of the Atchafalaya Diversion (Latimer and Schweizer, 1951). An additional contributing factor was the capture of the RR which allowed for channel enlargement and maintenance through seasonal low-water flows and sediment transport. Lastly, the final stage of development of the Atchafalaya Diversion was significantly impacted by human intervention. (Aslan et al., 2005).

2.3 Atchafalaya River Diversion and Anthropogenic Influences

In the early stages of the stream capture process the AR was highly impassible due to a raft of logs nearly 30 km long choking the stream at its upper end. The raft ceased to grow after Captain Shreve dredged his cutoff in 1831 to improve navigation at Turnbull Bend (Latimer and Schweizer, 1951; Shuman et. al., 1993; Mossa, 2013). While this cutoff reduced travel time, it also reduced scour velocities around the bend and began abandoning its connection with the Atchafalaya. It was only through extensive dredging that the channel between the two rivers could be maintained at through the lower arm of OR, while the upper arm silted in. While these dredging activities continued, private citizens and residents began efforts to remove the Atchafalaya log raft and by 1855 they were joined by the State of Louisiana to finish the job and

enable steamboat travel between the Atchafalaya and Mississippi. Immediately upon the removal of the obstruction, a rapid stream enlargement commenced (Fisk, 1952; Patrick, 1998; Nguyen et al., 2010; Bentley et al., 2016). Ironically, these improvements accomplished their goal of improving navigability between the Atchafalaya Basin and the MR, however they eventually accelerated the diversion development process toward ultimate stream capture. This led to the creation of the MRC in 1879 to put forth and implement rectification plans which included a series of sills and dams in the AR and its connection to the RR. A number of studies and reports also considered complete closure of OR, except for lock and navigation, however they concluded that the resulting rise in stage of about 4 feet could not be handled by the city of New Orleans and levee boards along the river (Latimer and Schweizer, 1951).

Under the 1928 Flood Control Act, the AR was improved to carry additional floodwaters of 650,000 cfs for an overall project flood of 3,000,000 cfs. Subsequently, favorable conditions lead to the Atchafalaya enlarging enough to exceed this portion of the project flood discharge at stages which were less than project heights. This prompted the Department of the Army to direct the MRC to engage in expedited engineering and geological studies to study the carrying capacity and alignment of the AR and OR. The directive also specified that the study should include “adequate profiles and actual sections to indicate with factual data the rate and extent of progressive changes in bank lines and sections of Old River and Atchafalaya River from its head in Old River through Grand and Six Mile Lakes to below Morgan City.” Additionally, the directive provided that a study on the influence of the geology of the Atchafalaya Basin on the river’s future regime was to compliment the engineering report for future planning. Lastly, the effectiveness of the Wax Lake Outlet in discharging excess waters from the lower Atchafalaya Basin was also to be assessed (Latimer and Schweizer, 1951).

Through the results of these studies which are discussed in the following section, it became evident that near term capture of the MR through the OR diversion was imminent. This led to the authorization and construction of the ORCS Complex at the point of diversion in 1963 to artificially terminate the total capture of MR flow. Since the structures became operational, federal law has mandated that the daily discharge into the AR be held static at 30% of the combined daily latitude flow of the MR and RR (Gagliano and van Beek, 1975; van Heerden and Roberts, 1988; Mossa and Roberts, 1990; Roberts et al., 2003; Allison et al., 2012).

2.4 Previous Research

The latest MR avulsion site at the AR Diversion has been of great interest to historians, engineers, scientists, and state and federal law makers since the 1800s (Ellicot, 1803; Schultz, 1810; Darby, 1816; Humphreys and Abbot, 1876; MRC, 1881). During the first half of the 20th century, studies of the diversion and its role in navigation, industry, and flood control grew from interest into concern (Elliot, 1932; Salisbury, 1937; Graves, 1949; Kemper, 1949; Halsey, 1950; Odom, 1950). The concerns raised in these studies were directly addressed by the MRC in the early 1950s through two extensive investigations which confirmed that the capture of the MR by the AR was imminent unless drastic federal action was taken (Latimer and Schweizer, 1951; Fisk, 1952). Although these reports resulted in the 1962 completion of the low sill and overbank structures of the ORCS which temporarily alleviated concerns over the diversion, fundamental questions remained regarding its long-term stability in the wake of the Flood of 1973 in which the low sill structure of the ORCS nearly failed (Kazmann and Johnson, 1980; Kolb, 1980; Martinez, 1986). This flood prompted the construction of an additional structure (auxiliary control structure) in 1986, followed by the Sidney A. Murray, Jr. hydroelectric station, completed in 1990 which takes advantage of the almost 5m head differential between the two

rivers (Bryan et al., 1998; Reuss, 2004; Piazza, 2014). Together these structures compose the complete ORCS complex which represents the largest continuous water diversion structure in the world (Knox and Latrubesse, 2016). Even with the abundance of research undertaken to investigate the effects of the ORCS (Mossa, 1996, 2013, 2016; Meade and Moody, 2010; Nittrouer et al., 2011b; Allison et al., 2012, Edmonds, 2012; Sounny-Slitine, 2012; Heath et al., 2015), many questions persist about the hydrogeomorphic stability of the overall fluvial system (Knox and Latrubesse, 2016).

2.4.1 Mississippi River Commission Studies

In a series of letters and memorandums in 1950, the Office of the Chief of Engineers for the U.S. Army (OCE) authorized the MRC to undertake and expedite the Atchafalaya River Study using engineering personnel from the Department of the Army who were well-versed in all phases of river hydraulics, mapping, and the design and construction of river control works. The OCE also authorized the MRC to employ Dr. Harold N. Fisk to report on the geology of the Atchafalaya Basin, with particular reference to the probable future regimen of the AR. Of particular note in the authorization correspondence, specific emphasis was repeatedly placed on the inclusion of sufficient survey information and factual engineering data to warrant conclusions in the form of adequate profiles, actual sections, and discharge measurements to indicate the rate and extent of progressive changes in the OR and AR.

Accordingly, the engineering study by Latimer and Schweizer (1951) includes three volumes of information. Volume 1 includes the directive from the OCE, a detailed description of the problem, analysis of the engineering data, a discussion of control structures and cost, and conclusions and recommendations. Volumes 2 and 3 include a plethora of relevant data sets for the MR, RR, OR, AR, Atchafalaya Basin, and Wax Lake Outlet. These include discharge

records and percent flow distributions; deterioration of main channel comparisons to other minor diversion chutes; dredging records; distribution of alluvial deposits; high water and low water profiles; 1950 plan, profile, and sections; various stage-discharge relationships; studies of suspended and bed material; accretion and sedimentation records; stage-salinity relationships; tidal effects; mapping of thalwegs, crevasses, and backwater areas; inventories of utility and bridge crossings; water surface profiles for various flows; cross-section elements by river reaches in relation to time; and rates of increase in discharge capacity for various stages; and comparison of stream widths and depths for various river reaches in relation to time. Of these data sets, the most relevant in determining OR and AR rates of enlargement are plotted in Figures 2.2 and 2.3.

In Volume 1 of the engineering study, Latimer and Schweizer estimated that the AR would become the main or master stream between 1968 and 1985 by visually extrapolating trends in discharge and cross-sectional area and comparing them to documented deterioration of the MR channel at locations which were abandoned by natural and artificial cutoffs. The two locations that were studied were diversions of MR flow through Island No. 8 Chute in Kentucky, 1481 km Above Head of Passes (AHP) and Brandywine Chute in Arkansas/Tennessee, 1207 km AHP. In both cases data was available from near inception (10 – 20% of flow in chute) to beyond main channel capture (>50%). These empirical examples showed that rates of capture initially increase linearly and then accelerate until the majority of the flow switches to the new course, and then decelerate towards the end of the process. When compared against flows through each chute, rates of enlargement of the chute cross-sectional areas increased very rapidly after 40% of the discharge of the main channel was diverted. Hence, Latimer and Schweizer considered capture beyond this discharge percentage to be uncontrollable and therefore suggested 40% as a critical threshold for capture. The engineering study concluded that the AR would enlarge to this

point of the total flow at the latitude of OR by 1960, while the geological study conducted by Fisk concluded that 40% of the MR only would be reached by 1971 without intervention.

To further demonstrate these trends, in Figure 2.2 we have plotted the same flow data used by Latimer and Schweizer and calculated polynomial regressions in order to revisit their capture progressions. The data used in Figure 2 is from the engineering study Volume 3 where it is listed in tabular format. The green line in the figure representing AR flow vs. total flow at the latitude of OR (combination of RR and MR flows) crosses the 40% flow threshold in 1971. The blue line in the figure representing OR flow vs. MR flow shows a slightly faster rate of capture without the influence of the RR. It is expected that because total flow in the MR is much greater than the RR, the capture rate regression calculated for the blue line would have greater influence over the combined flows calculated in the green line as deterioration progresses. Equation 1

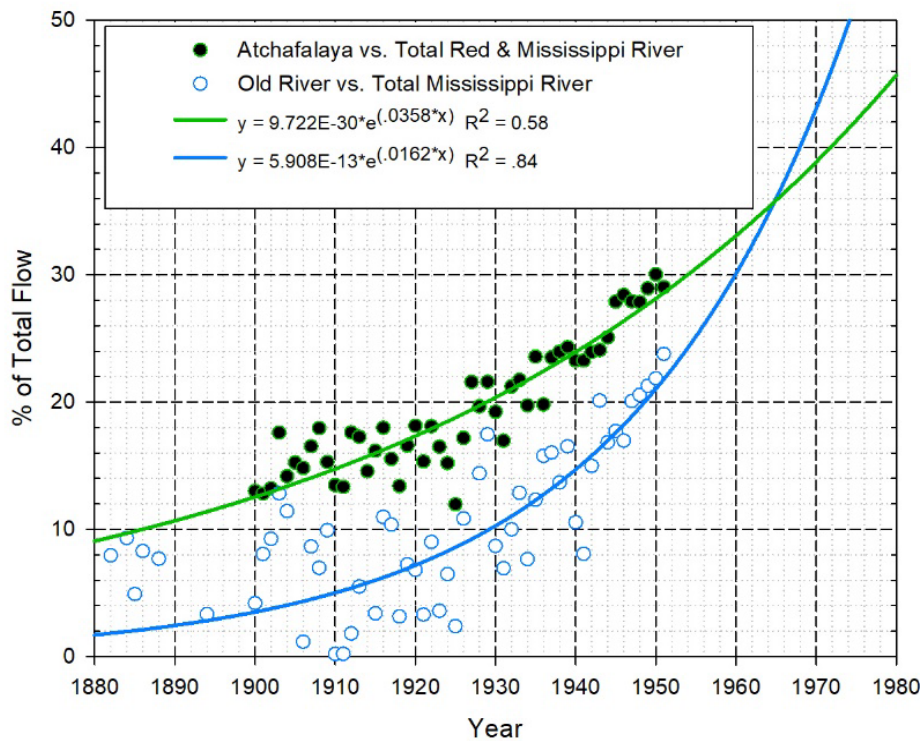


Figure 2.2. Historic records and projected rates of flow increase from the MR to OR and AR (data from Latimer and Schweizer, 1951).

below was formulated from the OR vs. MR dataset and will be used to compare against modeled results.

$$t_{capture\%} = \frac{\ln\left(\frac{\%Q_{OR}}{5.908E^{-13}}\right)}{0.0162} - 1962 \quad (\text{Eq. 1})$$

Where: $t_{capture\%}$ is the time in years to reach discrete values of $\%Q_{OR}$

$\%Q_{OR}$ is the percentage of total MR flow passing through OR

1962 represents the year of ORCS construction

Furthermore, in Figure 2.3A we show a pattern of enlargement in the initial 87 km of the AR to accommodate the increased flows. The diagram is a scatter plot of cross-sectional areas below bankfull stage taken from Volume 3 of the engineering study along with a 3rd order regression line which demonstrates acceleration rates along a similar time frame as those seen in Figure 2 for flow increases. Conversely, the scatter plot and 1st order regression line we configured in Figure 2.3B shows a pattern of increased accretion rates and slow channel deterioration in a 67 km stretch of the MR just south of its juncture with OR. Surveys were conducted by the USACE at multiple reaches in these locations to monitor diversion changes between 1880 and 1951.

To supplement the engineering study, the MRC employed Fisk to take a geological approach to the problem of the MR Diversion in order to corroborate the findings of the engineering study by analyzing historic evidence of past diversions and the factors which influenced their occurrence. In addition to the maps, graphs, and charts made available by the MRC, aerial photographs were used to reconstruct the geologic history and physiographic features of the Atchafalaya Basin. Additionally, over 200 borings were taken for this study and used along with thousands of additional borings from other sources to determine the character, configuration, and

sequence of ancient and modern distributary channels, deltaic and flood plain deposits, and overall geomorphology within the MR alluvial valley.

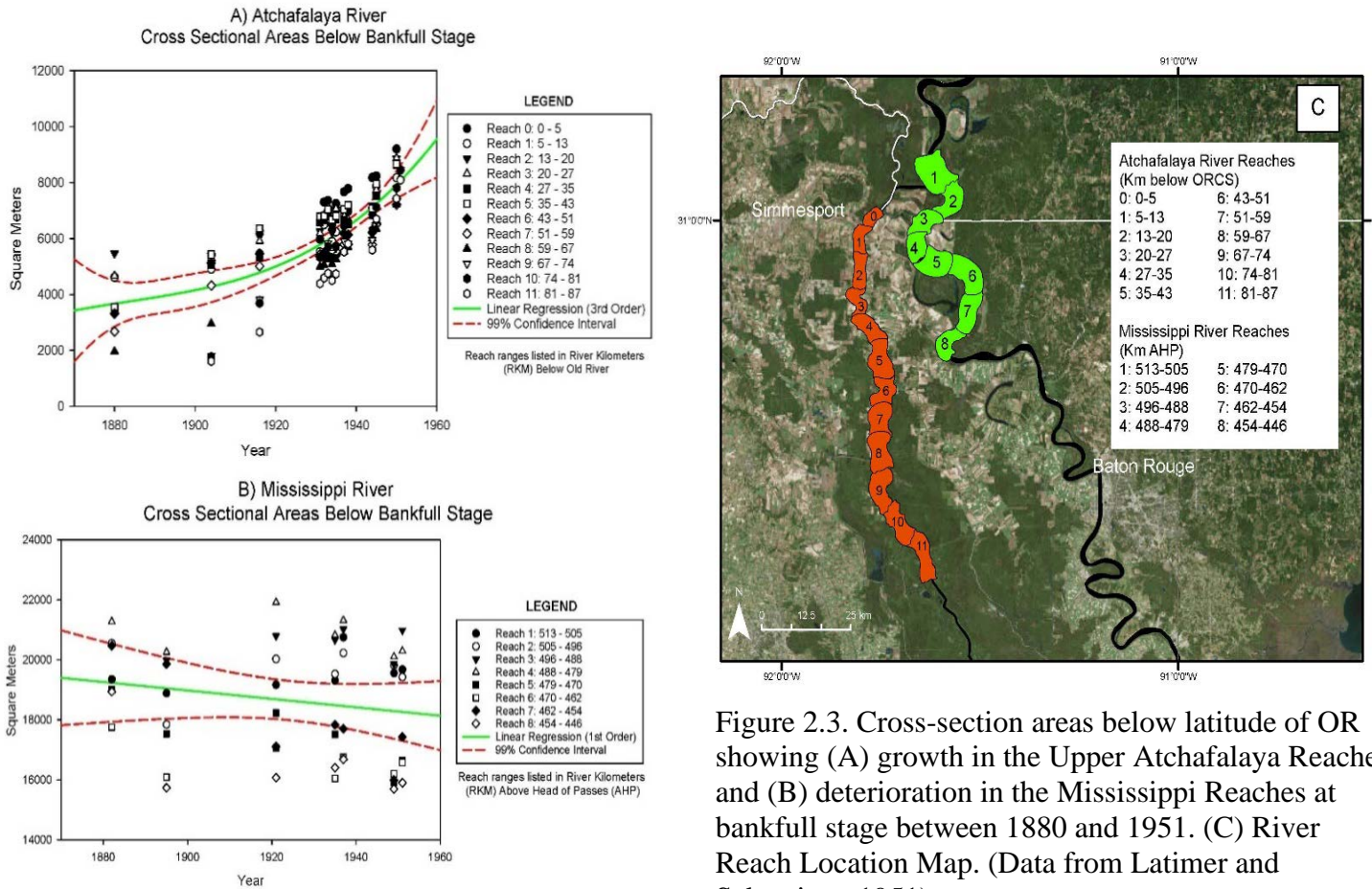


Figure 2.3. Cross-section areas below latitude of OR showing (A) growth in the Upper Atchafalaya Reaches and (B) deterioration in the Mississippi Reaches at bankfull stage between 1880 and 1951. (C) River Reach Location Map. (Data from Latimer and Schweizer, 1951).

Sedimentary records showed that historic MR courses are not abandoned rapidly like other more sediment-laden rivers such as the Yellow or Po Rivers (Fisk, 1952; Pickering et al., 2014, Zheng et al., 2017) which can shift course during a single flood. In most cases of overtopping during flood conditions in the MR, crevasses are healed unless conjoined with a previously formed distributary channel and minor alluvial valley stream. This is in large part due to the MR's deep channel throughout its entire length and its ability to efficiently transport its sediment load, regardless of slope, throughout the alluvial valley. Another key finding is that new channels must be able to carry the full flow of the river away from the point of diversion in order

to adequately transport the MR sediment load to the Gulf, otherwise they become plugged. In the case of all Mississippi valley diversions investigated, diversion arms only became dominant after deposits alluviated adjacent lowlands, formed a lengthened channel, constructed natural levees, and aggraded its flood basin. Historically, these processes were found to continue gradually until the course widens and deepens sufficiently to take the full MR flow. At this point, capture tends to accelerate similar to trends discussed in the engineering study and seen in Figures 2.2 and 2.3.

To focus on the closing stages of the capture process, Fisk placed particular emphasis on the Donaldsonville Diversion which abandoned the Lafourche course, in order to study the nature of the sediments filling the channel and gain perspective on the rate of abandonment. Borings made along present day Bayou Lafourche detected a longitudinal sand wedge, thickest near the MR at the point of diversion and thinning in a downstream direction. This indicates that a stage was reached where the old main Lafourche-Mississippi channel was rapidly plugged once it was isolated from low flows with adequate carrying capacity. Above the sand wedge the channel is filled with clay and silt, indicating that the channel was slowly filled thereafter with fine sediment from the river during high stages. Fisk described this rapid plugging of the main channel followed by slow infilling as the critical and final stages of diversion, respectively.

After fully understanding the nature of these diversion development conditions and stages, Fisk revisited the hydraulic assessments made by Latimer and Schweizer in the engineering study. In the case study presented in the engineering study for the Brandywine Chute, rapid deposition in the main channel began when 30% of the discharge flowed through the chute. While variable conditions exist at each diversion point controlling the relationship between discharge percentage and rapid sedimentation, Fisk deemed this comparison to be the right order

of magnitude. Hence, he forecasted this critical stage to be imminent and concurred with the engineering study that beyond 40% of the discharge down the AR, capture of the main stem would become uncontrollable (Fisk, 1952).

2.4.2 Delft 3D Model Background

More recently, hydraulic and sediment transport modelling was performed using the Delft 3D software suite developed by Deltares. Edmonds (2012) built a computational domain and grid (Figure 2.1) to study how backwater flow influenced the stability of the bifurcation. The domain began 45 km upstream of the bifurcation and extended to the Gulf on both the Mississippi and Atchafalaya branches. The grid is a 2D planform composed of ~20,000 cells with a typical size of 100 m x 900 m with the long axis extending downstream. The grid extends from bank to bank with this width remaining fixed but allowing the bed form to change with evolving hydrodynamics and sediment transport. Dry cells were added around the bifurcation to simulate its real-world complexity. The last constraint of the model setup was not to include tributaries or floodplains. These exclusions were considered justifiable given that man-made levees confine river flows in the majority of reaches. Sensitivity tests were run on the system's largest tributary, the RR, resulting in little to no impact on the results (Edmonds, 2012). The MRC Engineering similarly concluded that the RR has little influence over the development of the AR (Latimer and Schweizer, 1951).

In all model runs, bed roughness is a uniform Chezy value of $65 \text{ m}^{1/2} \text{ s}^{-1}$. A time step of 60 s was used. Bed adjustments were sped up by multiplying the bed sediment flux in each time step by a morphological scale factor set to 50. This is within the stable range (Ranasinghe et al., 2011) and was verified with sensitivity tests. At the upstream boundary, Edmonds specified the water discharge and sediment fluxes with the incoming discharge carrying two grain sizes, one

non-cohesive (200 μm) and one cohesive (15 μm). At the downstream boundaries, water surface elevations are set to zero. The initial bed topography in each river is from 2004 and 2006 hydrographic surveys of the Mississippi and Atchafalaya, respectively. For each river Edmonds calculated the cross-sectionally averaged centerline bed elevations every kilometer. In the subsurface, there is initially 10 m of sand and 2 m of mud available for erosion, consistent with observations (Galler and Allison, 2008; Nittrouer et al., 2011a). This model setup accurately predicts the water surface elevations in the MR to within 10–15% at different flow stages (Nittrouer et al., 2011b), corroborating these boundary condition choices. To assess the sensitivity of the results Edmonds conducted repeat experiments and varied the time step, bed roughness, the grid resolution, sediment transport formulas, sediment size, and initial volume of sediment in the subsurface. Varying each of these leads to a different solution in the details, but the behavior of the discharge ratio between the rivers is not different by more than 15% (Edmonds, 2012).

Edmonds conducted seven different model simulations with the ORCS removed and with different steady values of for the discharge upstream of the MR/AR bifurcation ranging from 5,000 m^3/s to 50,000 m^3/s . The simulations were run and monitored for an adequate length of time (ranging from \sim 12 to 22 years) to determine linear capture trends. For each simulation Edmonds observed that soon after the initial bed changes, one of the two rivers began to capture the discharge at a time and can alternate depending on the upstream flow (Q_{up}). By plotting the resulting Atchafalaya flow (Q_{Atch}) rates for each run over time and formulating linear regressions, distinct rates of capture (Q_{rc}) from the Mississippi to the Atchafalaya were determined for each steady state Q_{up} value. From these data, Edmonds demonstrated that the threshold for which the direction of capture switches from the Mississippi to the Atchafalaya is

$Q_{up} > 12,600 \text{ m}^3/\text{s}$. Additionally, with these results, the ultimate goal of predicting the capture timescale for the bifurcation in the absence of the ORCS was made possible by displaying the change in discharge of the Atchafalaya as:

$$dQ_{Atch} = \int_0^T Q_{rc} dt \quad (\text{Eq. 2})$$

$$\text{Where: } Q_{rc} = 0.012Q_{up} - 154 \quad (\text{Eq. 3})$$

dt is a time step in years, and $Q_{up} = f(t)$

Here, we modify Equation 3 to predict time to reach discrete percentages of capture after the hypothetical removal of the ORCS in Equation 4.

$$t_{capture\%} = \left(\frac{\%Q_{OR}}{100} - 0.3 \right) \left(\frac{Q_{up}}{0.012Q_{up} - 154} \right) \quad (\text{Eq. 4})$$

Where: 0.3 represents the fraction of Q_{up} already captured by OR and flowing into the AR prior to and maintained since the construction of the ORCS.

2.5 Methods

Ultimately the goal of this study is to extend the model by Edmonds to predict future long-term water and sediment management strategies through the MR/AR bifurcation via the ORCS. Because the extensive and exhaustive efforts in the MRC studies led to the construction of the ORCS, the Delft 3D model will be used to revisit the timescales and trends those studies put forth. Additionally, long-term semi-unsteady state input conditions will be developed in order to re-evaluate the bifurcation without the ORCS in place in addition to evaluating long-

term flow and stage developments in both branches with current management strategies unchanged.

Our goal is to observe the evolution of the MR/AR bifurcation using a variable hydrograph in a long-term simulation of 150 years to see the capture progression in this more realistic scenario. For this run, an average annual hydrograph was formulated using an 80+ year Q_{up} dataset from Vicksburg, MS for the time period from 1931 to 2015 acquired from USGS

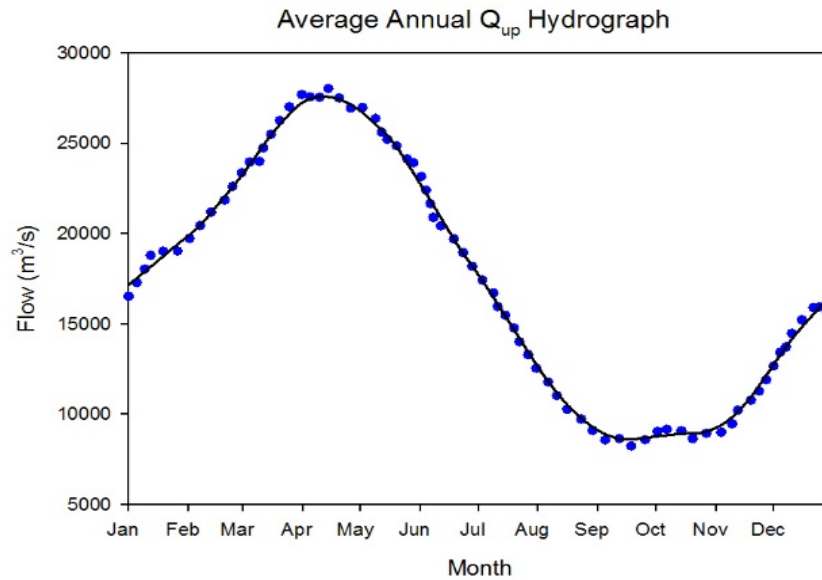


Figure 2.4. Average Annual Mississippi River Hydrograph at Vicksburg, MS. Generated from daily discharge data collected at USGS Site 07289000 from 1931-2015.

Site 07289000. The native data included average daily flows from October 1, 1931 to September 30, 2015. Flows were averaged for each day of the year over this time frame creating 365 discrete data points and plotted in Figure 2.4. The corresponding flow data was then repeated 150 times successively to create a text input file for the Delft 3D headwater boundary condition.

The Vicksburg USGS Gage location used to develop this headwater flow input is shown on the Figure 2.5 Location Map. This figure also shows Delft 3D grids for the MR and AR branches below the ORCS and for the MR above the ORCS. For model runs in which the MR/AR bifurcation is left uncontrolled with the ORCS removed, one complete grid encompassing both branches and the MR reach above the ORCS is used as shown in Figure 2.1. For a future without action (FWOA) model run in which the ORCS remains in place with operational schemes unchanged, individual MR and AR grids below the ORCS were developed. In order to simulate how the ORCS is currently operated in the upstream boundary flow conditions for the FWOA scenario, we apply 70% and 30% allocations of the average annual hydrograph from Figure 4 for the MR only and AR only grids, respectively. Lastly, Figure 2.5

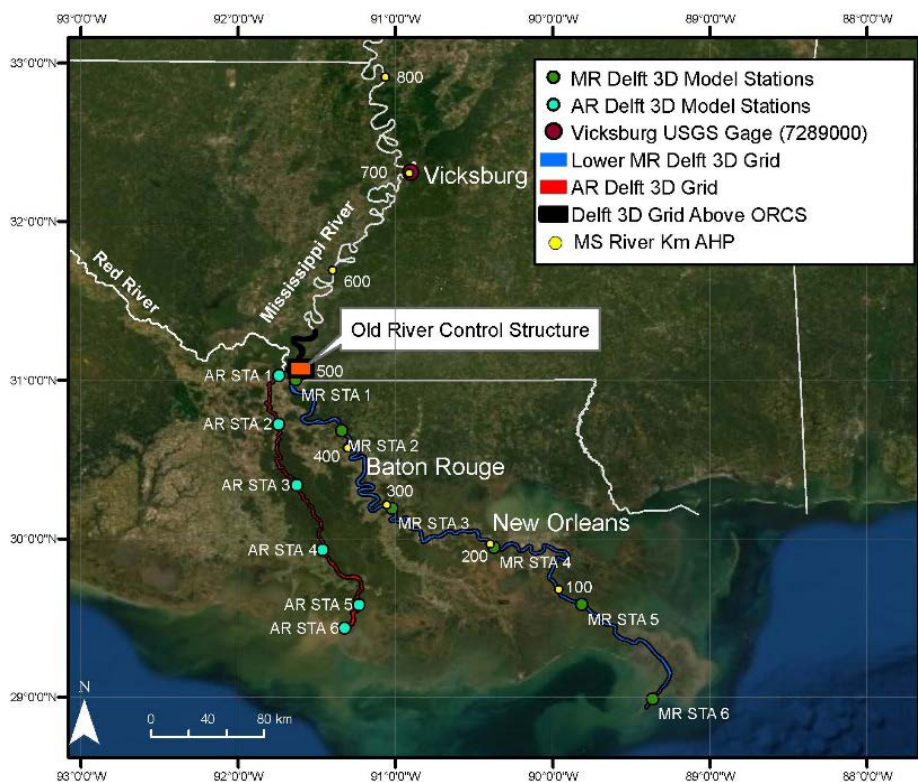


Figure 2.5. USGS River Gage and Delft 3D Grid and Output Station Location shows six observation locations chosen for each river branch and specified in the Delft 3D setup

files. Output parameters for each station include water level, discharge, and sediment transport rates broken down into cohesive, non-cohesive, bedload, and non-bedload components.

2.6 Results and Discussion

For the first set of model simulations, we simulated a long-term unsteady-state 150-year run with the ORCS removed and compared the results against the Edmonds 2012 steady-state simulations as well as the trends summarized in the MRC studies. We then used these comparisons to develop a complete capture lifecycle curve for the MR/AR bifurcation without the influences of the ORCS. Lastly, we then used the model to simulate future without action (FWOA) conditions with the ORCS in place and operational schemes unchanged.

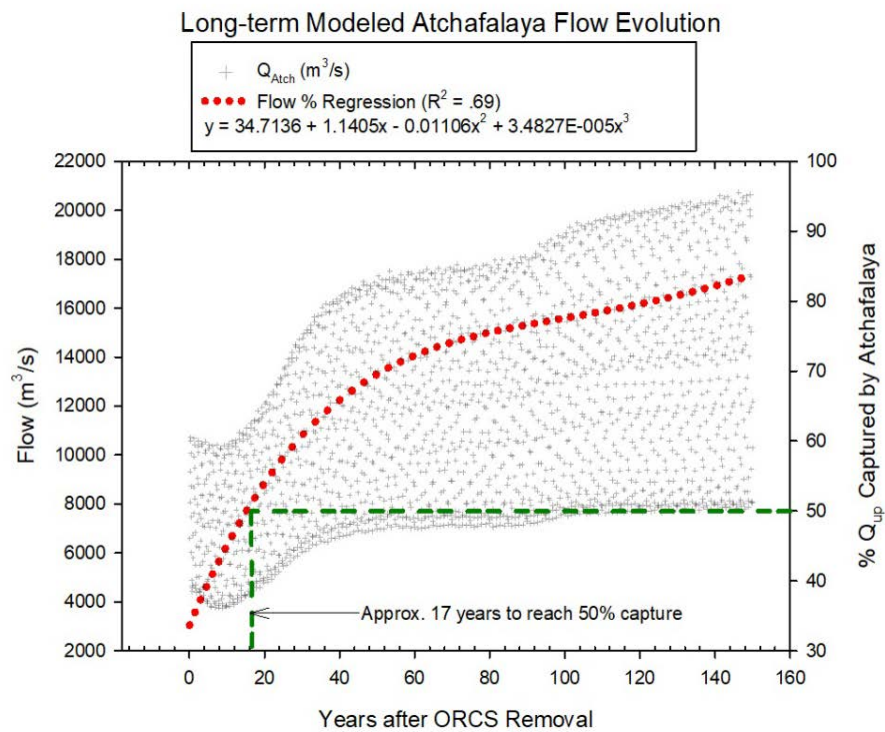


Figure 2.6. Simulated long-term AR flows and capture percentages for the average unsteady state MR hydrograph upstream (Q_{up}) of the MR/AR bifurcation after ORCS removal.

2.6.1 *Semi-Unsteady State 150-Year Simulation*

Using the average annual Q_{up} hydrograph developed in Figure 2.4 as the headwater boundary flow input, we modeled a semi- unsteady state simulation of the uncontrolled capture progression. By repeating this average annual flow input for a duration of 150 years continuously, the effects of long-term yearly high and low river stages were simulated and reflected in the upper and lower bounds of the output data. Figure 2.6 shows a plot of modeled flow evolution in the upper AR (Station 2) which indicates a rapid period of channel adjustment followed by a long and gradual increase in flow ranges and magnitudes similar to what is currently seen in the LMR. Figure 2.7 also plots a regression of the percentage of the total MR flow progressively captured by the AR over time. In this analysis, the 50% capture threshold is reached very quickly (~17 years) and then the slope along the regression line begins to flatten as the capture rate begins to decelerate. This deceleration is similar to the final stage trends observed for a new receiving channel at the Brandywine Chute and the inverse of the trends interpreted from sediment deposits found at the historic Donaldsonville Diversion for the abandonment of a main channel (Latimer and Schweizer, 1951; Fisk, 1952). From the plotted cubic polynomial regression, we can describe the capture time formulaically as:

$$t_{capture\%} = -426.2479 + 25.048\%Q_{OR} - 0.4836\%Q_{OR}^2 + 0.0032\%Q_{OR}^3 \quad (\text{Eq. 5})$$

Where: $\%Q_{OR} > 30\%$, as the initial model channel conditions reflect 30% previously captured and maintained since 1962.

$\%Q_{OR} = \%Q_{Atch}$ since inputs from the RR were justifiably excluded by sensitivity tests from the Edmonds 2012 study.

2.6.2 Comparison with Previous Studies

Given these modeling results, it is important to relate them to previous capture predictions which have greatly influenced the MR/AR system's water management strategies for many years.

Conclusions reached in the MRC studies resulted in the construction of the ORCS and significant Federal expenditures to protect public welfare and economic interests. With trends developed from many years of actual flow and cross-sectional data collected from both the MR and AR branches as well as geologic records from historic avulsion sites, they will serve as an important benchmark to evaluate the validity of the Delft 3D model constructed by Edmonds and modified by this study. Using Equations 1,4 & 5 developed to this point to estimate $t_{capture\%}$, we formulated Table 2.1 to compare the three predictive methodologies.

Table 2.1. Estimated Time to Capture Total Mississippi River Flow Percentages by the Atchafalaya River after ORCS Removal

Source Study	Equation No.	Time to Capture % by OR/AR (years)										
		40	45	50	55	60	65	70	75	80	85	90
Latimer & Swcheizer, 1951	1	3.8	11.1	17.6	23.5	28.8	33.8	38.4	42.6	46.6	50.3	53.9
Edmonds, 2012	4	32.7	49.0	65.3	81.7	98.0	114.3	130.7	147.0	163.3	179.7	196.0
Developed in this Study	5	6.7	13.2	17.2	20.9	26.9	37.5	55.1	82.1	121.0	174.0	243.7
Delta (4 vs. 1)	1,4	28.9	37.9	47.7	58.2	69.2	80.6	92.3	104.4	116.7	129.3	142.1
Delta (5 vs. 4)	4,5	-26.0	-35.8	-48.2	-60.8	-71.1	-76.9	-75.6	-64.9	-42.4	-5.7	47.7
Delta (5 vs. 1)	1,5	2.9	2.1	-0.4	-2.6	-2.0	3.7	16.7	39.5	74.4	123.7	189.8

Equation 1 developed from the data published in the MRC engineering study predicts an extremely swift capture (~54 years to reach 90%) which was described extensively in both the engineering and geologic studies. The equation very accurately agrees with the predictions made that the AR would overcome the MR at 50% by 1980 (the year of ORCS construction, 1962 + 17.6), however no empirical data was available at the scale needed to derive capture rate decreases qualitatively described for the final stages. In applying Equation 4 developed from Edmonds (2012), we used the USGS Mississippi River flow data set at Vicksburg, MS for the time period from 1931 to 2015 for which the average Q_{up} was $17,228 \text{ m}^3\text{s}^{-1}$. This produced a longer capture time (~196 years to reach 90%) and a linear capture time of 16.3 years for every

progressive 5%. Equation 5 derived from the long-term unsteady-state results presented in this study also produced a much longer capture time (~244 years to reach 90%), however results match those from Equation 1 extremely well (within 4 years) from 40-65% capture before the rate significantly slows down.

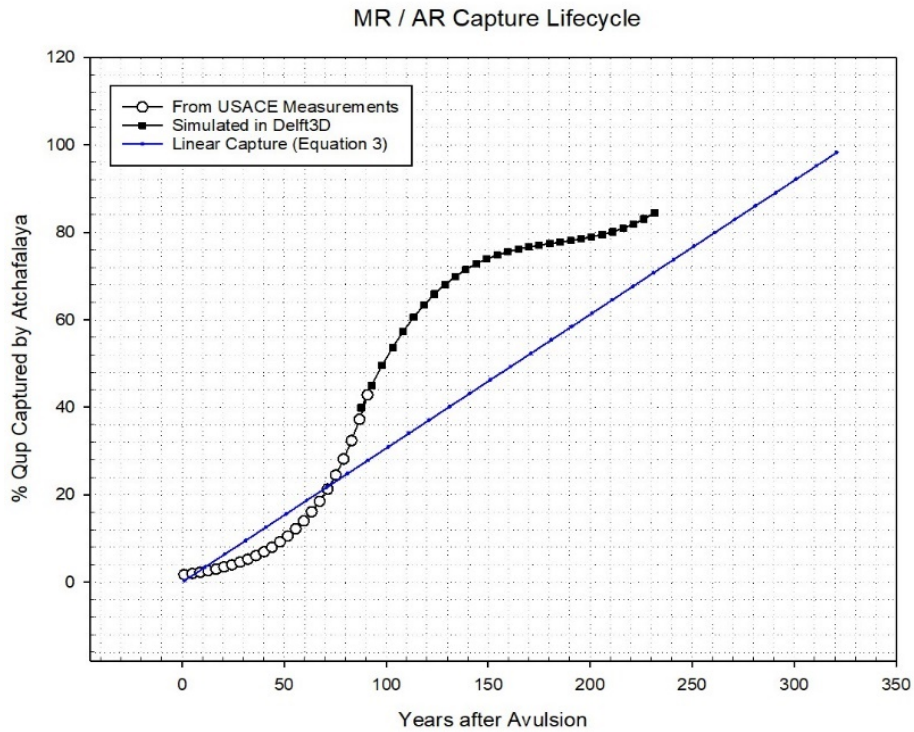


Figure 2.7. MR/AR Capture Lifecycle developed from Historic Measurements and Delft 3D Model (USACE Measurements from Latimer and Schweizer, 1951; Linear Capture from Edmonds, 2012)

In the MRC geologic study, Fisk described the final stage of capture to occur sometime after the balance is broken and a rapid decrease in velocity and increase in course bed load deposition causing the old main channel to become plugged. The pattern of capture deceleration predicted by Equation 5 between 65-75% fits this description and is also similar to that displayed by the Brandywine Chute example. Hence, it is surmised that applying the semi- unsteady state approach to the Edmonds Delft 3D model is an effective predictor of long-term trends for the MR/AR bifurcation and downstream impacts for both river branches. This further validates the

work of Edmonds in constructing the model and choosing its inputs such as grid resolution and boundary conditions; initial bed elevations, composition and thickness; sediment flux parameters and transport formulas, all of which were thoroughly tested against recent datasets and now replicate patterns found in long-term measurements and geologic tendencies of historic avulsions.

In Figure 2.7 we stitch together the OR vs. MR capture curve from Figure 2.2 and formed from the 70+ year USACE data set with the Delft 3D regression line formulated from the modeling conducted in this study and introduced in Figure 2.6. The two curves overlap somewhat seamlessly as seen in the comparison between Equations 1 and 5 in Table 1 which states time in terms of years after a theoretical removal of the ORCS. In Figure 2.8 we plot the curves from the inception of capture by the AR, and demonstrate a nearly completed lifecycle curve for the MR/AR bifurcation.

Towards the end of this lifecycle we see another increase in flow capture which could be due to variability in sediment transport rates and bed erosion. Without empirical data to predict capture patterns for the last 10-20%, Fisk's description of the final stages of capture did not include this degree of variability. Even at the Donaldsonville Diversion where Fisk utilized extensive geologic data in the 1951 MRC analysis, Bayou Lafourche remained naturally connected to the MR until 1904 when it was artificially dammed by the USACE (Penland et al., 1986; Reuss, 2004). Also included in Figure 2.8 is a plot of the linear capture rate from Equation 3 formulated in the Edmonds 2012 study. While this plot over estimates capture during the initial avulsion stages (up to ~20%) and underestimates capture during subsequent stages, it begins to converge with the semi-unsteady state regression plot as the avulsion nears total capture at 100% between 300 and 350 years. Hence, while the linear capture rate in Equation 3

can be used to estimate reasonable total capture time for MR avulsions, we will use the long-term semi-unsteady state modeling approach for evaluation of various management strategies moving forward.

2.6.3 Future Without Action Scenario

Comparisons made in Section 2.4.3 to long-term data trends from the MRC engineering study in 1951 coupled with the sensitivity tests performed by Edmonds in 2012, have verified the Delft 3D model as an adequate tool for making broad-scale, long-term assessments on the MR/AR system. While many management strategies have been considered for the MR/AR bifurcation over the years, since the ORCS became operational, federal law has mandated that the daily discharge into the AR be held static at 30% of the combined daily latitude flow of the MR and RR (Gagliano and van Beek, 1975; van Heerden and Roberts, 1988; Mossa and Roberts, 1990; Roberts et al., 2003; Allison et al., 2012). Any modifications to this operational scheme would have to undergo an arduous planning process under which potential planning alternatives would be scrutinized and evaluated. Potential changes could impact navigation, flood damage reduction and ecosystem restoration, as well as for storm damage prevention, hydroelectric power, recreation, and water supply. Major modifications to the Mississippi River and Tributaries (MR&T) project, the largest flood control project in the world, would encompass impacts to all of these categories. Engineering Regulation 1105-2-100 provides the overall direction by which USACE Civil Works projects are formulated, evaluated and selected for implementation (USACE, 2000). With the enormity of these potential planning deliberations, it is first important to gain insight into a future where ORCS operations remain unchanged.

In recent studies, researchers have raised concerns over rising stage levels and sedimentation within the MR system. Comparison of 1973 vs. 2011 flood records (the only two years in which

the Morganza Spillway was opened) from the USGS Vicksburg (RK 700) dataset show that between January and April during those floods prior to Morganza Spillway opening, the 1973 flood had a 46% higher average discharge and a 36% higher maximum discharge. Even so, the flood of 2011 produced approximately a 2 m higher peak stage (Kolker et al., 2014). Stage-discharge curves produced by Kemp et al. in 2014 at Tarbert Landing (RK 510) and Baton Rouge (RK 367) showed that stage was consistently 0.6 m and 0.4 m higher in 2011 than in 1973 at Tarbert Landing and Baton Rouge, respectively. Stage-discharge comparisons at Belle Chase (RK 120) produced lower stage values (-0.3 to -0.7 m) for 2011 vs. 1973. This represents a shift over 40 years toward an increase in high water slope upstream of New Orleans, and a flattening from there to the GOM (Kemp et al., 2014). The LMR below New Orleans is affected by proximity to GOM and mean sea level where the pressure gradient exerts greater influence over gravity flow and introduces the “backwater effect” (Lamb et al., 2012; Nittrouer, 2011b; Lane 1957; Chow, 1959). Typically, closer to the mouth of the river in this zone of water surface profile flattening, flow compensation may take place through increased velocities or loss of flow through lateral escape routes. The LMR has seen both scenarios in recent years, producing fluctuating depositional rates with an overall increasing trend of upstream depocenter movement from the mouth of the river, signifying loss of stream power and delta backstepping (Brown et al., 2009; Kemp et al., 2014; Bentley et al., 2016).

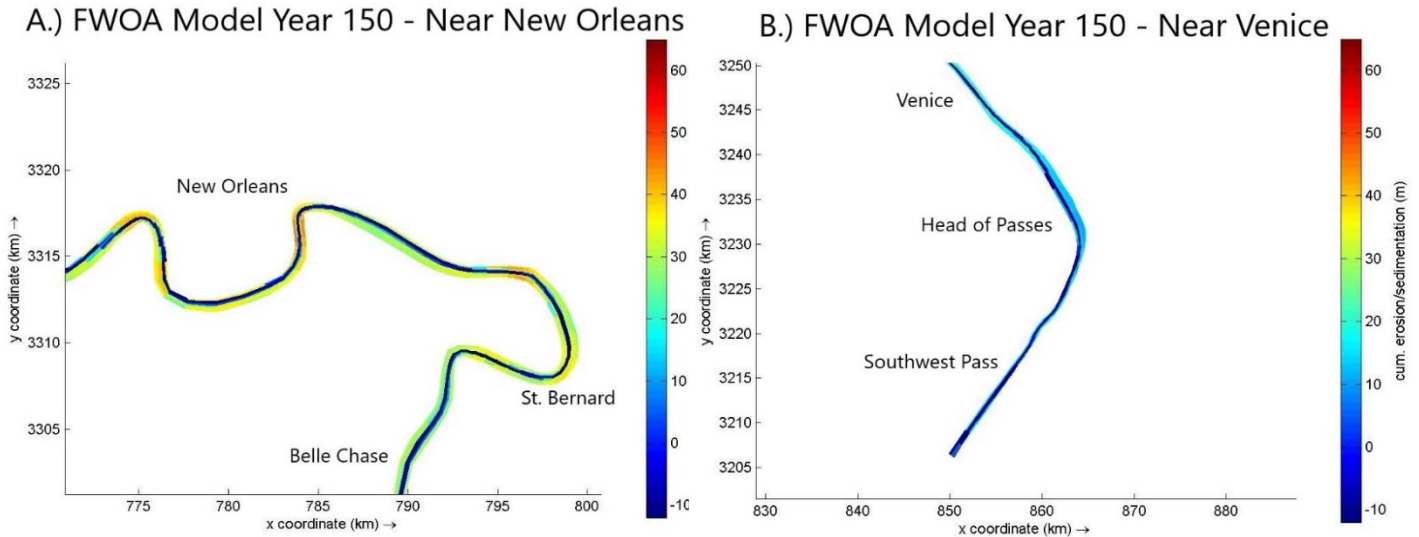


Figure 2.8. 150-Year Cumulative Bed Erosion/Sedimentation in the LMR Modeled in Delft 3D FWOA Scenario

A.) Near New Orleans, LA and B.) Near Venice, LA.

Results from the FWOA Delft 3D model scenario displays many of the same concerning trends. For example, we illustrate in Figure 2.8 cumulative bed erosion and deposition occurring over the 150-year time frame in the lower 200 km of the MR. Results show a tremendous amount of sedimentation of nearly 40 m in some locations adjacent to the main channel and a general trend of increased deposition moving upstream. Because the originally specified bed levels were cross-sectionally averaged centerline elevations from past surveys to minimize grid cells and reduce computational time, the model essentially rebuilds channel cross sections similar to those seen in the current river bathymetry. As time progresses beyond this point in the model, the major buildup of sediment in point bars and side slopes induces a channelizing effect and increases velocity in the main channel, causing erosion and deepening on the order of 10 m of erosion. Modeled depth-averaged velocities remained below 1 m/s in the beginning of the model run throughout this river reach, while in the last 50 years average velocities nearly doubled with peak velocities in the main channel that reach 3 m/s near river bends coupled with drastic declines in velocity near river banks. Velocity increases are also seen in the final

stretches of the river near the GOM, which is where the least deposition and most erosion occurs. This is consistent with the backwater effects explained by other researchers, however the river is channelized all the way to the GOM in the model and does not represent any lateral flow dispersion points which begin just below Venice on the West descending bank of the river and near Bohemia on the East descending bank.

Additionally, although the model also does not account for annual maintenance dredging conducted by the USACE to maintain navigation, these dredged volumes are offset by erosion modeled in the main channel. Dredging of shoals between river bends from New Orleans to Baton Rouge are pumped into deeper locations and these sediments stay within the system until deposited in shoals or point bars downstream or ultimately removed from Southwest Pass. Portions of the sediments dredged below Venice down into Southwest Pass are removed via offshore dumping or beneficial use. Erosion rates shown in Figure 2.8B below Venice more than

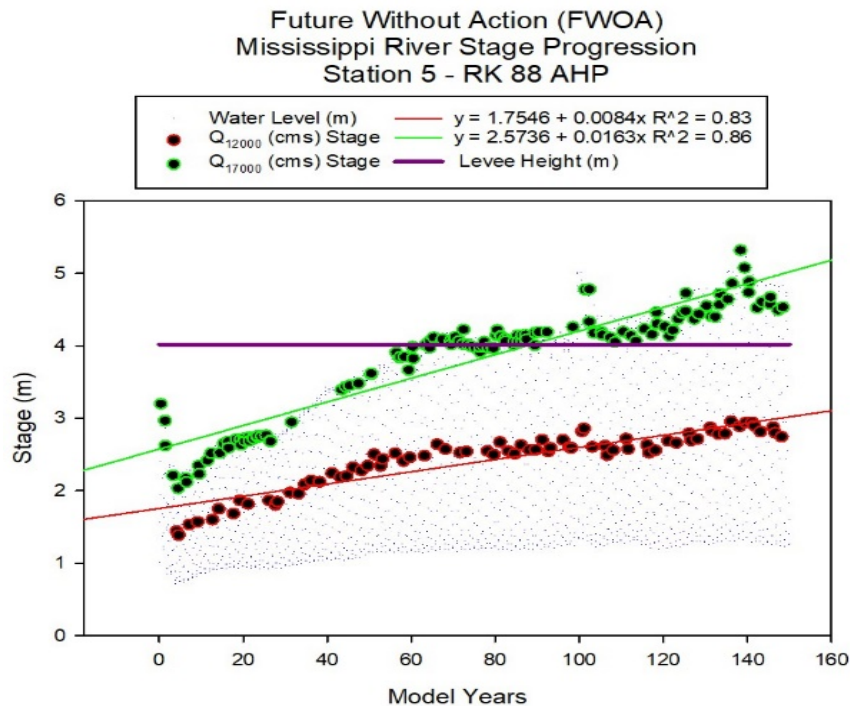


Figure 2.9. FWOA Model Scenario Mississippi River Stage Progression at MR Station 5.

account for these removed sediment volumes as the main channel at year 150 is more than 10 m below currently authorized dredging depth.

The level of sedimentation which occurs in the model over the 150-year period also causes major shifts in stage throughout the LMR. In Figure 2.9 we plot stage progression over time at MR Station 5 with highlighted values at average flows (12,000 m³/s) and higher flows (17,000 m³/s), which are typically experienced in annual Spring floods. While water levels at lower flows do not vary greatly over time, stages at higher flows increase by nearly 3 m. This is a cause for major concern as the model predicts that higher flow stages will overtop the river levee at this location in model year 88. We acquired levee heights at each station location by using NOAA’s Digital Coast data viewer (NOAA, 2019) and then converting the elevations using the USACE’s Corpscon software from the NAVD88 datum to the NGVD29 datum which is consistent with the USACE surveys used to assign elevations in the original model grid.

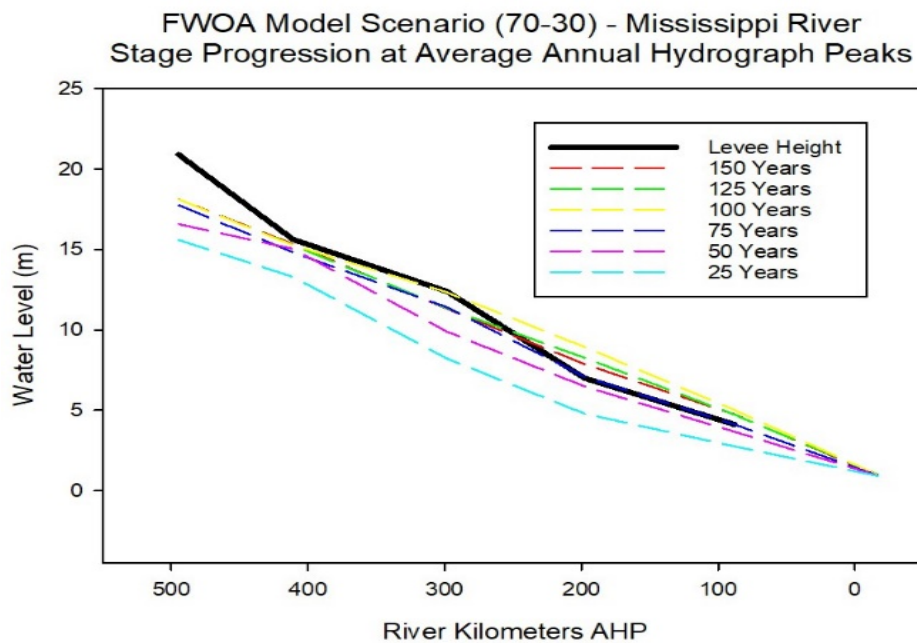


Figure 2.10. FWOA Model Scenario Mississippi River Stage Progression for MR Stations at Peak Hydrograph Flows (~17,000 m³/s) and 25-year intervals.

We performed this same analysis for each model station and plotted along the entire MR stretch from OR to the GOM in Figure 2.10 at 25-year intervals. This plot shows that at current elevations, MR levees near New Orleans and below will be highly vulnerable beyond 75 years and susceptible to overtopping during average Spring floods. These projected stage rises would also impose additional pressure on the ORCS and adjacent areas further contributing to its unsustainable predicament and increasing the likelihood of returning to an uncontrolled avulsion (Heath et al., 2015; Knox and Latrubesse, 2016).

Of course, these stage projections are made without incorporating any operation of flood alleviating spillways at Morganza or Bonnet Carré; constructed restoration diversions such as Davis Pond, Caernarvon, and West Bay; or future planned restoration diversions such as Mid Barataria and Mid Breton (CPRA, 2017). Operation of these spillways and diversions would lower these stages somewhat, however with approximately a meter of levee overtopping projected at some locations and nearly two meters of stage rise at the ORCS, more drastic safeguarding measures will need to be considered as these projections would only increase for higher than average Spring floods over 17,000 m³/s below OR. These measures could include some combination of raising levee heights, sediment dredging and removal from the MR system, or modifying the MR/AR 70%/30% flow split to more regularly send additional flows down the AR.

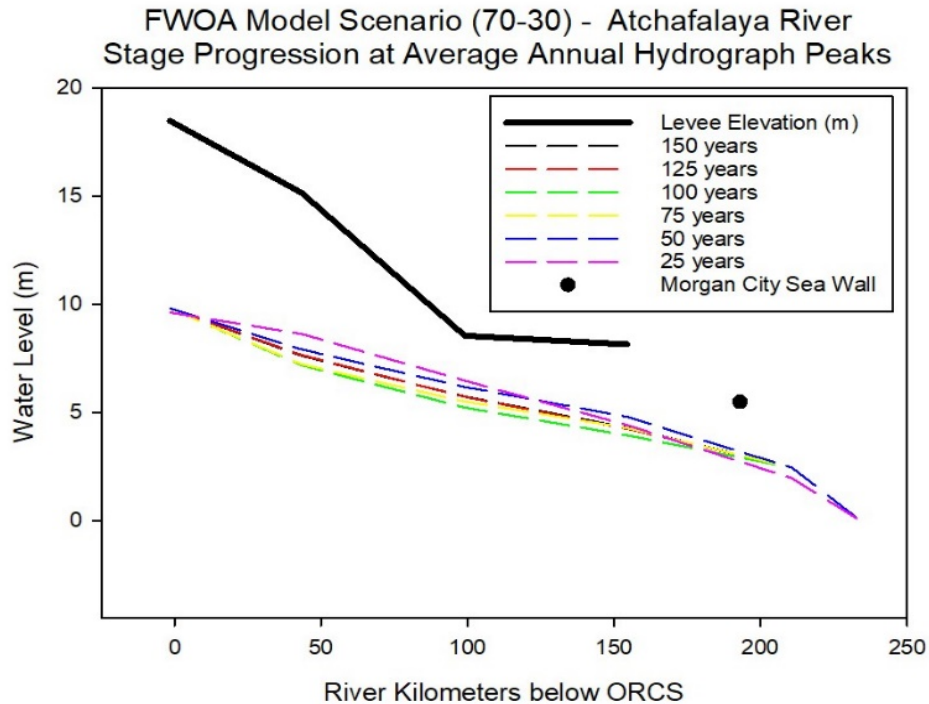


Figure 2.11. FWOA Model Scenario Atchafalaya River Stage Progression for AR Stations at Peak Hydrograph Flows ($\sim 7,500 \text{ m}^3/\text{s}$) and 25-year intervals.

In Figure 2.11 we enumerate a similar stage analysis for the AR branch which shows that for the FWOA model scenario, a decreasing stage trend develops over time at an average annual high flow of $7,500 \text{ m}^3/\text{s}$. General trends indicate that stages become lower over time likely due to further channel incising and flow accommodation, similar to the empirical trends shown in Figure 2.3A. The data in Figure 2.11 are also considered to be conservative since the AR levees encompass the entire AR basin floodway, while the model grid is only of the AR channel, meaning the additional unaccounted for overflow volume between the grid boundaries and the levee alignments would only lower stage values. Hence, current AR basin levee heights are not likely to be threatened by overtopping by average high river flows and could accommodate additional flow from the MR if necessary.

In addition to possibly alleviating flood pressure to the MR levee system and ORCS, diverting more flow into the AR could have potential land building benefits. In Figure 2.12 we plot total sediment transport rates which combines both cohesive and non-cohesive fractions for both the MR and AR over the 150-year modeled time period for both the ORCS Removed and FWOA scenarios. Sediment transport rates are plotted as instantaneous outputs for each time step at Delft 3D observation locations AR Station 4 and MR Station 5 (Figure 2.5) for the unsteady state model. As a frame of reference, towards the end of the model runs, the 70%/30% MR/AR flow split becomes approximately flipped for the ORCS Removed scenario (refer to regression line in Figure 2.6). Also, for clarity, only every 150th data point is shown, meaning the data set includes many additional oscillations between the upper and lower bounds.

For the most part, sediment transport rates remain about the same over the modeled duration in the FWOA scenario for both branches. In the ORCS Removed model run, sediment transport rates decline over time in the MR especially when compared to FWOA at the upper bounds

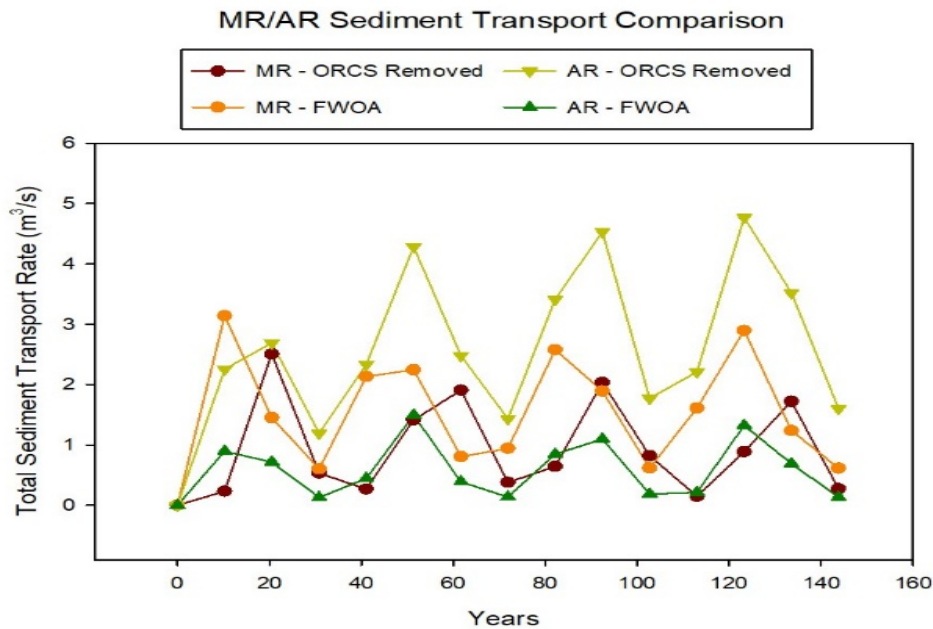


Figure 2.12. Comparison of Sediment Transport Rates between the Mississippi and Atchafalaya River Branches for ORCS Removal and FWOA Model Scenarios.

which correspond to annual Spring flow peaks in the hydrograph. Transport rates in the AR drastically increase when the ORCS is removed, equaling that of the MR almost immediately. Over time, the AR rates continue to significantly increase and by the end of the model run, the AR transports approximately 65% more sediment than the MR currently does and over 3 times the amount that the MR would in the ORCS Removed scenario at the upper bound.

While many factors govern the makeup of the deltaic systems which are regulated by the interaction between boundary conditions and forcing functions, sediment supply is one of the largest drivers (Coleman and Wright, 1975; Orton and Reading 1993; Overeem et al., 2005; Syvitski and Saito, 2007; Dean et al., 2012). Additionally, land building processes have initiated and accelerated in Atchafalaya Bay due to increased delivery of bedload sands and prodelta clays and silts as well as favorable receiving area conditions such as shallow depth and slope (Cratsley, 1975; Shlemon, 1975; Majersky et al., 1997; Roberts, 1999; Allison and Neill, 2002; Roberts et al., 2003; Bentley et al., 2003). Modeling results show that directing additional flow into the AR to reduce MR flood risks would increase sediment input into Atchafalaya and Wax Lake Deltas and potentially enhance already favorable delta-building conditions.

2.7 Conclusions

The problem of the Mississippi-Atchafalaya Diversion has vexed river engineers, scientists, and planners alike since the early 1800s. Over the years, researchers and governmental agencies have studied the diversion and formulated management plans to control its progression in order to protect life and property and allow river commerce to flourish. Conclusions reached in the AR Study conducted by the MRC in the early 1950s resulted in the construction of the ORCS in 1962 which has governed the diversion at a 70%/30% MR/AR flow split ever since.

In this study we revisit the basis of the MRC conclusion and carries them forward by conducting hydraulic and sediment transport modelling simulations using the Delft3D software suite and accounting for complex hydrodynamic interactions from the MR/AR bifurcation to the GOM. Using this tool, we verified MRC data trends to within ± 4 years for the 40-65% capture range and used the model to project forward the final stage of the capture lifecycle over a 150-year period.

Many recent studies have indicated that LMR system below the ORCS is on a retreating geologic trajectory due to contributing factors such as sea level rise, subsidence, faulting, declining hydraulic stream power, and increased sand storage between the LMR MR&T levees resulting in higher flood stages and backstepping of the Plaquemines-Belize bird's foot delta (Brown et al., 2009; Allison et al., 2012; Kemp et al., 2014; Kolker et al., 2014; Bentley et al., 2016). To further evaluate how these assessments project forward we simulated a 150-year FWOA scenario where the ORCS remains in place with operations unchanged. Results reveal that sedimentation will continue to be problematic within the MR branch where stages could increase by up to 3 m in the lower reaches at average annual peak flows, potentially placing the river levee system at New Orleans and below in jeopardy in the next 75 years. Additionally, rising stages from OR to the GOM diminish the sustainability of the LMR and ORCS as currently operated and maintained. Conversely, results from the FWOA stage analysis along the AR branch show stages decreasing accompanying a continually increasing capacity for discharge and sediment transport. All of these trends suggest that while the flow split at the MR/AR bifurcation continues to be regulated by the ORCS, the geologic evolution towards capture gradually continues.

Until recently in geologic history, natural MR avulsion processes went unabated and operated with maximum efficiency. With the current anthropogenic influences which have evolved out of necessity to sustain the development of delta communities and commerce, innovative balances must be sought between ecosystem restoration and protection of human investments. This challenge is being faced similarly around the world in delta systems such as Huanghe, Po, and Nile. Many planning efforts have been initiated in the Mississippi Delta system (CPRA, 2012, 2017; REC and EE, 2016; USACE, 2014; Changing Course, 2019) to develop near-term (50 to 100-year scale) solutions. This study presents a longer-term view of an uncontrolled MR/AR avulsion and capture results reiterate the ORCS's importance to socio-economic factors such as flood control and navigation. However, FWOA results also reveal long-term sustainability concerns for the MR system associated with current flow regulation. In subsequent work, the predictive modeling tool developed will be used to explore how the ORCS could be used to alleviate these concerns along with enhancing ecosystem restoration by augmenting the delta-building processes already at work.

CHAPTER 3: PROJECTED LONG-TERM DELTA-BUILDING RESPONSES TO FLOW MODIFICATIONS AT THE MISSISSIPPI – ATCHAFALAYA BIFURCATION

3.1 Introduction and Purpose

Human interventions have interrupted the latest Mississippi River's (MR) avulsion and the delta cycle which has occurred during the present sea-level high stand of the Holocene period (~7,500 years). Throughout this period the river has delivered sediment to the coast to build land at its mouth, annually extending the length of the river channel until a major flood or other disturbance causes the river to avulse, or change course, seeking a shorter, more efficient path to the GOM (Roberts, 1997). The most recent and currently active delta lobe is the Atchafalaya-Wax Lake (AWL) lobe, which consists of the Wax Lake Delta (WLD) and the Lower Atchafalaya Delta (LAD) and was initiated approximately 400 years ago as a result of ongoing MR stream capture by the Atchafalaya River (AR) (Fisk, 1944, 1952; Latimer and Schweizer, 1951; Gagliano and Van Beek, 1975; Tye and Coleman 1989a, b; Roberts, 1997, 1998; Coleman et al., 1998; Aslan et al., 2005). This capture process accelerated in the early to mid-1900s but further progress was prevented by construction and operation of the Old River Control Structure (ORCS) Complex. The complex originally became operational in 1963 with the low sill and overbank structures, was modified in 1986 with the auxiliary structure, and was completed in 1990 with the hydroelectric station as shown in Figure 3.1. Although this structure complex has limited flow from the Mississippi to the Atchafalaya to 30% of the total combined flow of the Mississippi and Red Rivers (RR) at the latitude of Old River (OR), the deltaic process has continued to advance in the Atchafalaya Basin, Wax Lake and Lower AR Outlets, and in the AWL Deltas.

Since its construction over 50 years ago the ORCS has played an integral part of the Mississippi River and Tributaries (MR&T) flood protection system which protects

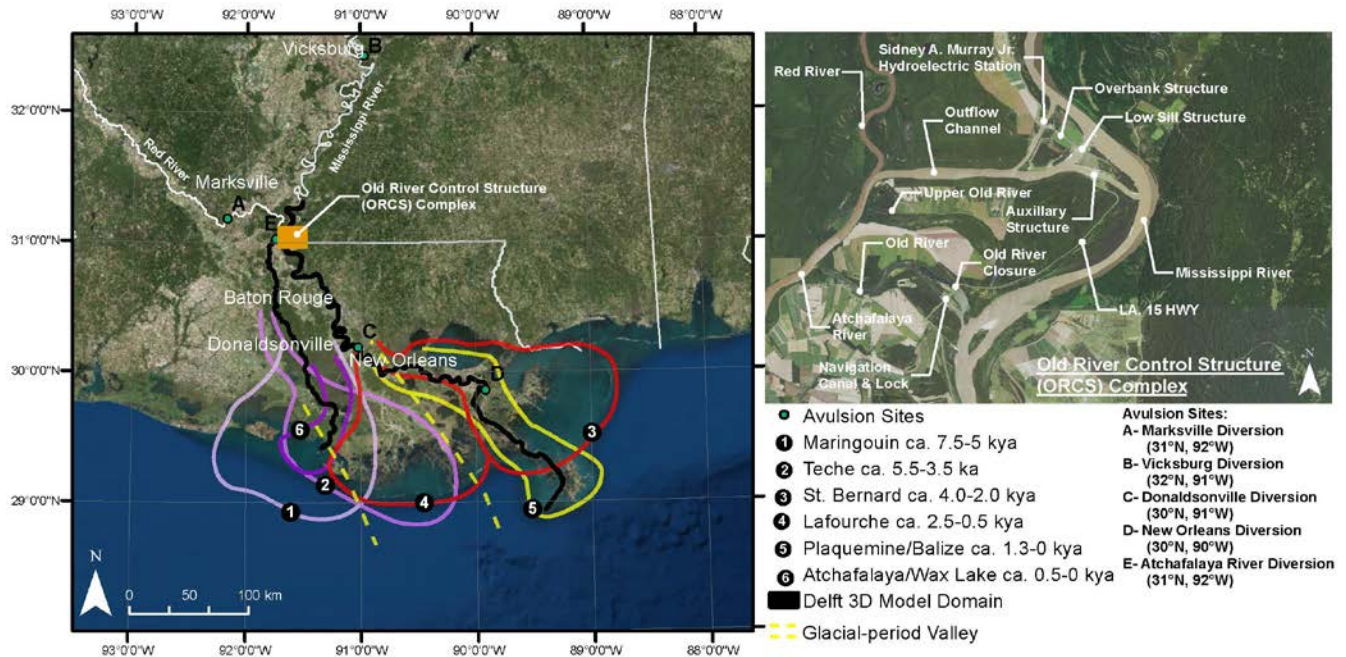


Figure 3.1. Study area depicting Holocene deltas of the Mississippi River (Blum and Roberts, 2012; from Roberts, 1997), Historic avulsion Mississippi River avulsion sites (from Fisk, 1952 and Aslan et al., 2005), Components of the Old River Control Structure Complex managed by the U.S. Army Corps of Engineers, and the Delft3D Model Domain used in this study (from Edmonds, 2012)

approximately 4 million people and prevents billions of dollars in flood damages. In 2011, the system prevented \$234 billion in flood damages alone. The system also provides tremendous benefit to the national economy and international trade markets. Each year, approximately 500 million tons of cargo move on the MR system and \$2.7 billion in domestic transport savings are realized from its operations (USACE, 2015). Below the ORCS between Baton Rouge and New Orleans, the Lower Mississippi River (LMR) is home to four of the fifteen largest ports in America which handle over 60% of all grain exports to the world. Barge traffic moving upriver supply petrochemicals, fertilizers, and raw materials which feed the U.S. agricultural industry among many others. It is estimated that shipping through the LMR is worth \$295 million per day. Additionally, the LMR provides fresh drinking water to over 1.5 million people (Masters, 2019).

This level of socio-economic sustainability has been made possible by the MR&T system and the ORCS, however geomorphic changes in the LMR make its future uncertain. Development of a large mid-channel bar near the ORCS, gradual loss of downstream cross-sectional area and flow capacity, and increased sedimentation and rising stages all contribute the rising concerns over the sustainability of the ORCS Complex and the long-term efficacy of its current operation mandate (Latimer and Schweizer, 1951; Fisk, 1952; Kesel et al., 1992; Hudson and Kesel, 2006; Heath et al., 2015; Knox and Latrubesse, 2016; Wang and Xu, 2016). The MR&T levees have also contributed to these issues by drastically reducing the connectivity of the MRDP with its riverine sediment source, thereby exacerbating land loss rates during the last century in which Louisiana has lost about 25% or 4800 km² of its coastal wetlands (Day et al., 2000, 2007, 2016b; Couvillion et al., 2011; CPRA, 2012, 2017a).

In the past few decades, a number of engineered solutions have been identified as large-scale restoration tools for reconnecting the river to its delta plain. Dredge-based projects use river sediments to build land by filling nearby open water areas to create marsh and barrier islands. This has proven to be a cost-effective measure for near-term, small-scale projects when benefit cost ratios and ecosystem service values are compared to existing river diversions which have been hampered by social constraints such as fisheries, landownership, and navigation interests which influence and limit diversion operations (Caffey et al., 2014). To date, the Louisiana Coastal Protection and Restoration Authority (CPRA) has constructed three river diversions: Caernarvon and Davis Pond diversions (227 and 285 m³/s, respectively) to control salinity intrusion, and the West Bay diversion (1,416 m³/s) to divert sediment to restore wetlands near the mouth of the river by reintroducing natural delta building processes. While the positive benefits of these projects represent progress, much bolder action is needed to mimic the MRDP's

historic functioning and combat the scale of the problem (CH2MHill, 2004; Condrey et al., 2014; Day et al., 2016b). Many studies have explored the efficacy of engineered sediment diversions and have demonstrated their potential for large-scale, long-term restoration (DeLaune et al., 2003; Simenstad et al., 2006; Day et al., 2007, 2016b, 2018; Kim et al., 2009; Allison and Meselhe, 2010; Paola et al., 2011; CPRA, 2012, 2017a; Dean et al., 2012, 2014; Nittrouer et al., 2012; Wang et al., 2014).

As such, CPRA is currently planning two large-scale MR sediment diversions below New Orleans. The Mid-Barataria (MBA) Diversion is being planned for River kilometer 97.7 on the west side of the river, near Myrtle Grove (Fig. 3.4b). The maximum planned flow of 2,124 m³/s is estimated to create approximately 120 km² in 50 years. The Mid-Breton (MBR) Diversion is currently being planned for River kilometer 110.4 near Wills Point on the east side of the river (Fig. 3.4b). The plan is to operate this diversion at a maximum flow of 991 m³/s to create an estimated 64 km² in 50 years (CPRA, 2012, 2017a). These two diversions are positioned with receiving areas which will intersect the late Holocene Lafourche and St. Bernard delta complexes which formed on the inner shelf. Potential diversion locations further downstream closer to the Plaquemines-Belize delta (PBD) at the shelf margin would create less sustainable land-surface area due to higher subsidence rates and less emergent marsh areas which help to retain clastic inputs and promote accumulation of organic material (Blum and Robert, 2012).

Building on the planning efforts of these two projects and CPRA's Comprehensive Master Plan for a Sustainable Coast (CMP), in 2015 the privately funded design competition, Changing Course, selected consulting teams to develop conceptual 100-year visions for restoring and sustaining the LMR Delta through channel realignment, while continuing to meet the needs of communities, fisheries, industry, navigation, and flood protection. The competition focused on

restoring the MR's natural land-building capacity to create a self-sustaining coastal ecosystem while continuing to support the high-functioning navigation system in the lower river. Solutions presented in the vision plans included increasing the number of diversions to reconnect coastal basins with their parent source; seasonal flood pulsing and ecosystem recovery periods; abandoning the PBD due to its unsustainable subsidence rates; creating a shorter navigation route to the gulf and relocating supporting port infrastructure; creating spillways, settling basins, and sediment traps that reorganize dredging operations and maximize beneficial use opportunities and take advantage of littoral transport patterns; and even modifying the 70/30 MR/AR flow split at the ORCS to 80/20 in order to send more freshwater and sediment through the LMR system and these proposed alterations (Changing Course, 2019).

Recognizing the efficacy of the suggested Changing Course solutions, no consideration was given to the feasibility of further enhancing the AWL Lobe as a sustainable progression of the delta cycle (Roberts, 1997). This would also involve a modification of the ORCS flow split by increasing the AR percentage into a basin that has been preparing geologically to receive it for over a century (Latimer and Schweizer, 1951; Fisk, 1952; Andrus, 2020). Conversely, many recent studies have indicated that LMR system below the ORCS is on a retreating geologic trajectory due to contributing factors such as sea level rise, subsidence, faulting, declining hydraulic stream power, and increased sand storage between the LMR MR&T levees resulting in higher flood stages and backstepping of the PBD (Brown et al., 2009; Allison et al., 2012; Kemp et al., 2014; Kolker et al., 2014; Bentley et al., 2016). Diversions along the LMR currently being planned by CPRA and suggested in the Changing Course vision documents would partially alleviate these risks by altering the LMR hydraulics and making flow paths shorter to the gulf which would increase gradient and stream power. However, many physical and socio-economic

challenges could limit the implementation and effectiveness of these suggested solutions in the LMR over the next century. The purpose of this study is to use various modeling techniques to alternatively explore the long-term land-building potential of progressively continuing the avulsion at the MR-AR bifurcation in a controlled manner through the ORCS. While abandoning LMR restoration efforts is not an option, results could give planners and policy makers another complimentary river management strategy to consider. Therefore, land-building in the AR will be compared to the MBA and MBR diversions in the MR as the largest, most-sustainable diversions currently being planned.

3.2 Methods

Since the early 1800s, much energy has been spent on scientific research, legislative mandates, engineering development, and construction of control structures and levees to protect public and private interests affected by the Mississippi-Atchafalaya bifurcation at Old River (Ellicot, 1803; Schultz, 1810; Darby, 1816; Humphreys and Abbot, 1876; MRC, 1881; Elliot, 1932; Salisbury, 1937; Graves, 1949; Kemper, 1949; Halsey, 1950; Odom, 1950; Latimer and Schweizer, 1951; Fisk, 1952). These efforts resulted in the construction of the ORCS low sill and overbank structures in 1962 however, they were nearly lost in Flood of 1973. While hundreds of millions of dollars were spent fortifying the system by adding additional structures (Figure 3.1), this led to fundamental questions regarding its long-term stability and consideration of alternate long-term strategies such as a controlled diversion of increasing flows through the Atchafalaya Basin over the course of decades (Kazmann and Johnson, 1980; Kolb, 1980; Martinez, 1986). More recently, river management research efforts have focused on coastal restoration implications along the lower delta reaches of both MR and AR systems (CPRA, 2012,

2017a). Ultimately, the delta building capabilities of these two rivers are highly driven by water and sediment inputs which have been regulated over the last sixty plus years at the ORCS.

This study uses both 1D and 2D numerical modeling techniques to evaluate the long-term effects of current water and sediment regulation mandates and test alternative regulation strategies with respect to delta-building goals. Riverine hydraulic and sediment transport modelling was performed using the Delft 3D modelling software suite developed by Deltares. Delft 3D is a unique, fully integrated modelling framework for a multi-disciplinary approach and 3D computations for coastal, river, lake, and estuarine areas. It can carry out numerical modelling of flows, sediment transport, waves, water quality, morphological developments and ecology. The Delft 3D framework is composed of several modules, grouped around a mutual interface, while being capable to interact with one another (Deltares, 2014). The modules that will be used in this study are Delft3D-FLOW and MOR 2D for hydrodynamic, salinity, temperature, transport and online coupling of morphology and Delft 3D-SED for cohesive and non-cohesive sediment transport. This study also makes use of a grid domain and input parameters developed by Edmonds (2012) and modified by Andrus (2020) that is relatively coarse to facilitate reasonable computational times for the large domain and duration. The domain extends down to meet the GOM but does not incorporate detailed deltaic planforms and channel structures.

In this study we set out to evaluate changes in overall delta area over long periods of time (i.e. hundreds of years). While Delft 3D models with fine resolution grids have been constructed of both delta systems (Hanegan, 2011; Meselhe et. al., 2016) to evaluate shorter-term evolution (i.e. sub-decadal and decadal scales as opposed to century scale), we chose to use a 1D spatially averaged equation developed by Dean et. al. (2012) (Dean model) which is capable of simulating

decades of delta growth using a spreadsheet without requiring multiprocessor computers and acceleration factors. The main goal of the Dean model is to predict the most important bulk properties of delta growth such as shoreline change and growth in delta area, given the water and sediment supply, general configuration and sediment retention properties of the receiving area, and local relative sea level rise. A recent study evaluated a similar 1D model by Kim et al. (2009) vs. a process-based 2D Delft 3D model to compare and contrast land-building simulations. Results showed that the 1D modeled consistently over predicted delta radii and areas by approximately 30%. While the 1D model does not produce the same level of detail with sinuous distributary channels and sediment stratigraphy, it remained relatively close in magnitude and ran 1200 times faster, giving it a distinct advantage for longer time scale evaluations (Baysal, 2014).

3.2.1 Delft 3D Model Background

In a recent study which evaluated backwater effects on the stability of the MR-AR bifurcation, hydraulic and sediment transport modelling was performed using the Delft 3D software suite where Edmonds (2012) built a computational domain and grid (Figure 1) which began 45 km upstream of the bifurcation and extended to the GOM on both the Mississippi and Atchafalaya branches, with the two branches connected through the bifurcation and the ORCS removed. The grid is a 2D planform composed of ~20,000 cells with a typical size of 100 m x 900 m with the long axis extending downstream. The grid extends from bank to bank with this width remaining fixed but allowing the bed form to change with evolving hydrodynamics and sediment transport. Dry cells were added around the bifurcation to simulate its real-world complexity. The last constraint of the model setup was not to include tributaries or floodplains. These exclusions were considered justifiable given that man-made levees confine river flows in

the majority of reaches. Sensitivity tests were run on the system's largest tributary, the RR, resulting in little to no impact on the results (Edmonds, 2012).

In all model runs, bed roughness is a uniform Chezy value of $65 \text{ m}^{1/2} \text{ s}^{-1}$. A time step of 60 s was used. Bed adjustments were sped up by multiplying the bed sediment flux in each time step by a morphological scale factor set to 50. This is within the stable range (Ranasinghe et al., 2011) and was verified with sensitivity tests. At the upstream boundary, Edmonds specified the water discharge and sediment fluxes with the incoming discharge carrying two grain sizes, one noncohesive ($200 \text{ }\mu\text{m}$) and one cohesive ($15 \text{ }\mu\text{m}$). At the downstream boundaries, water surface elevations are set to zero. The initial bed topography in each river is from 2004 and 2006 hydrographic surveys of the Mississippi and Atchafalaya, respectively. For each river Edmonds calculated the cross-sectionally averaged centerline bed elevations every kilometer. In the subsurface, there is initially 10 m of sand and 2 m of mud available for erosion, consistent with observations (Galler and Allison, 2008; Nittrouer et al., 2011a). This model setup accurately predicts the water surface elevations in the MR to within 10–15% at different flow stages (Nittrouer et al., 2011b), corroborating these boundary condition choices. To assess the sensitivity of the results Edmonds conducted repeat experiments and varied the time step, bed roughness, the grid resolution, sediment transport formulas, sediment size, and initial volume of sediment in the subsurface. Varying each of these leads to a different solution in the details, but the behavior of the discharge ratio between the rivers is not different by more than 15% (Edmonds, 2012).

As part of a previous phase of this study (Andrus, 2020), we collaboratively built on the Delft 3D model calibrated by Edmonds to conceptually resurrect the hydrographic and geomorphic evolution of the MR-AR bifurcation suspended by the ORCS. Using the model grid, boundary

conditions, and run parameters from the 2012 analysis, we created long-term semi-unsteady state input conditions in order to re-evaluate the bifurcation without the ORCS in place in addition to evaluating long-term flow and stage developments in both branches with current management strategies unchanged. For this run, an average annual hydrograph was formulated using an 80+ year Q_{up} dataset from Vicksburg, MS for the time period from 1931 to 2015 acquired from USGS Site 07289000 (Figure 2). This hydrograph was then repeated 150 times to observe the evolution of the capture progression in this long-term scenario. Using this tool, we compared against measured data trends published by the MRC (Latimer and Schweizer, 1951) and matched them to within ± 4 years for the 40-65% capture range and used the model to project forward the final stage of the capture lifecycle over a 150-year period. Hence, it is surmised that applying the semi-unsteady state approach to the Edmonds Delft 3D model is an effective predictor of long-term trends for the MR-AR bifurcation and downstream impacts for both river branches. This further validates the work of Edmonds in constructing the model and choosing its inputs such as grid resolution and boundary conditions; initial bed elevations, composition and thickness; sediment flux parameters and transport formulas, all of which were thoroughly tested against recent datasets and now replicate patterns found in long-term measurements and geologic tendencies of historic avulsions.

3.2.2 Delft 3D Model Modifications for this Study

Moving forward with a model that coalesces evolving geologic patterns associated with historic avulsions (Andrus, 2020) with recent realizations in backwater hydraulics (Edmonds, 2012), these updated model conditions are now used in this study to consider new flow split and delta-building scenarios. Understanding the magnitude of the policy deliberations leading to the legislative decision to construct and maintain the ORCS, the experimental design does not

consider a future without artificial control of the bifurcation and is intended to evaluate long-term, engineered changes which could be realistically implemented if future socio-economics assessments eventually justified them.

With the current MR to AR flow split being maintained at 70% to 30%, it can be logically postulated that a gradual flip of these percentages could be achievable. A MR to AR flow split transition to 30/70 (Scenario 9 in Table 3.1) would have to be carried out over a timeframe that would adequately allow for social, economic, and flood risk adjustments to be made on the same scale as what would be the largest modification to the MR&T project since its authorization by the 1928 Flood Control Act. To date the MR&T project is an estimated 87% complete, putting it on pace for a 100-year implementation timeline. The project provides flood protection for approximately 4 million people in the world's third largest watershed from Cape Girardeau, Mo. to Venice, LA (USACE, 2015). Louisiana's CMP projects a 50-year completion timeline (CPRA, 2012, 2017a) and the Dutch Delta Works were completed in 1997, 44 years after the "Deltaplan" was commissioned in 1953 to protect the southwestern portion of the Netherlands around the Rhine-Meuse-Scheldt delta from North Sea flooding (Aerts, 2009; Kind, 2014). Given that these two efforts are similar in scale and duration and must work in concert with larger national flood protection programs to protect lands and residents at their delta interfaces, a 50-year implementation timeframe for flow adjustments will be used for the experimental design in this study. Given the scale of the proposed action, an additional 50 years will be added to each scenario beyond implementation to sufficiently analyze delta response trends into the future. Another 50 years will be added to this timeframe on the front end to accommodate implementation of the CMP projects proposed by the State of Louisiana in 2017, many of which are underway.

Table 3.1 below outlines 12 scenarios (1 No Change scenario, 8 increased AR flow scenarios, and 3 increased MR flow scenarios) where flow adjustments are made gradually over time in 5% increments. The first two increments are made over 15 and 10 years, respectively, to account for modifications that would need to be made to the ORCS, levee and flood protection systems, dredging templates within navigation channels, and sediment management strategies the Atchafalaya Basin. It is assumed that subsequent modifications would be more manageable once the initial adjustments are engineered, constructed, and monitored with future adjustments in mind. Therefore, further flow adjustment increments are made over 5-year periods. In total, the duration of each scenario studied would be 150 years, which is approximately 10% of the life of historic Mississippi River delta complexes (Fisk, 1952; Frazier, 1967; Roberts, 1997).

To create these flow regimes two separate input files were created for each scenario, one for each river branch, where the flow percentages and respective durations from Table 3.1 were applied to the average upstream hydrograph created from the Vicksburg USGS Gage data. The complete model grid from Figure 3.1 was then broken into individual MR and AR model grids below the ORCS (Figure 3.2) for model runs in which the ORCS remains in place with operational schemes from Table 3.1. In order to simulate how the ORCS would be operated for each scenario, the modified hydrograph input files were used as the upstream boundary flow conditions for the MR only and AR only grids and run as two separate models. Lastly, Figure 3.2 shows six observation locations chosen for each river branch and specified in the Delft 3D setup files. Output parameters for each station include water level, discharge, and sediment transport rates broken down into cohesive, non-cohesive, bedload, and non-bedload components.

Table 3.1. Modeled flow split alteration scenarios at the MR-AR bifurcation

INCREASED ATCHAFALAYA SCENARIOS												
Scenario 1 (No Change)				Scenario 2 - 65/35 Split				Scenario 3 - 60/40 Split				
MR%	AR%	Duration (Yrs)	Period	MR%	AR%	Duration (Yrs)	Period	MR%	AR%	Duration (Yrs)	Period	
70	30	50	MP Implemetation	70	30	50	MP Implemetation	70	30	50	MP Implemetation	
70	30	100	No Change	65	35	100	Flow Adjustment & Delta Response	65	35	15	Flow Adjustment	
								60	40	85	Flow Adjustment & Delta Response	
Scenario 4 - 55/45 Split				Scenario 5 - 50/50 Split				Scenario 6 - 45/55 Split				
MR%	AR%	Duration (Yrs)	Period	MR%	AR%	Duration (Yrs)	Period	MR%	AR%	Duration (Yrs)	Period	
70	30	50	MP Implemetation	70	30	50	MP Implemetation	70	30	50	MP Implemetation	
65	35	15	Flow Adjustment	65	35	15	Flow Adjustment	65	35	15	Flow Adjustment	
60	40	10	Flow Adjustment	60	40	10	Flow Adjustment	60	40	10	Flow Adjustment	
55	45	75	Flow Adjustment & Delta Response	55	45	5	Flow Adjustment	55	45	5	Flow Adjustment	
				50	50	70	Flow Adjustment & Delta Response	50	50	5	Flow Adjustment	
								45	55	65	Flow Adjustment & Delta Response	
Scenario 7 - 40/60 Split				Scenario 8 - 35/65 Split				Scenario 9 - 30/70 Split				
MR%	AR%	Duration (Yrs)	Period	MR%	AR%	Duration (Yrs)	Period	MR%	AR%	Duration (Yrs)	Period	
70	30	50	MP Implemetation	70	30	50	MP Implemetation	70	30	50	MP Implemetation	
65	35	15	Flow Adjustment	65	35	15	Flow Adjustment	65	35	15	Flow Adjustment	
60	40	10	Flow Adjustment	60	40	10	Flow Adjustment	60	40	10	Flow Adjustment	
55	45	5	Flow Adjustment	55	45	5	Flow Adjustment	55	45	5	Flow Adjustment	
50	50	5	Flow Adjustment	50	50	5	Flow Adjustment	50	50	5	Flow Adjustment	
45	55	5	Flow Adjustment	45	55	5	Flow Adjustment	45	55	5	Flow Adjustment	
40	60	60	Flow Adjustment & Delta Response	40	60	5	Flow Adjustment	40	60	5	Flow Adjustment	
				35	65	55	Flow Adjustment & Delta Response	35	65	5	Flow Adjustment	
								30	70	50	Flow Adjustment & Delta Response	
INCREASED MISSISSIPPI SCENARIOS												
Scenario 10 - 75/25 Split				Scenario 11 - 80/20 Split				Scenario 12 - 85/15 Split				
MR%	AR%	Duration (Yrs)	Period	MR%	AR%	Duration (Yrs)	Period	MR%	AR%	Duration (Yrs)	Period	
70	30	50	MP Implemetation	70	30	50	MP Implemetation	70	30	50	MP Implemetation	
75	25	100	Flow Adjustment & Delta Response	75	25	15	Flow Adjustment	75	25	15	Flow Adjustment	
				80	20	85	Flow Adjustment & Delta Response	80	20	10	Flow Adjustment	
								85	15	75	Flow Adjustment & Delta Response	

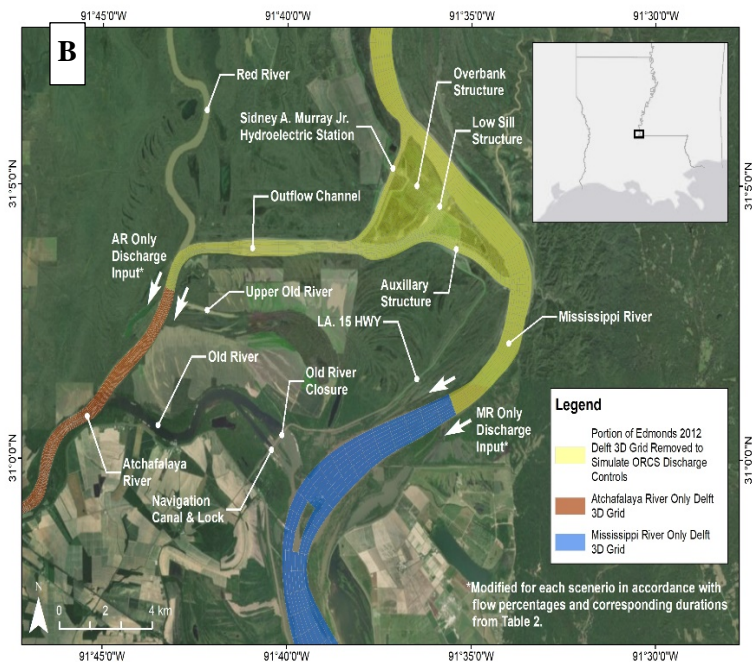
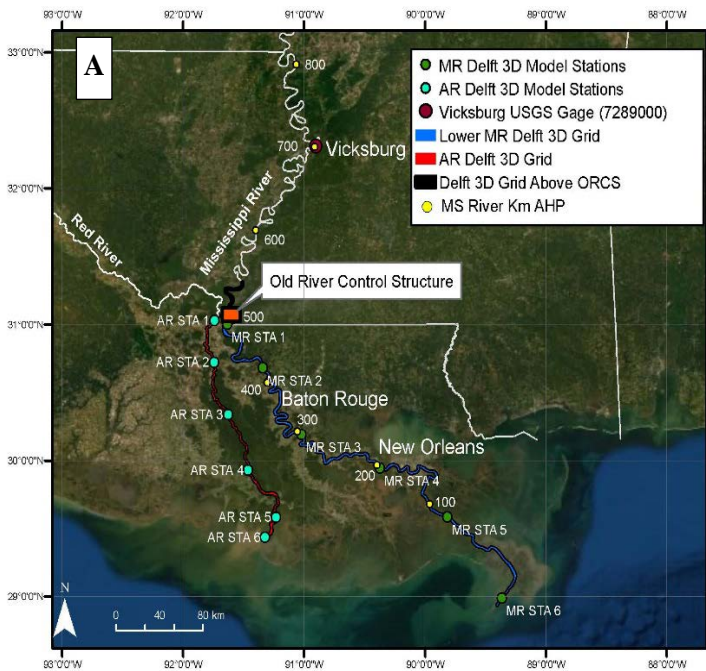


Figure 3.2. A) USGS river gage and Delft 3D grid and output station location map. B) Closeup of Delft 3D grids and model discharge input locations near ORCS.

3.2.3 1D Land-building Model Setup

In a guidance document prepared for the USACE, the State of Louisiana, and the U.S. Geological Survey, Dean et al. (2012) broadly categorized the factors that control the performance of river diversion as 1) basin geometry, 2) sediment characteristics, 3) biological factors, 4) water motion (e.g. sea level rise), and 5) design and operational strategies. The document used these broad concepts to formulate Equation 1 for the radius, r_0 of an idealized truncated cone receiving area delta geometry, as shown in Figure 3.3 and expressed as:

$$r_0 = -\frac{\alpha}{2m} + \sqrt{\frac{2V}{\alpha\Delta\theta} - \frac{\alpha^2}{12m^2}} \quad (\text{Eq. 1})$$

where m = front slope of the delta foreset; α = total depth of deposit, inclusive of sea level rise and subsidence; the volume of the truncated cone, $V = Qt$ and Q is the discharge rate of the retained sediments including “bulking” effects and t is time; $\Delta\theta$ = angle over which uniform angular radial spreading flow occurs. Inputs for V are taken from Delft 3D sediment transport rates at each time step exported from appropriate output stations shown in Figure 3.2. Once the r_0 is calculated, then the area of the subaerial portion of the delta can be found by using the formula for a circle segment, expressed as equation 2:

$$A = \frac{r_0^2}{2} \left(\frac{\pi}{180} \Delta\theta - \sin\Delta\theta \right) \quad (\text{Eq. 2})$$

While this formula does not account for the area of the foreset, this is considered to be negligible since most of the forest is subaqueous.

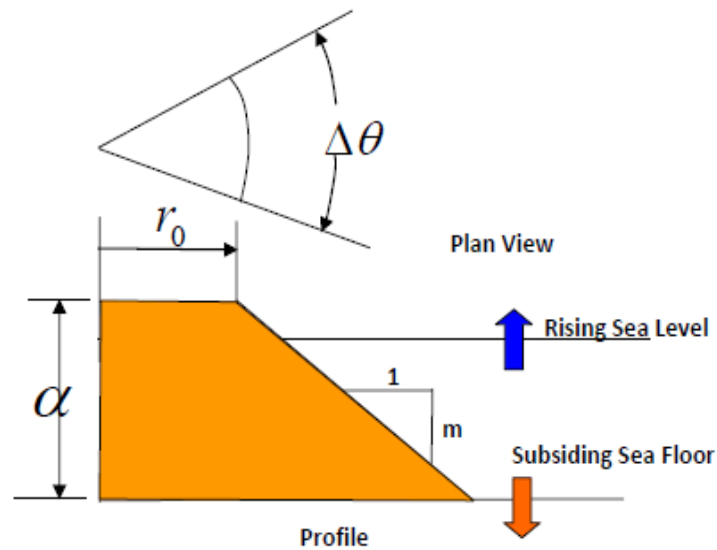


Figure 3.3. Definition sketch of a truncated cone in water of uniform/average depth (from Dean et al., 2012).

3.2.3.1 Receiving Area Characteristics

With the transgressive nature of the PBD at its outermost reaches near the GOM, upstream migration of stream power and depocenters, and delta backstepping trends, restoration planners have targeted land-building diversions for upstream locations with receiving basins in Barataria and Breton Sound Basins, which also have lower subsidence rates and higher sediment trapping efficiencies than the PBD (CPRA, 2017a). Therefore, this study uses the MBA and MBR planned diversions, their operating strategies, and receiving area characteristics to evaluate future long-term land building potential of the MR branch. While other diversions and outlets such as West Bay and Bohemia Spillway currently operate and provide restoration benefits, their outfalls are located in areas of radical subsidence and the future of the Lower MR will likely be greatly altered by extreme transgressive marine processes and drastically engineered solutions to combat them (CPRA, 2017; Changing Course, 2019). The MBA and MBR diversions also represent the two largest restoration project investments currently being considered with well documented

long-term flow regimes and land-building estimates that will be easily comparable to the AR (Kim et. al., 2009; CPRA, 2017).

In the AR branch, delta building currently occurs in the WLD and LAD in Atchafalaya Bay. Nearly 100% of the flow and sediment from the Lower AR feed these two deltas, therefore land building potential is maximized. Our approach is to evaluate all of this potential by modeling 1D land building by diverting all flow and sediment to only one of the deltas, namely WLD. This makes the calculations more straightforward as the receiving characteristics for both deltas are very similar. This is also consistent with the needs of the Port of Morgan City who would rather less sediment effecting shoaling rates in the navigational channel below the port (M. Wade, 2019). This could be achieved by

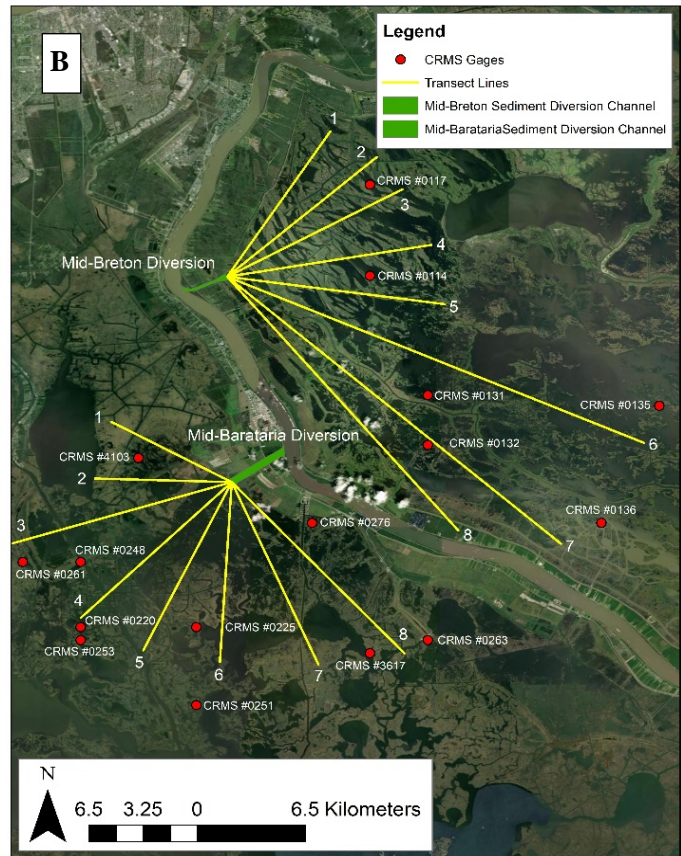
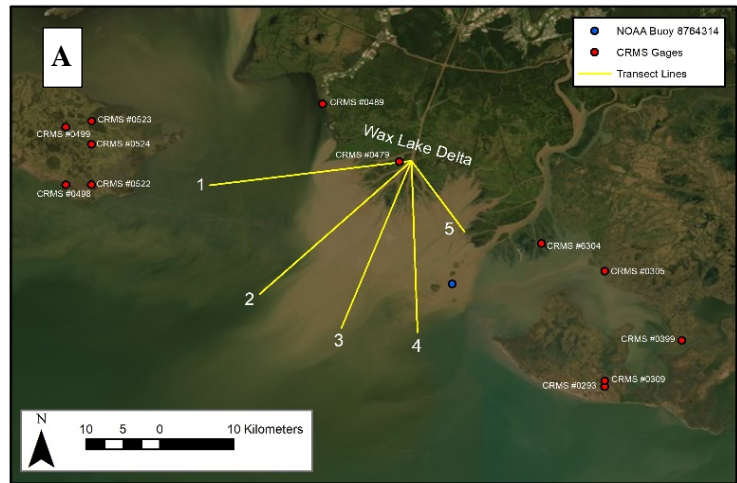


Figure 3.4. 1D modeled receiving areas showing transects used to acquire elevation data and diversion angle, $\Delta\theta$, and water level and subsidence monitoring locations for A) Wax Lake Delta in the AR and B) Mid-Barataria and Mid-Breton Diversions in the MR.

engineering a sediment control structure on the Lower AR downstream of the Wax Lake Outlet (WLO) channel diversion location. This concept will be further evaluated during a subsequent economic analysis.

Figure 3.4 shows the AR and MR modeled receiving areas, transects used to acquire elevation data from NOAA (2019) and water level monitoring stations provided by NOAA and CPRA's Coastwide Reference Monitoring System (CRMS). Monitoring stations datasets were analyzed to determine local mean water levels (MWL) as an upper bound for deltaic deposits and an approximate indicator for healthy marsh falling within optimal inundation levels of the intertidal zone (CPRA, 2017b). A normal tidal epoch lasts approximately 19 years; however, since recent sea level changes have been anomalous and each of the receiving areas are affected by diversions such as the WLO, Davis Pond, and Caernarvon, a modified tidal epoch of 5 years was used in order to capture the most recent water level trends (NOAA, 2003; CPRA, 2017a). For the WLD, a long-term dataset from NOAA Buoy 8764314 was used to determine a local MWL of 0.308 m in the NAVD88 elevation datum. CRMS stations 0248 and 0114 were used to determine MWL NAVD88 elevation values of 0.184 m and 0.211 m for the MBA and MBR receiving areas, respectively.

To account for elevation variations and bottom slopes, topography and bathymetry data were averaged over all transects for each receiving area resulting in average NAVD88 bottom elevations of -1.43 m, .003 m, and 0.104 m for the WLD, MBA, and MBR diversions, respectively. Diversion flow angle, $\Delta\theta$, was also measured between outermost transects for each receiving area resulting in angles of 115°, 164°, and 104° for the WLD, MBA, and MBR diversions, respectively. As can be seen in the 2019 aerial imagery in Figure 4, the MBA and MBR receiving areas are farther up in the estuary and contain more broken marsh habitat which

is more efficient in trapping sediment than the open bay setting for the WLD receiving area which is more susceptible to wave and tide erosion (Neumeier and Ciavola, 2004; Wilson and Allison, 2008; Li and Yang, 2009). Moreover, imagery analysis by Barras et al. (2003) indicated that the MBR receiving basin contains ~20% more emergent marsh than MBA.

Xu et al. (2019) plotted a semi-quantitative linear relationship between river kilometer (RK) (upstream of the Head of Passes of the MR or the river mouth of the AR) and sediment retention rate derived from 8 different studies and demonstrating a rough proxy of basin connectivity to the open ocean. Of the studies related to the proximity of our receiving areas Wells et al. (1984) reported a 27% retention rate in Atchafalaya Bay, Esposito et al. (2017) reported a range of 3-40% in WLD, Day et al. (2016a) reported a range of 55-75% at Caernarvon, just upstream of MBR, and Keogh et al. (2019) reported a range of 44-81% for the Davis Pond diversion which discharges into the Barataria Basin, although Davis Pond is located 98 RK upstream of the MBA diversion site. Furthermore, Bomer et al. (2019) concluded that MBR would be more likely to have a higher sediment retention rate than MBA due to the presence of ~40% more highly erodible organic-rich peat and muds and ~47% less interbedded deltaic sands and silts which are more erosion resistant in the MBA receiving area. Given the results of these previous studies, we have selected sediment retention rates of 30%, 50%, and 70% for the WLD, MBA, and MBR receiving areas, respectively. These retention rates will be applied to the cohesive mud fraction of the suspended sediment profile output from Delft 3D. Deposition of the coarsest material (fine sand, coarse silt) likely takes place roughly four channel widths into the receiving from the mouth of the diversion (Wright and Coleman, 1974).

Dean et al. (2012) defined bulk density as the dry mass per unit volume of the *in-situ* deposit, and also being a measure that reflects the relative amount of organic versus inorganic sediment,

and water content. Organic matter may contribute more than 50% of the sediment volume once a diversion deposit becomes subaerial and is accounted for through “bulking factors”. In estimating bulking factors, a sediment porosity of 75% with respect to 25% mineral sediment content was used and organic matter was varied based on water depth which effects time to become subaerial, open water area vs. marsh, and distance from the GOM which is a proxy for salinity. With a bottom elevation approximately 1.5 m deeper and a close proximity to the GOM, a low-level organic matter content of 40% was chosen for WLD. Situated 98 km upstream of the Head of Passes, a medium-level organic matter content of 50% was chosen for the MBA diversion site. Similarly, a slightly higher-level organic matter content of 55% was chosen for the MBR diversion site, being situate 110 km upstream of Head of Passes and having less open water than MBR. These inputs were then applied to Equation 3 to determine bulking factors:

$$B.F. = \frac{1}{M.C.(1-O.C.)} \quad (\text{Eq. 3})$$

where B.F. = bulking factor, M.C. = % mineral content, and O.C. = % organic content. The inputs selected for each diversion resulted in bulking factors of 6.7, 8.0, and 8.9 for WLD, MBA, and MBR, respectively. Moreover, these values are within the suggested ranges by Dean et al. (2012).

As with sediment retention and bulking factors, foreset slope is also affected by a diversion deposit’s proximity to the open GOM. Building on the earlier works of Parker et al. (1998), Kostic and Parker (2003), Parker et al. (2008), Twilley et al. (2009), and Kim et al. (2009), Dean et al. (2012) recommends a range of final foreset slopes between 0.002 and 0.005. The smaller slopes would be associated with smaller grain sizes and greater tidal current and wave action, conditions which decrease with distance away from the GOM. Slope values tend to be an order

of magnitude greater during early phases of a diversion where embryonic delta growth is mostly comprised of sandier material, there is very little vegetative biomass, and sediment trapping of fine-grained sediments is low. Given that this study has a long-term duration of 150 years, we use the recommended final deposit range for the analysis. Hence, we chose foreset slopes of 0.002, 0.004, and 0.005 for WLD, MBA, and MBR, respectively.

3.2.3.2 Subsidence and Sea Level Rise

Relative Sea Level Rise (RSLR), defined as Eustatic (global) Sea Level Rise (ESLR) combined with site-specific subsidence, will also play a major role in the rate of long-term delta growth. Coastal Louisiana has RSLR rates among the highest in the world (12 ± 8 mm per year) (Jankowski et al., 2017). Still, with adequate sediment input (> 20 mg/l) and in microtidal (< 2 m) environments, multiple marsh model dynamic models predict that susceptibility to drowning will not occur below ~ 10 - 12 mm per year of RSLR. This is especially true in the short-term where surface elevation change can increase through increased plant productivity, organic matter accretion, increased mineral deposition, and trapping of clastic sediment (Reed, 1995; Morris et al., 2002; Kirwan et al., 2010; Fagherazzi et al., 2012). Ultimately, this becomes an interplay between the vertical accretion rates and subsidence in determining whether net surface elevation gain occurs by outpacing RSLR (Cahoon et al., 1995).

Accordingly, some efforts through various techniques and data sources have been made to quantify subsidence in south Louisiana (Dokka et al., 2006; Kent and Dokka, 2013; Reed and Yuill, 2016). However, the most comprehensive undertaking to date by Jankowski et al. (2017) used the worlds' largest data set by far of 274 CRMS records and a well-established method rod surface-elevation table marker horizon (RSET-MH) measurements (Steyer et al., 2003; Webb et al., 2013). Table 3.2 lists the most applicable sites (also shown in Figure 3.4) and summarizes

subsidence data for each diversion. Previous work has suggested that subsidence rates increase with the thickness of Holocene strata (Meckel et al., 2006; Törnqvist et al., 2008), however Jankowski et al. (2017) showed rates to be similar across varying Holocene thicknesses and more dependent on site specific shallow subsidence within the uppermost 5-10 m.

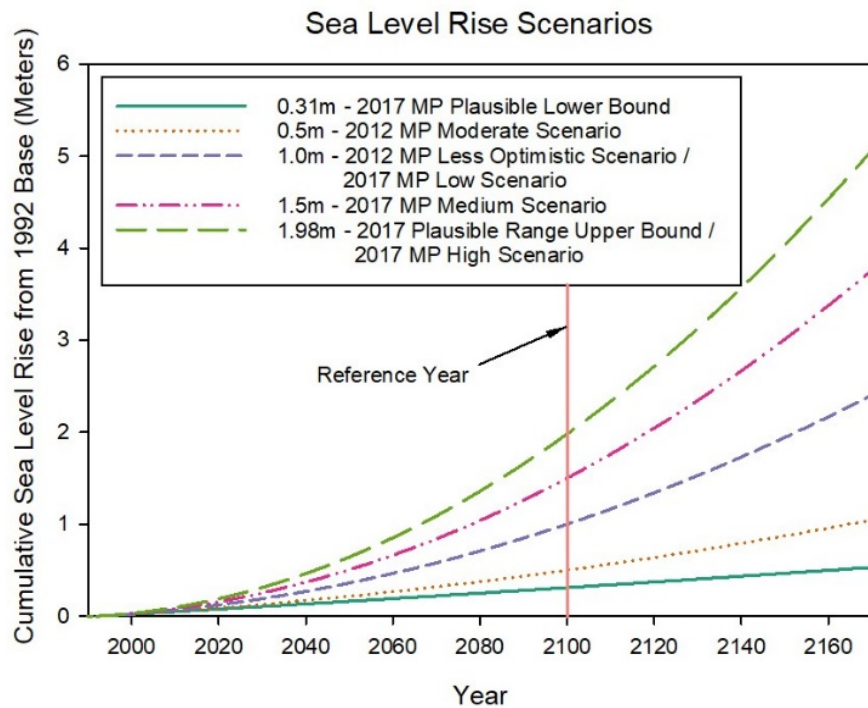


Figure 3.5. Eustatic Sea Level Rise Scenarios used for 1D land-building estimates (modified from CPRA, 2012, 2017a).

The scientific community has long recognized that the global ESLR pattern is highly variable and non-linear. For its 2017 CMP, CPRA analyzed 15 different recent studies which predicted ESLR ranges by the year 2100 using various techniques including expert opinion, process-based models, and semi-empirical models which use a vast network of long-term gage datasets to capture regional variations and satellite altimetry records tying together global patterns. Considering this immense body of work, CPRA aggregated the results to give a full range of values of 0.31 - 1.98 meters GOM Regional SLR by 2100 and developed non-linear curves with a base year of 1992 to represent these lower and upper bounds with acceleration constants of

$1.5775 \times 10^{-6} \text{ m/y}^2$ and $1.44753 \times 10^{-4} \text{ m/y}^2$, respectively (Pahl, 2016). This range was used to develop a suite of scenarios to evaluate 2017 CMP projects (updated from 2012). For this study curves for each of these scenarios were carried beyond the reference year of 2100 to 2170 in accordance with the 150-year model durations from Table 3.1. As can be seen in Figure 3.5, by extrapolating these curves another 70 years, the range of uncertainty nearly triples, which makes considering multiple scenarios even more important.

3.2.3.3 Diversion Operations

As previously stated, land building in the WLD is evaluated as if 100% of the sediment transported by the lower AR is diverted through the WLO. This would be achieved by design and construction of a control structure and or lock system downstream of the WLO that would facilitate navigation to and from the Port of Morgan City and through the LAD. The MBA and MBR diversions are currently in the design phase by CPRA. Structural details, flow capacities, sediment intake rates, impact studies, modeled benefit projections, permit restrictions, and construction costs and schedules are all currently being developed. Therefore, the latest published planning goals and estimates were taken from the 2017 CMP for 1D input drivers. In the CMP, the MBA diversion is planned to operate at 150 m³/s for MR flows below 6,000 m³/s; at flows which vary linearly between MR flows of 6,000 and 37,500 m³/s; and at a maximum 2,250 m³/s when MR flows are at 37,500 m³/s or above. In this operational scheme the ratio of diverted flow to total MR flow ranges from 2.5% to 6.0%, with a median of 4.25%. Similarly, the MBR diversion is planned to operate at 150 m³/s for MR flows below 6,000 m³/s; at flows which flows vary linearly between MR flows of 6,000 and 37,500 m³/s; and at a maximum of 1,050 m³/s when MR flows are at 30,000 m³/s or above. In this operational scheme the ratio of diverted flow to total MR flow ranges from 2.5% to 3.5%, with a median of 3.0%. For

simplicity, the median diverted flow percentages for the MBA and MBR diversions are used in the respective 1D models and are applied to the MR sediment transport rates across all time steps since sediment intake rates are not specified in the CMP (CPRA, 2017a).

Table 3.2. CRMS Sites and data used for subsidence estimations. (From Jankowski et al., 2017)

CRMS Site	Longitude	Latitude	Diversion Site	Shallow Subsidence Rate (mm/yr)	Average Shallow Subsidence Rate (mm/yr)	Deep Subsidence Rate (mm/yr)	Average Deep Subsidence Rate (mm/yr)	Total Subsidence Rate (mm/yr)	Average Total Subsidence Rate (mm/yr)
114	-89.9167	29.7591	MBR	17.4	14.3	3.7	3.9	21.1	18.3
117	-89.9167	29.8099	MBR	19.6		3.5		23.1	
131	-89.8855	29.6925	MBR	17.3		4.0		21.2	
132	-89.8855	29.6648	MBR	14.2		4.1		18.2	
135	-89.7605	29.6865	MBR	5.5		4.0		9.4	
136	-89.7917	29.6212	MBR	12.1		4.2		16.4	
220	-90.0730	29.5632	MBA	3.6	4.9	4.4	4.4	8.0	9.3
225	-90.0105	29.5632	MBA	-2.1		4.4		2.4	
248	-90.0730	29.5994	MBA	-0.6		4.3		3.7	
251	-90.0105	29.5196	MBA	5.4		4.6		10.0	
253	-90.0730	29.5559	MBA	10.5		4.5		15.0	
261	-90.1042	29.5994	MBA	5.1		4.3		9.4	
263	-89.8855	29.5559	MBA	11.0		4.5		15.4	
276	-89.9480	29.6212	MBA	0.4		4.2		4.6	
3617	-89.9167	29.5486	MBA	17.3		4.5		21.8	
4103	-90.0417	29.6575	MBA	-1.2		4.1		2.9	
293	-91.1980	29.2438	WLD	2.3		8.5		5.6	
305	-91.1980	29.3890	WLD	4.8	5.1		9.9		
309	-91.1980	29.2511	WLD	12.3	5.6		17.9		
399	-91.1043	29.3019	WLD	9.0	5.4		14.4		
479	-91.4480	29.5269	WLD	28.4	4.6		32.9		
489	-91.5418	29.5994	WLD	2.7	4.3		7.0		
498	-91.8543	29.4978	WLD	6.2	4.7		10.9		
499	-91.8543	29.5704	WLD	3.8	4.4		8.2		
522	-91.8230	29.4978	WLD	5.8	4.7		10.5		
523	-91.8230	29.5777	WLD	10.0	4.4		14.4		
524	-91.8230	29.5486	WLD	6.3	4.5		10.8		
6304	-91.2752	29.4238	WLD	10.2	5.0		15.2		

3.2.3.4 Summary of 1D Land-building Model Inputs

Table 3.3 summarizes the 1D model inputs for all variables for the WLD, MBA, and MBR diversions. These variables are applied in a three-step process in the spreadsheet model. Step 1 multiplies instantaneous Delft 3D cohesive and non-cohesive sediment transport rates by each 25-day output time step, multiplies both resulting volumes by the bulking factor, multiplies the cohesive sediment volume by the fine sediment retention percentage, and then adds the two

volumes together. In Step 2, the resulting volume is applied along with $\Delta\theta$, m , and α to Equation 1 to determine r_0 . In determining α , the average bottom elevation is subtracted from the MWL which is added to the amount of subsidence and SLR which has occurred up to the end of each time step depending on the SLR scenario. In the final Step 3, r_0 is then applied with $\Delta\theta$ to Equation 2 to find the area of the diversion deposit at each time step.

Table 3.3. Summary of 1D Land-building Model Inputs.

	WLD	MBA	MBR	Source
<i>Diversion Flow Angle, $\Delta\theta$ =</i>	115°	164°	104°	Measured between Figure 3.4 outermost transects
<i>Foreset Slope, m =</i>	0.002	0.004	0.005	Dean et al., 2012
<i>Average Bottom Elevation (m) =</i>	-1.430	0.003	0.104	Averaged from Figure 3.4 transects
<i>MWL (m) =</i>	0.308	0.184	0.211	NOAA and CRMS Stations
<i>% Fine Sediment Retention =</i>	0.3	0.5	0.7	Xu et al., 2019; Bomer et al., 2019
<i>Bulking Factor =</i>	6.7	8	8.9	Dean et al., 2012; Equation 3
<i>Subsidence ($m/year$) =</i>	0.0133	0.0093	0.0183	Jankowski et al., 2017
<i>% Sediment Diverted =</i>	100%	4.25%	3.00%	CPRA, 2017a

3.3 Results

Results in the following subsections present land-building area curves for the WLD, MBA, and MBR diversions for various ESLR scenarios in comparison with results from previous studies in order to focus on the most representative ESLR rate. From there, all flow spit scenarios are presented and compared for each diversion and vs. the other two diversions to assess the long-term land-building potential of the MR vs. the AR.

3.3.1 Comparison with Other Studies

Using the inputs from Table 3.3, 1D land-building models were run for each diversion under current flow (no change to 70/30 flow split) conditions under the five ESLR scenarios from Figure 3.5, giving a wide range of delta area outputs. In Figure 3.6, these output curves are

plotted along with land building reference points using growth rates documented from previous studies for the WLD (Fig. 3.6a) and previous modeling predictions made by Kim et al. (2009) and CPRA (2017a) for the MBA (Fig. 3.6b) and MBR (Fig. 3.6c) diversions. In all three cases, the previous studies bracket the 1D land-building curves with results which predict subaerial delta areas on both the higher and lower ends of the range. This indicates a wide range of variability amongst the scientific community studying these diversions. For each diversion, the 1.0 m ESLR scenario falls approximately in the middle of the ranges given by both 1D results and those of the previous studies. Therefore, the 1.0 m ESLR scenario was chosen to report all further results for all modeling scenarios.

3.3.2 All Modeling Scenarios

Sediment transport rates produced in Delft 3D from each of the twelve flow scenarios from Table 3.1 were fed into the 1D spreadsheets for each diversion to produce discrete land building curves. In Figure 3.7, each of the twelve curves are presented for the WLD (Fig. 3.7a), MBA (Fig. 3.7b), and MBR (Fig. 3.7c) diversions. The WLD diversion produces the widest range of land building results from 351 km² to 1,616 km² (a difference of 1,265 km²) when the AR receives 15% and 70% of the total flow above OR, respectively. The MBA diversion produces the smallest range of land building results from 157 km² to 288 km² (a difference of 131 km²) when the MR receives 30% and 85% of the total flow above OR, respectively. The MBR diversion produces a range of land building results from 192 km² to 346 km² (a difference of 154 km²) when the MR receives 30% and 85% of the total flow above OR, respectively. For each diversion, all curves maintain similar land building trajectories until 50 years when flow regime adjustment begins for each scenario.

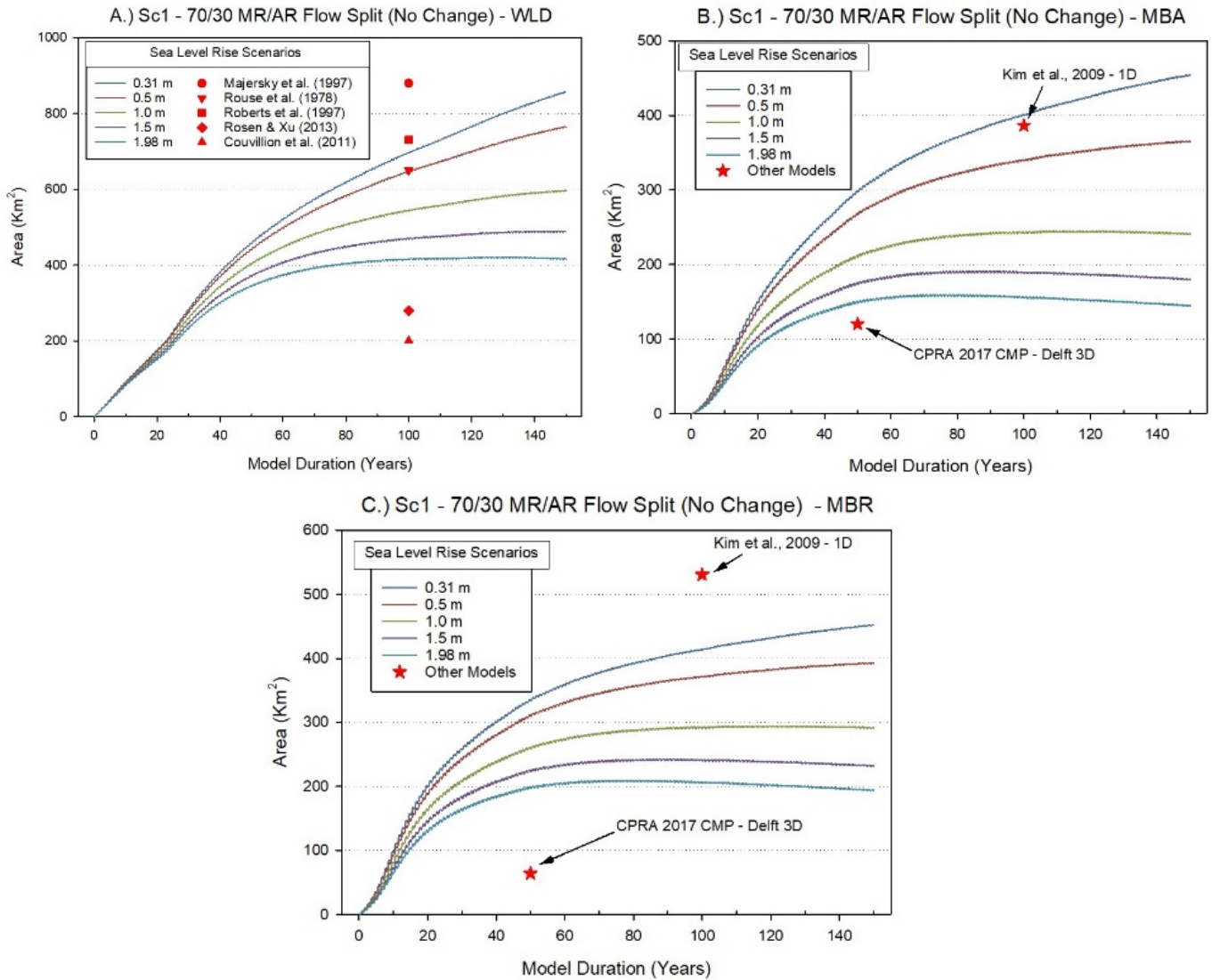


Figure 3.6. Land-building curves for all ESLR scenarios for Modeling Scenario 1 – 70/30 MR/AR Flow Split (No Change). Comparisons made with previous studies for A.) WLD B.) MBA and C.) MBR diversions.

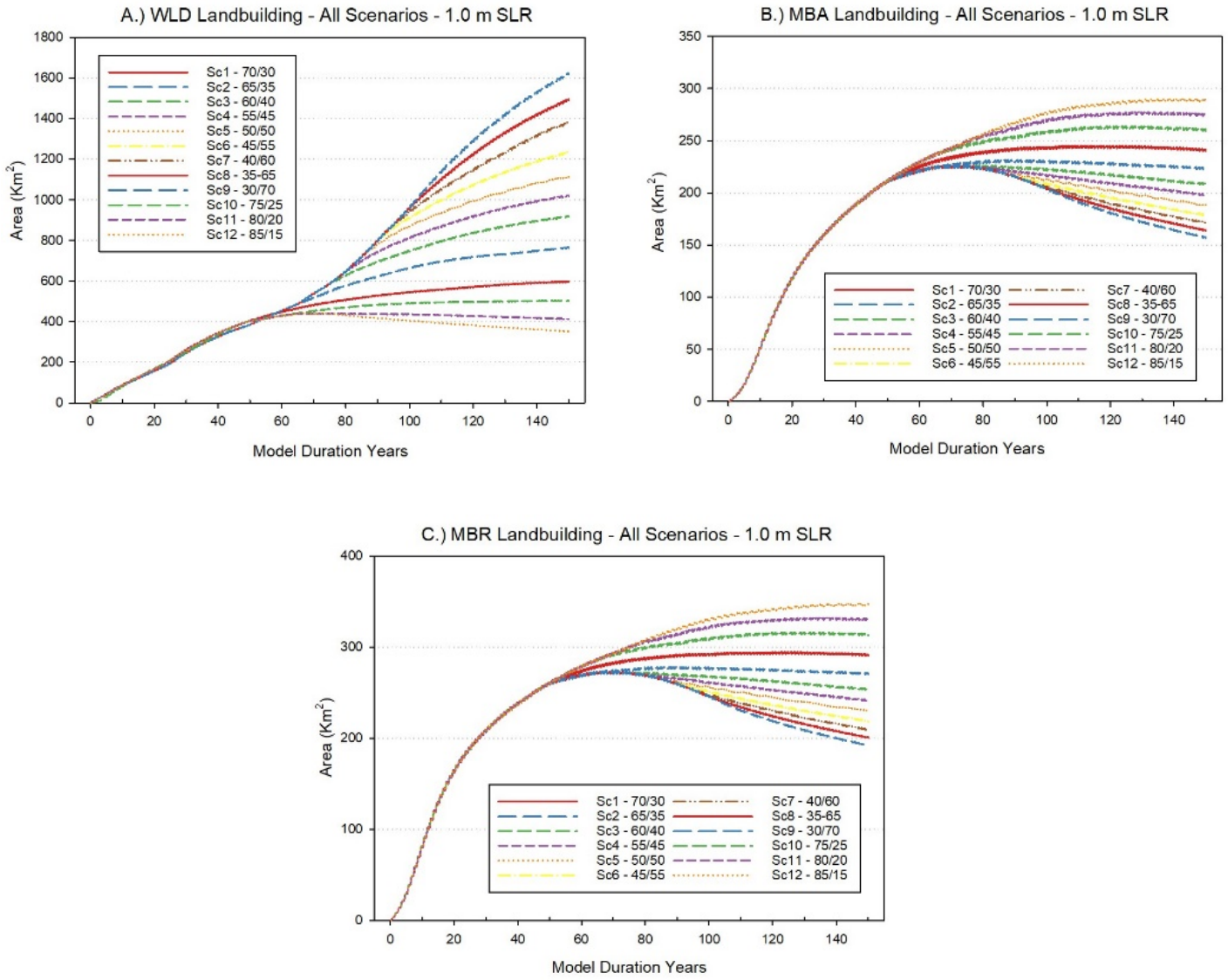


Figure 3.7. Land-building curves for all Modeling Scenarios for A.) WLD B.) MBA and C.) MBR diversions using 1.0 m ESLR.

3.3.3 Diversion Comparisons

The main goal of this study is to compare the land building capacity of the MR vs. the AR along their current alignments, gradients, and receiving area conditions at various flow regulation percentages. Hence, land-building curves were plotted together for all three diversions with the WLD curve representing the capacity of the AR while the combination of the MBA and MBR

diversions representing the capacity of the MR. Results for six of the twelve scenarios are shown in Figure 3.8. Flow percentages increase from Fig. 3.8a to 3.8e by 10% increments from the MR to the AR. In Fig. 3.8f, the flow increases by 10% in the opposite direction from the AR to the MR.

For Scenario 1 in Fig. 3.8a, the MR produces more subaerial delta area than the AR until year 93 where its growth begins to flatten and the AR delta growth continues to increase slowly, resulting in a small difference of 64 km² at year 150. This assessment is determined by comparing instantaneous values along the land building curves at discrete points in time. A more comprehensive assessment is determined by averaging the subaerial land area at each time step to get an average delta area maintained over time. For Scenario 1, the average area maintained is 447 km²/y and 425 km²/y for the MR over the 150-year model duration and the running averages along the curve do not break even, meaning the MR diversions are more effective at building and maintaining land for the majority of the time frame even though there is slightly more land present in the WLD at the end of model run. Table 3.4 lists total area present at the end of the model duration and average area maintained by the MR and AR for each scenario in addition to the year in which the land area curves cross or “break even” and when running averages break even. The AR progressively builds more land by year 150 in Scenarios 1-9 and maintains more land on average in Scenarios 2-9 as AR flows and sediment loads increase. The MR progressively builds and maintains more land in Scenarios 10-12 as MR flows and sediment

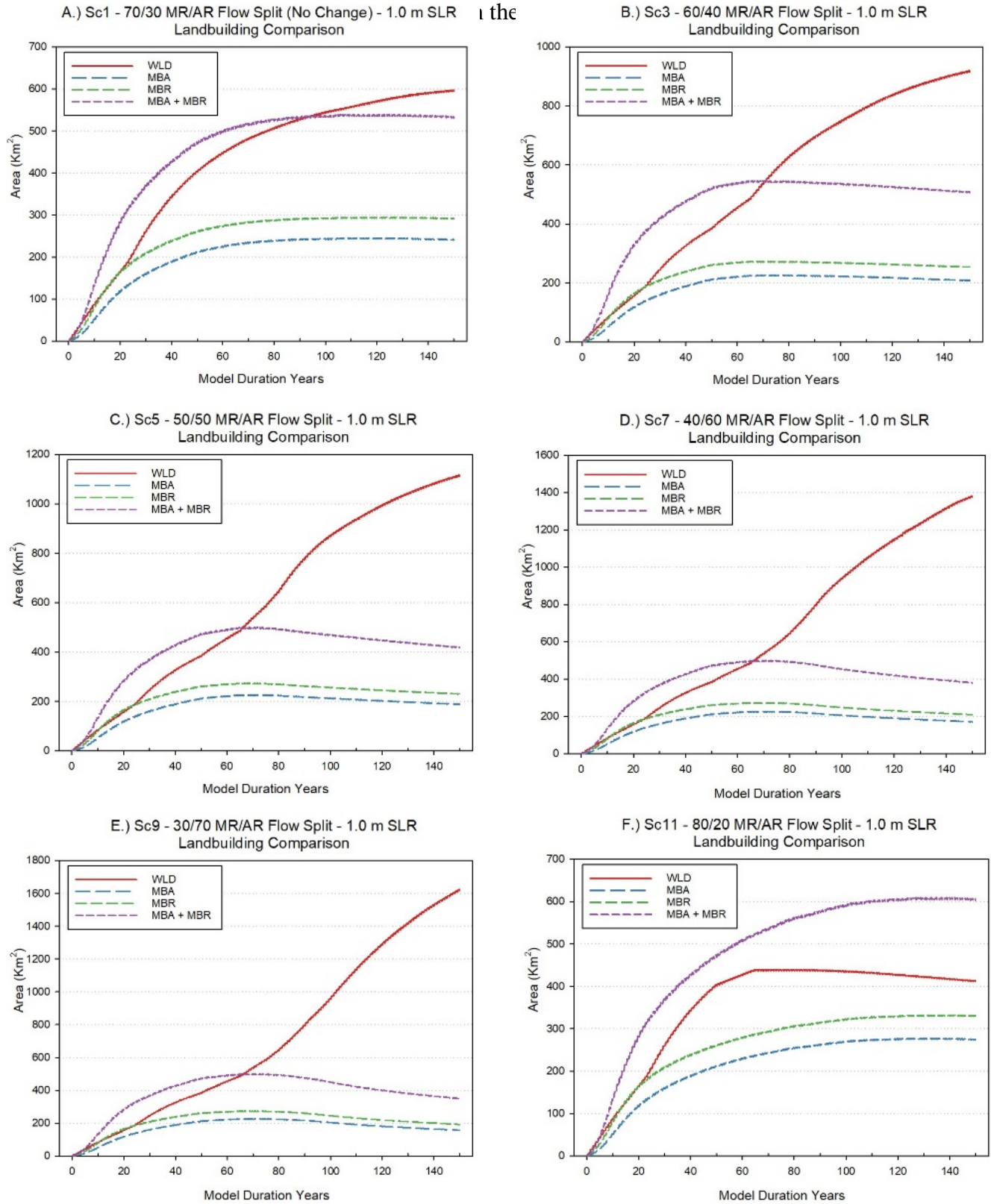


Figure 3.8. Comparison of Land-building curves for WLD, MBA, MBR and combined MBA + MBR diversions using 1.0 m ESLR for select modeling scenarios.

as large as those between the MR and AR in Scenarios 1-9. Figure 3.9 also compares 150-year resulting land areas for each diversion and the MR vs. the AR at discrete flow percentages. The resulting plots demonstrate a clear land-building capacity advantage in the AR. For common flow percentages the AR builds 1.7 times more land at 30% of the total river flow and 3.0 times more land at 70% of the total river flow.

Table 3.4. Results Comparison for End Year Areas and Breakeven Years between the MR and AR for All Scenarios.

Scenario	MR %	AR %	150 Year MR Area (Km ²)	150 Year AR Area (Km ²)	150 Year MR Avg. Area (Km ² /y)	150 Year AR Avg. Area (Km ² /y)	Breakeven Year	Breakeven Year of Running Average
1	70	30	531	595	447	425	93	NA
2	65	35	493	762	430	488	67	113
3	60	40	461	915	419	542	66	101
4	55	45	438	1018	412	576	66	97
5	50	50	417	1111	406	607	66	95
6	45	55	396	1231	400	638	66	95
7	40	60	380	1375	396	668	66	95
8	35	65	364	1489	392	695	66	95
9	30	70	348	1617	389	719	66	95
10	75	25	572	501	466	387	NA	NA
11	80	20	603	412	479	357	NA	NA
12	85	15	633	350	488	338	NA	NA

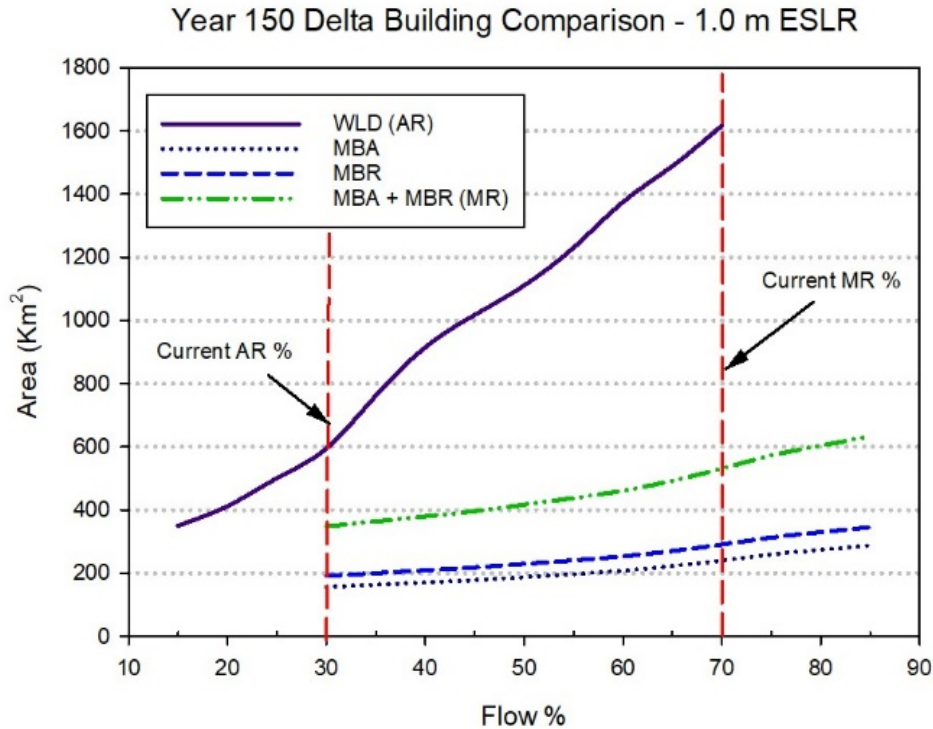


Figure 3.9. Land-building areas vs. flow percentages at year 150 for the WLD, MBA, MBR and MBA + MBR diversions using 1.0 m ESLR

3.4 Discussion

Results from the coupled 3D and 1D modeling produce a relatively wide range of results for all three diversions that depend highly on ESLR, however this range is well within documented land-building rates and previous modeling studies (Figure 3.6). While this validates the formulation of inputs for other variables such as subsidence, sediment retention, bulking factors, bottom elevations, average water levels, foreset slopes, diversion flow angles, and % sediment diverted, a ESLR rate of 1.0 m by 2100 was chosen to avoid the higher and lower extremes of the previously documented ranges. This rate of ESLR contributes to declining delta areas towards the end of the study duration for three diversions in portion of the 12 scenarios, some more drastic than others. This occurs in eight of the scenarios for the MBA and MBR diversions with flow percentages of 65% down to 30% (Figure 3.7). When flows are increased from 70% to

85%, the MR diversion keep pace with ESLR and even realize slight gains beyond 100 years. Land-building curves for the WLD diversion experience declines in only two scenarios when existing flows are decreased to 15% and 20%. All other scenarios either keep pace with ESLR or dramatically increase in land-building rates and continue to accelerate up to and beyond the 150-year duration, especially when receiving 50% or more of the total flow.

Depending on the goals of restoration planners, introducing flexibility into the operations of the ORCS complex could make management of the MRDP much more adaptive as coastal landscapes, communities and industry continue to evolve. For example, if the goal is to strike a balance in deltaic wetland growth between the MR and AR systems, Scenario 1 – 70/30 MR/AR Flow Split (No Change) would produce approximately equal 150-year land area growth of 531 km² vs. 595 km² for the MR vs. AR, respectively (Fig. 3.8a, Table 3.4). If the goal is to produce the most system-wide deltaic land possible in the MRDP through the use of diversions, Scenario 9 – 30/70 MR/AR Flow Split would produce a 150-year land area growth of 348 km² vs. 1,617 km² for the MR vs. AR, respectively, for a total of 1,965 km² (Fig. 3.8e, Table 3.4). This total would represent a regain of ~ 40% of the coastal land area lost in the MRDP since the early 1930's (Couvillion et al., 2011) in addition to any ancillary benefits to surrounding marshes from fine sediments that bypass the diversion receiving areas. It is also noted that the AR curve produced by the WLD diversion in Figure 3.8e is on an accelerating trajectory at year 150, meaning additional land-building benefits would be forthcoming before hitting a delta cycle peak where regressive processes would shift to transgressive (Roberts, 1997). Scenario 9 would build and maintain the least amount of deltaic land by the MR, however this could be supplemented with hardened structures such as storm surge barriers and additional marsh created through mechanical dredging means, especially if a cost savings is realized by reducing stress on the

MR&T levee system. If the goal is to produce the most deltaic land possible by the MR which effects the highest population density and industry, Scenario 12 – 85/15 MR/AR Flow Split would produce a 150-year land area growth of 633 km² vs. 350 km² for the MR vs. AR, respectively (Fig. 3.8f, Table 3.4). However, this would produce the lowest total system-wide deltaic land area total of 984 km² and would be the most problematic in terms of rising river stages and levee maintenance (Andrus, 2020). Insights gained from a cost impact analysis to river maintenance programs in a subsequent phase of this study could further elucidate overall recommendations and identify needs for more extensive evaluations.

Despite having the least favorable receiving area characteristics for land building (closest proximity to GOM and most energetic, deepest bottom, highest water levels, least existing wetlands for trapping) the AR is much more efficient at building land through the WLD diversion than the MR is through the MBA and MBR diversions at common flow rates (Figure 3.9). This can be attributed to higher sediment transport rates, a significant gradient advantage, and a much higher % sediment diverted. The gradient advantage of the AR over the MR at its present point of diversion at OR is approximately 3:1, making it the most advantageous river course for land-building since the Holocene period began ~7,500 years ago, from a gradient perspective (Fisk, 1952). Additionally, there are no restrictions on how much of the sediment transported to the Lower AR can be delivered to the WLD receiving area. Combined, the MBA and MBR diversions will only be designed to divert ~7.25% of the total MR sediment transported. The higher 150-year land-building totals of the AR could potentially be even higher if the flow increases transitioned to the AR were implemented in the model prior to year 50.

With more favorable receiving area conditions (shallower water bottoms, higher sediment retention rates, etc.) over the WLD, MBA and MBR land-building rates would be proportionally

greater with additional diverted flow and sediment. Similarly, additional diversions along the MR with favorable receiving area characteristics such as the Maurepas Swamp Diversion, currently in planning, could add to the MR land-building projections (Rutherford et al., 2018). Furthermore, future land-building analysis performed for the MR branch could be more comprehensive by including all outlets and diversions, even those that are located in less sustainable locations nearer to the GOM. The methodologies provided herein for the MBA and MBR diversions could provide a viable approach for such analyses.

While the results are the land-building projections decisively favor the AR, some study limitations must be underscored. Given the limited budgetary resources available, a previously developed Delft 3D model (from Edmonds, 2012) was retrofitted for this study. While the model was sufficiently calibrated and tested, it uses river elevation data from the early 2000's which was averaged along river course centerlines to reduce computational complexity. The model also does not incorporate any flood plains or minor distributary outlets present in the LMR or the AR Basin. Additionally, the average hydrograph used at the upstream Delft 3D model boundary could be improved upon by incorporating more variable flows which mimic actual river flow extremes where lower flows could induce more shoaling and higher flow peaks could simulate more sediment flushing and higher stream power (Rodi, 2017). Lastly, a more intricate 3D network of deltaic channels and deposits as opposed to the simpler 1D Dean model outputs would offer much more spatial detail to the analysis. Without these exclusions and simplifications, hydraulic model interactions and computational requirements would be much more resource intensive, but could reveal more detailed results of different magnitudes and additional contributing factors to consider. These potential inadequacies highlight even more the

importance of placing the reported trends within the context of the previous studies listed in Figure 3.6 which do account for the limitations listed.

3.5 Conclusions

- (1) While the models used for this study are simplified with respect to river bathymetry, floodplains and distributary outlets, flow hydrographs, and deltaic receiving area detail, model inputs are sufficient to produce results within the range of peer-reviewed scientific studies which account for these limitations.
- (2) The AR river branch displays a clear land-building advantage over the MR due to its extreme gradient advantage over the MR and the lack of restrictions to deliver all of the AR's sediment supply to its receiving area.
- (3) If eventually justified by overcoming extensive socio-economic factors, altering the MR/AR flow split at the ORCS to a maximum of 30/70, rendering the AR path as the new dominant river branch, land-building potential of the MR and AR combined could effectively combat ESLR and reclaim up to 40% of the last century's coastal land loss that has occurred in the MRDP in the next 150 years.
- (4) Land-building trends associated with long-term management of the ORCS flow split in favor of the AR as the dominant river branch would continue to accelerate beyond 150 years, continuing a regressive land-building phase along a sustainable delta cycle curve towards a peak much further into the future.

(5) With the potential to as much as triple land-building rates through sediment diversions in the next 150 years and continue long-term ecosystem sustainability well into the future, further in-depth evaluations which analyze implementation and maintenance costs in addition to socio-economic impacts of altering the control of river flows through the MR-AR bifurcation are warranted.

CHAPTER 4: A FIRST ORDER COST-BENEFIT ANALYSIS OF MODELED COASTAL LAND-BUILDING POTENTIAL OF THE MISSISSIPPI AND ATCHAFALAYA RIVER-DELTA SYSTEMS

4.1 Introduction and Purpose

The present sea-level high stand has given rise to delta-building processes of the Mississippi River (MR) that are cyclic in nature and involve a wide array of depositional environments. Through alternating regressive (fluvial/depositional) and transgressive (marine/erosional) phases, the MR has occupied at least six major courses in the deltaic plain during the Holocene geologic period as depicted in Figure 4.1 (Roberts, 1997; Blum and Roberts, 2012). Throughout this period the river has delivered sediment to the coast to build land at its mouth, annually extending the length of the river channel until a major flood or other disturbance causes the river to avulse, or change course, seeking a shorter, more efficient path to the Gulf of Mexico (GOM). Historically these processes have maintained approximately 40% of the total MR deltaic plain through active delta lobes at any one time, leaving the remaining coastline in retreat (Kolb and van Lopik, 1958; Roberts, 1997; Bentley et al., 2014). Currently, it is estimated that the river is maintaining less than 10-15% of the coast due to drastically decreased sediment loads resulting from upriver dam construction, increased sediment storage within the river levee system, and sediment and nutrient bypassing into the GOM (Barras et al., 2003; Day et al., 2007).

While the MR delta cycle has continued up to the present day, it has been largely influenced by human activities and intense river engineering in the last two centuries which mark the advent of the Anthropocene (Zalasiewicz et al. 2011). Recent research on global deltas has shown anthropogenic activities such as agriculture, mining, reservoir construction, transportation infrastructure, oil and gas extraction, water diversions, flood control, and navigational channels now heavily impact and many times dominate sediment dispersal and depositional patterns at today's river mouth locations (Syvitski et al., 2005; Fan et al., 2006; Syvitski and Saito, 2007;

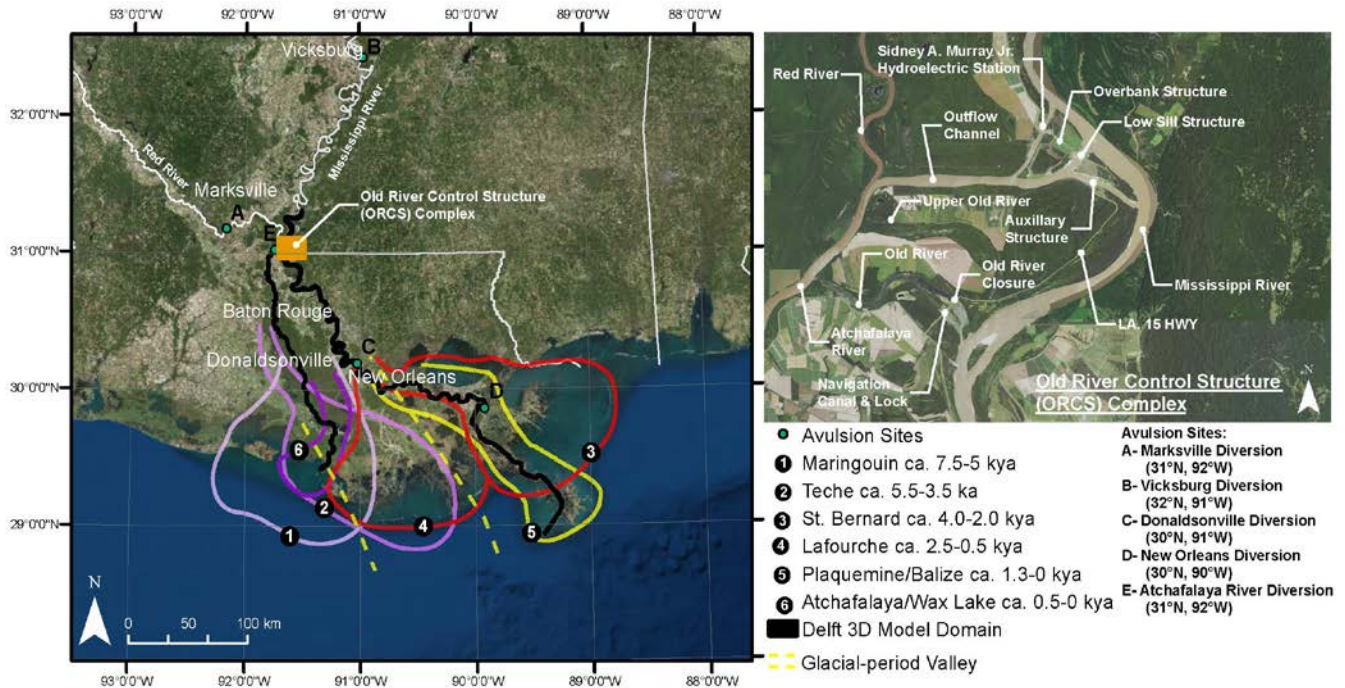


Figure 4.1. Study area depicting Holocene deltas of the Mississippi River (Blum and Roberts, 2012; from Roberts, 1997), Historic avulsion Mississippi River avulsion sites (from Fisk, 1952 and Aslan et al., 2005), Components of the Old River Control Structure Complex managed by the U.S. Army Corps of Engineers, and the Delft3D Model Domain used in this study (from Edmonds, 2012).

Bergillos et al., 2016; Yang et al., 2017). Many of these factors are at play in the heavily engineered Mississippi River Delta Plain (MRDP) which is largely influenced by control of water flow and sediment at the bifurcation which connects the MR to the Atchafalaya River (AR) via the Old River Control Structure Complex (ORCS). The complex originally became operational in 1963 with the low sill and overbank structures, was modified in 1986 with the auxiliary structure, and was completed in 1990 with the hydroelectric station as shown in Figure 4.1. Although this structure complex has limited flow from the Mississippi to the Atchafalaya to 30% of the total combined flow of the Mississippi and Red Rivers (RR) at the latitude of Old River (OR), the deltaic process has continued to advance in the Atchafalaya Basin and in the Atchafalaya and Wax Lake (AWL) Deltas.

Since its construction over 50 years ago the ORCS has played an integral part of the Mississippi River and Tributaries (MR&T) flood protection system, authorized as part of the

1928 Flood Control Act. The system protects approximately 4 million people and prevents billions of dollars in flood damages, with an estimated \$234 billion prevented in the 2011 flood alone. The system also provides tremendous benefit to the national economy and international trade markets. Each year, approximately 500 million tons of cargo move on the MR system and \$2.7 billion in domestic transport savings are realized from its operations (USACE, 2015).

Below the ORCS between Baton Rouge and New Orleans, the Lower Mississippi River (LMR) is home to four of the fifteen largest ports in America which handle over 60% of all grain exports to the world. Barge traffic moving upriver supply petrochemicals, fertilizers, and raw materials which feed the U.S. agricultural industry among many others. It is estimated that shipping through the LMR is worth \$295 million per day. Additionally, the LMR provides fresh drinking water to over 1.5 million people (Masters, 2019).

Given these overwhelming positive economic benefits, much energy has been spent since the early 1800s on scientific research, legislative mandates, engineering development, and construction of control structures and levees to protect public and private interests affected by the MR-AR bifurcation at Old River (Ellicot, 1803; Schultz, 1810; Darby, 1816; Humphreys and Abbot, 1876; MRC, 1881; Elliot, 1932; Salisbury, 1937; Graves, 1949; Kemper, 1949; Halsey, 1950; Odom, 1950; Latimer and Schweizer, 1951; Fisk, 1952). These efforts resulted in the construction of the ORCS low sill and overbank structures in 1963 however, they were nearly lost in Flood of 1973. While hundreds of millions of dollars were spent fortifying the system by adding additional structures (Figure 4.1), this led to fundamental questions regarding its long-term stability. One study by Kazman and Johnson (1980) which accounted for transportation failures and interruptions, property flood damage, pipeline failures, and water supply failures estimated the economic consequences of a catastrophic structure failure at the ORCS to be

between \$1.6B and \$4B (\$5B and \$12.5B when inflated to 2020). Considering this, alternate long-term strategies such as a controlled diversion of increasing flows through the Atchafalaya Basin over the course of decades have been suggested (Kolb, 1980; Martinez, 1986). In addition to the massive flood protection and economic implications such modifications would entail, the delta building capabilities of the MR and AR would be altered since they are highly driven by water and sediment volumes regulated by the ORCS.

More recently, river management research efforts have focused on coastal restoration implications along the lower delta reaches of both MR and AR systems (CPRA 2012, 2017). Because the natural geologic processes of the MR system have been interrupted, many studies have explored the efficacy of engineered sediment diversions and have demonstrated their potential for large-scale, long-term restoration of these processes (DeLaune et al., 2003; Simenstad et al., 2006; Day et al., 2007, 2016, 2018; Kim et al., 2009; Allison and Meselhe, 2010; Paola et al., 2011; CPRA, 2012, 2017; Dean et al., 2012, 2014; Nittrouer et al., 2012; Wang et. al, 2014). As such, the Louisiana Coastal Protection and Restoration Authority (CPRA) is currently planning two large-scale MR sediment diversions below New Orleans. The Mid-Barataria (MBA) Diversion is being planned for River kilometer 97.7 on the west side of the river, near Myrtle Grove (Fig. 4.4b). The maximum planned flow of 2,124 m³/s is estimated to create approximately 120 km² in 50 years. The Mid-Breton (MBR) Diversion is currently being planned for River kilometer 110.4 near Wills Point on the east side of the river (Fig. 4.4b). The plan is to operate this diversion at a maximum flow of 991 m³/s to create an estimated 64 km² in 50 years (CPRA, 2012, 2017).

The MRDP is critically important to the United States as a whole. The region is the third largest source of natural gas and one of the top ten producers of oil in the country (USEIA,

2014). The delta's marshes also provide critical nursery habitat for aquatic and marine species – Louisiana has the second-highest commercial fisheries landings in the United States and is the tenth most popular state for recreational fishing (ASA, 2013; De Mutsert et al., 2013). Negative impacts to these industries, either through action or inaction, would have severe economic repercussions. It is therefore understood that the proposed diversions have potentially tremendous socio-economic implications. As such, hurricane storm protection, water supplies, navigation, commercial fishing, wildlife habitat, recreational opportunities, jobs, incomes, and the impact on individual parishes were all examined in a basin-wide socio-economic study conducted by CPRA in 2016. The socio-economic analysis is driven by biophysical and fisheries modeling of the diversions, conducted under the Louisiana Coastal Area Mississippi River Hydrodynamic and Delta Management Study (MRHDMS), which provided input data on land creation, vegetation patterns, fisheries abundance, distribution, and catch, salinity levels, and more. The results of this analysis did not indicate any region-wide negative socio-economic impacts to the 10-parish area as a result of implementing sediment diversions. On the contrary, many of the socio-economic indicators analyzed showed marked improvement with diversions over a future without action/no diversion scenario (REC and EE, 2016).

While the MBA and MBR diversions have received much attention regarding their potential for restoration in the transgressive MR branch, their effectiveness hinges upon the long-term sustainability of the ORCS and its ability to maintain the current 70%/30% MR/AR flow split. This study aims to assess their project performance beyond the next 50 years comparatively with the delta building capacity of the regressive AR branch. Previous phases of this study (Andrus, 2020a, 2020b) used various modeling techniques to evaluate the complex hydrodynamic interactions of an uncontrolled MR-AR bifurcation as well as future flow, stage, and sediment

transport trends in the MR and AR branches under currently implemented management controls. These models were also used to explore the long-term land-building potential of delta regions of the MR and AR branches under modified control scenarios. The purpose of this study is to evaluate the potential cost impacts of these modifications which will place the environmental benefits into the perspective of how the river channels and flood protection systems would have to be altered and maintained to achieve them. Holistically speaking, river maintenance costs such as levee enlargements and navigational dredging, are only pieces of the economic puzzle that includes ecosystem services like commercial and recreational fisheries production, storm surge protection, nitrogen removal, and carbon sequestration. While some ecological and economical links have been developed between estuarine wetlands and some specific ecosystem service categories for different geographical locations, much uncertainty and need for additional research still exists (Engle, 2011). Therefore, this study will focus on river management costs, namely levee enlargement and dredging costs, as economic indicators that are directly related to river discharge, stage, and sedimentation rates. All costs are listed in 2019 dollars, not accounting for inflation rates or rises in energy costs.

4.2 Methods

The methodologies used in this study were employed in a three step process of 1) 2D river hydrodynamic modeling of various flow split alternatives, 2) coupling the resulting 2D sediment transport rates with a 1D delta-building model to estimate land built in receiving areas, and 3) estimating annual river maintenance costs associated with rising stages and changes in depositional rates within the MR and AR channels for each scenario.

4.2.1 1D and 2D Modeling

This study uses both 1D and 2D numerical modeling techniques to evaluate the long-term effects of current water and sediment regulation mandates and test alternative regulation strategies with respect to delta-building goals. Riverine hydraulic and sediment transport modelling was performed using the Delft 3D modelling software suite developed by Deltares. Delft 3D is a unique, fully integrated modelling framework for a multi-disciplinary approach and 3D computations for coastal, river, lake, and estuarine areas. It can carry out numerical modelling of flows, sediment transport, waves, water quality, morphological developments and ecology. The Delft 3D framework is composed of several modules, grouped around a mutual interface, while being capable to interact with one another (Deltares, 2014). The modules that will be used in this study are Delft3D-FLOW and MOR 2D for hydrodynamic, salinity, temperature, transport and online coupling of morphology and Delft 3D-SED for cohesive and non-cohesive sediment transport. This study also makes use of a grid domain and input parameters developed by Edmonds (2012) and modified by Andrus (2020a, 2020b) that is relatively coarse to facilitate reasonable computational times for the large domain and duration. The domain extends down to meet the GOM but does not incorporate detailed deltaic planforms and channel structures.

In this study we set out to evaluate changes in overall delta area over long periods of time (i.e. hundreds of years). While Delft 3D models with fine resolution grids have been constructed of both delta systems (Hanegan, 2011; Meselhe et. al., 2016) to evaluate shorter-term evolution (i.e. sub-decadal and decadal scales as opposed to century scale), we chose to use a 1D spatially averaged equation developed by Dean et. al. (2012) (Dean model) which is capable of simulating decades of delta growth using a spreadsheet without requiring multiprocessor computers and acceleration factors. The main goal of the Dean model is to predict the most important bulk

properties of delta growth such as shoreline change and growth in delta area, given the water and sediment supply, general configuration and sediment retention properties of the receiving area, and local relative sea level rise. A recent study evaluated a similar 1D model by Kim et al. (2009) vs. a process-based 2D Delft 3D model to compare and contrast land-building simulations. Results showed that the 1D modeled consistently over predicted delta radii and areas by approximately 30%. While the 1D model does not produce the same level of detail with sinuous distributary channels and sediment stratigraphy, it remained relatively close in magnitude and ran 1200 times faster, giving it a distinct advantage for longer time scale evaluations (Baysal, 2014).

With the current MR to AR flow split being maintained at 70% to 30%, it can be logically postulated that a gradual flip of these percentages could be achievable. A MR to AR flow split transition to 30/70 (Scenario 9 in Table 4.1) would have to be carried out over a timeframe that would adequately allow for social, economic, and flood risk adjustments to be made on the same scale as what would be the largest modification to the MR&T project since its authorization by the 1928 Flood Control Act. To date the MR&T project is an estimated 87% complete, putting it on pace for a 100-year implementation timeline. The project provides flood protection for approximately 4 million people in the world's third largest watershed from Cape Girardeau, Mo. to Venice, LA (USACE, 2015). Louisiana's CMP projects a 50-year completion timeline (CPRA, 2012, 2017) and the Dutch Delta Works were completed in 1997, 44 years after the "Deltaplan" was commissioned in 1953 to protect the southwestern portion of the Netherlands around the Rhine-Meuse-Scheldt delta from North Sea flooding (Aerts, 2009; Kind, 2014). Given that these two efforts are similar in scale and duration and must work in concert with larger national flood protection programs to protect lands and residents at their delta interfaces, a

50-year implementation timeframe for flow adjustments will be used for the experimental design in this study. Given the scale of the proposed action, an additional 50 years will be added to each scenario beyond implementation to sufficiently analyze delta response trends into the future. Another 50 years will be added to this timeframe on the front end to accommodate implementation of the CMP projects proposed by the State of Louisiana in 2017, many of which are underway.

Table 4.1 below outlines 12 scenarios (1 No Change scenario, 8 increased AR flow scenarios, and 3 increased MR flow scenarios) where flow adjustments are made gradually over time in 5% increments. The first two increments are made over 15 and 10 years, respectively, to account for modifications that would need to be made to the ORCS, levee and flood protection systems, dredging templates within navigation channels, and sediment management strategies the Atchafalaya Basin. It is assumed that subsequent modifications would be more manageable once the initial adjustments are engineered, constructed, and monitored with future adjustments in mind. Therefore, further flow adjustment increments are made over 5-year periods. In total, the duration of each scenario studied would be 150 years, which is approximately 10% of the life of historic Mississippi River delta complexes (Fisk, 1952; Frazier, 1967; Roberts, 1997).

To create these flow regimes two separate input files were created for each scenario, one for each river branch, where the flow percentages and respective durations from Table 4.1 were applied to the average upstream hydrograph created from the Vicksburg USGS Gage (#7289000) data. The complete model grid from Figure 4.1 was then broken into individual MR and AR model grids below the ORCS (Figure 4.2) for model runs in which the ORCS remains in place with operational schemes from Table 4.1. In order to simulate how the ORCS would be operated for each scenario, the modified hydrograph input files were used as the upstream boundary flow

conditions for the MR only and AR only grids and run as two separate models. Lastly, Figure 4.2 shows six observation locations chosen for each river branch and specified in the Delft 3D setup files. Output parameters for each station include water level, discharge, and sediment transport rates broken down into cohesive, non-cohesive, bedload, and non-bedload components.

Table 4.1. Modeled flow split alteration scenarios at the MR-AR bifurcation.

INCREASED ATCHAFALAYA SCENARIOS											
Scenario 1 (No Change)				Scenario 2 - 65/35 Split				Scenario 3 - 60/40 Split			
MR%	AR%	Duration (Yrs)	Period	MR%	AR%	Duration (Yrs)	Period	MR%	AR%	Duration (Yrs)	Period
70	30	50	MP Implemetation	70	30	50	MP Implemetation	70	30	50	MP Implemetation
70	30	100	No Change	65	35	100	Flow Adjustment	65	35	15	Flow Adjustment
							& Delta Response	60	40	85	Flow Adjustment
											& Delta Response
Scenario 4 - 55/45 Split				Scenario 5 - 50/50 Split				Scenario 6 - 45/55 Split			
MR%	AR%	Duration (Yrs)	Period	MR%	AR%	Duration (Yrs)	Period	MR%	AR%	Duration (Yrs)	Period
70	30	50	MP Implemetation	70	30	50	MP Implemetation	70	30	50	MP Implemetation
65	35	15	Flow Adjustment	65	35	15	Flow Adjustment	65	35	15	Flow Adjustment
60	40	10	Flow Adjustment	60	40	10	Flow Adjustment	60	40	10	Flow Adjustment
55	45	75	Flow Adjustment	55	45	5	Flow Adjustment	55	45	5	Flow Adjustment
			& Delta Response	50	50	70	Flow Adjustment	50	50	5	Flow Adjustment
							& Delta Response	45	55	65	Flow Adjustment
											& Delta Response
Scenario 7 - 40/60 Split				Scenario 8 - 35/65 Split				Scenario 9 - 30/70 Split			
MR%	AR%	Duration (Yrs)	Period	MR%	AR%	Duration (Yrs)	Period	MR%	AR%	Duration (Yrs)	Period
70	30	50	MP Implemetation	70	30	50	MP Implemetation	70	30	50	MP Implemetation
65	35	15	Flow Adjustment	65	35	15	Flow Adjustment	65	35	15	Flow Adjustment
60	40	10	Flow Adjustment	60	40	10	Flow Adjustment	60	40	10	Flow Adjustment
55	45	5	Flow Adjustment	55	45	5	Flow Adjustment	55	45	5	Flow Adjustment
50	50	5	Flow Adjustment	50	50	5	Flow Adjustment	50	50	5	Flow Adjustment
45	55	5	Flow Adjustment	45	55	5	Flow Adjustment	45	55	5	Flow Adjustment
40	60	60	Flow Adjustment	40	60	5	Flow Adjustment	40	60	5	Flow Adjustment
			& Delta Response	35	65	55	Flow Adjustment	35	65	5	Flow Adjustment
							& Delta Response	30	70	50	Flow Adjustment
											& Delta Response
INCREASED MISSISSIPPI SCENARIOS											
Scenario 10 - 75/25 Split				Scenario 11 - 80/20 Split				Scenario 12 - 85/15 Split			
MR%	AR%	Duration (Yrs)	Period	MR%	AR%	Duration (Yrs)	Period	MR%	AR%	Duration (Yrs)	Period
70	30	50	MP Implemetation	70	30	50	MP Implemetation	70	30	50	MP Implemetation
75	25	100	Flow Adjustment	75	25	15	Flow Adjustment	75	25	15	Flow Adjustment
			& Delta Response	80	20	85	Flow Adjustment	80	20	10	Flow Adjustment
							& Delta Response	85	15	75	Flow Adjustment
											& Delta Response

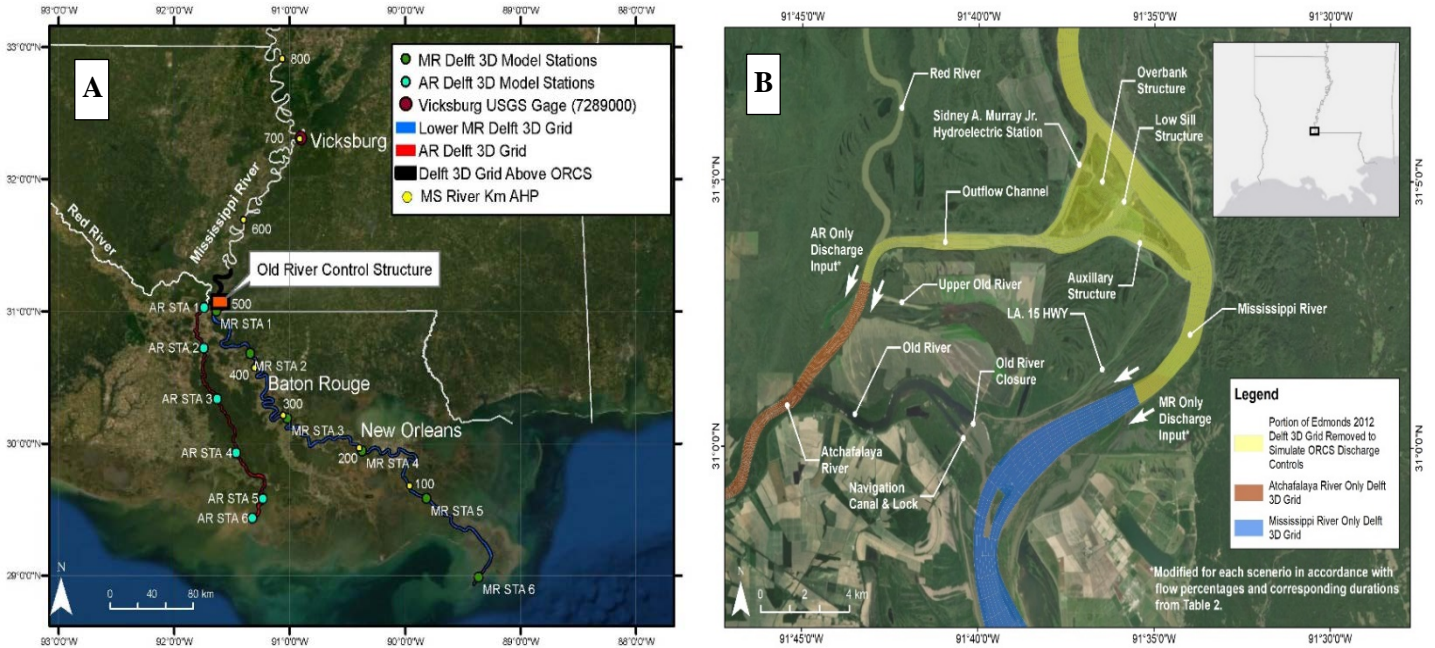


Figure 4.2. A) USGS river gage and Delft 3D grid and output station location map. B) Closeup of Delft 3D grids and model discharge input locations near ORCS.

In a guidance document prepared for the USACE, the State of Louisiana, and the U.S. Geological Survey, Dean et al. (2012) broadly categorized the factors that control the performance of river diversion as 1) basin geometry, 2) sediment characteristics, 3) biological factors, 4) water motion (e.g. sea level rise), and 5) design and operational strategies. The document used these broad concepts to formulate Equation 1 for the radius, r_0 of an idealized truncated cone receiving area delta geometry, as shown in Figure 3 and expressed as:

$$r_0 = -\frac{\alpha}{2m} + \sqrt{\frac{2V}{\alpha\Delta\theta} - \frac{\alpha^2}{12m^2}} \quad (1)$$

where m = front slope of the delta foreset; α = total depth of deposit, inclusive of sea level rise and subsidence; the volume of the truncated cone, $V = Qt$ and Q is the discharge rate of the retained sediments including “bulking” effects and t is time; $\Delta\theta$ = angle over which uniform angular radial spreading flow occurs. Inputs for V are taken from Delft 3D sediment transport

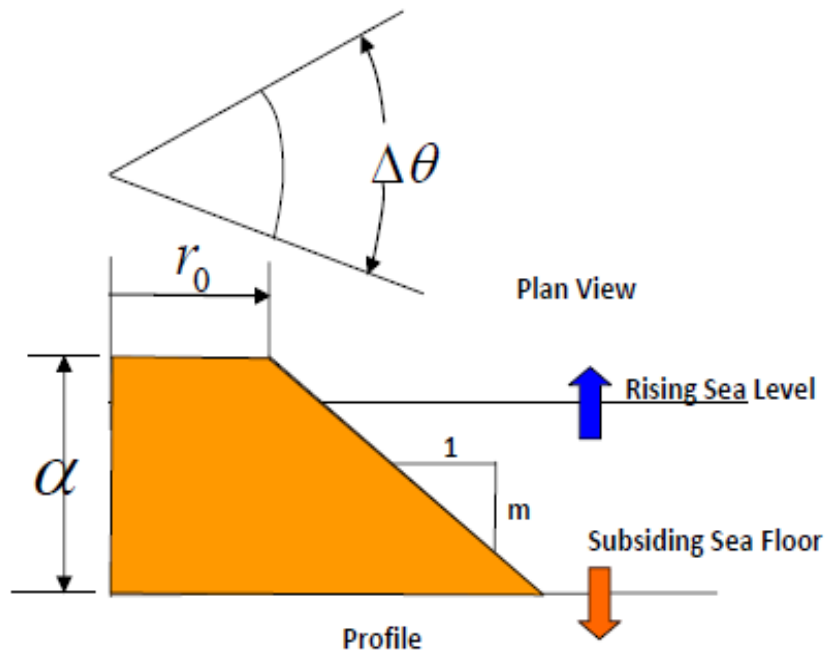


Figure 4.3. Definition sketch of a truncated cone in water of uniform/average depth (from Dean et al., 2012).

rates at each time step exported from appropriate output stations shown in Figure 4.2. Once the r_0 is calculated, then the area of the subaerial portion of the delta can be found by using the formula for a circle segment, expressed as equation 2:

$$A = \frac{r_0^2}{2} \left(\frac{\pi}{180} \Delta\theta - \sin\Delta\theta \right) \quad (2)$$

While this formula does not account for the area of the foreset, this is considered to be negligible since most of the forest is subaqueous.

Figure 4.4 shows the AR and MR modeled receiving areas, transects used to acquire elevation data from NOAA (2019) and water level monitoring stations provided by NOAA and CPRA's Coastwide Reference Monitoring System (CRMS). This study uses the MBA and MBR planned diversions, their operating strategies, and receiving area characteristics to evaluate future long-term land building potential of the MR branch. In the AR branch, delta building currently occurs in the WLD and LAD in Atchafalaya Bay. Nearly 100% of the flow and sediment from

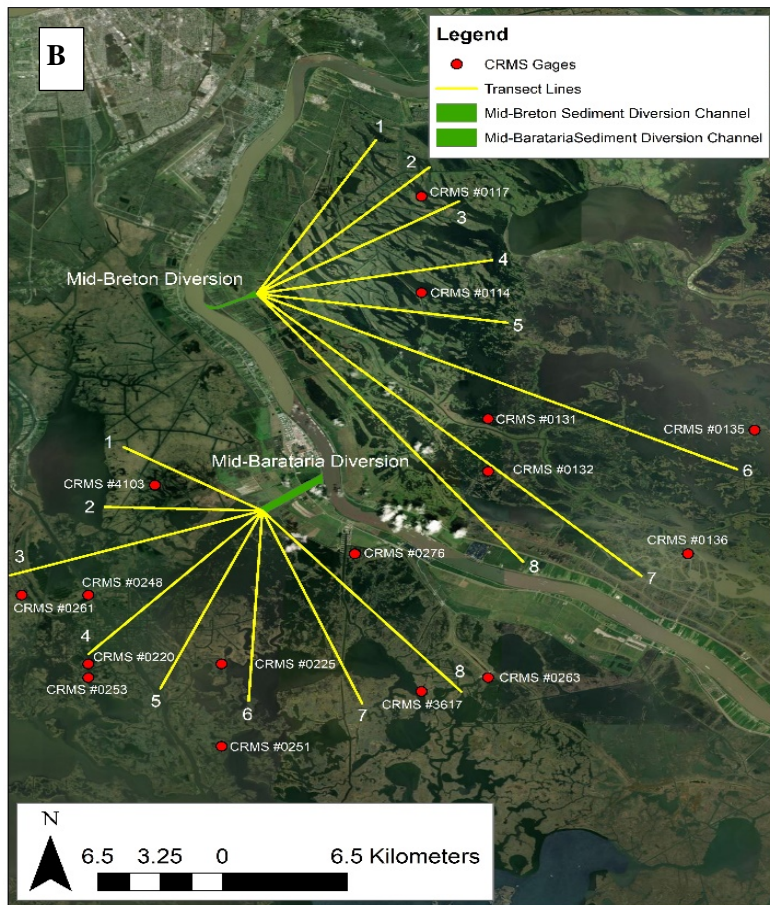
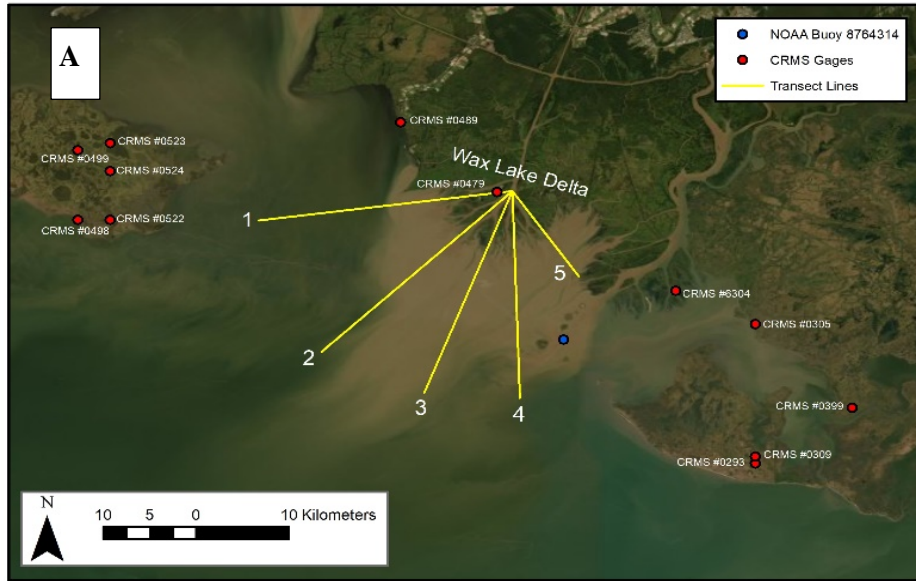


Figure 4.4. 1D modeled receiving areas showing transects used to acquire elevation data and diversion angle, $\Delta\theta$, and water level and subsidence monitoring locations for A) Wax Lake Delta in the AR and B) Mid-Barataria and Mid-Breton Diversions in the MR.

the Lower AR feed these two deltas, therefore land building potential is maximized. The approach is to evaluate all of this potential by modeling 1D land building by diverting all flow and sediment to only one of the deltas, namely WLD. This makes the calculations more straightforward as the receiving characteristics for both deltas are very similar. This is also consistent with the needs of the Port of Morgan City who would rather less sediment effecting shoaling rates in the navigational channel below the port (Wade, 2019). This could be achieved by engineering a sediment control structure on the Lower AR downstream of the Wax Lake Outlet (WLO) channel diversion location.

Relative Sea Level Rise (RSLR), defined as Eustatic (global) Sea Level Rise (ESLR) combined with site-specific subsidence, will also play a major role in the rate of long-term delta growth. Coastal Louisiana has RSLR rates among the highest in the world (12 ± 8 mm per year) (Jankowski et al., 2017). Still, with adequate sediment input (> 20 mg/l) and in microtidal (< 2 m) environments, multiple marsh model dynamic models predict that susceptibility to drowning will not occur below ~ 10 - 12 mm per year of RSLR. This is especially true in the short-term where surface elevation change can increase through increased plant productivity, organic matter accretion, increased mineral deposition, and trapping of clastic sediment (Reed, 1995; Morris et al., 2002; Kirwan et al., 2010; Fagherazzi et al., 2012). Ultimately, this becomes an interplay between the vertical accretion rates and subsidence in determining whether net surface elevation gain occurs by outpacing RSLR (Cahoon et al., 1995).

Accordingly, some efforts through various techniques and data sources have been made to quantify subsidence in south Louisiana (Dokka et al., 2006; Kent and Dokka, 2013; Reed and Yuill, 2016). However, the most comprehensive undertaking to date by Jankowski et al. (2017) used the worlds' largest data set by far of 274 CRMS records and a well-established method rod

surface-elevation table marker horizon (RSET-MH) measurements (Steyer et al., 2003; Webb et al., 2013). Figure 4.4 shows the most applicable sites for which subsidence data was used for each diversion. Previous work has suggested that subsidence rates increase with the thickness of Holocene strata (Meckel et al., 2006; Törnqvist et al., 2008), however Jankowski et al. (2017) showed rates to be similar across varying Holocene thicknesses and more dependent on site specific shallow subsidence within the uppermost 5-10 m.

The scientific community has long recognized that the global ESLR pattern is highly variable and non-linear. For its 2017 CMP, CPRA analyzed 15 different recent studies which predicted ESLR ranges by the year 2100 using various techniques including expert opinion, process-based models, and semi-empirical models which use a vast network of long-term gage datasets to capture regional variations and satellite altimetry records tying together global patterns. Considering this immense body of work, CPRA aggregated the results to give a full range of values of 0.31 - 1.98 meters GOM Regional SLR by 2100 and developed non-linear curves with a base year of 1992 to represent these lower and upper bounds with acceleration constants of $1.5775 \times 10^{-6} \text{ m/y}^2$ and $1.44753 \times 10^{-4} \text{ m/y}^2$, respectively (Pahl, 2016). This range was used to develop a suite of scenarios to evaluate 2017 CMP projects (updated from 2012). For this study curves for each of these scenarios were carried beyond the reference year of 2100 to 2170 in accordance with the 150-year model durations from Table 4.1. As can be seen in Figure 4.5, by extrapolating these curves another 70 years, the range of uncertainty nearly triples, which makes considering multiple scenarios even more important. Andrus (2020b) showed that for all three diversions, results from previous studies bracket the 1D land-building curves with results which predict subaerial delta areas on both the higher and lower ends of the range predicted by the models used in this study. For each diversion, the 1.0 m ESLR scenario falls approximately in

the middle of the ranges given by both 1D results and those of the previous studies. Therefore, the 1.0 m ESLR scenario was chosen to report all further land-building and river maintenance cost results for all modeling scenarios.

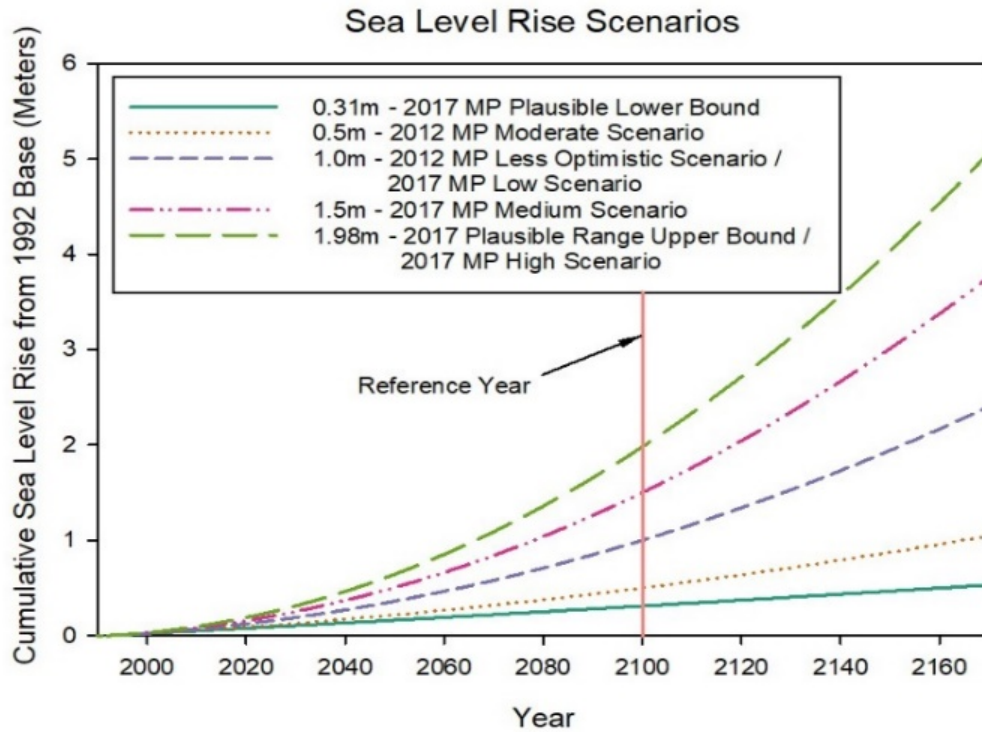


Figure 4.5. Eustatic Sea Level Rise Scenarios used for 1D land-building estimates (modified from CPRA, 2012, 2017).

As previously stated, land building in the WLD is evaluated as if 100% of the sediment transported by the lower AR is diverted through the WLO. This would be achieved by design and construction of a control structure and or lock system downstream of the WLO that would facilitate navigation to and from the Port of Morgan City and through the LAD. The MBA and MBR diversions are currently in the design phase by CPRA. Structural details, flow capacities, sediment intake rates, impact studies, modeled benefit projections, permit restrictions, and construction costs and schedules are all currently being developed. Therefore, the latest published planning goals and estimates were taken from the 2017 CMP for 1D input drivers. In

the CMP, the MBA diversion is planned to operate at 150 m³/s for MR flows below 6,000 m³/s; at flows which vary linearly between MR flows of 6,000 and 37,500 m³/s; and at a maximum 2,250 m³/s when MR flows are at 37,500 m³/s or above. In this operational scheme the ratio of diverted flow to total MR flow ranges from 2.5% to 6.0%, with a median of 4.25%. Similarly, the MBR diversion is planned to operate at 150 m³/s for MR flows below 6,000 m³/s; at flows which flows vary linearly between MR flows of 6,000 and 37,500 m³/s; and at a maximum of 1,050 m³/s when MR flows are at 30,000 m³/s or above. In this operational scheme the ratio of diverted flow to total MR flow ranges from 2.5% to 3.5%, with a median of 3.0%. For simplicity, the median diverted flow percentages for the MBA and MBR diversions are used in the respective 1D models and are applied to the MR sediment transport rates across all time steps since sediment intake rates are not specified in the CMP (CPRA, 2017).

Table 4.2 summarizes the 1D model inputs for all variables for the WLD, MBA, and MBR diversions. These variables are applied in a three-step process in the spreadsheet model. Step 1 multiplies instantaneous Delft 3D cohesive and non-cohesive sediment transport rates by each 25-day output time step, multiplies both resulting volumes by the bulking factor, multiplies the cohesive sediment volume by the fine sediment retention percentage, and then adds the two volumes together. In Step 2, the resulting volume is applied along with $\Delta\theta$, m , and α to Equation 1 to determine r_0 . In determining α , the average bottom elevation is subtracted from the MWL which is added to the amount of subsidence and SLR which has occurred up to the end of each time step depending on the SLR scenario. In the final Step 3, r_0 is then applied with $\Delta\theta$ to Equation 2 to find the area of the diversion deposit at each time step.

Table 4.2 Summary of 1D Land-building Model Inputs.

	WLD	MBA	MBR	Source
<i>Diversion Flow Angle, $\Delta\theta$ =</i>	115°	164°	104°	Measured between Figure 4.4 outermost transects
<i>Foreset Slope, m =</i>	0.002	0.004	0.005	Dean et al., 2012
<i>Average Bottom Elevation (m) =</i>	-1.430	0.003	0.104	Averaged from Figure 4.4 transects
<i>MWL (m) =</i>	0.308	0.184	0.211	NOAA and CRMS Stations
<i>% Fine Sediment Retention =</i>	0.3	0.5	0.7	Xu et al., 2019; Bomer et al., 2019
<i>Bulking Factor =</i>	6.7	8	8.9	Dean et al., 2012
<i>Subsidence (m/year) =</i>	0.0133	0.0093	0.0183	Jankowski et al., 2017
<i>% Sediment Diverted =</i>	100%	4.25%	3.00%	CPRA, 2017

4.2.2 River Maintenance Cost Estimating

The level of sedimentation and erosion which occurs in the model over the 150-year period causes major shifts in stage throughout the MR and AR river branches. In Figure 4.6 is a plot of stage progression over time for Scenario 1 – 70/30 MR/AR Flow Split (No Change) at MR Station 5 with highlighted values at average flows (12,000 m³/s) and higher flows (17,000 m³/s), which are typically experienced in annual Spring floods. While water levels at lower flows do not vary greatly over time, stages at higher flows increase by nearly 3 m. This is a cause for major concern as the model predicts that higher flow stages will overtop the river levee at this location in model year 88. We acquired levee heights at each station location by using NOAA’s Digital Coast data viewer (NOAA, 2019) and then converting the elevations using the USACE’s Corpsccon software from the NAVD88 datum to the NGVD29 datum which is consistent with the USACE surveys used to assign elevations in the original model grid.

This same analysis was performed for each model station and plotted along the entire MR stretch from OR to the GOM in Figure 4.7A at 25-year intervals. This plot shows that at current elevations, MR levees near New Orleans and below will be highly vulnerable beyond 75 years and susceptible to overtopping during average Spring floods. In Figure 4.7B, a similar stage analysis is presented for the AR branch which shows that for Scenario 1, a decreasing stage trend

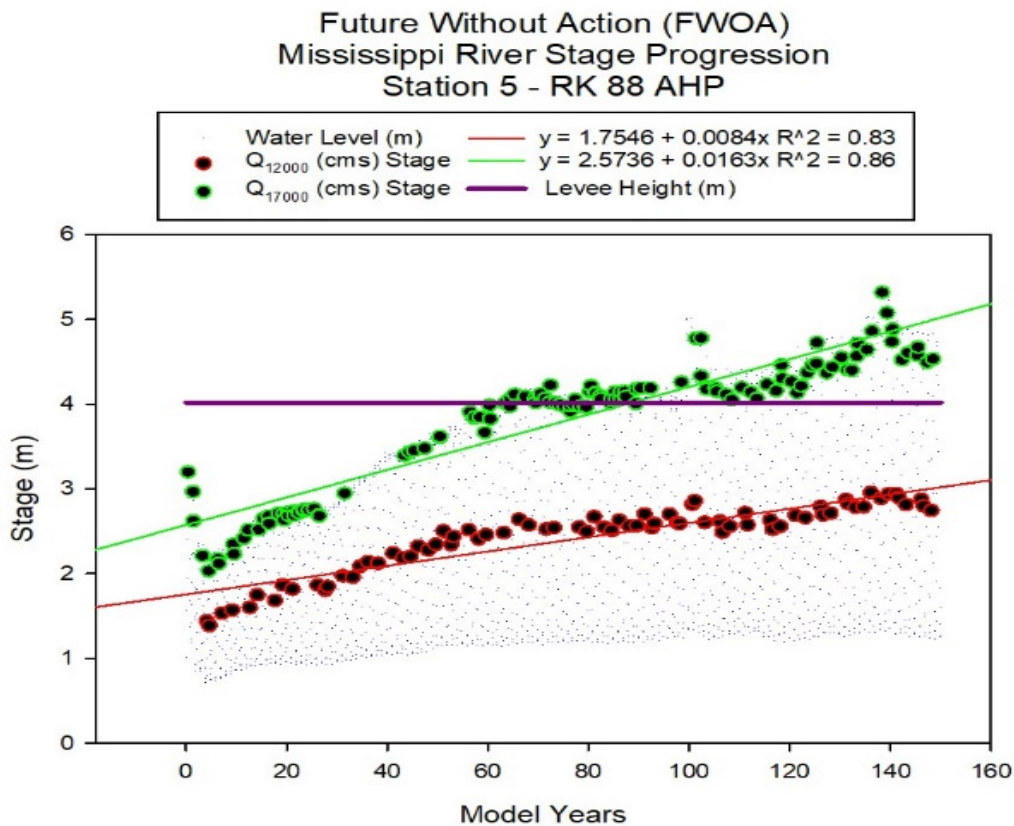
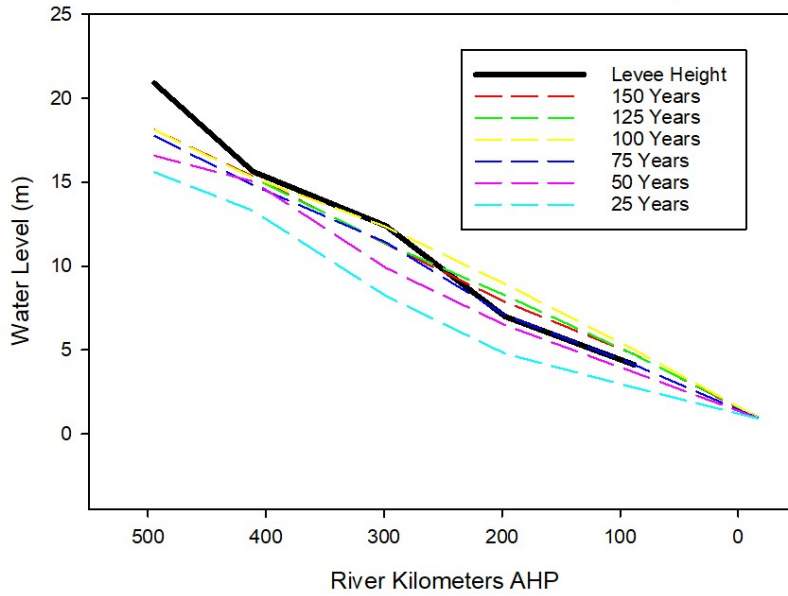


Figure 4.6. FWOA Model Scenario Mississippi River Stage Progression at MR Station 5.

develops over time at an average annual high flow of 7,500 m³/s. General trends indicate that stages become lower over time likely due to further channel incising and flow accommodation. Similar analyses were performed for all twelve scenarios with results presented in Appendix A and analyzed for levee enlargement requirements to maintain the flood protection integrity of each river branch.

A.) FWOA Model Scenario (70-30) - Mississippi River Stage Progression at Average Annual Hydrograph Peaks



B.) FWOA Model Scenario (70-30) - Atchafalaya River Stage Progression at Average Annual Hydrograph Peaks

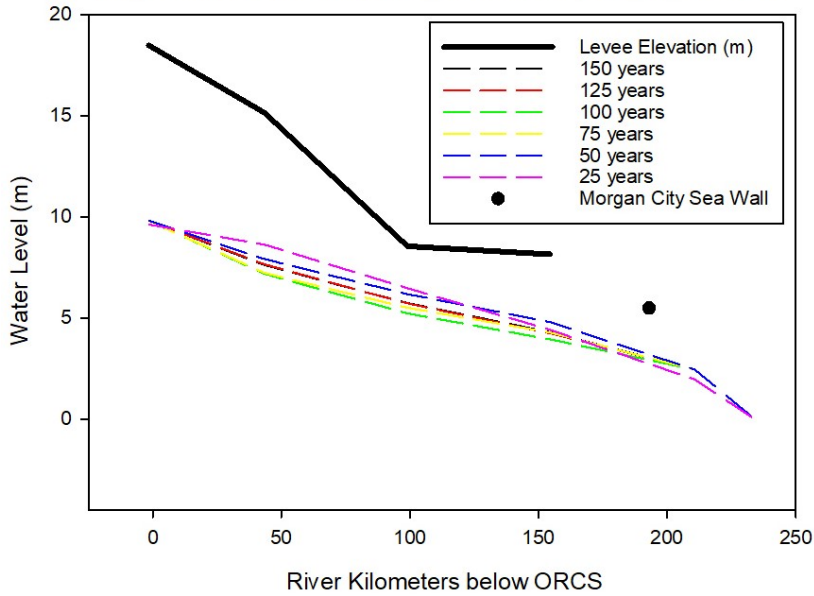


Figure 4.7. Scenario 1 Stage Progression for A) MR Stations at Peak Hydrograph Flows ($\sim 17,000 \text{ m}^3/\text{s}$) and B) AR Stations at Peak Hydrograph Flows ($\sim 7,500 \text{ m}^3/\text{s}$).

As flows increase from the MR to the AR from Scenarios 1-9, stages rise and cause some overtopping in the AR branch at a low-lying area near Station 3 in Scenarios 4-9. The overtopping is not as extreme as in the MR branch due to channel deepening through scour processes which creates additional flow capacity. As flow percentages are increased into the MR in Scenarios 10-12, overtopping becomes more extreme and farther upstream, nearly all the way up to OR.

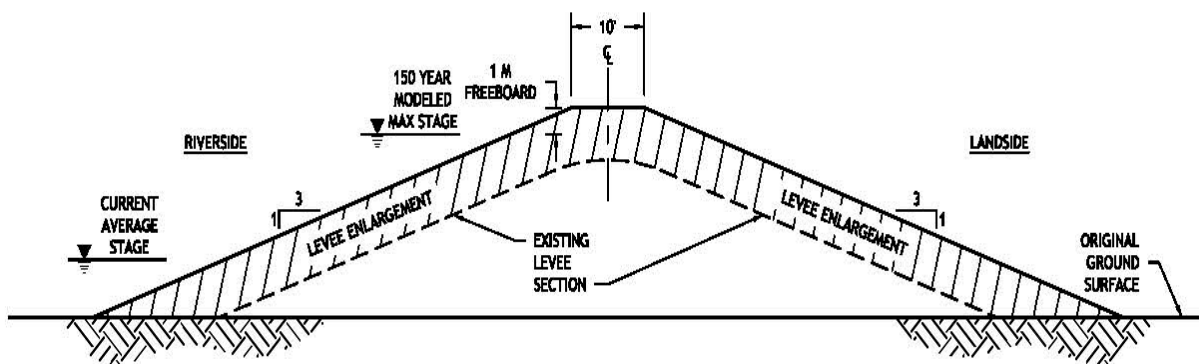


Figure 4.8. Typical section for a “Straddle” type levee enlargement (USACE, 2000).

These overtopping events which would occur annually when peak flows are reached in the average hydrograph. Current operational schemes within the MR&T call for opening of the Bonnet Carré and Morganza Spillways to relief flood pressure from the levee system, however these instances were meant to take place during extreme events of much higher flow magnitudes than the average annual hydrograph. Therefore, it is expected that levee enlargements would need to be implemented in addition to operation of spillways and diversions. Typical levee enlargement design principles are presented in U.S. Army Corps of Engineers (USACE) Engineering Manual No. 1110-2-1913 (USACE, 2000). Figure 4.8 shows an illustration of a typical “straddle” type enlargement section used in estimating earthen embankment volumes that would be required to build levees which would compensate for the modeled maximum stage

rises predicted in each scenario and shown in Appendix A. Design details include a 10 foot crown width, 3 to 1 side slopes, and builds in 1 m of freeboard above the maximum stage from the model results. Currently existing levee crown and ground surface elevations were approximated at each station from NOAA (2019). Segment lengths between stations on each side of both river branches were measured from recent aerial photography in google earth and summarized in Table 4.3. Applicable percentages of these segments which experience overtopping were then multiplied by an average of the two cross-sectional levee enlargement areas calculated at the upstream and downstream stations to arrive at an embankment volume to be added to the existing levee section. Lastly, estimated volumes do not account for any subsidence which may occur to the existing levee sections over the course of the 150-year duration.

Estimated levee enlargement volumes and distances were then used to project construction costs by examining past river levee projects available from recent USACE construction projects below New Orleans summarized by bid tabulation sheets in Appendix B. The average bid price per cubic meter of fill volume required to enlarge levees from the two projects listed is \$43.92. In addition to borrowing and placing compacted embankment fill, there are many other aspects of levee construction such as ground preparation, erosion control, seeding and fertilizing, drainage, and road construction. These costs are more dependent on the length of the levee rather than the height or thickness. The average cost for these items is \$6,896.56 per linear meter. Construction projects of this nature also break out mobilization and demobilization of equipment and labor as a separate cost which averaged 6.41% of the total project cost. Engineering, construction management, and inspection generally costs around 15% of

construction and planning estimates generally include a contingency of 25% or more to account for unknowns and market variability.

Table 4.3. Levee Segment Lengths for the MR and AR East and West Banks

<i>Mississippi River - West Bank</i>							
Segment	Upstream Model Station	Downstream Model Station	feet	yards	miles	meters	km
1	1	2	234,045	78,015	44.3	23,779.0	71.4
2	2	3	325,515	108,505	61.7	33,072.3	99.2
3	3	4	328,785	109,595	62.3	33,404.6	100.2
4	4	5	375,150	125,050	71.1	38,115.2	114.4
5	5	End	207,960	69,320	39.4	21,128.7	63.4
TOTALS:			1,471,455	490,485	278.7	149,499.8	448.6

<i>Mississippi River - East Bank</i>							
Segment	Upstream Model Station	Downstream Model Station	feet	yards	miles	meters	km
1	1	2	225,360	75,120	42.7	68,689.7	68.7
2	2	3	328,245	109,415	62.2	100,049.1	100.1
3	3	4	328,785	109,595	62.3	100,213.7	100.2
4	4	5	375,150	125,050	71.1	114,345.7	114.4
5	5	End	31,320	10,440	5.9	9,546.3	9.5
TOTALS:			1,288,860	429,620	244.1	392,844.5	392.9

<i>Atchafalaya River - West Bank</i>							
Segment	Upstream Model Station	Downstream Model Station	feet	yards	miles	meters	km
1	1	2	218,745	656,235	41.4	200,020.4	66.7
2	2	3	153,780	461,340	29.1	140,616.4	46.9
3	3	4	191,910	575,730	36.3	175,482.5	58.5
4	4	End	133,665	400,995	25.3	122,223.3	40.8
TOTALS:			698,100	2,094,300	132.2	638,342.6	212.8

<i>Atchafalaya River - East Bank</i>							
Segment	Upstream Model Station	Downstream Model Station	feet	yards	miles	meters	km
1	1	2	129,750	389,250	24.6	39,547.8	39.6
2	2	3	157,686	473,058	29.9	48,062.7	48.1
3	3	4	180,243	540,729	34.1	54,938.1	55.0
4	4	End	117,240	351,720	22.2	35,734.8	35.7
TOTALS:			584,919	1,754,757	110.8	178,283.3	178.3

The second major river maintenance cost category is dredging to maintain adequate depth for navigation. The USACE New Orleans districts has jurisdiction over the MR and AR lower reaches and has published 22 years of dredging records on their website from 1996-2018 (USACE, 2020) which are summarized in Figure 4.9. No dredging occurred in the AR in 2017 or 2018 as funding was directed towards design and construction of a dedicated dredge for that

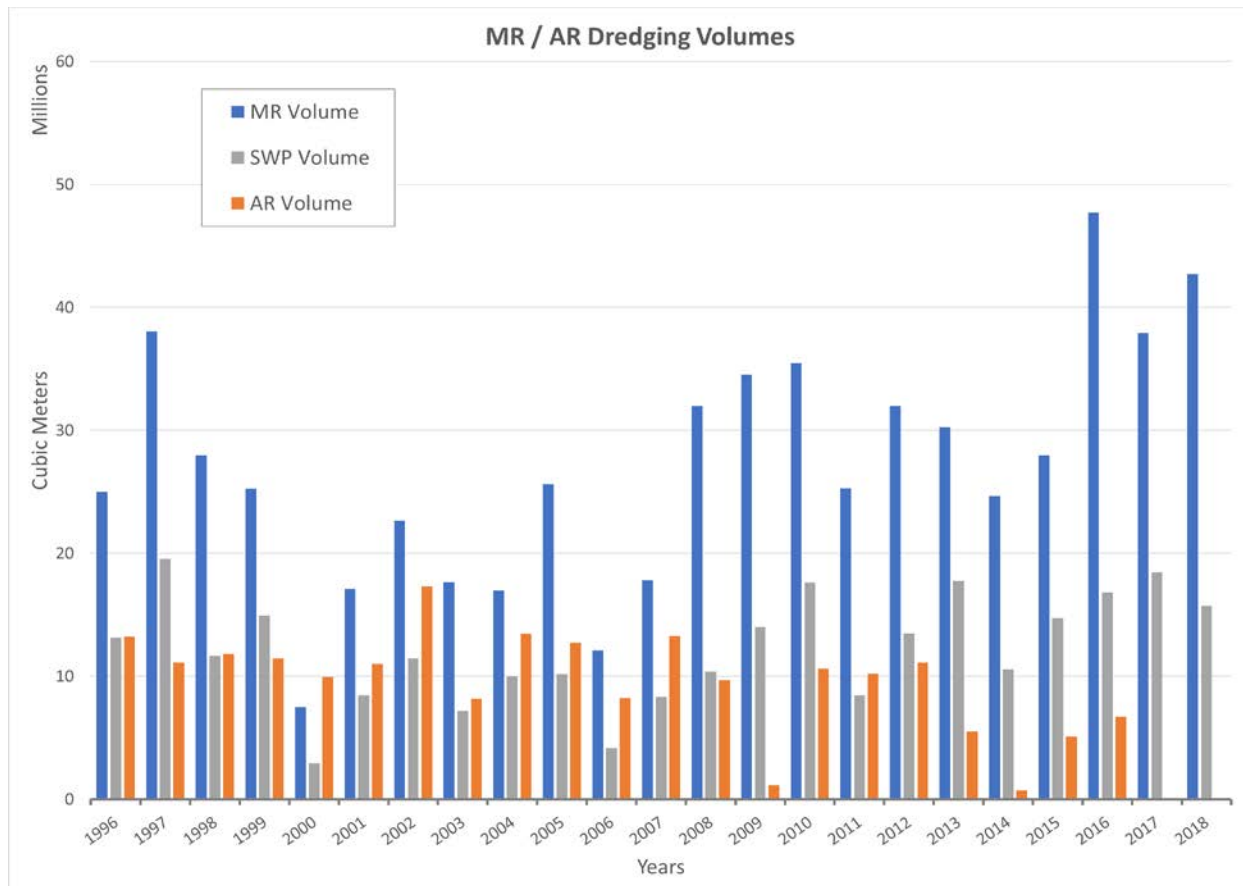


Figure 4.9. Annual Dredging Volumes for the MR and AR from 1996-2018 (USACE, 2020).

location. Also, volumes for Southwest Pass (SWP), the farthest downstream reach located below Head of Passess, are also listed as the largest component of MR volumes. It is noted that the percentage of MR dredging volume comprised by SWP has declined over the 22 year period from ~49% to ~42%, supporting the contention that the MR is losing stream power and its ability to transport sediment to its farthest reaches downstream (Fisk, 1952; Roberts, 1997; Kemp et al., 2014; Bentley et al., 2016).

This argument is further supported by the comparisons of flow vs. dredged volumes in Figure 4.10. Linear interpolations of the data reveal that dredging needs generally with flow rate increase in the MR, indicating its declining ability to transport sediment into deltaic receiving areas or beyond. Conversely, dredging needs in the AR decrease with increasing flow rates,

indicating an increasing stream power and ability to self-maintain its primary channel and more effectively deliver delta building sediments to its confluences with Atchafalaya Bay. It is acknowledged that these data contain a high degree of variability, likely due to funding inconsistencies, equipment availability, high water interruptions to safe working conditions, and evolving river geomorphology. However, the overall trends are consistent with prior research as previously established (Fisk, 1952; Roberts, 1997; Allison et al., 2000; Allison and Neill, 2002; Kemp et al., 2014; Kolker et al., 2014; Bentley et al., 2016). Therefore, the linear regression equations from Figure 4.10 will be used to project dredging volumes using upstream boundary flow conditions from the individual MR and AR model domains. This is consistent with the flow data presented in Figure 4.10 which are average annual flow values from just below old river for the time period of the dredging records. Average costs of $\$2.80/\text{m}^3$ and $\$2.39/\text{m}^3$ for the

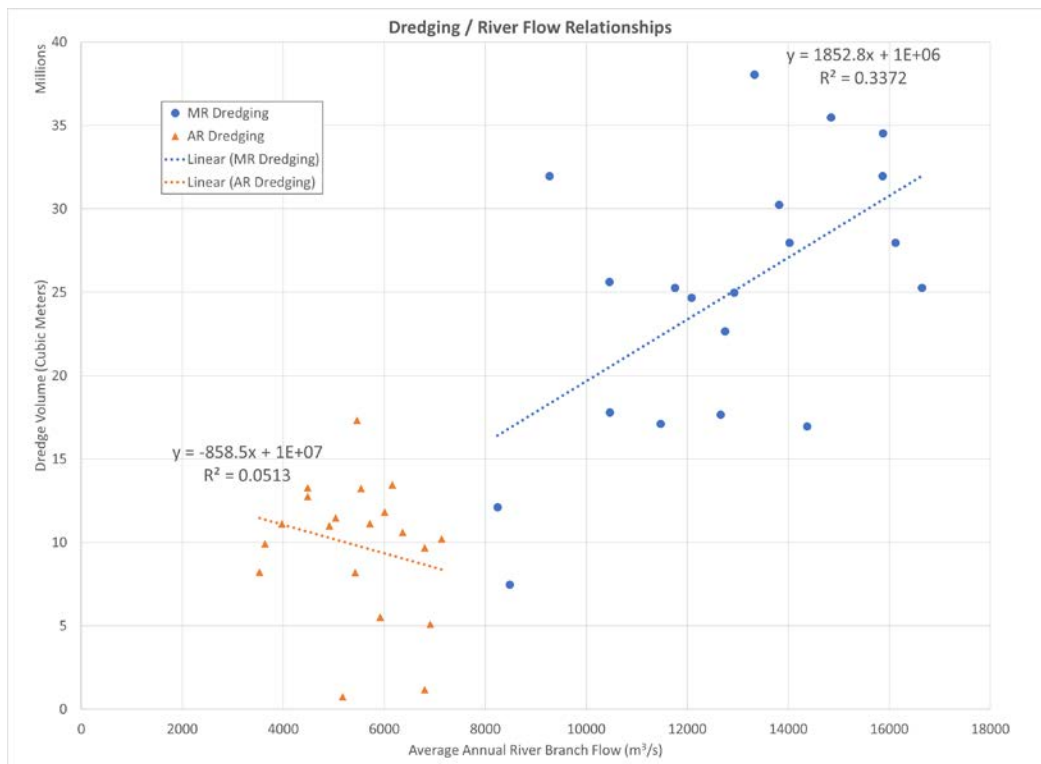


Figure 4.10. Dredging vs. River Flow Relationships for the MR and AR (Data from taken USACE Dredging Records from 1996-2016).

MR and AR, respectively from the 2015 and 2016 dredging cycles were then applied to the projected dredging volumes to estimate annual dredging costs over the course of the 150-year study duration.

4.3 Results

Results are categorized into land-building area analysis for the WLD, MBA, and MBR diversions and for the overall MR vs. AR branches, levee building cost estimating results, and dredging cost estimating results. Land-building area benefits are then compared to river maintenance costs to evaluate cost-effectiveness.

4.3.1 Summary of MR and AR Land-building

Using the inputs from Table 2 and sediment transport rates from Delft 3D for each scenario from Table 4.1, 1D land-building models were run for each diversion under the 1.0 m ESLR scenario from Figure 4.5, giving a wide range of delta area outputs (Andrus, 2020b). The WLD diversion produces the widest range of land building results from 351 km² to 1,616 km² (a difference of 1,265 km²) when the AR receives 15% and 70% of the total flow above OR, respectively. The MBA diversion produces the smallest range of land building results from 157 km² to 288 km² (a difference of 131 km²) when the MR receives 30% and 85% of the total flow above OR, respectively. The MBR diversion produces a range of land building results from 192 km² to 346 km² (a difference of 154 km²) when the MR receives 30% and 85% of the total flow above OR, respectively. Each diversion maintains similar land building trajectories until 50 years when flow regime adjustment begins for each scenario.

The main goal of this study is to compare the land building capacity of the MR vs. the AR along their current alignments, gradients, and receiving area conditions at various flow regulation percentages. Figure 4.11 compares 150-year resulting land areas for each diversion and the MR

vs. the AR at discrete flow percentages. The resulting plots demonstrate a clear land-building capacity advantage in the AR. For common flow percentages the AR builds 1.7 times more land at 30% of the total river flow and 3.0 times more land at 70% of the total river flow.

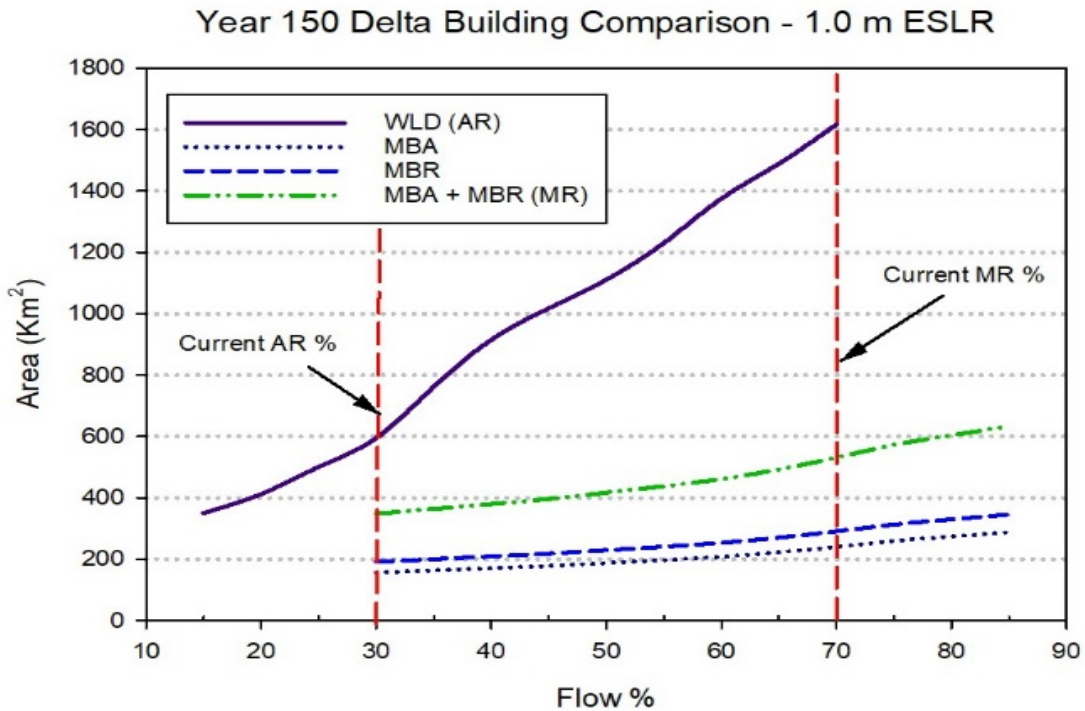


Figure 4.11. Land-building areas vs. flow percentages at year 150 for the WLD, MBA, MBR and MBA + MBR diversions using 1.0 m ESLR.

4.3.2 Levee Building Cost Estimates

Estimated levee building enlargement costs to accommodate rising stages project by the Delft 3D model are presented in Table 4.4. In the MR, levees are overtopped in Scenarios 1-4 and 10-12. For these scenarios, stage height reached above the current levee elevations was identified and used to determine the height of the enlargement section. Using the methods described in Section 2.2, enlargement costs were estimated and applied ten years prior to the year levees were overtopped by the modeled stages. In Scenarios 5-9, which all have decreased flow split percentages of 50% down to 30%, stages do continue to rise but do not overtop current

levee elevations. For Scenario 1 – 70/30 MR/AR Flow Split (No Change), \$8.5B in levee enlargement costs are estimated to compensate for a 1.93 m rise above current levee heights. Scenario 12 – 85/15 MR/AR Flow Split produces the most expensive levee enlargement cost of \$14.5B.

In the AR, levees are overtopped in Scenarios 4-9, with Scenario 9 - 30/70 MR/AR Flow Split causing the highest rise in stage of 1.78 m above current levee elevations resulting in the most expensive AR levee enlargement cost of \$3.9B. In Scenarios 1-3, which flow split percentages increase in the AR from 30% down to 40%, some minor stage rises occur along with some stage decreases due to channel enlargement and no levee overtopping occurs. In Scenarios 10-12, which flow split percentages decrease in the AR from 30% down to 15%, stages decrease over time.

4.3.3 Dredging Cost Estimates

Using equations from Figure 4.10, dredging volumes required to maintain existing navigation standards were projected and used to estimate average annual and total 150-year duration costs for the MR and AR branches in Table 5. Average annual and total 150-year dredging costs for the MR ranged from \$48.0M and \$7.2B, respectively in Scenario 9 to \$72.4M and \$10.9B, respectively in Scenario 12. Average annual and total 150-year dredging costs for the AR ranged from \$19.4M and \$2.9B, respectively in Scenario 9 to \$29.0M and \$4.4B, respectively in Scenario 12. Therefore, Scenario 9 – 30/70 MR/AR Flow Split produced the lowest combined maintenance dredging costs while Scenario 12 – 85/15 MR/AR Flow Split produced the highest.

Table 4.4. Levee Enlargement Summary

Mississippi River						
Scenario	MR %	Levees Overtopped? (Yes/No)	Year Overtopped	Max Stage Differential Above Levee Height (m)	Upstream River Km Overtopped*	Levee Enlargement Cost
1	70	Yes	75	1.93	300	\$8,475,656,826
2	65	Yes	75	1.68	275	\$7,457,081,057
3	60	Yes	100	1.17	240	\$5,591,577,212
4	55	Yes	100	0.18	220	\$4,215,279,596
5	50	No				
6	45	No				
7	40	No				
8	35	No				
9	30	No				
10	75	Yes	50	1.26	400	\$6,478,056,127
11	80	Yes	50	1.52	440	\$10,060,823,905
12	85	Yes	50	2.36	460	\$14,469,676,155
Atchafalaya River						
Scenario	AR %	Levees Overtopped? (Yes/No)	Year Overtopped	Max Stage Differential Above Levee Height (m)	Upstream River Km Overtopped*	Levee Enlargement Cost
1	30	No				
2	35	No				
3	40	No				
4	45	Yes	75	0.47	90	\$404,692,680
5	50	Yes	75	0.47	90	\$404,692,680
6	55	Yes	75	0.47	90	\$404,692,680
7	60	Yes	75	0.47	90	\$404,692,680
8	65	Yes	75	0.93	85	\$1,401,037,626
9	70	Yes	75	1.78	75	\$3,882,170,154
10	25	No				
11	20	No				
12	15	No				

*MR Km represents distance above Head of Passes. AR Km represents distance below OR.

Table 4.5. Dredging Projection Volumes and Costs

Scenario	MR %	AR %	Dredging Vol. (m ³)	Avg. Annual MR Dredging Cost	MR Dredging Cost	Dredging Vol. (m ³)	Avg. Annual AR Dredging Cost	AR Dredging Cost
1	70	30	23,104,814	\$64,671,116	\$9,700,667,413	10,854,633	\$25,981,267	\$3,897,190,091
2	65	35	22,040,992	\$61,693,444	\$9,254,016,584	10,361,703	\$24,801,408	\$3,720,211,213
3	60	40	21,136,743	\$59,162,423	\$8,874,363,379	9,942,713	\$23,798,528	\$3,569,779,166
4	55	45	20,338,876	\$56,929,168	\$8,539,375,257	9,573,016	\$22,913,633	\$3,437,045,007
5	50	50	19,594,201	\$54,844,798	\$8,226,719,677	9,227,965	\$22,087,732	\$3,313,159,792
6	45	55	18,902,717	\$52,909,311	\$7,936,396,638	8,907,560	\$21,320,823	\$3,198,123,521
7	40	60	18,264,423	\$51,122,708	\$7,668,406,140	8,611,803	\$20,612,908	\$3,091,936,193
8	35	65	17,679,321	\$49,484,988	\$7,422,748,184	8,340,691	\$19,963,985	\$2,994,597,810
9	30	70	17,147,410	\$47,996,152	\$7,199,422,769	8,094,226	\$19,374,056	\$2,906,108,371
10	75	25	24,168,636	\$67,648,788	\$10,147,318,242	11,347,562	\$27,161,126	\$4,074,168,970
11	80	20	25,072,885	\$70,179,810	\$10,526,971,447	11,766,553	\$28,164,007	\$4,224,601,017
12	85	15	25,870,751	\$72,413,064	\$10,861,959,569	12,136,250	\$29,048,901	\$4,357,335,176

4.3.4 Overall Cost-Benefit Analyses

Presented in Table 4.6 are the combinations of levee enlargement costs associated with flood protection maintenance against rising stages and river dredging costs projected for changing flow rates to maintain currently authorized navigation channels in each river branch for

each scenario. For each scenario the total maintenance costs for the MR and AR are also summed to arrive at total system maintenance cost for each scenario. This cost is then compared against the cost of Scenario 1 – 70/30 Flow Split (No Change) to determine the cost of each scenario vs. no future action. Scenarios 2 – 10 all produce cost savings compared to Scenario 1, while Scenarios 11 and 12 would increase river maintenance costs. Scenario 7 produces the largest cost savings of \$10.9B over the 150-year model duration when compared to the current 70/30 flow split management mandate.

Table 4.6. Total Cost Comparisons

Scenario	MR %	AR %	Total 150-Year MR Maintenance Cost	Total 150-Year AR Maintenance Cost	Total MR + AR Maintenance Cost	MR - AR Cost Difference	Total Cost Difference from Sc1 (No Change)
1	70	30	\$18,176,324,238	\$3,897,190,091	\$22,073,514,330	\$14,279,134,147	\$0
2	65	35	16,711,097,641	\$3,720,211,213	\$20,431,308,854	\$12,990,886,428	(\$1,642,205,476)
3	60	40	14,465,940,591	\$3,569,779,166	\$18,035,719,757	\$10,896,161,426	(\$4,037,794,573)
4	55	45	12,754,654,853	\$3,841,737,687	\$16,596,392,540	\$8,912,917,167	(\$5,477,121,790)
5	50	50	8,226,719,677	\$3,717,852,472	\$11,944,572,148	\$4,508,867,205	(\$10,128,942,182)
6	45	55	7,936,396,638	\$3,602,816,200	\$11,539,212,838	\$4,333,580,437	(\$10,534,301,492)
7	40	60	7,668,406,140	\$3,496,628,873	\$11,165,035,013	\$4,171,777,267	(\$10,908,479,317)
8	35	65	7,422,748,184	\$4,395,635,437	\$11,818,383,621	\$3,027,112,748	(\$10,255,130,709)
9	30	70	7,199,422,769	\$6,788,278,525	\$13,987,701,294	\$411,144,245	(\$8,085,813,036)
10	75	25	16,625,374,369	\$4,074,168,970	\$20,699,543,339	\$12,551,205,398	(\$1,373,970,991)
11	80	20	20,587,795,352	\$4,224,601,017	\$24,812,396,369	\$16,363,194,335	\$2,738,882,039
12	85	15	25,331,635,724	\$4,357,335,176	\$29,688,970,900	\$20,974,300,548	\$7,615,456,570

The total costs for each river branch and the system as a whole were then applied to the end year resulting delta areas and listed in Table 4.7 to determine the cost effectiveness of each scenario.

The most cost-effective scenario for the MR is Scenario 5 – 50/50 MR/AR Flow Split at \$19.7M/Km² with the least cost effective being Scenario 12 – 85/15 MR/AR Flow Split at \$40.0M/Km² even though it produces the most land area at 633 Km². The most cost-effective scenario for the AR is Scenario 7 – 40/60 MR/AR Flow Split at \$2.5M/Km² with the least cost effective being Scenario 12 – 85/15 MR/AR Flow Split at \$12.4M/Km² even though it produces the most land area at 633 Km². Lastly, the most cost-effective system-wide combination is Scenario 7 – 40/60 MR/AR Flow Split at \$6.4M/Km². Yearly cost-benefit progressions for each

river branch and the system-wide combination are shown in Figure 4.12. If inflation were accounted for, costs per area would be greater impacted for the MR since levee enlargement events for some scenarios occur in later years, incurring more inflation and because both levee enlargement and dredging costs are much larger in the MR. Inflation would also pose greater impacts to dredging costs since they occur every year as opposed to one-time levee enlargement events. While this may change the most cost-effective flow split percentages into the AR slightly up or down, all increased AR flow percentage scenarios are expected to be more cost-effective than no change.

Table 4.7. Cost Benefit Analysis

Scenario	MR 150-Year Delta		AR 150-Year		MR - AR			
	MR %	AR %	Area (km ²)	Delta Area (km ²)	MR (\$/km ²)	AR (\$/km ²)	Difference (\$/km ²)	Overall (\$/km ²)
1	70	30	531	595	\$34,239,573	\$6,553,262	\$27,686,312	\$19,611,281
2	65	35	493	762	\$33,916,389	\$4,880,412	\$29,035,977	\$16,280,076
3	60	40	461	915	\$31,371,940	\$3,900,204	\$27,471,736	\$13,103,632
4	55	45	438	1,018	\$29,130,029	\$3,773,449	\$25,356,580	\$11,399,015
5	50	50	417	1,111	\$19,727,748	\$3,345,334	\$16,382,414	\$7,815,251
6	45	55	396	1,231	\$20,021,334	\$2,927,896	\$17,093,437	\$7,092,715
7	40	60	380	1,375	\$20,199,233	\$2,542,505	\$17,656,728	\$6,362,177
8	35	65	364	1,489	\$20,396,291	\$2,951,918	\$17,444,374	\$6,377,958
9	30	70	348	1,617	\$20,672,546	\$4,199,076	\$16,473,469	\$7,118,885
10	75	25	572	501	\$29,052,277	\$8,139,625	\$20,912,652	\$19,295,013
11	80	20	603	412	\$34,116,538	\$10,256,801	\$23,859,737	\$24,437,575
12	85	15	633	350	\$39,999,137	\$12,433,387	\$27,565,751	\$30,179,111

4.4. Discussion

For many years, researchers have realized the land-building potential of the MR and AR by studying the historic transitions made through river avulsions which have led to the development of major delta lobes as part of the delta cycle (Fisk, 1952; Roberts, 1997). Andrus (2020a, b) explored the possibility of continuing this cycle through the MR-AR bifurcation in both controlled and uncontrolled manners. While allowing an uncontrolled diversion to occur would be disastrous (Latimer and Schweizer, 1951; Kazman and Johnson, 1980), altering flow split regulations at the ORCS could effectively combat ESLR and reclaim up to 40% of the last century’s coastal land loss that has occurred in the MRDP in the next 150 years (Couvillion et

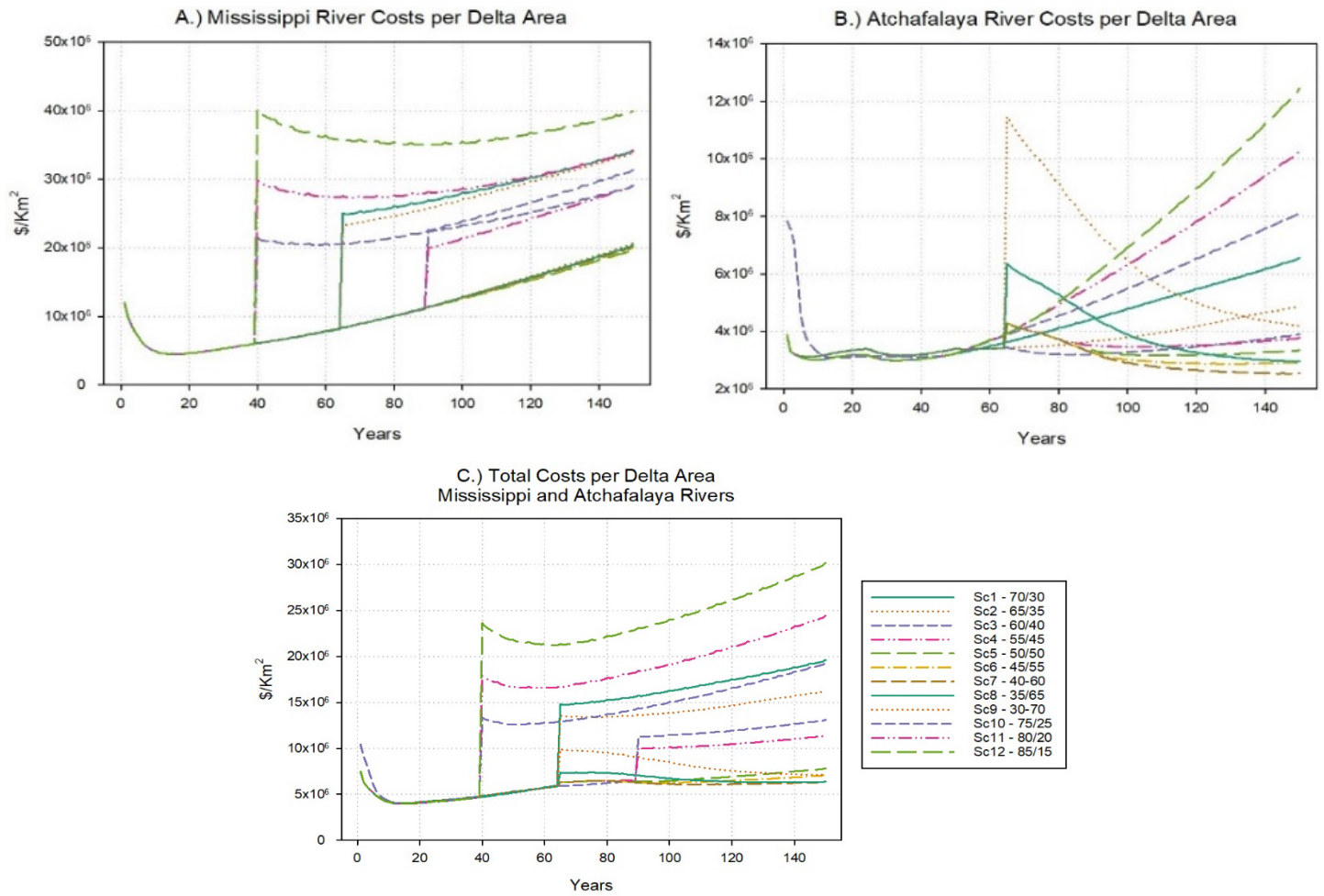


Figure 4.12. Cost Benefit Analysis in terms of River Maintenance costs vs. Delta Land Built for A.) MR Branch B.) AR Branch and C.) MR and AR Branches Combined.

al., 2011; Andrus 2020,b). However, this assessment did not account for impacts to river maintenance costs or socio-economic factors which greatly effect communities across the MRDP, the gulf coast, and beyond.

The analysis presented herein shows that when two of the largest impact categories of dredging and levee enlargement costs are accounted for, gradually increasing flows into the AR makes sense below a certain threshold. System-wide costs of maintaining flood protection and navigation go down with increasing AR flow percentage from 30% to 60%. Beyond this point, costs per benefit area begin to incrementally increase again as flow percentage into the AR

increases, flow accommodation begins to decrease, and stages begin to rise in the AR at a rate that outpaces the additional deltaic areas being built.

The most cost-effective scenario analyzed is Scenario 7 – 40/60 MR/AR Flow Split with a cost-benefit ratio of \$22.7M/Km², a total river maintenance cost of \$11.2B and a benefit are of 1,755 Km² at year 150. Figure 4.13 illustrates the land-building progression curves in Scenario 7 of the WLD diversion which represents the AR and the MBA and MBR diversions which represent the MR. While the MR reaches its land-building peak in the first 60 years, the AR continues an accelerating trajectory through year 150 and beyond. Scenario 7 is almost twice as cost-effective as maintaining the status quo of a 70/30 MR/AR flow split in Scenario 1 and builds ~ 629 Km² more land and saves ~ \$10.9B.

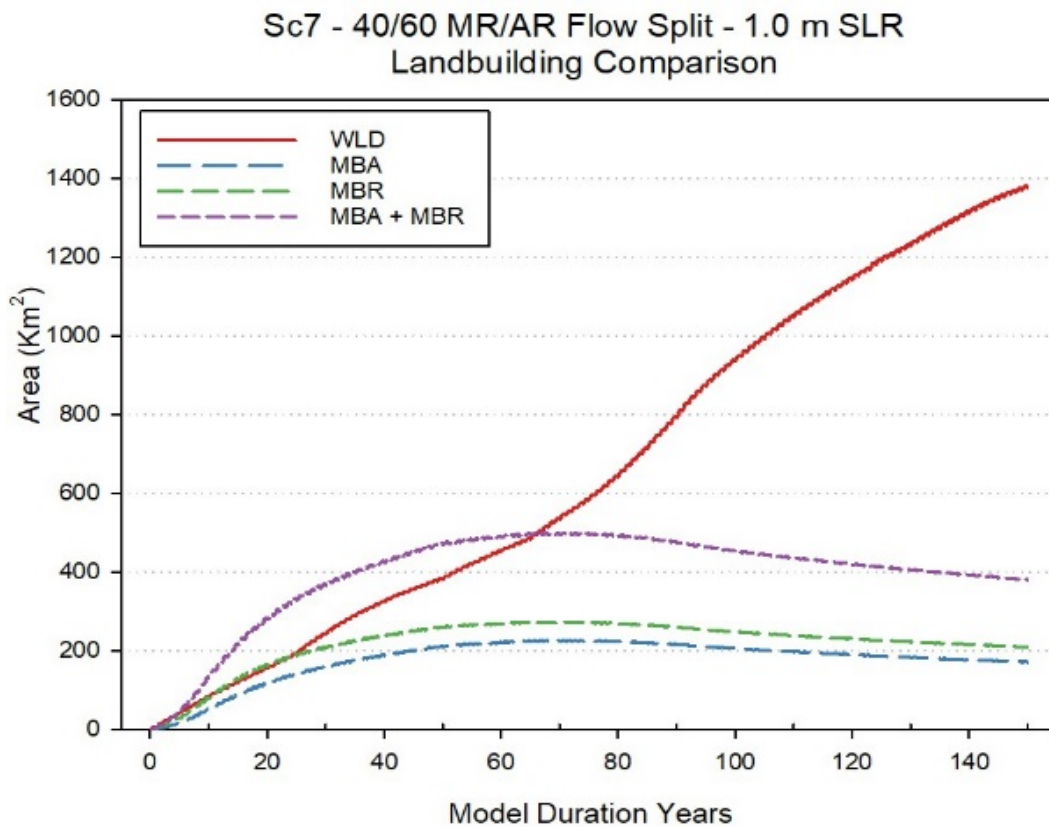


Figure 4.13. Scenario 7 – 40/60 MR/AR Flow Split Land-building Curves.

Some concerns that would remain would be municipal and industrial freshwater supply in the MR, higher AR velocities that could impact navigation and scour protection to municipal and industrial infrastructure, and elevated average water levels in the AR basin, Morgan City, and backwater areas below AR basin flood protection levees. In past years of extreme drought, the USACE has constructed an underwater sill in the MR below New Orleans to prevent denser salt water from migrating further upstream and contaminating water supplies. Additionally, for rising stage concerns in the AR basin, the model does not take into account significant water storage capacity between the extents of the main AR channel and the AR basin levees, meaning actual stages would be lower than those projected by the model in this river branch. Even so, the \$10.9B in cost savings could be used to mitigate for rising stages by additional fortification of levees, sea walls, and backwater flood protection. For example, a structural protection project was added across Bayou Chene near Amelia, LA in the CMP (CPRA, 2017) at an estimated cost of \$80M to protect against backwater flooding during high river flows. While this is a substantial cost, it represents less than 1% of the total cost savings of over the no flow split change scenario. Similarly, communities such as Butte la Rose, LA which reside inside of the AR basin levee system and have a higher flood risk, would likely be eligible for non-structural mitigation programs or relocation programs. Comparatively, in a precedent setting National Disaster Resilience Competition in January of 2016, the U.S. Department of Housing and Urban Development awarded the state of Louisiana \$48.3M in Community Development Block Grant for the Resettlement of Isle de Jean Charles, LA (IDJCR, 2020). Lastly, the maximum discharge reached in the AR near WLO and Morgan City was 22,709 m³/s during the 2011 flood event which even eclipsed the peak of ~20,000 m³/s in 1973 (Roberts, et al., 2003; Kolker et al., 2014). The maximum flow reached over the 150-day duration near this location in the model for

Scenario 7 – 40/60 MR/AR Flow Split is 16,360 m³/s. Even during the only two major flood events which resulted in the opening of the Morgana Spillway which drastically increased the normally mandated 30% AR flow restriction, no insurmountable, catastrophic impacts were realized in the AR basin.

While the results of the cost-benefit projections favor altering the MR/AR flow split to increase AR flows, some study limitations must be underscored. Given the limited budgetary resources available, a previously developed Delft 3D model (from Edmonds, 2012) was retrofitted for this study. While the model was sufficiently calibrated and tested, it uses river elevation data from the early 2000's which was averaged along river course centerlines to reduce computational complexity. The model also does not incorporate any flood plains or minor distributary outlets present in the LMR or the AR Basin. Additionally, the average hydrograph used at the upstream Delft 3D model boundary could be improved upon by incorporating more variable flows which mimic actual river flow extremes where lower flows could induce more shoaling and higher flow peaks could simulate more sediment flushing and higher stream power (Rodi, 2017). Also, a more intricate 3D network of deltaic channels and deposits as opposed to the simpler 1D Dean model outputs would offer much more spatial detail to the analysis. Without these exclusions and simplifications, hydraulic model interactions and computational requirements would be much more resource intensive, but could reveal more detailed results of different magnitudes and additional contributing factors to consider.

The estimation of river maintenance costs are based on reconnaissance level analysis of dredging vs. annual river flow relationships and desktop measurement of levee elevations and lengths using online resources. Additionally, costs were determined by evaluating past construction contracts which do not factor in inflation or other changing physical, environmental,

or market driven factors such as rising energy costs. Results are only presented in terms of two major maintenance categories and do not account for other municipal or industrial impacts or any sophisticated ecosystem service categories. Nevertheless, estimated cost savings and added environmental benefits associated with modifying flow management regimes to take advantage of the AR's future discharge accommodation and land-building potential is significant and warrants additional research in these areas of limitation.

4.5. Conclusions

- (1) Model results show that the AR river branch displays a clear land-building advantage over the MR due to its extreme gradient advantage over the MR and the lack of restrictions to deliver all of the AR's sediment supply to its receiving area.

- (2) Rising stage in the MR due to declining stream power and ability to adequately transport sediment loads threatens the current status of the MR&T flood protection system in the LMR and could result in significantly increased maintenance costs without consideration of major flow diversion.

- (3) Using model results and reconnaissance-level cost estimating methods, shows that flow diversion of up to 60% of total MR river flow above the MR-AR bifurcation into the AR would result in cost-effective alternative management strategies for both flood alleviation and deltaic land-building in the MRDP over the next 150 years. Potential cost savings of such alternatives could also be used to mitigate for negative impacts to communities in both the MR and AR branches.

- (4) If eventually justified by overcoming extensive socio-economic factors, altering the MR/AR flow split at the ORCS to a maximum of 40/60, rendering the AR path as the new dominant river branch, land-building potential of the MR and AR combined could effectively combat ESLR and reclaim up to 38% of the last century's coastal land loss that has occurred in the MRDP in the next 150 years.

- (5) Land-building trends associated with long-term management of the ORCS flow split in favor of the AR as the dominant river branch would continue to accelerate beyond 150 years, continuing a regressive land-building phase along a sustainable delta cycle curve towards a peak much further into the future.

- (6) With the potential to as much as triple land-building rates through sediment diversions in the next 150 years and continue long-term ecosystem sustainability well into the future, further in-depth evaluations which analyze implementation and maintenance costs in addition to socio-economic impacts of altering the control of river flows through the MR-AR bifurcation are warranted.

CHAPTER 5: SUMMARY AND CONCLUSIONS

For thousands of years as part of glacial processes, the MR has forged its alluvial valley through the heart of North America and shaped the south Louisiana coastal plain through its delta cycle. Many researchers, universities, and agencies over the last century have collected valuable data, conducted comprehensive investigations, and made significant contributions to the knowledge base on MR evolution. The MR supports our nation's economy, the livelihood of Louisiana communities, and the sustainability of the gulf coast ecosystem. As the world's third largest river, the MR provides the country's most important navigational corridor, hydroelectric power, drinking water, freshwater to fisheries, nutrients to wetlands, and land-building sediments to coastal landscapes. Prior to human intervention to control its course, engineer its channels for navigation, and fortify its banks to prevent adjacent flooding, the MR flowed freely and naturally built wetlands at the gulf interface in the form of delta complexes over hundreds of years. Once these historic deltas became hydraulically inefficient and susceptible to marine processes, the MR would gradually shift courses through an upstream avulsion and repeat this geologic process in a new location.

Today the MR is a highly engineered system which includes the ORCS constructed in 1962 at the MR-AR bifurcation which is the location of the most recent and currently active MR avulsion. The avulsion was initiated approximately 400 years ago and capture of the main stem of the MR by the AR began to accelerate in the early to mid-1900's, jeopardizing federal investments, local communities, industrial infrastructure, and regional and national economic stability. The construction of the ORCS prevented certain capture of the MR and suspended the flow split between the MR and AR at 70%/30% where it has been maintained ever since. While this federal action brought economic stability and certainty for decades by providing mostly predictable short-term flow and stage conditions, coastal wetlands in the MRDP continue to

deteriorate at alarming rates and recent evidence of changing river dynamics could increase flood vulnerability.

The intent of this dissertation was to gain a more comprehensive understanding of the role that the MR-AR bifurcation and the ORCS will likely play in long-term river management and coastal restoration strategies. Using state of the art Delft 3D modeling software, Chapter 2 revisited the AR engineering study conducted in 1951 and its companion geologic investigation conducted in 1952 by the MRC in which avulsion capture rates were evaluated and ultimately used to authorize the ORCS construction and operation. The capture analysis modeled in Chapter 2 produced convincing results that compare well with past avulsion investigations and provided a foundational approach to land-building analyses conducted in Chapter 3 for twelve alternative flow split scenarios. Chapter 3 coupled Delft 3D outputs from lower AR and MR locations with a 1D spreadsheet model using Dean et. al., 2012 delta building equations over a 150-year time frame. Chapter 4 also utilized Delft 3D stage and flow outputs across the entire domains of both the MR and AR branches to evaluate river maintenance costs in the two major categories of levee enlargements to protect floods which would be caused by rising river stages and navigational dredging expenses which are largely influenced by flow and sedimentation rates.

In Chapter 2, Delft 3D riverine modeling was conducted over a model domain developed by Edmonds (2012) that expanded from Vicksburg, MS above the MR-AR bifurcation down to the GOM interface below Venice, LA for the MR and below Morgan City, LA for the AR. At the MR-AR bifurcation, Edmonds removed the ORCS the model by splicing together bathymetry data and developing detailed gridwork that connected the two river branches together. In his 2012 study, Edmonds tested the capture hypothesis by running steady-state upstream flows over short decadal-scale durations. To further this work an unsteady average annual upstream

hydrograph was developed using a historical daily flow data set. This hydrograph was then applied as a revised upstream boundary input and repeated 150 times in succession to create a semi-unsteady state model which re-evaluated avulsion dynamics. Results were then used to develop a time to capture percentage equation and compared to similar equations developed using data regressions from MRC investigations from the early 1950's. The new semi-unsteady state results predict 40% capture by the AR in 6.7 years and 50% capture in 17.2 years which varies from the MRC results by 2.9 and -0.4 years, respectively. This is considered to be a high degree of agreement with capture trends from actual measurements taken prior to ORCS construction. This agreement with MRC regression data continues through a capture prediction of 65% before the Delft 3D model begins to deviate with a rate that slows down significantly. While this is inconsistent with earlier capture stage trends, later stage Delft 3D capture outputs do agree well with qualitative assessments made in the MRC geological investigation regarding later-stage avulsion evolution based on full life-cycle analogs from smaller streams and analysis of geologic deposits from historic avulsion sites.

Using the newly developed Delft 3D semi-unsteady state model approach proven to be effective in predicting capture trends, twelve new alternative flow split scenarios (1 No Change scenario, 8 increased AR flow scenarios, and 3 increased MR flow scenarios) were developed for coastal land-building analyses in Chapter 3. The combined Delft 3D grid which connect the MR to the AR at OR was broken in to two individual grids below the bifurcation and headwater boundary conditions were adjusted in both branches to simulate ORCS flow and sediment controls. Output monitoring locations were also setup within the model at six strategic locations in both river branches. Sediment transport time-series files were output at monitoring locations near MBA and MBR diversion locations in the MR and near the WLD diversion in the AR. A

1D spreadsheet model was then developed using a delta building equation from Dean et al. (2012) for each diversion location which used sediment volumes from each Delft 3D time step along with various inputs gathered from published data sources for each receiving area. The 150-year resulting land areas built for the MR vs. the AR at discrete flow percentages demonstrate a clear land-building capacity advantage in the AR. For common flow percentages, the AR builds 1.7 times more land at 30% of the total river flow and 3.0 times more land at 70% of the total river flow. Scenario 9 – 30/70 MR/AR Flow Split produced the most system-wide deltaic land in the MRDP at 1,965 km² with a 150-year land area growth of 348 km² vs. 1,617 km² for the MR vs. AR, respectively. Scenario 12 – 85/15 MR/AR Flow Split produced the least system-wide deltaic land in the MRDP at 984 km² with a 150-year land area growth of 633 km² vs. 350 km² for the MR vs. AR, respectively.

While the coastal restoration metrics of land area built are straightforward, planners must consider the complex task of evaluating associated costs of implementation. Chapter 3 provides a first-order estimation of river maintenance costs by applying cost data from recent federal levee enlargement and dredging projects to quantities developed using reconnaissance-level desktop measurements combined with Delft 3D stage and flow outputs for each scenario. Levee enlargement volume and length requirements to prevent future flooding were determined using long-term stage profiles for 25-year increments along each river branch. Dredging volume requirements to maintain navigation were determined using dredging vs. river flow equations developed for each river branch using 22 years of dredging data from the USACE and flow data from the USGS. Dredging and levee enlargement costs were combined for each river branch and divided by land-building outputs from Chapter 3 to determine the most costs per benefit for each scenario. The most cost-effective scenario analyzed is Scenario 7 – 40/60 MR/AR Flow Split

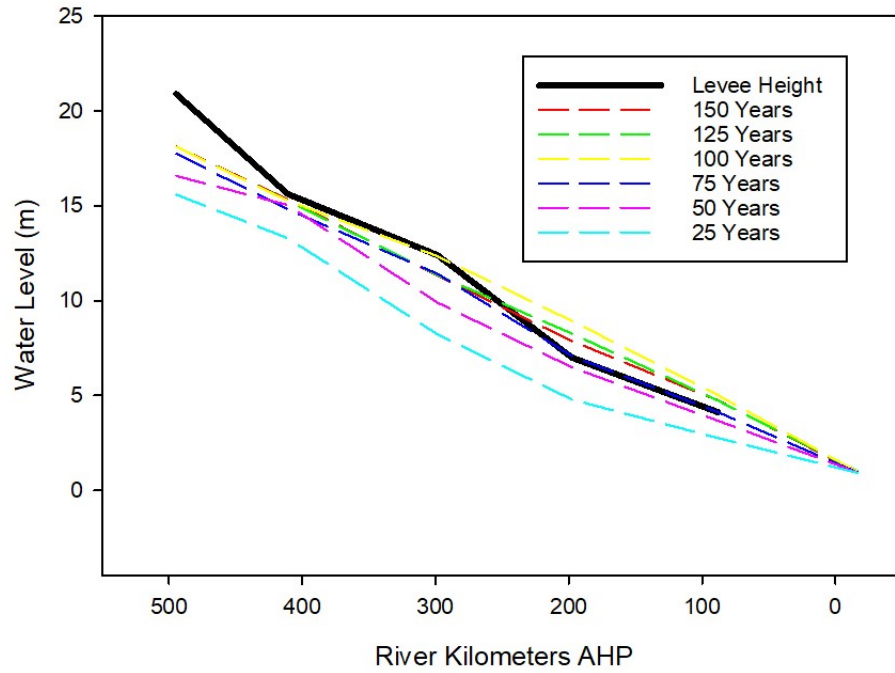
with a cost-benefit ratio of \$22.7M/km², a total river maintenance cost of \$11.2B and a benefit are of 1,755 Km² at year 150. This is almost twice as cost-effective as maintaining the status quo of a 70/30 MR/AR flow split in Scenario 1 and builds ~ 629 km² more land and saves ~ \$10.9B.

These estimated cost savings and land-building benefits are over the next 150 years could have vast implications for federal, state, and local planning authorities and funding agencies. While this study uses scientifically based trends, published data sets, and proven modeling techniques to arrive at its conclusions, many improvements could be made through future needed research. The Delft 3D model should be improved by incorporating more variable flows which mimic actual river flow extremes, more recent river bathymetry and finer grid spacing to better define channel side slopes and bed geomorphology, inclusion of minor distributary outlets and overflow areas in the lower MR reaches and AR basin, and development of deltaic receiving area grids which account for physics and complex gulf-interface boundary conditions. Future cost analyses should also account for inflation factors which would more accurately capture rising energy costs and reflect the rising impacts of maintenance events which occur in later years. They should also account for additional river maintenance categories such as revetment maintenance and impacts to infrastructure such as bridges, locks, jetties, docks, and pipelines. Ecosystem services valuations which consider benefits to fisheries, storm protection, recreation, water supply, carbon sequestration, etc. would also be integral to future comprehensive evaluations which could lead to action.

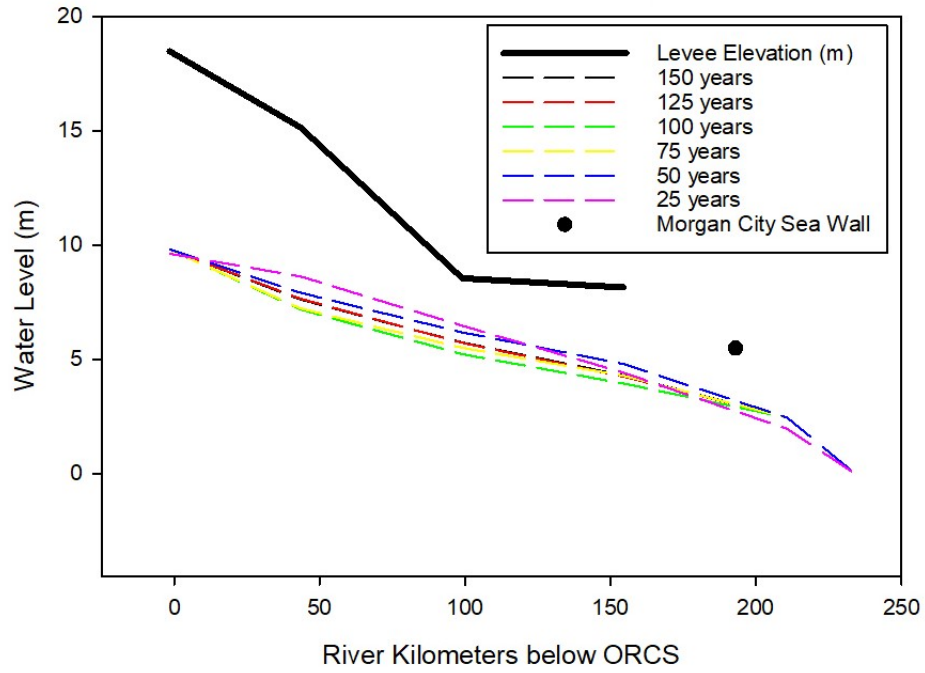
APPENDIX A: MODELED STAGE AND LEVEE PLOTS

SCENARIO 1 – 70/30 MR/AR FLOW SPLIT (NO CHANGE)

FWOA Model Scenario (70-30) - Mississippi River
Stage Progression at Average Annual Hydrograph Peaks

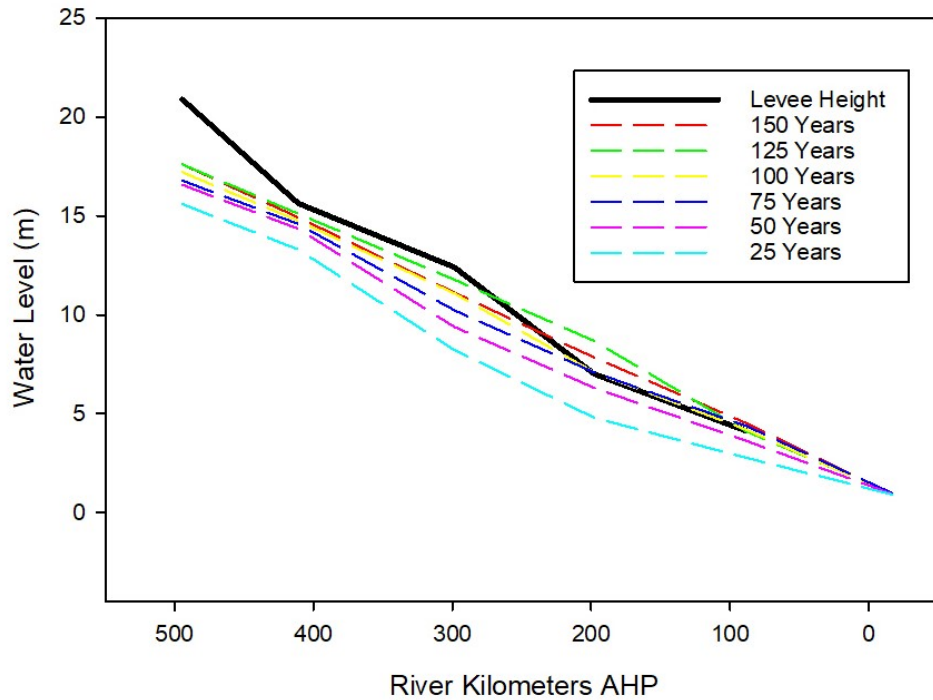


FWOA Model Scenario (70-30) - Atchafalaya River
Stage Progression at Average Annual Hydrograph Peaks

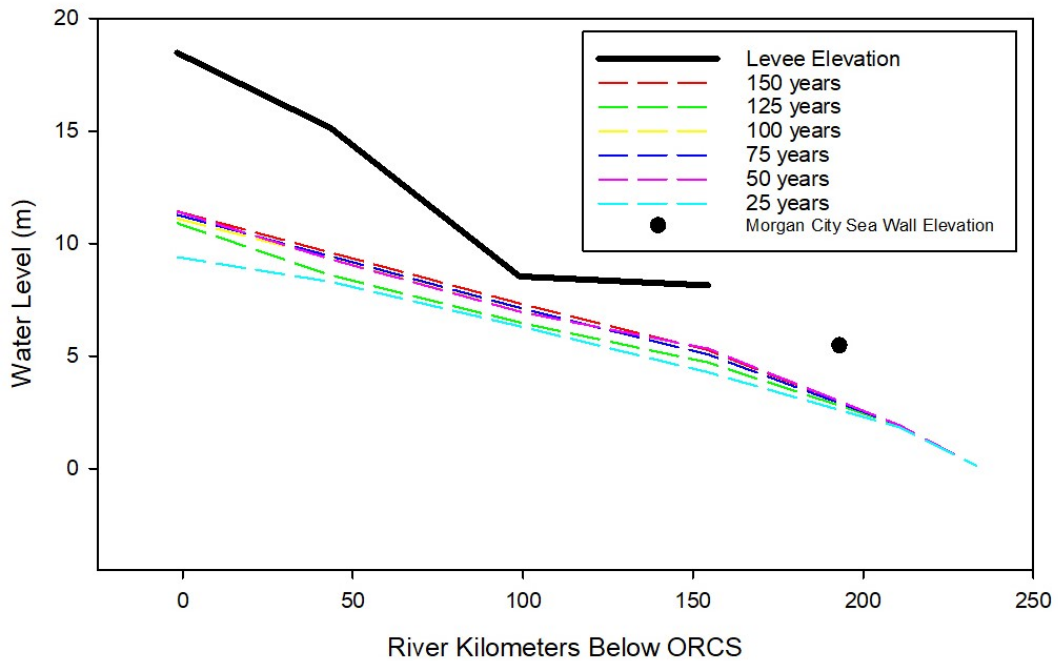


SCENARIO 2 – 65/35 MR/AR FLOW SPLIT

Model Scenario 2 (65-35) - Mississippi River
Stage Progression at Average Annual Hydrograph Peaks

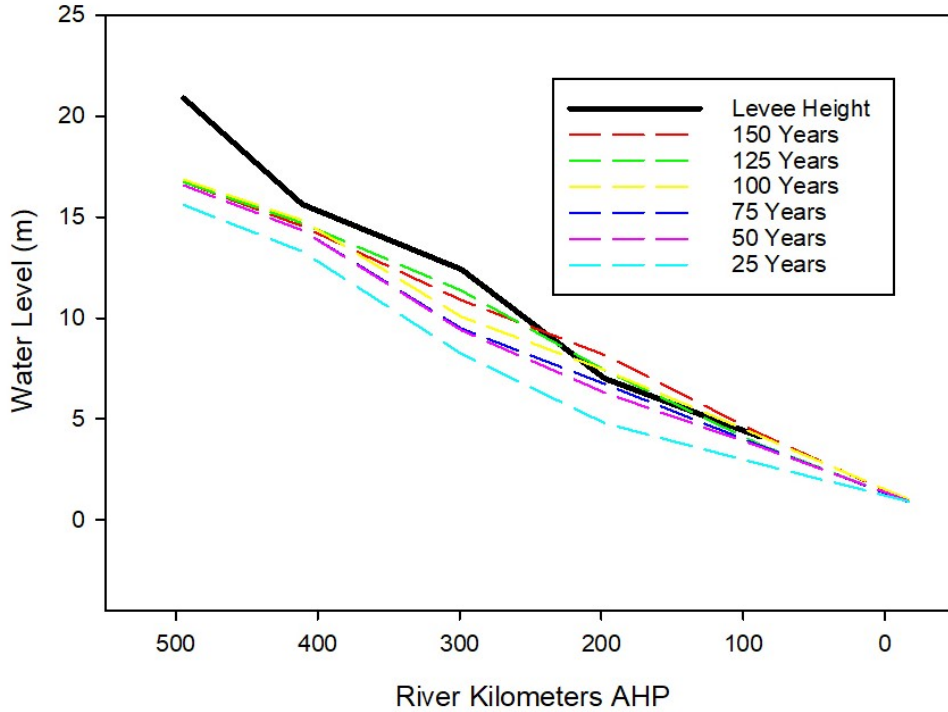


Model Scenario 2 (65 - 35) - Atchafalaya River
Stage Progression at Average Annual Hydrograph Peaks

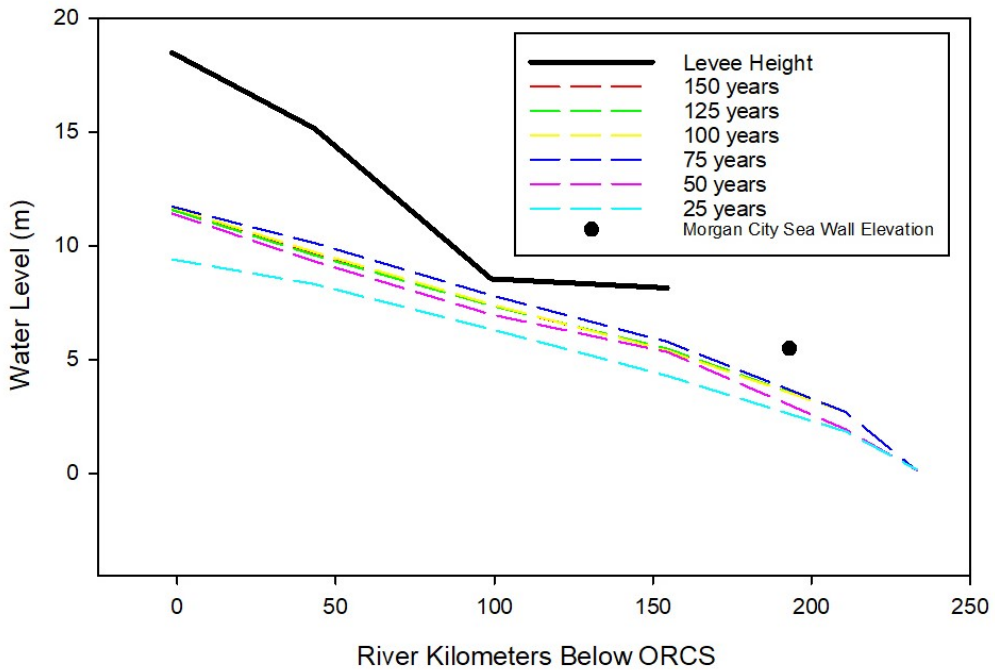


SCENARIO 3 – 60/40 MR/AR FLOW SPLIT

Model Scenario 3 (60-40) - Mississippi River
Stage Progression at Average Annual Hydrograph Peaks

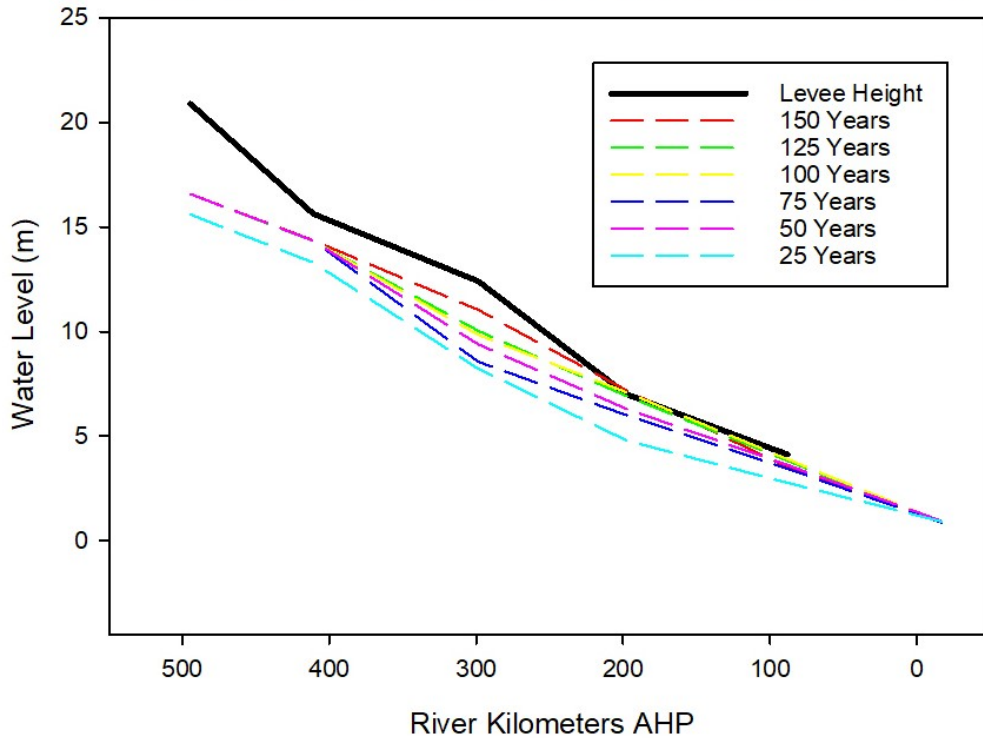


Model Scenario 3 (60-40) - Atchafalaya River
Stage Progression at Average Annual Hydrograph Peaks

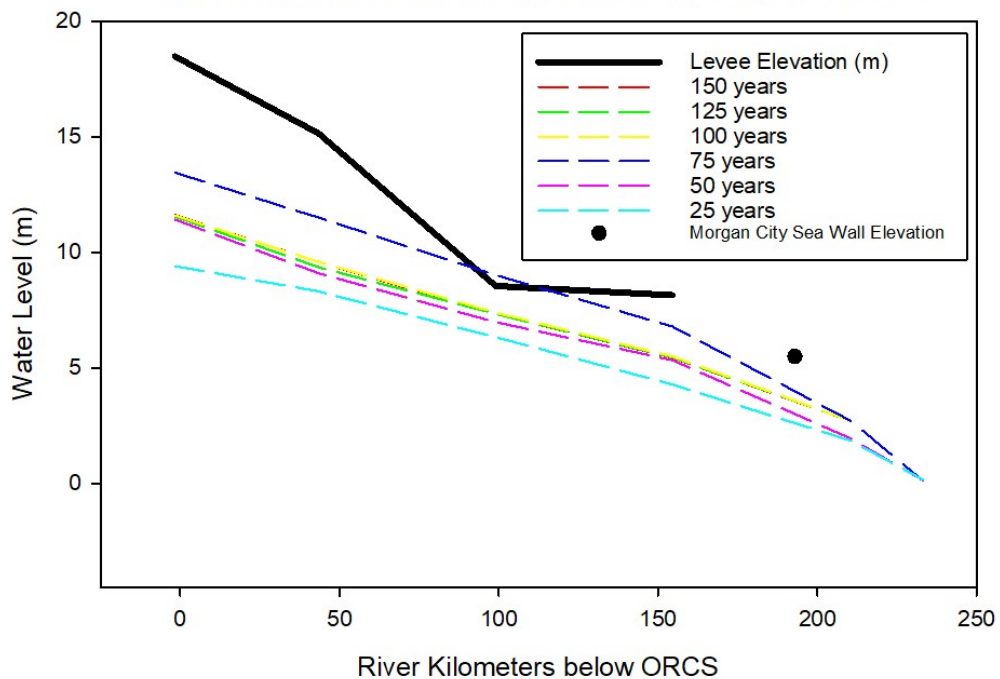


SCENARIO 4 – 55/45 MR/AR FLOW SPLIT

Model Scenario 4 (55-45) - Mississippi River
Stage Progression at Average Annual Hydrograph Peaks

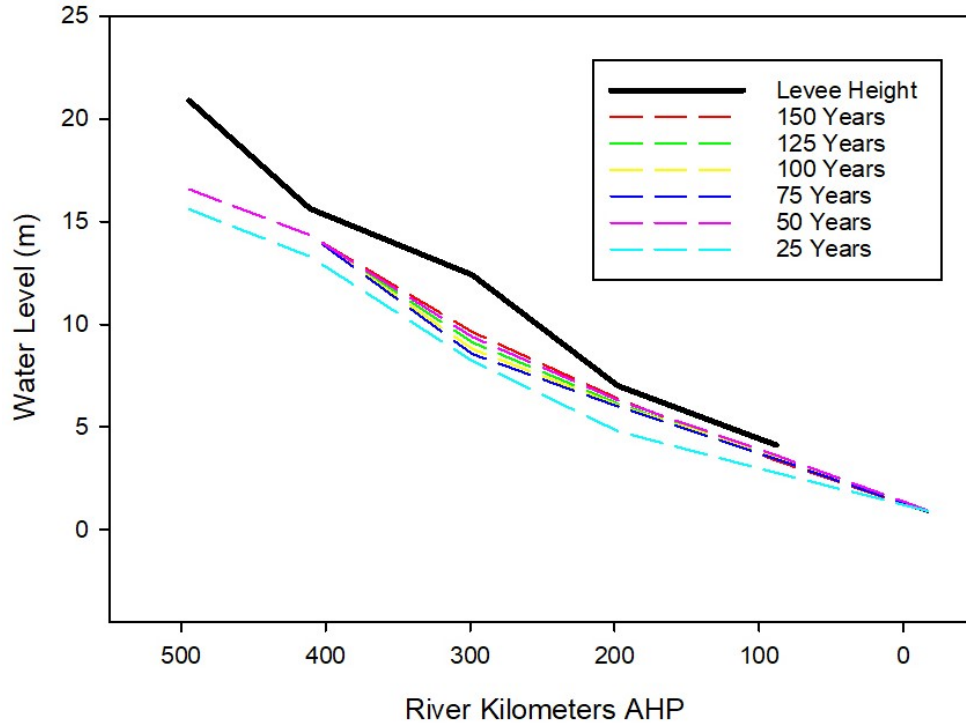


Model Scenario 4 (55 - 45) - Atchafalaya River
Stage Progression at Average Annual Hydrograph Peaks

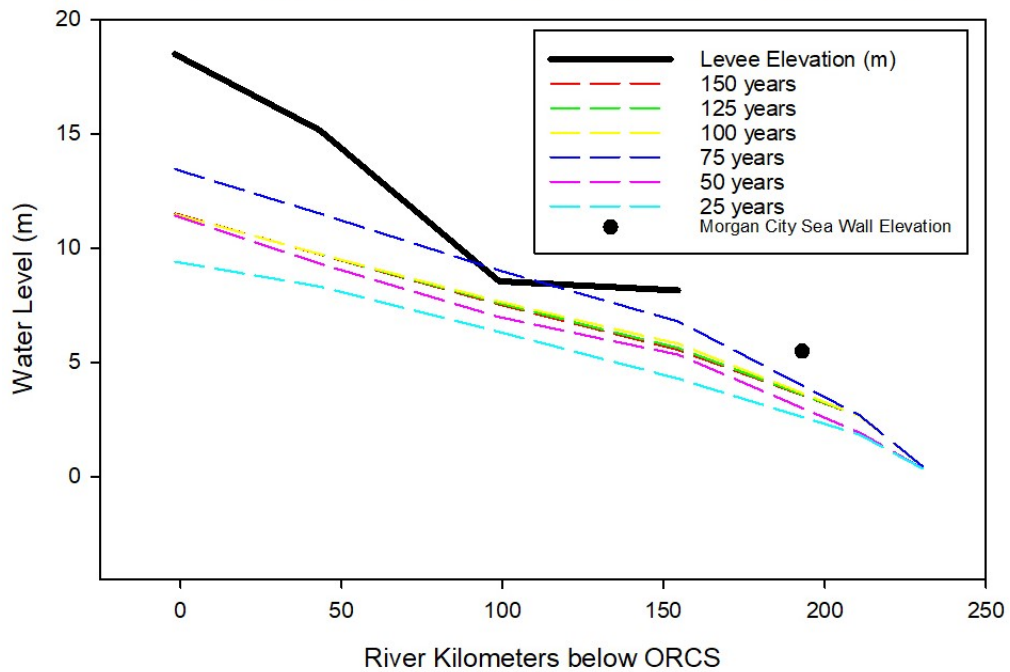


SCENARIO 5 – 50/50 MR/AR FLOW SPLIT

Model Scenario 5 (50-50) - Mississippi River
Stage Progression at Average Annual Hydrograph Peaks

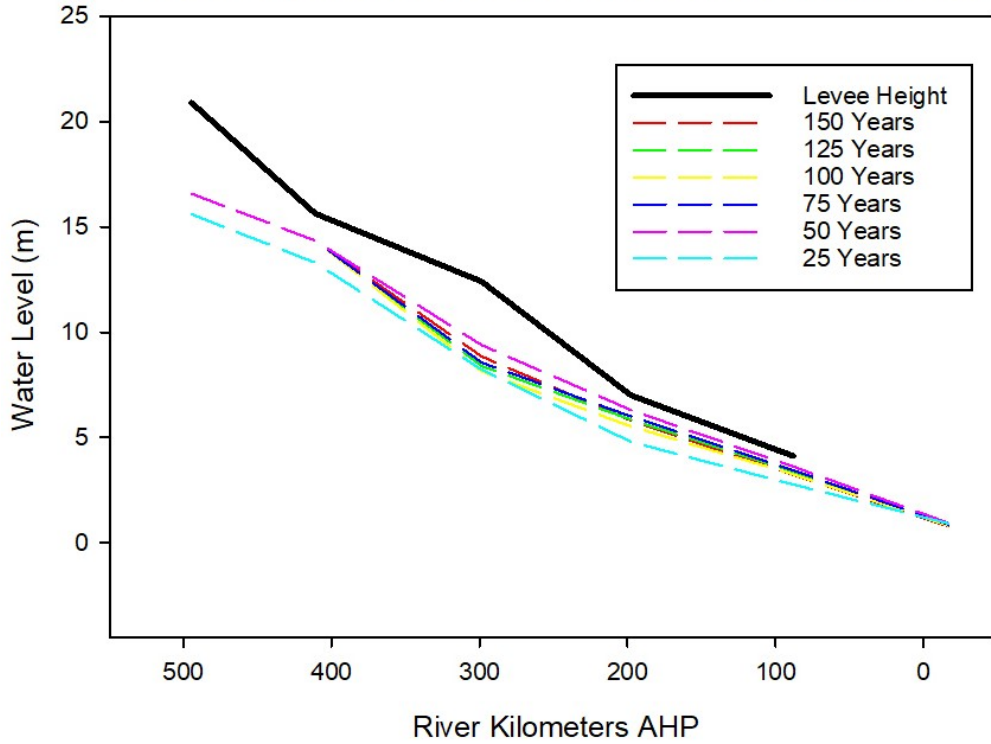


Model Scenario 5 (50-50) - Atchafalaya River
Stage Progression at Average Annual Hydrograph Peaks

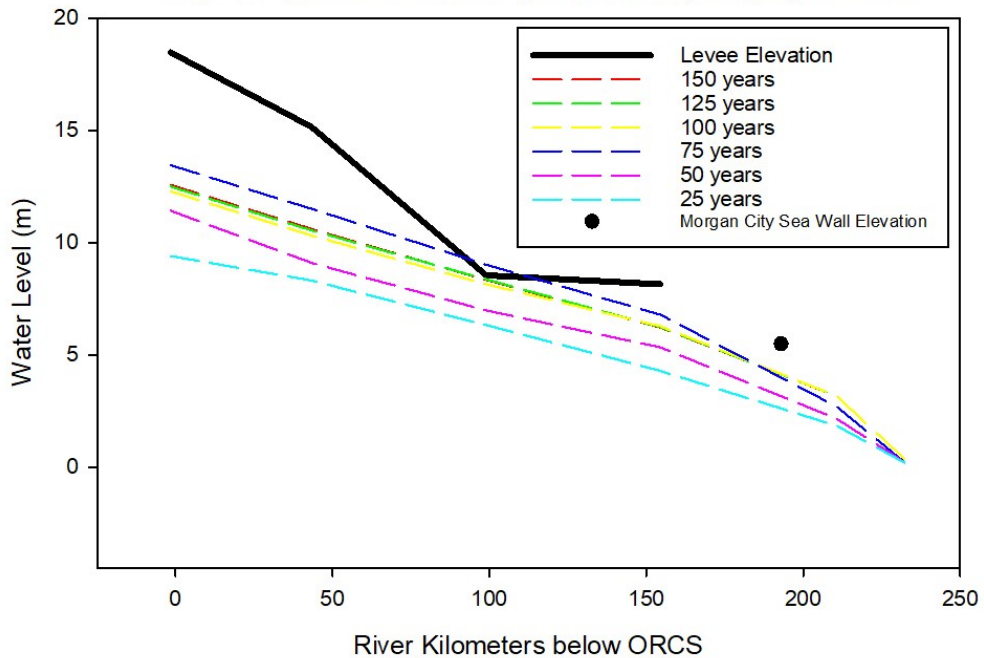


SCENARIO 6 – 45/55 MR/AR FLOW SPLIT

Model Scenario 6 (45-55) - Mississippi River
Stage Progression at Average Annual Hydrograph Peaks

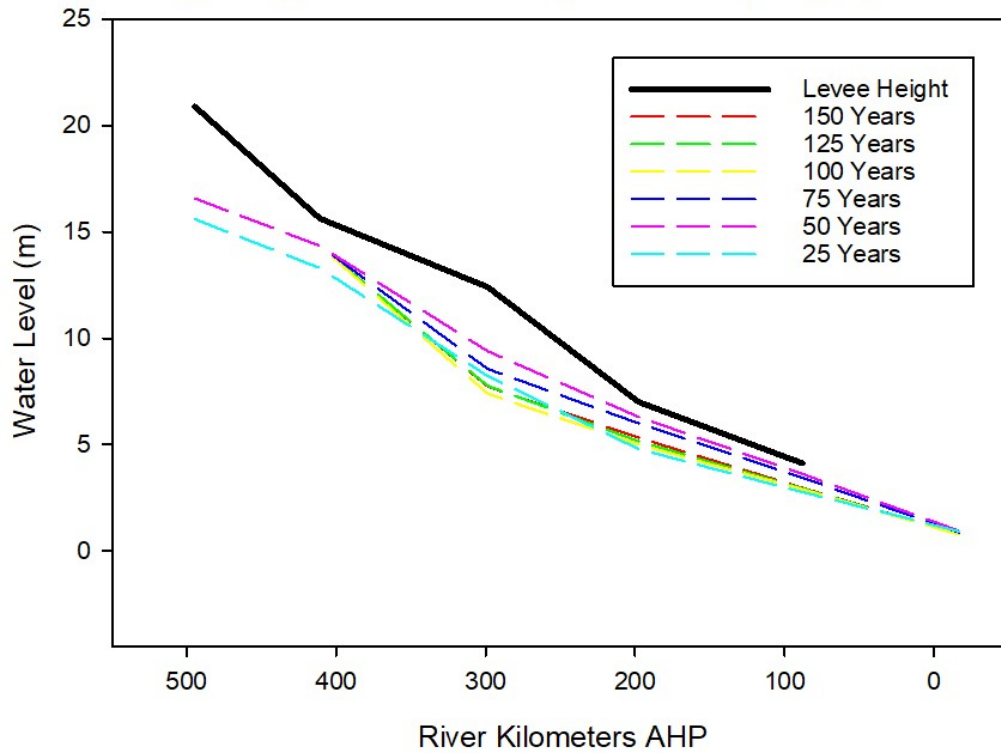


Model Scenario 6 (45-55) - Atchafalaya River
Stage Progression at Average Annual Hydrograph Peaks

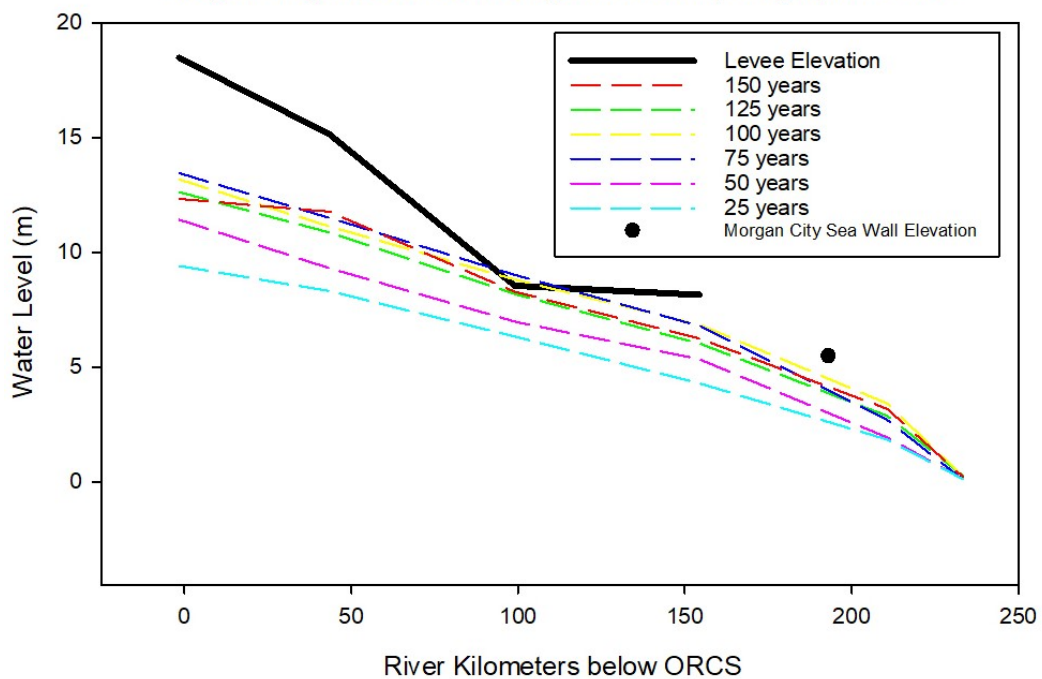


SCENARIO 7 – 40/60 MR/AR FLOW SPLIT

Model Scenario 7 (40-60) - Mississippi River
Stage Progression at Average Annual Hydrograph Peaks

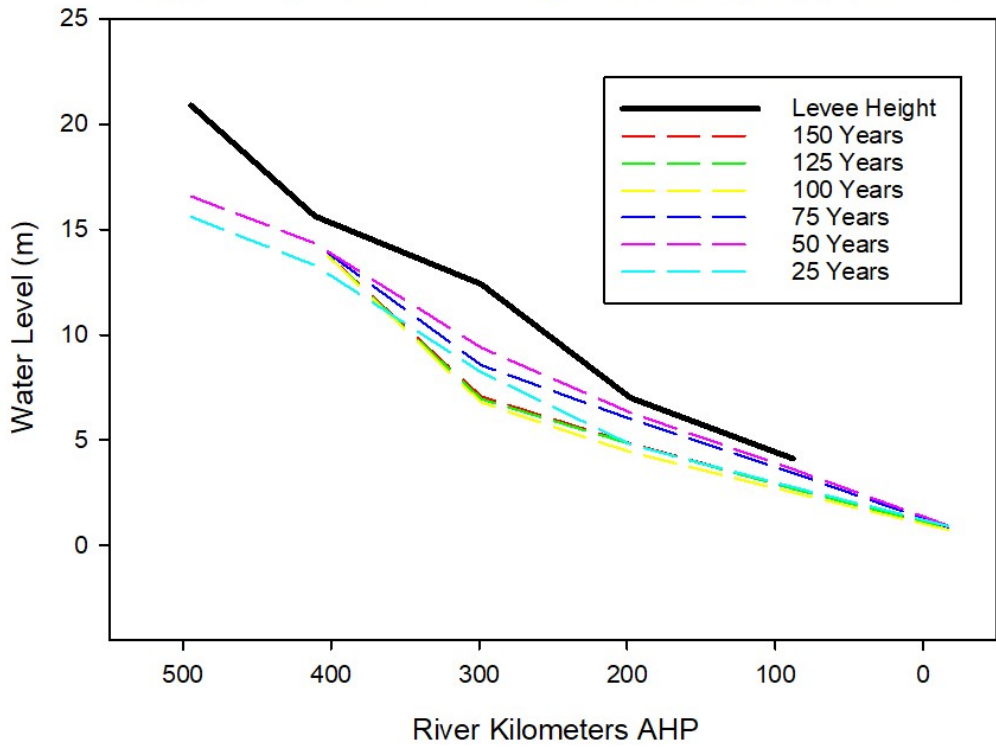


Model Scenario 7 (40- 60) - Atchafalaya River
Stage Progression at Average Annual Hydrograph Peaks

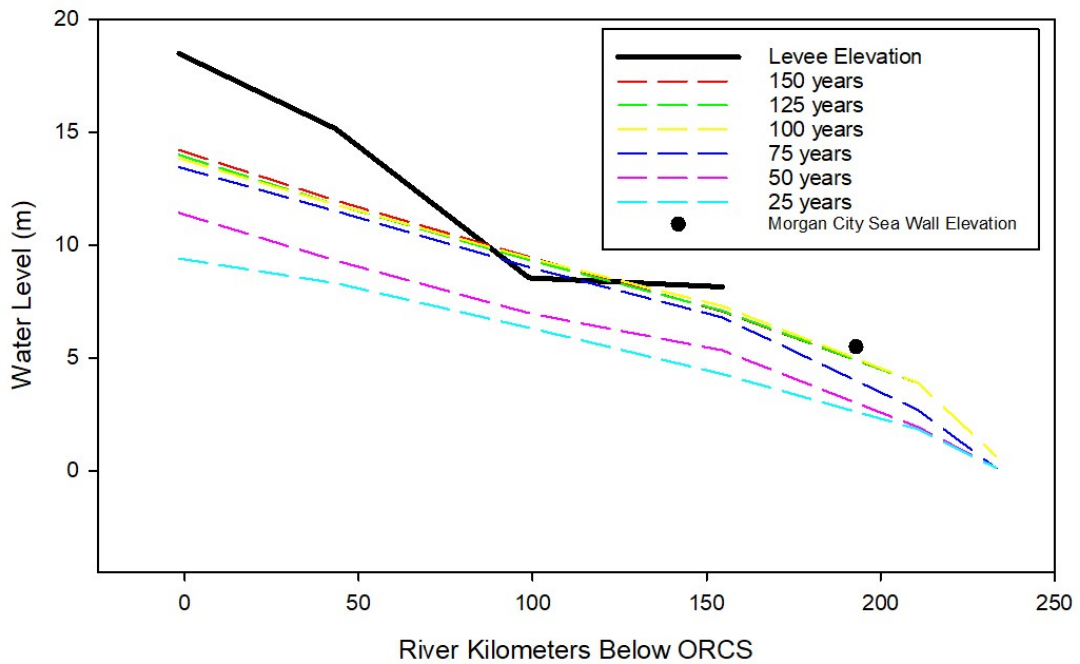


SCENARIO 8 – 35/65 MR/AR FLOW SPLIT

Model Scenario 8 (35-65) - Mississippi River
Stage Progression at Average Annual Hydrograph Peaks

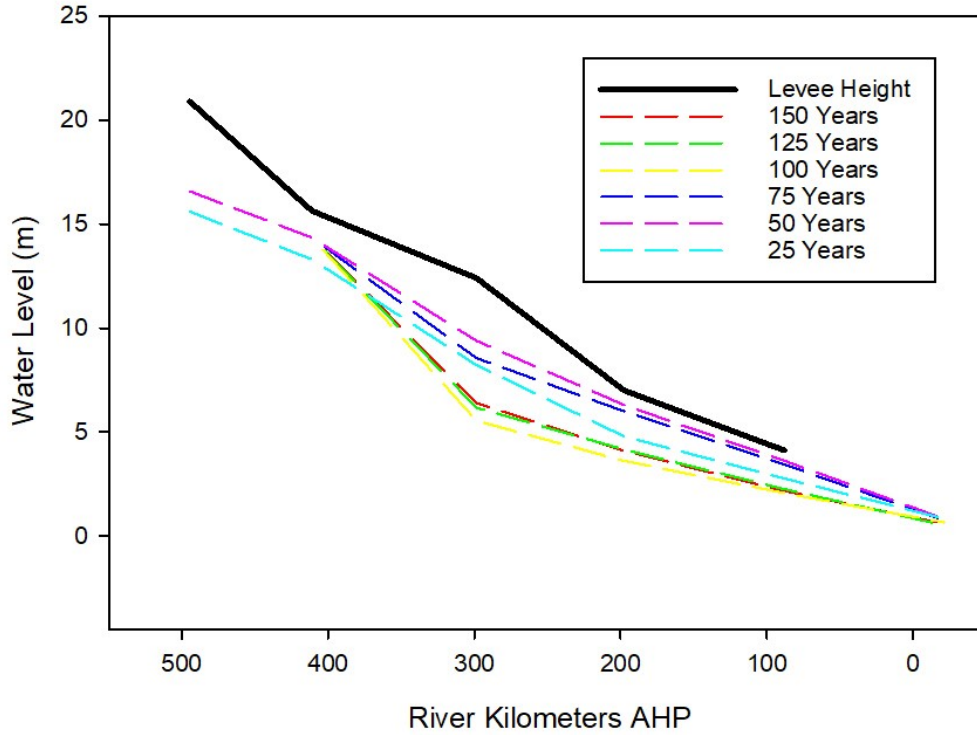


Model Scenario 8 (35-65) - Atchafalaya River
Stage Progression at Average Annual Hydrograph Peaks

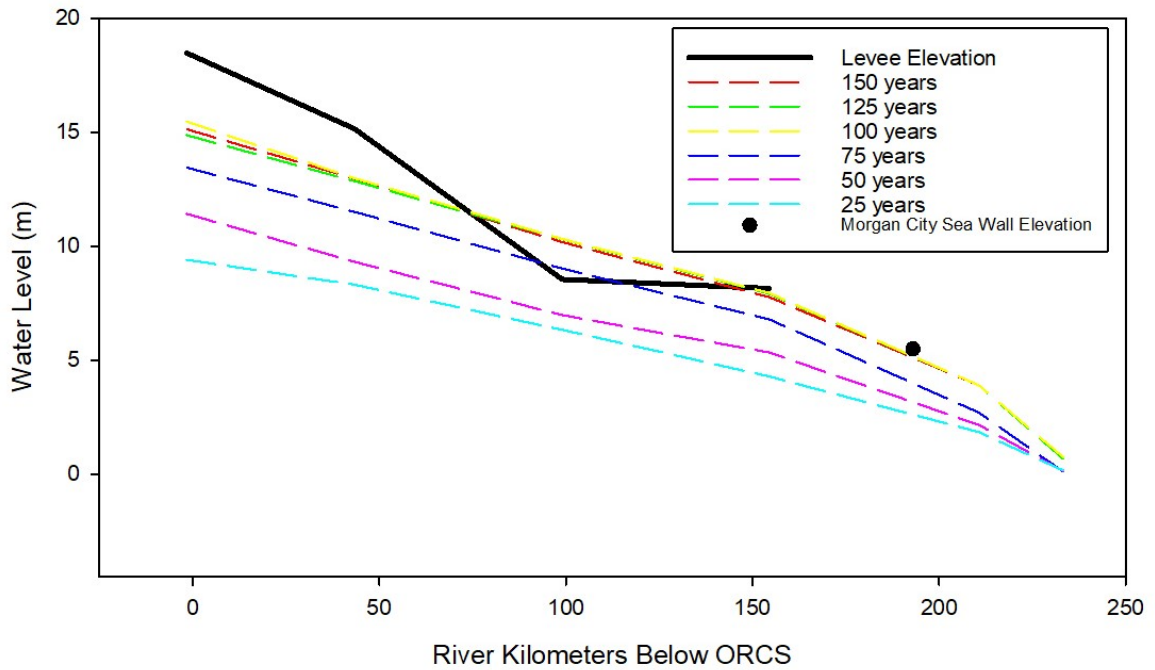


SCENARIO 9 – 30/70 MR/AR FLOW SPLIT

Model Scenario 9 (30-70) - Mississippi River
Stage Progression at Average Annual Hydrograph Peaks

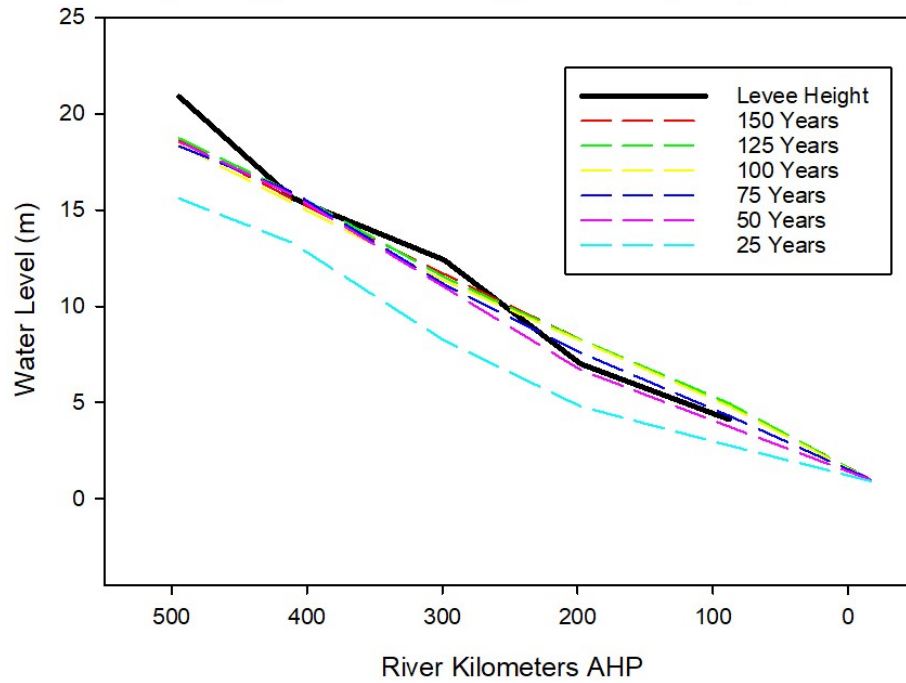


Model Scenario 9 (30-70) - Atchafalaya River
Stage Progression at Average Annual Hydrograph Peaks

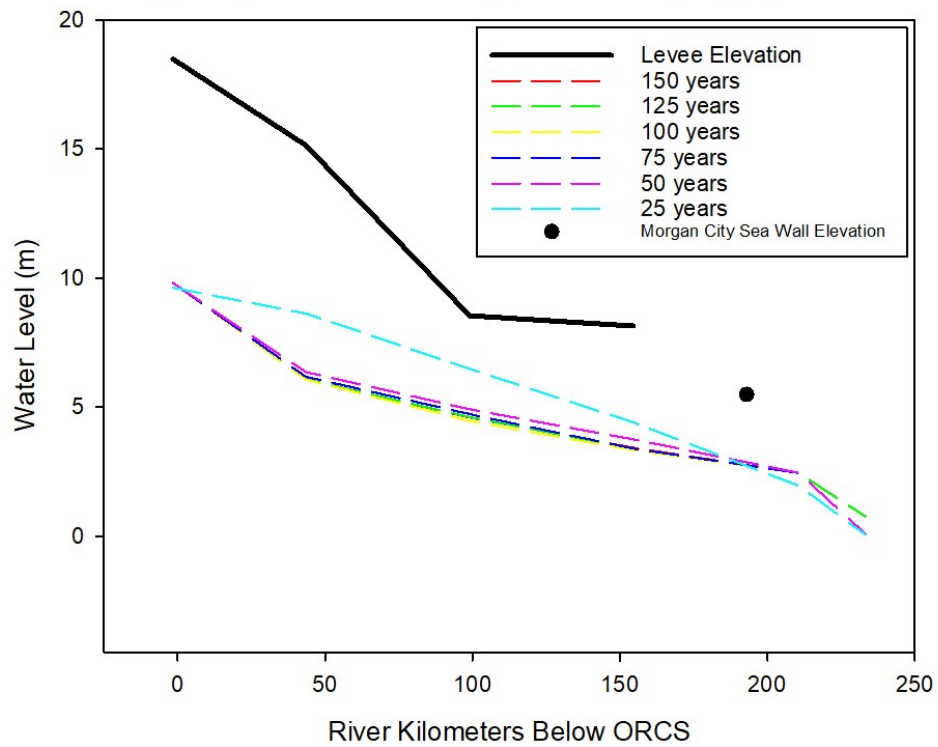


SCENARIO 10 – 75/25 MR/AR FLOW SPLIT

Model Scenario 10 (75-25) - Mississippi River
Stage Progression at Average Annual Hydrograph Peaks

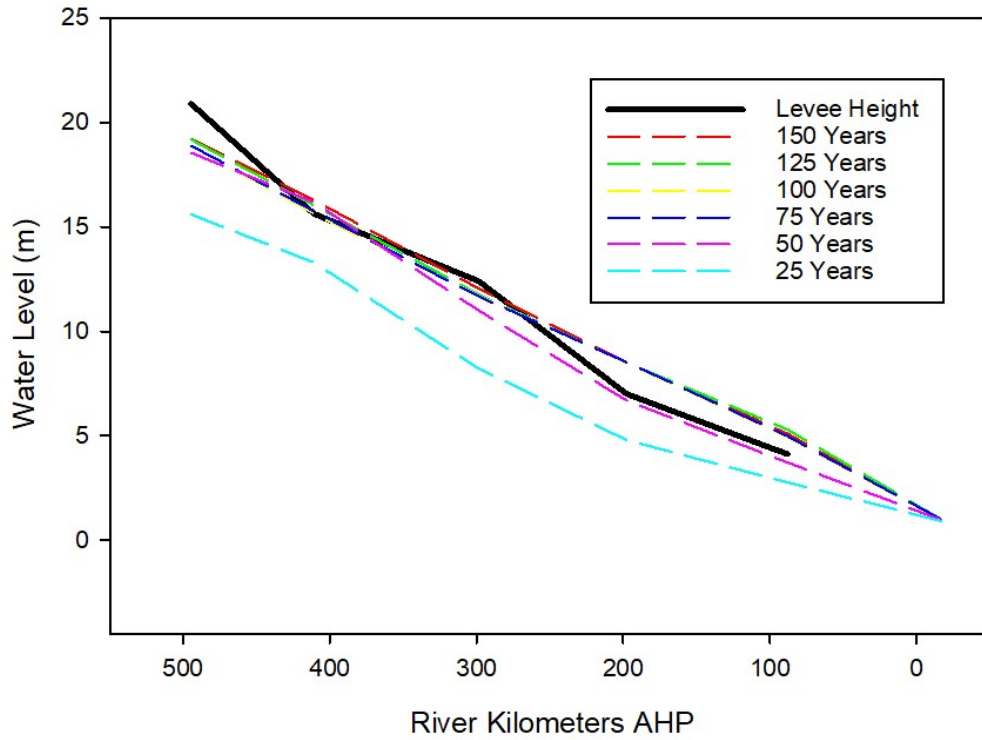


Scenario Model 10 (75-25) - Atchafalaya River
Stage Progression at Average Annual Hydrograph Peaks

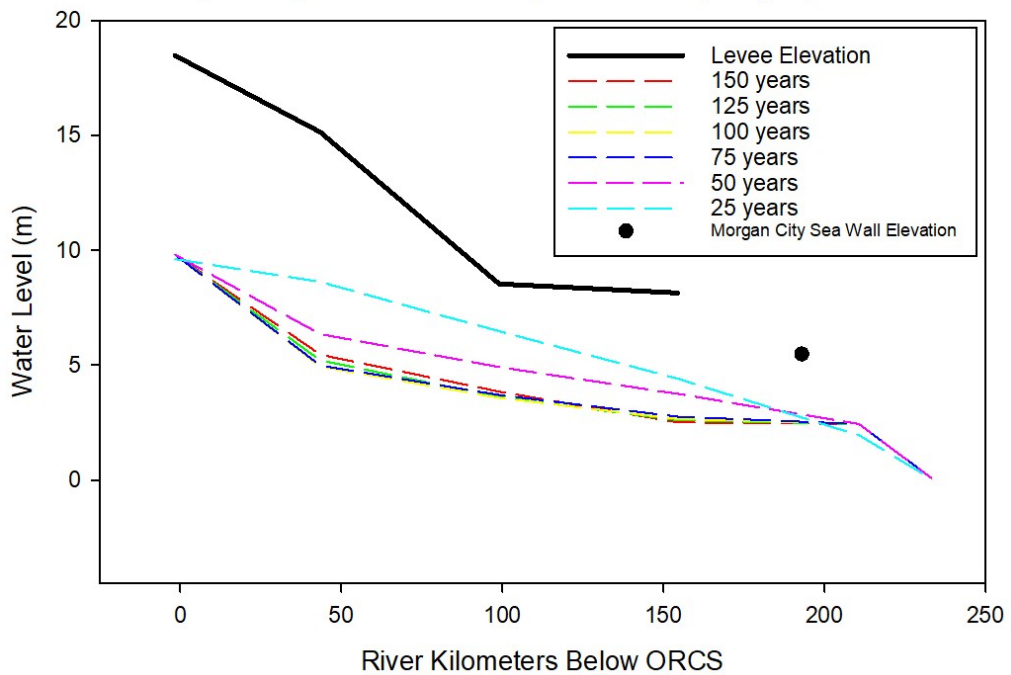


SCENARIO 11 – 80/20 MR/AR FLOW SPLIT

Model Scenario 11 (80-20) - Mississippi River
Stage Progression at Average Annual Hydrograph Peaks

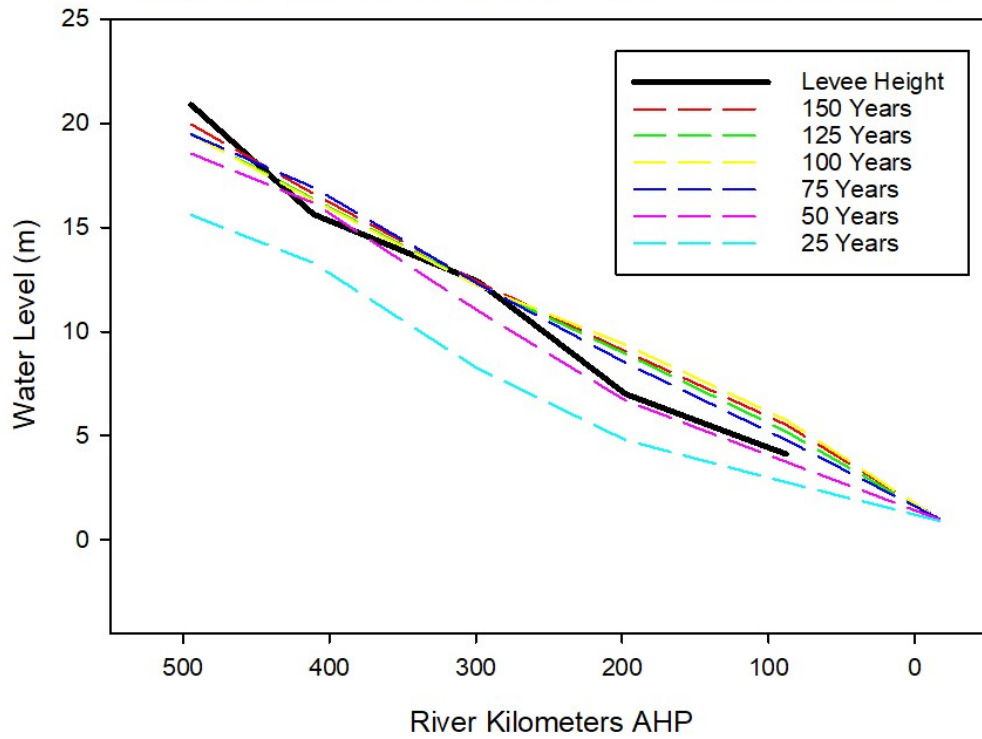


Model Scenario 11 (80-20) - Atchafalaya River
Stage Progression at Average Annual Hydrograph Peaks

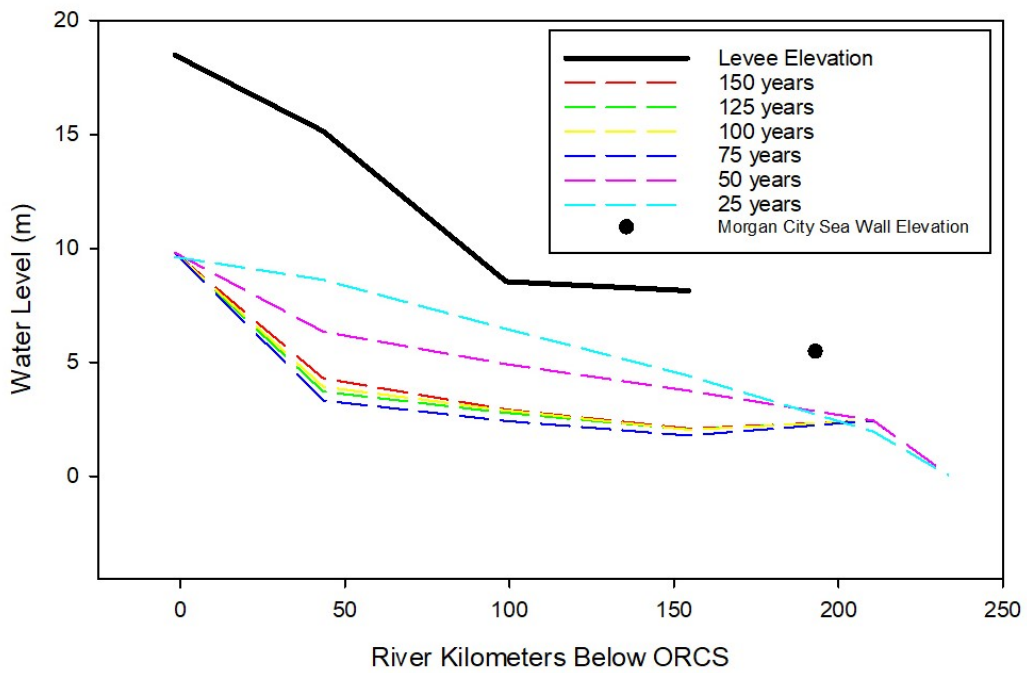


SCENARIO 12 – 85/15 MR/AR FLOW SPLIT

Model Scenario 12 (85-15) - Mississippi River
Stage Progression at Average Annual Hydrograph Peaks



Model Scenario 12 (85-15) - Atchafalaya River
Stage Progression at Average Annual Hydrograph Peaks



**APPENDIX B: RIVER LEVEE CONSTRUCTION COSTS
EXAMPLE USACE BID TABULATIONS**

Westbank Mississippi River Levee New Orleans to Venice, Nov-09, 2018													
St. Jude to City Price Requirements Parish, Louisiana													
LineItem	Description	Estimated Quantity	Unit of Measure	Low Bidder - B&K Construction	PhyWay Construction	Cycle Construction	Randy/Kinder Excavating	Average					
Linear Feet of Levee													
LineItem	Description	Estimated Quantity	Unit of Measure	Unit Price	Total	Unit Price	Total	Unit Price	Total	Unit Price	Total	Average	
2	Traffic Control and Coordination	1.00	Job	\$ 52,000.00	\$ 52,000.00	\$ 50,000.00	\$ 50,000.00	\$ 59,900.00	\$ 59,900.00	\$ 50,075.00	\$ 50,075.00	\$ 59,900.00	
3a	Silt Fence First 25,000 LF	25,000.00	LF	\$ 4.00	\$ 100,000.00	\$ 3.00	\$ 75,000.00	\$ 5.50	\$ 137,500.00	\$ 1.54	\$ 38,500.00	\$ 3.51	
3b	Silt Fence Over 25,000 LF	7,000.00	LF	\$ 1.50	\$ 10,500.00	\$ 3.00	\$ 21,000.00	\$ 5.50	\$ 38,500.00	\$ 1.50	\$ 10,500.00	\$ 2.88	
4	Ground Improvements	1.00	Job	\$ 11,641,727.00	\$ 11,641,727.00	\$ 10,000,000.00	\$ 10,000,000.00	\$ 9,650,000.00	\$ 12,996,450.00	\$ 11,069,544.25	\$ 11,069,544.25	\$ 11,069,544.25	
6	Separator Gravel	18,852.00	SY	\$ 2.00	\$ 37,704.00	\$ 2.30	\$ 42,936.00	\$ 3.00	\$ 54,156.00	\$ 4.60	\$ 83,092.20	\$ 3.03	
7	Cleaning and Grubbing	1.00	Job	\$ 680,000.00	\$ 680,000.00	\$ 800,000.00	\$ 800,000.00	\$ 650,000.00	\$ 1,296,450.00	\$ 717,000.00	\$ 717,000.00	\$ 717,000.00	
8	Excavation New Drainage Ditch	2,200.00	CY	\$ 11.00	\$ 24,200.00	\$ 6.00	\$ 13,200.00	\$ 19.00	\$ 41,800.00	\$ 10.68	\$ 23,488.00	\$ 10.68	
9	Degrading Existing Levees	1,900.00	CY	\$ 6.50	\$ 12,350.00	\$ 6.00	\$ 11,400.00	\$ 23.00	\$ 43,700.00	\$ 6.75	\$ 21,750.00	\$ 11.74	
10	Enbanment, Compacted Fill	460,000.00	CY	\$ 23.00	\$ 10,580,000.00	\$ 29.00	\$ 13,340,000.00	\$ 34.00	\$ 15,640,000.00	\$ 56.25	\$ 25,875,000.00	\$ 35.56	
12	Granular Base Course	900.00	SY	\$ 23.00	\$ 20,700.00	\$ 33.00	\$ 29,700.00	\$ 33.00	\$ 29,700.00	\$ 14.60	\$ 13,140.00	\$ 25.90	
13	Asphaltic Pavement	900.00	SY	\$ 70.00	\$ 63,000.00	\$ 60.00	\$ 54,000.00	\$ 44.00	\$ 39,600.00	\$ 50.15	\$ 45,135.00	\$ 56.04	
15	Seeding and Mutching	3,300.00	AC	\$ 3,000.00	\$ 9,900.00	\$ 900.00	\$ 2,700.00	\$ 1,600.00	\$ 382,800.00	\$ 93.55	\$ 308,715.00	\$ 92.39	
16	Fertilizer - First 21,600 US	21,600.00	US	\$ 2.04	\$ 44,064.00	\$ 1.25	\$ 27,000.00	\$ 1.00	\$ 21,600.00	\$ 1.70	\$ 36,720.00	\$ 1.46	
17a	Fertilizer - Over 21,600 US	3,300.00	US	\$ 1.88	\$ 6,204.00	\$ 1.25	\$ 4,125.00	\$ 1.00	\$ 3,300.00	\$ 1.70	\$ 5,610.00	\$ 1.46	
18	Lime Soil Amendment	72.00	TON	\$ 2,000.00	\$ 14,400.00	\$ 225.00	\$ 16,200.00	\$ 150.00	\$ 10,800.00	\$ 1,400.00	\$ 82,800.00	\$ 431.25	
19	Sulfur Soil Amendment	36.00	TON	\$ 750.00	\$ 27,000.00	\$ 300.00	\$ 10,800.00	\$ 90.00	\$ 3,240.00	\$ 85.50	\$ 3,078.00	\$ 70.125	
Total Bid Price				\$ 23,759,969.00	\$ 25,642,755.00	\$ 27,113,856.00	\$ 39,924,464.20	\$ 28,860,111.05	\$ 28,860,111.05	\$ 36,469,765.05	\$ 2,580,750.00	\$ 7,008	
Mobilization and Demobilization 45 BD				\$ 2,900,000.00	\$ 2,075,000.00	\$ 2,100,000.00	\$ 2,960,000.00	\$ 4,712,204.20	\$ 2,580,750.00	\$ 2,580,750.00	\$ 3,050,000.00	\$ 1,744.50	
Mobilization and Demobilization Percentage of Total				9.28%	6.49%	6.01%	6.20%	16.36%	9.32%	7.69%	4.73%	2.44%	
Contract Balance Dollars (Job Specific Items)				\$ 4,600,390.00	\$ 4,856,500.00	\$ 5,717,500.00	\$ 4,827,860.00	\$ 5,000,615.00	\$ 5,000,615.00	\$ 5,000,615.00	\$ 5,000,615.00	\$ 5,000,615.00	\$ 5,000,615.00
Total Construction Cost per Linear Foot of Levee				\$ 2,312.56	\$ 2,352.36	\$ 2,352.36	\$ 2,352.36	\$ 2,352.36	\$ 2,352.36	\$ 2,352.36	\$ 2,352.36	\$ 2,352.36	\$ 2,352.36
Non-Enhancement Construction Cost per Linear Foot of Levee				\$ 1,793.87	\$ 1,616.47	\$ 1,673.41	\$ 1,844.23	\$ 1,744.50	\$ 1,744.50	\$ 1,744.50	\$ 1,744.50	\$ 1,744.50	\$ 1,744.50
Westbank Mississippi River Levee, New Orleans to Venice, Nov-10, 2019													
Happo Lock to Naim Plaquemine Parish, Louisiana													
LineItem	Description	Estimated Quantity	Unit of Measure	Low Bidder - PhyWay Construction	Durr Heavy Construction	Porchman Frames	B&K Construction	Cycle Construction					
Linear Feet of Levee													
LineItem	Description	Estimated Quantity	Unit of Measure	Unit Price	Total	Unit Price	Total	Unit Price	Total	Unit Price	Total	Average	
2	Traffic Control and Coordination	1.00	Job	\$ 60,000.00	\$ 60,000.00	\$ 37,000.00	\$ 37,000.00	\$ 52,000.00	\$ 52,000.00	\$ 100,000.00	\$ 100,000.00	\$ 90,000.00	
5	Cleaning and Grubbing	1.00	Job	\$ 1,700,000.00	\$ 1,700,000.00	\$ 1,675,000.00	\$ 1,675,000.00	\$ 400,000.00	\$ 400,000.00	\$ 1,571,623.00	\$ 1,571,623.00	\$ 1,465,324.60	
6	Ground Improvement	1.00	Job	\$ 11,900,000.00	\$ 11,900,000.00	\$ 10,764,000.00	\$ 10,764,000.00	\$ 10,575,000.00	\$ 10,575,000.00	\$ 11,788,129.00	\$ 11,788,129.00	\$ 13,850,000.00	
7	Embankment/Compacted Fill	336,480.00	CY	\$ 32.00	\$ 10,767,360.00	\$ 30.70	\$ 10,229,984.00	\$ 26.90	\$ 9,051,312.00	\$ 34.40	\$ 11,574,912.00	\$ 34.00	
8A	Silt Fence First 16,800 LF	16,800.00	LF	\$ 3.50	\$ 59,000.00	\$ 2.50	\$ 42,150.00	\$ 2.14	\$ 36,864.00	\$ 2.50	\$ 42,150.00	\$ 2.75	
8B	Silt Fence Over 16,800 LF	3,300.00	LF	\$ 3.00	\$ 9,900.00	\$ 2.20	\$ 7,260.00	\$ 2.07	\$ 6,866.40	\$ 1.50	\$ 5,070.00	\$ 3.00	
9	Strawing	3,800.00	CY	\$ 80.00	\$ 304,800.00	\$ 130.00	\$ 495,300.00	\$ 65.00	\$ 246,900.00	\$ 80.00	\$ 304,800.00	\$ 87.12	
10	Separator Gravel	3,800.00	SY	\$ 2.30	\$ 8,740.00	\$ 2.00	\$ 7,600.00	\$ 2.18	\$ 8,358.00	\$ 5.00	\$ 19,050.00	\$ 9.25	
11	Seeding and Mutching	80.00	AC	\$ 4,100.00	\$ 328,000.00	\$ 4,200.00	\$ 336,000.00	\$ 3,625.00	\$ 290,000.00	\$ 6,800.00	\$ 544,000.00	\$ 4,565.00	
12	Lime Soil Amendment	80.00	TON	\$ 225.00	\$ 18,000.00	\$ 110.00	\$ 8,800.00	\$ 212.50	\$ 17,000.00	\$ 1,000.00	\$ 8,000.00	\$ 1,000.00	
13	Sulfur Soil Amendment	40.00	TON	\$ 500.00	\$ 20,000.00	\$ 810.00	\$ 32,400.00	\$ 675.00	\$ 27,000.00	\$ 750.00	\$ 30,000.00	\$ 500.00	
14A	Fertilizer for 24,000 US	24,000.00	US	\$ 2.20	\$ 52,800.00	\$ 1.00	\$ 24,000.00	\$ 1.11	\$ 26,640.00	\$ 0.75	\$ 18,000.00	\$ 3.00	
14B	Fertilizer Over 24,000 US	3,600.00	US	\$ 2.20	\$ 7,920.00	\$ 1.00	\$ 3,600.00	\$ 1.17	\$ 4,212.00	\$ 0.50	\$ 1,800.00	\$ 1.57	
15	Asphaltic Pavement	100.00	SY	\$ 160.00	\$ 16,000.00	\$ 100.00	\$ 10,000.00	\$ 150.00	\$ 15,000.00	\$ 500.00	\$ 50,000.00	\$ 280.00	
16	Granular Base Course	100.00	SY	\$ 24.00	\$ 2,400.00	\$ 25.00	\$ 2,500.00	\$ 60.00	\$ 6,000.00	\$ 40.00	\$ 4,000.00	\$ 35.00	
18	Degrading Existing Levees	48,200.00	CY	\$ 7.00	\$ 337,400.00	\$ 14.00	\$ 675,200.00	\$ 4.00	\$ 192,800.00	\$ 11.40	\$ 549,820.00	\$ 23.00	
19	Excavation New Drainage Ditch	280.00	CY	\$ 9.00	\$ 2,520.00	\$ 22.00	\$ 6,160.00	\$ 10.71	\$ 2,988.00	\$ 30.00	\$ 8,400.00	\$ 14.00	
Total Bid Price				\$ 25,959,330.00	\$ 24,657,122.00	\$ 24,657,122.00	\$ 26,619,765.00	\$ 26,619,765.00	\$ 29,174,750.00	\$ 25,959,330.00	\$ 25,959,330.00	\$ 25,959,330.00	
Mobilization and Demobilization AS BD				\$ 48,540,995.00	\$ 50,640,996.00	\$ 50,640,996.00	\$ 52,480,999.00	\$ 52,480,999.00	\$ 53,001,995.00	\$ 53,001,995.00	\$ 53,001,995.00	\$ 53,001,995.00	
Mobilization and Demobilization Percentage of Total				4.96%	7.41%	7.16%	7.19%	7.50%	7.50%	3.96%	3.96%	5.82%	
River Channel Bypass Rip Rap Cost				\$ 20,181,120.00	\$ 21,820,836.00	\$ 21,820,836.00	\$ 22,861,425.00	\$ 22,861,425.00	\$ 21,127,100.00	\$ 21,127,100.00	\$ 21,127,100.00	\$ 21,127,100.00	
Rip Rap Percent Cost of Total				41.86%	43.09%	43.09%	51.79%	51.79%	39.66%	39.66%	43.78%	43.78%	
Contract Balance Dollars (Job Specific Items)				\$ 1,678.87	\$ 1,698.67	\$ 1,698.67	\$ 1,698.67	\$ 1,698.67	\$ 1,764.74	\$ 1,764.74	\$ 1,764.74	\$ 1,764.74	
Construction Cost per Linear Foot of Levee				\$ 2,270.84	\$ 2,416.15	\$ 2,416.15	\$ 2,833.07	\$ 2,833.07	\$ 2,517.06	\$ 2,517.06	\$ 2,517.06	\$ 2,517.06	
Non-Enhancement Construction Cost per Linear Foot of Levee				\$ 2,270.84	\$ 2,416.15	\$ 2,416.15	\$ 2,833.07	\$ 2,833.07	\$ 2,517.06	\$ 2,517.06	\$ 2,517.06	\$ 2,517.06	

REFERENCES

- Aerts, J.C.J.H., 2009. Adaptation cost in the Netherlands: Climate Change and flood risk management. *Climate Changes Spatial Planning and Knowledge for Climate*. pp. 34–36. ISBN 9789088150159.
- Allen, J.R.L., 1965. A review of the origin and characteristics of recent alluvial sediments. *Sedimentology*, v. 5:2, p. 89-101.
- Allen, Y.C., B.R. Couvillion, and J.A. Barras, 2012. Using multitemporal remote sensing imagery and inundation measures to improve land change estimates in coastal wetlands. *Estuaries Coasts* 35 (1), 190-200.
- Allison, M.A., C.R. Demas, B.A Ebersole, B.A. Kliess, C.D. Little, E.A. Meselhe, N.J. Powell, T.C. Pratt, B.M. Vosburg, 2012. A water and sediment budget for the lower Mississippi-Atchafalaya River in flood years 2008-2010: implications for sediment discharge to the oceans and coastal restoration in Louisiana. *Journal of Hydrology*, 432-433, 84-87.
- Allison, M.A., G.C. Kineke, E.S. Gordon, M.A. Goni, 2000. Development and reworking of a seasonal flood deposit on the inner continental shelf off the Atchafalaya River. *Continental Shelf Research*, 20, 2267-2294.
- Allison, M.A., and E.A. Meselhe, 2010. The use of large water and sediment diversions in the lower Mississippi River (Louisiana) for coastal restoration. *J. Hydrol.* 387 (3), 346–360.
- Allison, M.A. and C.F. Neill, 2002. Accumulation Rates and Stratigraphic Character of the Modern Atchafalaya River prodelta, Louisiana. *Transactions, Gulf Coast Association of Geological Societies*, v. 52, p. 1031-1040.
- Allison, M.A., B.M. Vosburg, M.T. Ramirez, and E.A. Meselhe, 2013. Mississippi River channel response to the Bonnet Carré Spillway opening in the 2011 flood and its implications for the design and operation of river diversions. *J. Hydrol.* 477, 104-118.
- Allison, M.A., B.T. Yuill, E.A. Meselhe, J.K. Marsh, A.S. Kolker, A.D. Ameen, 2017. Observational and numerical particle tracking to examine sediment dynamics in a Mississippi River delta diversion. *Estuar. Coast Shelf Sci.* 194, 97-108.
- Andrus, T.M., 2007. Sediment Flux and Fate in the Mississippi River Diversion at West Bay: Observation Study (MS Thesis), Louisiana State University).
- Andrus, T.M., 2020a. The capture timescale of and uncontrolled Mississippi-Atchafalaya bifurcation revisited with future lower river management strategy implications. *Doctoral Dissertation, Chapter 2, Louisiana State University.*

- Andrus, T.M., 2020b. Projected long-term delta-building responses to flow modifications at the Mississippi-Atchafalaya bifurcation. Doctoral Dissertation, Chapter 3, Louisiana State University.
- Andrus, T.M., and S.J. Bentley, 2007. Sediment flux and fate in the Mississippi river diversion at West Bay: observation study. In: Coastal Sediments'. vol. 07. pp. 722-735.
- Andrus, T.M., S.J. Bentley, G.P. Kemp, and J. Hoffman, 2012. West Bay case study: A coastal restoration success with policy implications for future land-building sediment diversions. Presented at the State of the Coast Conference, New Orleans, LA. Abstract available at: https://3887972e-b695-41d9-b719-f333cf15ac7e.filesusr.com/ugd/8be722_12887e7704384488a47fd2d6260b8eec.pdf
- (ASA) American Sportfishing Association. 2013. Sportfishing in America - An Economic Force for Conservation. American Sportfishing Association, Alexandria.
- Aslan, A., W.J. Autin, and M.D. Blum, 2005. Causes of River Avulsion: Insights from the Late Holocene Avulsion History of the Mississippi River, U.S.A. *Journal of Sedimentary Research*, v. 75, p. 650-664.
- Barras, J., S. Beville, D. Britsch, S. Hartley, S. Hawes, J. Johnston, P. Kemp, P. Kinler, A. Martucci, J. Porthouse, D. Reed, K. Roy, S. Sapkota, J. Suhayda, 2003. Historical and predicted coastal Louisiana land changes. 1978–2050.
- Barry, J.M., 1997. *Rising Tide: The Great Mississippi Flood of 1927 and How It Changed America*. Simon and Schuster, New York.
- Basyal, G.P., 2009. Comparison of land building by Mississippi River diversion using one and two dimensional numerical models. MS Thesis, Department of Civil and Environmental Engineering, Louisiana State University, 95p.
- Bentley, S.J., Blum, M.D., Maloney, J., Pond, L., Paulsell, R., 2016. The Mississippi River source-to-sink system: Perspectives on tectonic, climatic, and anthropogenic influences, Miocene to Anthropocene. *Earth-Science Reviews*, 153: 139-174.
- Bentley, S.J., A.M. Freeman, C.S. Willson, J.E. Cable, and L. Giosan, 2014. Using What We Have: Optimizing Sediment Management in Mississippi River Delta Restoration to Improve the Economic Viability of the Nation. J.W. Day et al. (eds.), *Perspectives on the Restoration of the Mississippi Delta, Estuaries of the World*, p. 85-97.
- Bentley, S.J. and C. Magliolo, 2018. Overbank sediment capture in the upper delta plain of the Mississippi River. In: *Proceedings of the American Geophysical Union Fall Meeting*, Washington D.C. Abstract # 378721.

- Bentley, S.J., H.H. Roberts, and K. Rotondo, 2003. The sedimentology of muddy coastal systems: The research legacy and new perspectives from the Coastal Studies Institute. Transactions, Gulf Coast Association of Geological Societies, v. 53.
- Bergillos, R.J., A. Lopez-Ruiz, M. Ortega-Sanchez, G. Masselink, and M.A. Losada, 2016. Implications of delta retreat on wave propagation and longshore sediment transport – Guadelfeo case study (southern Spain). *Mar. Geol.* 382, 1–16.
- Blum M.D. and H.H. Roberts, 2009. Drowning of the Mississippi Delta due to insufficient sediment supply and global sea-level rise. *Nat Geosci* 2:488–491, 18p. supplementary information. doi:10.1038/NGE0553
- Blum, M.D. and H.H. Roberts, 2012. The Mississippi Delta Region: Past, Present, and Future. *Annu. Rev. Earth Planet. Sci.* 40: 655-83.
- Blum, M.D. and H.H. Roberts, 2014. Is sand in the Mississippi River delta a sustainable resource? *Nat. Geosci.* 7 (12), 851.
- Bomer E.J., S.J. Bentley, J.E.T. Hughes, C.A. Wilson, F. Crawford, and K. Xu, 2019. Deltaic morphodynamics and stratigraphic evolution of Middle Barataria Bay and Middle Breton Sound regions, Louisiana, USA: Implications for river-sediment diversions. *Estuarine, Coastal and Shelf Science* 224, 20-33.
- Bridge, J.S. and M.R. Leeder, 1979. A simulation model of alluvial stratigraphy. *Sedimentology*, v. 26, p. 617–644.
- Brown, G., Callegan, C., Heath, R., Hubbard, L., Little, C., Luong, P., Martin, K., McKinney, P., Perky, D., Pinkard, F., Pratt, T., Sharp, J., Tubman, M., 2009. West Bay sediment diversion effects. ERDC workplan report—draft. Coastal and Hydraulics Lab, U.S. Army Engineer Research and Development Center, Vicksburg, MS (250 pp., Apps).
- Bryan, C.F., W.E. Kelso, D.A. Rutherford, L.F. Hale, D.G. Kelly, B.W. Bryan, F. Monzyk, J. Noguera, and G. Constant, 1998. Atchafalaya River Basin hydrological management plan: research and development. Final Report. FEMA, LADWF Contract 512-3019. Baton Rouge: Louisiana State University, Louisiana Cooperative Fish and Wildlife Research Unit.
- Bryant, M., P. Falk, and C. Paola, 1995. Experimental study of avulsion frequency and rate of deposition. *Geology*, v. 23, p. 365–368.
- Caffey, R.H., H. Wang, and D.R. Petrolia, 2014. Trajectory economics: assessing the flow of ecosystem services from coastal restoration. *Ecol. Econ.* 100, 74e84.
- Cahoon, D.R., D.J. Reed, and J.W. Day, 1995. Estimating shallow subsidence in microtidal salt marshes of the southeastern United States: Kaye and Barghoorn revisited. *Mar. Geol.* 128, 1–9.

- Caldwell, R.L. and D.A. Edmonds, 2014. The effects of sediment properties on deltaic processes and morphologies: A numerical modeling study. *Journal of Geophysical Research: Earth Surface*, 119: 961-982.
- Carle, M., C. Sasser, and H. Roberts, 2015. Accretion and vegetation community change in the Wax Lake Delta following the historic 2011 Mississippi River flood. *J. Coast. Res.* 313, 569–587.
- Changing Course, 2019. Navigating the future of the Lower Mississippi River Delta. <http://changingcourse.us/>. Accessed 5 October 2019.
- Chapman, A.D., S.E. Darby, H.M. Hong, E.L. Thompkins, and V.P.D. Tri, 2016. Adaptation and development trade-offs: fluvial sediment deposition and the sustainability of rice-cropping in An Giang Province, Mekong Delta. *Clim. Change* 137 (3-4), 593-608.
- Chow V.T., 1959. *Open-channel hydraulics*. McGraw-Hill, New York, 680 p.
- CH2M Hill, Mussetter Engineering, Inc., Mobile Boundary Hydraulics, PLLC, and Eustis Engineering Company, Inc., 2004. Phase 1 Reconnaissance-level Evaluation of the Third Delta Conveyance Channel Project. Final Report Prepared for the Louisiana Department of Natural Resources.
- Coleman, J.M., 1988. Dynamic changes and processes in the Mississippi River Delta. *Geol. Soc. Am. Bull.*, 100(7), p. 999-1015.
- Coleman, J.M., Boyd Professor, Louisiana State University, Coastal Studies Institute, 2006. Personal communication with Mitch Andrus and approval to use unpublished data on November 27, 2006.
- Coleman, J.M. and S.M. Gagliano, 1964. Cyclic sedimentation in the Mississippi River deltaic plain. *Gulf Coast Association of Geological Societies Transactions* 14, pp. 67–80.
- Coleman, J.M. and S.M. Gagliano, 1965. Sedimentary structures: Mississippi River deltaic plain. In: B.V. Middleton (Editor), *Primary sedimentary structures and their hydrodynamic interpretation*. *Am. Assoc. Petr. Geols., Spec. Publ.* 12: 133-148.
- Coleman, J.M. and L.E. Garrison, 1977. Geological aspects of marine slope stability, northwestern Gulf of Mexico. *Mar. Geotechnol.* 2, 9-44.
- Coleman, J.M. and H.H. Roberts, 1988. Late Quaternary depositional framework of the Louisiana continental shelf and upper continental slope. *Trans. Gulf Coast Assoc. Geol. Soc.* 38, 407–419.
- Coleman, J.M., H.H. Roberts, and G.W. Stone, 1998. Mississippi River delta: an overview. *Journal of Coastal Research*, 14: 698-716.

- Coleman, J.M. and L.D. Wright, 1975. Modern river deltas; variability of processes and sand bodies. In: Broussard, M.L. (Ed.), *Deltas; Models for Exploration*. Houston Geological Society, pp. 99-149.
- Condrey, R.E., P.E. Hoffman, D.E. Evers, 2014. The Last Naturally Active Delta Complexes of the Mississippi River (LNDM): Discovery and Implications. J.W. Day et al. (eds.), *Perspectives on the Restoration of the Mississippi Delta*, *Estuaries of the World*, p. 33-50.
- Couvillion, B.R., J. Barras, G. Steyer, W. Sleavin, M. Fischer, H. Beck, N. Trahan, B. Griffin, and D. Heckman, 2011. Land Area Change in Coastal Louisiana from 1932 to 2010: U.S. Geological Survey Scientific Investigations Map 3164, Scale 1:265, 000, p. 12 (pamphlet).
- (CPRA) Coastal Protection and Restoration Authority, State of Louisiana, 2012. Louisiana's Comprehensive Master Plan for a Sustainable Coast. Prepared for Louisiana State Legislature, 190 p.
- (CPRA) Coastal Protection and Restoration Authority, State of Louisiana, 2017. Louisiana's Comprehensive Master Plan for a Sustainable Coast. Prepared for Louisiana State Legislature, 93 p.
- Cratsley, D.W., 1975. Recent deltaic sedimentation, Atchafalaya Bay, Louisiana: MS thesis, Department of Marine Sciences, Louisiana State University, Baton Rouge, LA, 142 p.
- Darby, W., 1816. *A Geographical Description of the State of Louisiana*. Philadelphia, John Melish.
- Day, J.W., D.F. Boesch, E.J. Clairain, G.P. Kemp, S.B. Laska, W.J. Mitsch, K. Orth, H. Mashriqui, D.J. Reed, L. Shabman, C.A. Simenstad, B.J. Streever, R.R. Twilley, C.C. Watson, J.T. Wells, D.F. Whigham, 2007. Restoration of the Mississippi Delta: lessons from Hurricanes Katrina and Rita. *Science* 315: 1679-1684.
- Day, J.W., L.D. Britsch, S.R. Hawes, G.P. Shaffer, D.J. Reed, and D. Cahoon, 2000. Pattern and process of land loss in the Mississippi Delta: a spatial and temporal analysis of wetland habitat change. *Estuar. Coast* 23 (4), 425e438.
- Day, J.W., J.E. Cable, R.R. Lane, and G.P. Kemp, 2016a. Sediment deposition at the Caernarvon crevasse during the great Mississippi flood of 1927: implications for coastal restoration. *Water* 8 (2), 38.
- Day, J.W., R.D. DeLaune, J.R. White, R.R. Lane, R.G. Hunter, and G.P. Shaffer, G.P., 2018. Can Denitrification Explain Coastal Wetland Loss: A Review of Case Studies in the Mississippi Delta and New England. pp. 294-304. <https://doi.org/10.1016/j.ecss.2018.08.029>.

- Day, J., R. Hunter, R.F. Keim, R. DeLaune, G. Shaffer, E. Evers, D. Reed, C. Brantley, P. Kemp, and M. Hunter, 2012. Ecological response of forested wetlands with and without large-scale Mississippi River input: implications for management. *Ecol. Eng.* 46, 57-67.
- Day, J.W., R.R. Lane, C.F. D'Elia, A.R. Wiegman, J.S. Rutherford, G.P. Shaffer, C.G. Brantley, and G.P. Kemp, 2016. Large infrequently operated river diversions for Mississippi delta restoration. *Estuarine, Coastal and Shelf Science* 183, 292e303.
- Dean, R.G., J.T. Wells, J. Fernando, and P. Goodwin, 2012. River Diversions: Principles, Processes, Challenges and Opportunities – A Guidance Document. Prepared for: U.S. Army Corps of Engineers, State of Louisiana, U.S. Geological Survey, 40 p.
- Dean, R.G., J.T. Wells, J. Fernando, and P. Goodwin, 2014. Sediment diversions on the lower Mississippi river: insight from simple analytical models. *J. Coast Res.* 30 (1), 13e29.
- DeLaune, R.D., A. Jugsujinda, G.W. Peterson, and W.H. Patrick Jr., 2003. Impact of Mississippi River freshwater reintroduction on enhancing marsh accretionary processes in a Louisiana estuary. *Estuar. Coast. Shelf Sci.* 58 (3), 653–662.
- Deltares Academy, 2014. Introductory course for Modelling of hydrodynamics, sediment transport, and bed dynamics in Delft 3D. Delft, the Netherlands, Version: 4.00.33026, September 30, 2014.
- De Mutsert, K., J. Cowan, and C. Walters, 2012. Using Ecopath with Ecosim to explore nekton community response to freshwater diversion into a Louisiana estuary. *Mar. Coast. Fish.* 4, 104–116.
- De Mutsert, K., K.A. Lewis, J. Buszowski, J. Steenbeek, and S. Milroy, 2016. Louisiana Coastal Area Delta Management Ecosystem Modeling, Delta Management Fish and Shellfish Ecosystem Model, Ecopath with Ecosim plus Ecospace (EwE) model description. Final Report to the Louisiana Coastal Protection and Restoration Authority. Baton Rouge, LA.
- Dokka, R.K., G.F. Sella, and T.H. Dixon, 2006. Tectonic control of subsidence and southward displacement of southeast Louisiana with respect to stable North America. *Geophysical Research Letters*, Vol. 33, L23308, doi:10.1029/2006GL027250.
- Edmonds, D.A., 2012. Stability of backwater-influenced river bifurcations: A study of the Mississippi-Atchafalaya system. *Geophysical Research Letters*, Vol. 39, L08402, 5 p.
- Edmonds, D.A. and R.L. Slingerland, 2007. Mechanics of river mouth bar formation: Implications for the morphodynamics of the delta distributary networks. *Journal of Geophysical Research*, 112(F2): F02034.
- Edmonds, D.A. and R.L. Slingerland, 2010. Significant effect of sediment cohesion on delta morphology. *Nature Geoscience*, 3(2): 105-109.

- Ellicott, A., 1803. *The Journal of Andrew Ellicott*. Philadelphia, Budd and Bartram.
- Elliot, D.O., 1932. *The Improvement of the Lower Mississippi River for Flood Control and Navigation*. Vicksburg, Waterways Experiment Station.
- Esposito, C.R., Z. Shen, T.E. Törnqvist, J. Marshak, and C. White, 2017. Efficient retention of mud drives land building on the Mississippi Delta plain. *Earth Surface Dynamics* 5 (3), 387–397.
- Fagherazzi, S. et al., 2012. Numerical models of salt marsh evolution: Ecological, geomorphic, and climatic factors. *Rev. Geophys.* 50, RG1002.
- Falcini, F., N.S. Khan, L. Macelloni, B.P. Horton, C.B. Lutken, K. L. McKee, R. Santoleri, S. Colella, C. Li, G. Volpe, M. D’Emidlo, A. Salsusti, and D.J. Jerolmack, 2012. Linking the historic 2011 Mississippi River flood to coastal wetland sedimentation. *Nat.Geosci.* 5, 803–807.
- Fan, H., H. Huang, and T. Zeng, 2006. Impacts of anthropogenic activity on the recent evolution of the huanghe (yellow) river delta. *J. Coast. Res.* 22 (4), 919–929.
<http://dx.doi.org/10.2112/04-0150.1>.
- Fisk, H.N., 1944, *Geological investigations of the alluvial valley of the lower Mississippi River*. Vicksburg, Mississippi, U.S. Army Corps of Engineers, Mississippi River Commission, 78 p.
- Fisk, H.N., 1952. *Geological investigation of the Atchafalaya Basin and the problem of the Mississippi River diversion*. Vicksburg, Mississippi, U.S. Army Corps of Engineers, Waterways Experiment Station, 145 p.
- FitzGerald, D.M., 1998. *Sand Body Geometry of the Wax Lake Outlet Delta, Atchafalaya Bay, Louisiana*. Baton Rouge, Louisiana: Louisiana State University, Master’s thesis, 130p.
- Frazier, D.E., 1967. Recent deltaic deposits of the Mississippi River: their development and chronology: *Gulf Coast Association of Geological Societies Transactions*, 17: 287-315.
- Gagliano, S., E. Kemp, K. Wicker, K. Wiltenmuth, and R. Sabate, 2003. Neotectonic framework of Southeast Louisiana and applications to coastal restoration. *Trans Gulf Coast Assoc Geol Soc* 53:262–272.
- Gagliano, S.M., K.J. Meyer-Arendt, and K.M. Wicker, 1981. Land loss in the Mississippi River deltaic plain. *Gulf Coast Association of Geological Societies Transactions*. 31, 295-306.
- Gagliano, S.M. and J.L. van Beek, 1975. *Environmental base and management study Atchafalaya Basin, Louisiana*. EPA Socioeconomic Environmental Studies Series, EPA-600/5-75-006.
- Galler, J. J., and M.A. Allison, 2008. Estuarine controls on fine-grained sediment storage in the

- Lower Mississippi and Atchafalaya rivers. *Geol. Soc. Am. Bull.*, 120(3–4), 386–398, doi:10.1130/B26060.1.
- Gaweesh, A., and E. Meselhe, 2016. Evaluation of sediment diversion design attributes and their impact on the capture efficiency. *J. Hydraul. Eng.* 142 (5), 04016002.
- Geleynse, N., J.E.A. Storms, et al., 2010. Modeling of a mixed-load fluvio-deltaic system. *Geophysical Research Letters*, 37(5): L05402.
- Geleynse, N., J.E.A. Storms, et al., 2011. Controls on river delta formation; insights from numerical modelling. *Earth and Planetary Science Letters*, 302(1-2): 217-226.
- Giosan, L. and A.M. Freeman, 2014. How Deltas Work: A Brief Look at the Mississippi River Delta in a Global Context. J.W. Day et al. (eds.), *Perspectives on the Restoration of the Mississippi Delta*, *Estuaries of the World*, p. 29-32.
- Graves, E.A., 1949. Enlargement of Atchafalaya and Old Rivers; estimates of time lapse before the Atchafalaya will carry an increased proportion of latitude flow. Unpublished paper in Mississippi River Commission files, Vicksburg.
- Guidroz, W.S., 2009. Subaqueous, Hurricane-Initiated Shelf Failure Morphodynamics Along the Mississippi River Delta Front, North-Central Gulf of Mexico. Unpublished, Louisiana State University PhD dissertation.
- Hajek, E.A. and D.A. Edmonds, 2014, Is river avulsion style controlled by floodplain morphodynamics?. *Geology*, doi:10.1130/G35045.1.
- Hajek, E.A. and M.A. Wolinsky, 2012, Simplified process modeling of river avulsion and alluvial architecture: Connecting models and field data. *Sedimentary Geology*, v. 257–260, p. 1–30, doi:10.1016/j.sedgeo.2011.09.005.
- Halsey, J.F., 1950. Discussion of the “Atchafalaya Diversion and Its Effect on the Mississippi River”. *Proceedings, Am. Soc. of Civil Engineers*, v. 76.
- Hanegan, K., 2011. Modeling the Evolution of the Wax Lake Delta in Atchafalaya Bay, Louisiana. Erasmus Mundus MSc Programme, Coastal and Marine Engineering and Management CoMEM, Delft University of Technology.
- Harmar, O.P., and N.J. Clifford, 2007. Geomorphological explanation of the long profile of the Lower Mississippi River. *Geomorphology* 84 (3–4), 222–240.
- Heath, R.E., G.L. Brown, C.D. Little, T.C. Pratt, J.J. Ratcliff, D.D. Abraham, D. Perkey, N.B. Ganesh, K. Martin, D.P. May, 2015. Old River Control Complex Sedimentation Investigation. U.S. Army Engineer Research and Development Center, 149 pp.
- Hillen, M., 2009. Wave reworking of a delta: Process-based modelling of sediment reworking

under wave conditions in the deltaic environment. Faculty of Civil Engineering and Geosciences. Delft, the Netherlands, Delft University of Technology.

Hudson, P.F., and R.H. Kesel, 2006. Spatial and temporal adjustment of the Lower Mississippi River channel to major human impacts. *Z. Geomorphol.* 143, 17–33.

Humphreys, A.A. and H.L. Abbot, 1876. Report upon the Physics and Hydraulics of the Mississippi River; upon the Protection of the Alluvial Region against Overflow; and upon the Deepening of the Mouths; based upon Surveys and Investigations. Washington, Gov't Printing Office.

(IDJCR) Isle de Jean Charles Resettlement, 2020. isledejeancharles.la.gov. Accessed 31 January 2020.

Jankowski, K.L., T.E. Törnqvist, and A.M. Fernandes, 2017. Vulnerability of Louisiana's coastal wetlands to present-day rates of relative sea-level rise. *Nature Communications*. DOI: 10.1038/ncomms14792.

Jerolmack, D.J., 2009. Conceptual framework for assessing the response of delta channel networks to Holocene sea level rise. *Quaternary Science Reviews*, 28, p. 1786-1800.

Jerolmack, D.J. and D. Mohrig, 2007. Conditions for branching in depositional rivers. *Geology* 35 (5), 463–466.

Kazmann, R.G. and D.B. Johnson, 1980. If the Old River Control Structure Fails? (The Physical and Economic Consequences). Louisiana Water Resources Research Institute, Bulletin 12: Louisiana State University, Baton Rouge, LA, 135 p.

Kemp, G.P., 2012. West Bay Delta Development Since 2009 (Draft). National Audubon Society, Louisiana Coastal Initiative. 26 pp.

Kemp, G.P., J.W. Day, J.D. Rogers, L. Giosan, and N. Peyronnin, 2016. Enhancing mud supply from the lower Missouri River to the Mississippi river delta USA: dam bypassing and coastal restoration. *Estuar. Coast Shelf Sci.* 183, 304–313.

Kemp, G.P., C.S. Willson, J.D. Rogers, K.A. Westphal, and S.A. Binselam, 2014. Adapting to Change in the Lowermost Mississippi River: Implications for Navigation, Flood Control and Restoration of the Delta Ecosystem. J.W. Day et al. (eds.), *Perspectives on the Restoration of the Mississippi Delta, Estuaries of the World*, p. 51-84.

Kemper, J.P., 1949. *Rebellious River*. Boston, Bruce Humphries, Inc.

Kent, J.D. and R.K. Dokka, 2013. Potential impacts of long-term subsidence on the wetlands and evacuation routes in coastal Louisiana. *GeoJournal* 78, 641-655.

Keogh, M.E., A.S. Kolker, G.A. Snedden, and A.A. Renfro, 2019. Hydrodynamic controls on

- sediment retention in an emerging diversion-fed delta. *Geomorphology* 332, 100-111.
- Keown, M.P., E.A. Dardeau Jr., and E.M. Causey, 1986. Historic trends in the sediment flow regime of the Mississippi River. *Water Resour. Res.* 22 (11), 1555–1564.
- Kesel, R.H., 1988. The decline in the suspended load of the lower Mississippi River and its influence on adjacent wetlands. *Environ. Geol. Water Sci.* 11 (3), 271-281.
- Kesel, R.H., 2003. Human modification to the sediment regime of the lower Mississippi River flood plain. *Geomorphology*, 56:10.
- Kesel, R.H., E.G. Yodis, and D.J. McCraw, 1992. An approximation of the sediment budget of the lower Mississippi River prior to major human modification. *Earth Surf. Process. Landf.* 17 (7), 711–722.
- Kim, W., D. Mohrig, R. Twilley, C. Paola, and G. Parker, 2009. Is it feasible to build new land in the Mississippi River Delta? *Eos Trans. AGU* 90 (42), 373e374.
- Kind, J.M., 2014. Economically efficient flood protection standards for the Netherlands. *Journal of Flood Risk Management* 7, 103-117. DOI: 10.1111/jfr3.12026.
- Kirwan, M.L. and G.R. Guntenspergen, 2012. Feedbacks between inundation, root production, and shoot growth in a rapidly submerging brackish marsh. *J. Ecol.* 100, 764–770.
- Knox, R.L. and E.M. Latrubesse, 2016. A geomorphic approach to the analysis of bedload and bed morphology of the Lower Mississippi River near the Old River Control Structure. *Geomorphology*, 268, p. 35-47.
- Kolb, C.R., 1980. Should we permit the Mississippi-Atchafalaya Diversion? *Transactions, Gulf Coast Association of Geological Societies*, v. XXX, p. 145-150.
- Kolb, C.R. and J.R. van Lopik, 1958. *Geology of the Mississippi Deltaic Plain-Southeastern Louisiana*.
- Kolker, A.S., C. Li, N.D. Walker, C. Pilley, A.D. Ameen, G. Boxer, C. Ramatchandirane, M. Ullah, and K.A. Williams, 2014. The impacts of the great Mississippi/Atchafalaya River flood on the oceanography of the Atchafalaya Shelf. *Continental Shelf Research*, 17 p.
- Kolker, A.S., Miner, M.D., Weathers, H.D., 2012. Depositional dynamics in a river diversion receiving basin: the case of the West Bay Mississippi River Diversion. *Estuar. Coast. Shelf Sci.* 106, 1–12.
- Kostic, S. and B. Parker, 2003. Progradational sand-mud deltas in lakes and reservoirs. Part 1. Theory and numerical modeling. *Journal of Hydraulic Research*, 41(2): 127-140. doi: 10.1080/00221680309499956.

- Kulp M., D. Fitzgerald, S. Penland, 2005. Sand-rich lithosomes of the Holocene Mississippi river Delta Plain. In: Giosan L, Bhattacharya JP (eds) River deltas-concepts, models, and examples. Soc Sediment Geol Special Publ 83:279–293.
- Kulp, M., P. Howell, S. Adiau, S. Penland, J. Kindinger, and S.J. Williams, 2002. Latest Quaternary stratigraphic framework of the Mississippi River delta region. In: Transactions - Gulf Coast Association of Geological Societies. 52.
- Lamb, M.P., J.A. Nittrouer, D. Mohrig, and J. Shaw, 2012. Backwater and river plume controls on scour upstream of river mouths: implications for fluvio-deltaic morphodynamics. J. Geophys. Res. 117, F01002. <https://doi.org/10.1029/2011JF002079>.
- Lane E.W., 1957. A study of the shape of channels formed by natural streams flowing in erodible material. M.R.D. Sediment series, Vol 1. U.S. Army Engineer Division, Missouri River, Corps of Engineers, Omaha, 121 p.
- Latimer, R.A. and C.W. Schweizer, 1951. The Atchafalaya River Study: A Report Based upon Engineering and Geological Studies of the Enlargement of Old and Atchafalaya Rivers. U.S. Army Corps of Engineers, Mississippi River Commission, Vicksburg, Mississippi, 3 vol., 375 p.
- LCWCRTF and WCRA, 1998. Coast 2050: toward a sustainable coastal Louisiana. Louisiana coastal wetlands conservation and restoration task force and the wetlands conservation and restoration authority. Louisiana Department of Natural Resources, Baton Rouge, La, 161 p. <http://www.coast2050.gov/report.pdf>.
- Li, H., and S.L. Yang, 2009. Trapping effect of tidal marsh vegetation on suspended sediment, Yangtze Delta. J. Coast. Res. 25, 915-924.
- Lopez, J.A., T.K. Henkel, A.M. Moshogianis, A.D. Baker, E.C. Boyd, E.R. Hillmann, P.F. Conner, and D.B. Baker, 2014. Examination of deltaic processes of Mississippi River outlets—Caernarvon delta and Bohemia Spillway in southeastern Louisiana. Gulf Coast Association of Geological Sciences Transactions 6, 707–708.
- (LPBF) Lake Pontchartrain Basin Foundation, 2019. <https://saveourlake.org/lpbf-programs/coastal/coastal-projects/bohemia-spillway/>. Accessed 10 November 2019.
- Mack, G.H. and M.R. Leeder, 1998. Channel shifting of the Rio Grande, southern Rio Grande rift: implications for alluvial stratigraphic models. Sedimentary Geology, v. 117:3-4, p. 207-219.
- Mackey, S.D., and J.S. BRIDGE, 1995. Three-dimensional model of alluvial stratigraphy: theory and application. Journal of Sedimentary Research v. B65, p. 7–31.
- Magliolo, C., 2017. Overbank Deposition of Sand and Mud within Two Point Bars Bound by the Mississippi River Levee System: Implications for Coastal Restoration Sediment Budgets.

- Louisiana State University Masters Thesis, pp. 60. https://digitalcommons.lsu.edu/gradschool_theses/4326/.
- Maloney, J.M., S.J. Bentley, K. Xu, J. Obelcz, I.Y. Georgiou, and M.D. Miner, 2018. Mississippi River subaqueous delta is entering a stage of retrogradation. *Mar. Geol.* 400, 12-23.
- Majersky, S., H.H. Roberts, R. Cunningham, G.P. Kemp, and C.J. John, 1997. Facies development in the Wax Lake Outlet delta: Present and future trends. *Basin Research Institute Bulletin* 7, p. 50-66.
- Martinez, J.D., 1986. Mississippi-Atchafalaya Diversion: A New Perspective. *Bulletin of the Association of Engineering Geologists*, v. XXIII, No. 1, p. 93-100.
- Masters, J., 2019. America's Achilles' Heel: the Mississippi River's Old River Control Structure. <https://www.wunderground.com/cat6/Americas-Achilles-Heel-Mississippi-Rivers-Old-River-Control-Structure>.
- McIntire, W.G., 1954. Correlation of prehistoric settlements and delta development. LA State Univ., Coastal Studies Inst., Baton Rouge, LA, Tech. Rept. 5, 65 pp.
- McKee, B.A., R.C. Aller, M.A. Allison, T.S. Bianchi, and G.C. Kineke, 2004. Transport and transformation of dissolved and particulate materials on continental margins influenced by major rivers: benthic boundary layer and seabed processes. *Cont. Shelf Res.* 24, 899-926.
- Meade, R.H., and J.A. Moody, 2010. Causes for the decline of suspended-sediment discharge in the Mississippi River system, 1940-2007. *Hydrol. Process.* 24 (1), 35-49.
- Meckel, T.A., U.S. ten Brink, and S.J. Williams, 2006. Current subsidence rates due to compaction of Holocene sediments in southern Louisiana. *Geophys. Res. Lett.* 33, L11403.
- Meselhe, E., M. Baustian, and M.A. Allison, 2016. Basin Wide Model Development for the Louisiana Coastal Area Mississippi River Hydrodynamic and Delta Management Study (Draft). The Water Institute of the Gulf.
- Meselhe, E.A., I. Georgiou, M.A. Allison, and J.A. McCorquodale, 2012. Numerical modeling of hydrodynamics and sediment transport in lower Mississippi at a proposed delta building diversion. *J. Hydrol.* 472, 340-354.
- Morris, J.T., P.V. Sundareshwar, C.T. Nietch, B. Kjerfve, B. and D.R. Cahoon, 2002. Responses of coastal wetlands to rising sea level. *Ecology* 83, 2869-2877.
- Morton, R. A., et al., 2005. Historical subsidence and wetland loss in the Mississippi delta plain, *Gulf Coast Assoc. Geol. Soc. Trans.*, 55, 555-571.
- Morton, R.A., C.J. Bernier, J.A. Barras, and F.N. Ferina, 2005. Historical subsidence and wetland loss in the Mississippi delta plain. *Transactions, Gulf Coast Association of*

- Geological Societies, 55: 555-571.
- Mossa, J., 1996. Sediment dynamics in the lowermost Mississippi River. *Eng. Geol.* 45, 457–479.
- Mossa, J., 2013. Historical channel geometry of a major juncture: Lower Old River, Louisiana. *Physical Geography*, v. 34(4-5), pp. 314-334.
- Mossa, J., 2016. The changing geomorphology of the Atchafalaya River, Louisiana: a historical perspective. *Geomorphology* 252, 112–127.
- Mossa, J. and H.H. Roberts, 1990. Synergism of riverine and winter storm-related sediment transport processes in Louisiana's coastal wetlands. *Transactions of the Gulf Coast Association of Geological Societies*, 40: 635-642.
- (MRC) Mississippi River Commission, 1881. Report of the Commission with Minority Report 47. 47th Congress, 1st Session, S. Document 10.
- Neumeier, U., and P. Ciavola, 2004. Flow resistance and associated sedimentary processes in a *Spartina maritima* salt-marsh. *J. Coast. Res.* 20, 435-447.
- Nguyen, I., A. Cox, J. Brown, R. Davinroy, J. Floyd, E. Rivera, 2010. Mississippi River and Old River Control Complex Sedimentation Investigation and Hydraulic Sediment Response Model Study. U.S. Army Corps of Engineers, St. Louis District.
- Nicholls, R.J. and C. Small, 2002. Improved estimates of coastal population and exposure to hazards released. *Eos* 8 (2), 301–305. <https://doi.org/10.1029/2002EO000216>.
- Nittrouer, J.A., J.L. Best, C. Brantley, R.W. Cash, M. Czapiga, P. Kumar, and G. Parker, 2012. Mitigating land loss in coastal Louisiana by controlled diversion of Mississippi River sand. *Nat. Geosci.* 5, 534–537.
- Nittrouer, J., D. Mohrig, M.A. Allison, and A. Peyret, 2011a. The lowermost Mississippi River: A mixed bedrock alluvial channel. *Sedimentology*, 58: 1914-1934.
- Nittrouer, J. A., D. Mohrig, and M. Allison, 2011b. Punctuated sand transport in the lowermost Mississippi River. *J. Geophys. Res.*, 116, F04025, doi:10.1029/2011JF002026.
- Nittrouer, J.A and E. Viparelli, 2014. Sand as a stable and sustainable resource for nourishing the Mississippi River delta. *Nat. Geosci.* 7 (5), 350.
- (NOAA) U. S. Department of Commerce, National Oceanic and Atmospheric Administration, 2019. Data Access Viewer. <https://coast.noaa.gov/dataviewer/#/>. Accessed 15 June 2019.
- (NOAA) United States Department of Commerce, National Oceanic and Atmospheric Administration National Ocean Service Center for Operational Oceanographic Products and

- Services, 2003. Computational Techniques for Tidal Datums Handbook. NOAA Special Publication NOS CO-OPS 2.
- Odom, L.M., 1950. Atchafalaya Diversion and its effect on the Mississippi River. Proceedings, American Society of Civil Engineers, vol. 76.
- Orton, G.J. and H.G. Reading, 1993. Variability of deltaic processes in terms of sediment supply, with particular emphasis on grain size. *Sedimentology* 40: 475-517.
- Overeem, I., J.P.M. Syvitski, and E.W.H. Hutton, 2005. Three-dimensional numerical modeling of deltas. In: Giosan, L. Bhattacharya, J.P. (Eds.), *River Deltas – Concepts, Models, and Examples*. SEPM Special Publication, 83: 13-30.
- Pahl, James. 2016. 2017 Coastal Master Plan: Attachment C-2: Eustatic Sea Level Rise. Version I. Baton Rouge, Louisiana: Coastal Protection and Restoration Authority.
- Paola, C., R.R. Twilley, D.A. Edmonds, W. Kim, D. Mohrig, G. Parker, E. Viparelli, and V.R. Voller, V.R., 2011. Natural processes in delta restoration: application to the Mississippi delta. *Annu. Rev. Mater. Sci.* 3, 7e91.
- Parker, G., C. Paola, K. Whipple, and D. Mohrig, 1998. Alluvial fans formed by channelized fluvial and sheet flow: theory. *Journal of Hydraulic Engineering* 124:1-11.
- Parker, G., T. Muto, Y. Akamatsu, W.E. Dietrich, and J.W. Lauer, 2008. Unraveling the conundrum of river response to rising sea-level from laboratory to field: Part 1. Laboratory experiments. *Sedimentology* 55:1643-1655.
- Patrick, R., 1998. Rivers of the United States, Volume IV, Part A: The Mississippi River and Tributaries North of St. Louis. John Wiley & Sons.
- Penland, S., W. Ritchie, R. Boyd, R.G. Gerdes, J.R. Suter, 1986. The Bayou Lafourche delta, Mississippi River delta plain, Louisiana. *Geol. Soc. of Am. Centennial Field Guide-Southeastern Section*, p. 447-452.
- Peyronnin, N.S., R.H. Caffey, J.H. Cowan, D. Justic, A.S. Kolker, S.B. Laska, A. McCorquodale, E. Melancon, J.A. Nyman, R.R. Twilley, and J.M. Visser, 2017. Optimizing sediment diversion operations: working group recommendations for integrating complex ecological and social landscape interactions. *Water* 9 (6), 368.
- Piazza, B.P., 2014. The Atchafalaya River Basin: history and ecology of and American wetland. Supported by the Louisiana Chapter of The Nature Conservancy. College Station: Texas A&M University Press. 305 p.
- Pickering, J.L., S.L. Goodbred, M.D. Reitz, T.R. Hartzog, D.R. Mondal, M.S. Hossain, 2014. Late Quaternary sedimentary record and Holocene channel avulsions of the Jamuna and Old Brahmaputra River valleys in the upper Bengal delta plain. *Geomorphology*, 227, p. 123-136.

- Ramatchandirane, C.G., 2013. Coastal Marsh Formation and its Relation to Sediment Exchange Along the Chenier Plain in Southwest Louisiana. Department of Earth and Environmental Sciences, Tulane University, New Orleans, LA 113.
- Ranasinghe, R., C. Swinkels, A. Luijendijk, D. Roelvink, J. Bosboom, M. Stive, and D. J. Walstra, 2011. Morphodynamic upscaling with the MORFAC approach: Dependencies and sensitivities. *Coastal Eng.*, 58, 806–811.
- (REC & EE) Royal Engineers and Consultants, LLC., and Earth Economics, 2016. Basin-wide Socio-economic Analysis of Four Proposed Sediment Diversions. Final Report to the Louisiana Coastal Protection and Restoration Authority in Fulfillment of Task 3/5 of the Scope of Work. CPRA Contract No. 2035-14-27, Task Order 1.
- Reed, D. J., 1995. The response of coastal marshes to sea-level rise: Survival or submergence? *Earth Surf. Process. Landf.* 20, 39–48.
- Reed, D.J. and B. Yuill, 2016. 2017 Coastal Master Plan: Attachment C2-2: Subsidence. Version I. Baton Rouge, Louisiana: Coastal Protection and Restoration Authority.
- Reuss, M., 2004. Designing the Bayous: The Control of Water in the Atchafalaya Basin. Texas A&M University Press, pp. 1800–1995 (No. 4).
- Roberts, H.H., 1997. Dynamic Changes of the Holocene Mississippi River Delta Plain: The Delta Cycle. *Journal of Coastal Research*, v. 13, no. 3, p. 605-627.
- Roberts, H.H., 1998. Delta switching: early responses of the Atchafalaya diversion. *Journal of Coastal Research*, 14:882.
- Roberts, H.H., 1999. Atchafalaya Basin and Atchafalaya-Wax Lake deltas: Guidebook. AAPG Modern Deltas field Seminar, 68 p.
- Roberts, H.H. and J.M. Coleman, 1996. Holocene evolution of the deltaic plain: a perspective – from Fisk to present. *Engineering Geology* 45, 113-138.
- Roberts, H.H., J.M. Coleman, S.J. Bentley, and N. Walker, 2003. An Embryonic Major Delta Lobe: A New Generation of Delta Studies in the Atchafalaya – Wax Lake Delta System. *Transactions, Gulf Coast Association of Geologic Societies / GCSSEPM*, v. 53, p. 690–703.
- Roberts, H.H. and I.L. van Heerden, 1992. Atchafalaya-Wax Lake delta complex: The new Mississippi River delta lobe. Annual Coastal Studies Institute Industrial Associates Research Program, Research Report #1, 45 p.
- Rodi, R.J., 2017. Unsteady Flow Simulations to Develop Model Scale Discharge Hydrographs for the Expanded Small Scale Physical Model of the Mississippi River. Master's Thesis, Louisiana State University.

- Rosen, T. and Y.J. Xu, 2013. Recent decadal growth of the Atchafalaya River Delta complex: Effects of variable riverine sediment input and vegetation succession. *Geomorphology* 194, 108-120.
- Rouse, L.J., Jr., H.H. Roberts, and R.H.W. Cunningham, 1978. Satellite observation of the subaerial growth of the Atchafalaya delta, Louisiana: *Geology*, v. 6, p. 405-408.
- Rutherford, J.S., J.W. Day, C.F. D'Elia, A.R. Wiegman, C.S. Willson, R.H. Caffey, G.P. Shaffer, R.R. Lane, and D. Batker, 2018. Evaluating trade-offs of a large, infrequent sediment diversion for restoration of a forested wetland in the Mississippi delta. *Estuarine, Estuar. Coast Shelf Sci.* 203, 80-89.
- Salisbury, E.F., 1937. Influence of diversion on the Mississippi and Atchafalaya Rivers. *Transactions, American Society of Civil Engineers*, vol. 102.
- Safak, I., A. Sheremet, J. Davis, and J.M. Kaihatu, 2017. Nonlinear wave dynamics in the presence of mud-induced dissipation on Atchafalaya Shelf, Louisiana, USA. *Coastal Engineering* 130, 52-64.
- Saito, Y., Z. Yang, & K. Hori, 2001. The Huanghe (YellowRiver) and Changjiang (YangtzeRiver) deltas: A review on their characteristics, evolution and sediment discharge during the Holocene. *Geomorphology*, 41(2), 219-231.
- Salisbury, E.F., 1937. Influence of diversion on the Mississippi and Atchafalaya Rivers. *Transactions, American Society of Civil Engineers*, vol. 102.
- Schultz, C., 1810. *Travels on an Inland Voyage*. New York, Isaac Riley, v. 2.
- Schumm, S.A., 1986. Alluvial river response to active tectonics, in Schumm, S.A., Dumont, J.F., and Holbrook, J.M., eds., *Active Tectonics: Washington D.C., National Academy Press, Studies in Geophysics*, p. 80-94.
- Sherement, A. and G.W. Stone, 2003. Observation of nearshore wave dissipation over muddy sea beds. *Journal of Geophysical Research* v. 108, no. C11, 3357, doi:10.1029/2003JC001885.
- Shlemon, R.J., 1975. Subaqueous delta formation-Atchafalaya Bay, Louisiana. In: Broussard, M.L. (Ed.), *Deltas: Models for Exploration*. Houston Geological Society, pp. 209-221.
- Shi, C.X., and D. Zhang, 2003. Processes and mechanisms of dynamic channel adjustment to delta progradation: The case of the mouth channel of the Yellow River, China. *Earth Surface Processes and Landforms*, 28(6), 609-624.
- Shuman, M., D. Jones, J. Mossa, T. Smith, 1993. *Cultural Resources Survey of Fort Adams Reach Revetment, Mile 312.2 to 306.0-L, Mississippi River, Wilkinson County, Mississippi*.

Cultural Resources Series U.S. Army Corps of Engineers, New Orleans District.

- Siadatmousavi, S.M., M.N. Allahdaddi, Q. Chen, F. Jose, and H.H. Roberts, 2012. Simulation of wave damping during a cold front over the muddy Atchafalaya shelf. *Continental Shelf Research* 47, 165-177.
- Simenstad, C., D. Reed, and M. Ford, 2006. When is restoration not? Incorporating landscapescale processes to restore self-sustaining ecosystems in coastal wetland restoration. *Ecol. Eng.* 26 (1), 27–39.
- Slingerland, R. and N.D. Smith, 1998. Necessary conditions for a meandering-river avulsion. *Geology* 26 (5), 435–438.
- Snedden, G.A., J.E. Cable, C. Swarzenski, and E. Swenson, 2007. Sediment discharge into a subsiding Louisiana deltaic estuary through a Mississippi River diversion. *Estuar. Coast Shelf Sci.* 71 (1-2), 181-193.
- Smith, M., and S.J. Bentley, 2014. Sediment capture in floodplains of the Mississippi river: a case study in cat island national wildlife Refuge, Louisiana. In: *Sediment Dynamics from the Summit to the Sea*. vol. 367. IAHS Publ, pp. 442-446 2014.
- Sommerfield, C.K., C.A. Nittrouer, and C.R. Alexander, 1999. Be-7 as a tracer of flood sedimentation on the northern California continental margin. *Cont. Shelf Res.* 19, 335–361.
- Sounny-Slitine, A., 2012. *Geomorphic and Anthropogenic Influences on Hydrologic Connectivity Along the Lower Mississippi River*. University of Texas, Austin, M.S. Thesis.
- Steyer, G. D. et al., 2003. A proposed coast-wide reference monitoring system for evaluating wetland restoration trajectories in Louisiana. *Environ. Monit. Assess.* 81, 107–117.
- Storms, J.E.A., M.J.F. Stive, et al., 2007. Initial Morphologic and Stratigraphic Delta Evolution Related to Buoyant River Plumes. *Proceedings of the Sixth International Symposium on Coastal Engineering and Science of Coastal Sediment Process*, New Orleans, Louisiana, American Society of Civil Engineers.
- Stouthamer, E. and J.A.H. Berendsen, 2000. Factors controlling the Holocene avulsion history of the Rhine-Meuse Delta (The Netherlands). *Journal of Sedimentary Research*, v. 70:5, p. 1051-1064.
- Stouthamer, E., and J.A.H. Berendsen, 2007. Avulsion: the relative roles of autogenic and allogenic processes. *Sediment. Geol.*, v. 198 (3–4), p. 309–325.
- Syvitski, J. and S. Higgins, 2012. Swamped. *New Scientist* 40-43.

- Syvitski, J.P., A.J. Kettner, I. Overeem, E.W. Hutton, M.T. Hannon, G.R. Brakenridge, J. Day, C. Vörösmarty, Y. Saito, L. Giosan, and R.J. Nicholls, 2009. Sinking deltas due to human activities. *Nat. Geosci.* 2 (10), 681.
- Syvitski, J.P.M. and Saito, Y., 2007. Morphodynamics of deltas under the influence of humans. *Global and Planetary Change*, 57:261-282.
- Syvitski, J.P.M., Vörösmarty, C., Kettner, A.J., Green, P., 2005. Impact of humans on the flux of terrestrial sediment to the global coastal ocean. *Science* 308, 376–380.
- Thompson, W.C., 1951. Oceanographic analysis of Atchafalaya Bay, Louisiana and adjacent continental shelf area marine pipeline problems: Texas A&M Foundation, Department of Oceanography, Sec. 2, Project 25, 31p.
- Thompson, W.C., 1955. Sandless coastal terrain of the Atchafalaya Bay area, Louisiana: SEPM Special Publication No. 3, p. 52-76.
- Törnqvist, T.E., 1993. Holocene alternation of meandering and anastomosing fluvial systems in the Rhine-Meuse Delta (central Netherlands) controlled by sea-level rise and subsoil erodibility. *J. Sediment. Res.* 63 (4), 683–693.
- Törnqvist, T.E., T.R. Kidder, W.J. Autin, K. van der Borg, K., A.F.M. de Jong, C.J.W. Klerks, E.M.A. Snijders, J.E.A. Storms, R.L. van Dam, and M.C. Wiemann, 1996. A revised chronology for Mississippi river subdeltas. *Science* 273 (5282), 1693–1696.
- Törnqvist, T. E. et al., 2008. Mississippi Delta subsidence primarily caused by compaction of Holocene strata. *Nat. Geosci.* 1, 173–176.
- Twilley, R.R., B.R. Couvillin, I. Hossain, C. Kaiser, and A.B. Owens, 2008. Coastal Louisiana ecosystem assessment and restoration (CLEAR) program: the role of ecosystem forecasting in evaluating restoration planning in the Mississippi River deltaic plain. In: *Mitigating Impacts of Natural Hazards on Fishery Ecosystems*, McLaughlin, K.D. (Ed.), American Fisheries Society.
- Tye, R.S. and J.M. Coleman, 1989a. Evolution of Atchafalaya lacustrine deltas, south-central Louisiana. *Sedimentary Geology* 65:95-112.
- Tye, R.S. and J.M. Coleman, 1989b. Depositional processes and stratigraphy of fluvially dominated lacustrine deltas: Mississippi Delta plain. *Journal of Sedimentary Petrology* 59:973-996.
- (USACE) U.S. Army Corps of Engineers, 1935. Studies of river bed materials and their movement, with special reference to the Lower Mississippi River. Paper 17, Vicksburg, Waterways Experiment Station.

- (USACE) U.S. Army Corps of Engineers, 2000. Engineer Regulation 1105-2-100: Planning Guidance Notebook.
- (USACE) U.S. Army Corps of Engineers, 2002. New Orleans, District Water Control Section: Web site [Http://www.mvn.usace.army.mil/eng/edhd/wcontrol/discharge.htm](http://www.mvn.usace.army.mil/eng/edhd/wcontrol/discharge.htm).
- (USACE) U.S. Army Corps of Engineers, 2004. Louisiana Coastal Area (LCA) Ecosystem Restoration Study, Appendix D – Louisiana Gulf Shoreline Restoration Report.
- (USACE) U.S. Army Corps of Engineers, Engineer Research and Development Center, 2014. Mississippi River Hydrodynamic and Delta Management Study (MRHDM)-Geomorphic Assessment. Prepared by Charles D. Little and David S. Biedenham. Sponsored by Louisiana Coastal Protection and Restoration Authority. 309pp.
- (USACE) U.S. Army Corps of Engineers, New Orleans District, 2014. Bonnet Carre Spillway Informational Booklet.
<https://www.mvn.usace.army.mil/Portals/56/docs/PAO/Brochures/BCspillwaybooklet.pdf>.
- (USACE) U.S. Army Corps of Engineers, Mississippi Valley Division, 2015. MR&T Project. Informational Paper. 4 p.
- (USACE) U.S. Army Corps of Engineers, New Orleans District Website, 2019.
<https://www.mvn.usace.army.mil/Missions/Mississippi-River-Flood-Control/Bonnet-Carre-Spillway-Overview/Spillway-Operation-Information/>. Accessed 15 November 2019.
- (USACE) U.S. Army Corps of Engineers, Mississippi Valley Division, New Orleans District, 2020. Maintenance Dredging Activities.
<https://www.mvn.usace.army.mil/About/Offices/Operations/Beneficial-Use-of-Dredged-Material/>. Accessed 5 January 2020.
- (USEIA) U.S. Energy Information Administration, 2014. Rankings: Natural Gas Marketed Production, 2014. Retrieved from www.eia.gov: www.eia.gov/state/rankings/#/series/47.
- Van Beek, J.L. and K.J. Meyer-Arendt, 1982. Louisiana's eroding coastline: Recommendations for protection. Off. Coastal Zone Mgt. Rept., Baton Rouge, LA, 143 pp.
- van Heerden, I.L. and H.H. Roberts, 1988. Facies development of Atchafalaya Delta, Louisiana: a modern bayhead delta. The American Association of Petroleum Geologists Bulletin, 72: 439-453.
- Wade, R., Executive Director, Morgan City Harbor and Terminal District, 2019. Personal communication with Mitch Andrus on February 15, 2019.
- Walker, N.D. and A.B. Hammack, 2000. Impacts of Winter Storms on Circulation and Sediment Transport: Atchafalaya-Vermilion Bay Region, Louisiana, U.S.A. Journal of Coastal Research 16:4, 996-1010.

- Walker, N.D., W.J. Wiseman, L.J. Rouse, and A. Babin, 2005. Seasonal and wind-forced changes in surface circulation, suspended sediments, and temperature fronts of the Mississippi River plume, Louisiana. *J. Coast. Res.* 21, 1228–1244.
- Wang, B. and Y.J. Xu, 2016. Long-term geomorphic response to flow regulation in a 10-km reach downstream of the Mississippi-Atchafalaya River diversion. *Journal of Hydrology: Regional Studies*, 8:10-25.
- Wang, B. and Y.J. Xu, 2018a. Dynamics of 30 large channel bars in the Lower Mississippi River in response to river engineering from 1985 to 2015. *Geomorphology* 300, 31–44.
- Wang, B. and Y.J. Xu, 2018b. Decadal scale riverbed deformation and sand budget of the last 500 km of the Mississippi River: insights into natural and river engineering effects on a large alluvial river. *J. Geophys. Res.: Earth Surface* 123, 874–890.
<https://doi.org/10.1029/2017JF004542>.
- Wang, H., G.D. Steyer, B.R. Couvillion, J.M. Rybczyk, H.J. Beck, W.J. Sleavin, E.A. Meselhe, M.A. Allison, R.G. Boustany, C.J. Fischenich, and V.H. Rivera-Monroy, 2014. Forecasting landscape effects of Mississippi River diversions on elevation and accretion in Louisiana deltaic wetlands under future environmental uncertainty scenarios. *Estuarine, Coastal & Shelf Science* 138, 57e68.
- Wang, Z.Y., and Z.Y. Liang, 2000. Dynamic characteristics of the Yellow River mouth. *Earth Surface Processes and Landforms*, 25(7), 765–782.
- Webb, E. L. et al., 2013. A global standard for monitoring coastal wetland vulnerability to accelerated sea-level rise. *Nat. Clim. Change* 3, 458–465.
- Welder, F.A., 1959. Processes of deltaic sedimentation in the lower Mississippi River. Louisiana State University, Baton Rouge, LA, Coastal Studies Institute, Tech. Rept. 12, 90 pp.
- Wells, J.T., 1983. Dynamics of coastal fluid muds in low-, moderate-, and high-tide-range environments. *Can. J. Fish. Aquat. Sci.* 40(Suppl.1): 130 - 142.
- Wells, J.T., S.J. Chinburg, and J.M. Coleman, 1984. The Atchafalaya River Delta. Report 4. Generic Analysis of Delta Development. Louisiana State University Baton Rouge, Coastal Studies Institute, pp. 105.
- Wells, J.T. and J.M. Coleman, 1987. Wetland loss and the subdelta life cycle. *Estuarine, Coastal and Shelf Science*. 25, 111 – 125.
- Wilson, C.A. and M.A. Allison 2008. An equilibrium profile model for retreating marsh shorelines in southeast Louisiana. *Estuar. Coast Shelf Sci.* 80, 483-494.

- Wright, L.D., 1977. Sediment transport and deposition at river mouths: a synthesis. *Geol. Soc. Am. Bull.* 88, 857–868.
- Wright, L.D. and J.M. Coleman, 1974. Effluent expansion and interfacial mixing in the presence of a salt wedge, Mississippi River Delta. *Journal of Geophysical Research.* 76, 8649-8661.
- Xu, J.X., 2008. Response of land accretion of the Yellow River delta to global climate change and human activity. *Quaternary International*, 186(1), 4–11.
- Xu, K., S.J. Bentley, J.W. Day, and A.M. Freeman, 2019. A review of sediment diversion in the Mississippi River Deltaic Plain. *Estuarine, Coastal and Shelf Science* 225, 106241. <https://doi.org/10.1016/j.ecss.2019.05.023>.
- Yang, H.F., S.L. Yang, K.H. Xu, H. Wu, B.W. Shi, Q. Zhu, W.X. Zhang, and Z. Yang, 2017. Erosion potential of the Yangtze Delta under sediment starvation and climate change. *Sci. Rep.* 7, 10535. <http://dx.doi.org/10.1038/s41598-017-10958-y>.
- Zalasiewicz, J., M. Williams, A. Haywood, and M. Ellis, M., 2011. The Anthropocene: a new epoch of geological time? *Philosophical Transactions of the Royal Society A: MathematicalPhys. Eng. Sci.* 369 (1938), 835–841.
- Zheng, S., D.A. Edmonds, B. Wu, S. Han, 2019. Backwater controls on the evolution and avulsion of the Qingshuigou channel on the Yellow River Delta. *Geomorphology*, v. 333, p. 137-151.
- Zheng, S., B.S. Wu, K.C. Wang, G.M. Tan, S.S. Han, C.R. Thorne, 2017. Evolution of the Yellow River delta, China: impacts of channel avulsion and progradation. *Int. J. Sediment Res.* 32, 34–44.

VITA

Thomas Mitchell Andrus was born in 1974, in Rayne, Louisiana. He is the son of Cotton and Sheila Andrus and the older brother of Mackenzie and Jordan. He and his wife, Hallie, have three children, Evelyn, Kate, and Thomas. He graduated from Notre Dame High School in 1992 and went on to receive a Bachelor of Science degree in Civil and Environmental Engineering in December of 1997 and a Master of Science degree in Oceanography and Coastal Science in December of 2007 from Louisiana State University (LSU). Mitch began his engineering career in 1998 and has been a registered professional engineer since 2002. He has worked in state government as well as private consulting with a primary focus in the coastal engineering field. As an avid outdoorsman reared in south Louisiana, Mitch aimed to learn more about the history and function of America's largest coastal wetland system. In doing so, he found great disappointment in the rate at which this national treasure is being lost. Early in his career, Mitch became interested in the role of major river diversions as a long-term sustainable restoration method and the feasibility of incorporating them with vital flood protection systems. He currently serves as a principal engineer and part-owner at Royal Engineers and Consultants, LLC. He is expected to receive his Doctor of Philosophy degree in Geology and Geophysics from LSU in May of 2020.